ORGANOMETALLIC PRECURSORS FOR PILLARED CLAY SYNTHESIS.

Rachael Claire Ashcroft.

A Thesis Submitted for the Degree of
Doctor of Philosophy.

THE UNIVERSITY OF ASTON IN BIRMINGHAM.

June 1993

The University of Aston in Birmingham

ORGANOMETALLIC PRECURSORS FOR PILLARED CLAY SYNTHESIS

Rachael Claire Ashcroft

A thesis submitted for the degree of Doctor of Philosophy 1993

The synthetic hectorite, laponite has been used within the paper industry to produce mildly conducting paper for use in electrographic printing. The aim of this research was to modify laponite in order to improve the electrical conductivity.

In a continuation of a previous investigation involving organotin intercalation of laponite, the organotin precursor $(p\text{-}CH_3OC_6H_4)_4Sn$ was synthesised and characterised using Mass Spectroscopy, Infrared Spectroscopy and Elemental analysis. Results of intercalation with this compound and a range of organobismuth and organoantimony compounds suggested that a halide content within the precursor was necessary for improvement in conductivity to be observed.

Organometallic intercalation of a range of organotellurium compounds with laponite provided evidence that a hydrolysis reaction on the clay surface followed by the release of hydrochloric acid was an important first step if a reaction was to occur with the clay. Atomic Absorption Spectroscopy studies have shown that the acid protons underwent exchange with the interlayer sodium ions in the clay to varying degrees. Gas-liquid Chromatography and Infrared Spectroscopy revealed that the carbon-tellurium bond remained intact. Powder X-ray diffraction revealed that there had been no increase in the basal spacing.

The a.c. conductivity of the modified clays in the form of pressed discs was studied over a frequency range of 12Hz - 100kHz using two electrode systems, silver paste and stainless steel. The a.c. conductivity consists of two components, ionic and reactive. The conductivity of laponite was increased by intercalation with organometallic compounds. The most impressive increase was gained using the organotellurium precursor $(p\text{-}CH_3OC_6H_4)_2TeCl_2$.

Conductivity investigations using the stainless steel electrode where measurements are made under pressure showed that in the case of laponite, where poor particle-particle contact exists at ambient pressure, there is a two order of magnitude increase in the measured a.c. conductivity. This significant increase was not seen in modified laponites where the particle-particle contact had already been improved upon.

Investigations of the clay surface using Scanning Electron Microscopy suggested that the improvement in particle-particle contact is the largest factor in the determination of the conductivity. The other important factor is the nature and the concentration of the interlayer cations.

A range of clays were synthesised in order to increase the concentration of sodium interlayer cations. A sol-gel method was employed to carry out these syntheses. A conductivity evaluation showed that increasing the concentration of the sodium cations within the clay led to an increase in the conductivity.

KEY WORDS: laponite, organotellurium, conductivity, clay synthesis, tetra(*p*- methoxyphenyl tin(IV)

To Martin

and

My Family

ACKNOWLEDGEMENTS

I would like to express my sincere gratitude and thanks to Professor W.R. McWhinnie for his encouragement, guidance and advice during the course of this research.

I would like to thank the S.E.R.C. and James River Graphics, Chartham Paper Mill, for funding this research, in particular to Carl Willetts for his interest and help during the past three years.

I am grateful to Dr. M. Perry for providing N.M.R. data and Professor F.J. Berry for supplying Mossbauer spectra.

Many thanks are due to the technical staff within the chemisty department and also to Roger Howell from outside the department.

I would like to thank the members of the research group both past and present for making my time at Aston an interesting and enjoyable one.

Finally I would like to express my thanks to Martin Greaves and to my family for their support and encouragement during the course of this work.

CONTENTS.

List of Tables.

List of Figures.

CHAPTER ONE
Introduction

CHAPTER ONE

1.1 Introduction

Clays have been defined in many ways. In geological terms a clay is any naturally occurring material with a particle size of no more than 2μ. A little more precise is the term "clay mineral". Again the particle size must be less than 2μ, but by adding the term 'mineral' we are thus implying that the material has a specific composition and defined structure.

Chemically a clay mineral can be regarded as a hydrous silicate (usually of aluminium or magnesium). Much of the information regarding the structures and basic properties of clay minerals was gained through the work of mineralogists and soil scientists[1-3]. More recent work has concentrated on refining the properties and developing new applications for the clay minerals[4]. Clay minerals can be used in pottery, ceramics,as rubber, plastic, paint and paper fillers, as absorbents, in drilling muds and as catalysts, clarifyers and filters (see section 1.4)

Clay mineral notation is standardised by using lower case letters. Strictly speaking laponite, a synthetic clay used extensively throughout this work, is a trade name but in this thesis the clay will be written to conform with natural clay notation.

1.2 The Structure of Layered Silicate Minerals

Most silicates contain the tetrahedral SiO_4 unit as a structural starting point. The hydrous silicates consist of two-dimensional tetrahedral sheets of composition Si_2O_5 with tetrahedra linked by sharing three corners of each. In ideal configuration a hexagonal mesh is formed as in Figure 1.1.

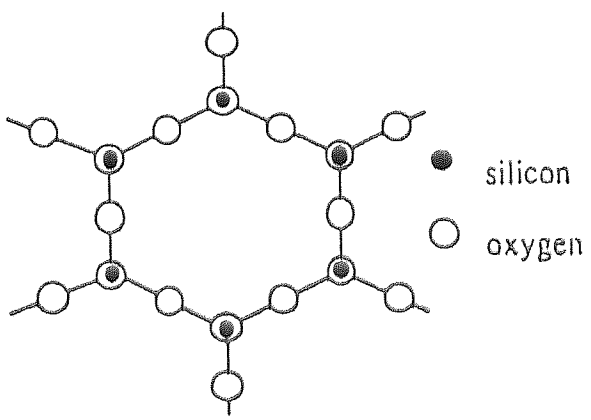

Figure 1.1 The configuration of the hexagonal mesh

The remaining (apical) oxygen is directed perpendicularly to the sheet and hence forms part of the adjacent octahedral sheet, where the octahedra are linked *via* shared edges. Thus the junction plane between the octahedral and the tetrahedral sheets consists of shared apical oxygen atoms and unshared hydroxy groups lying at the centre of each sixfold ring of tetrahedra. Coordinating cations in the octahedral sheet are usually Al^{3+}, Mg^{2+}, Fe^{3+} or Fe^{2+}.

The nature of the layers enables the clay minerals to be sub-divided into several main groups. The first division is for the clay to be classified as dioctahedral or trioctahedral. This is dependent on to what extent the available cation sites are filled. A trioctahedral clay has all available cation sites occupied, usually with divalent cations. A dioctahedral clay has 2/3 of available sites occupied, mainly with trivalent cations.

The second division is by the ratio of tetrahedral to octahedral sheets. For example if one octahedral sheet is linked to one tetrahedral sheet, the clay is classed as a 1:1 layer silicate. Alternatively if one octahedral sheet links to two tetrahedral sheets, a 2:1 layer structure is produced.

The final sub-division deals with a possible layer charge. A structure is classed as electronically neutral when no substitution occurs in the octahedral or tetrahedral sheet and consequently all the charges balance. In some clay minerals some isomorphous substitution occurs, Mg^{2+} could substitute for Al^{3+}, or Al^{3+} could substitute for Si^{4+}. This substitution results in the layers possessing a net negative charge. In consequence this leads to the presence of cations in the interlayer region in order to balance the charge deficiency. These interlayer cations are bound strongly within the clay structure in some minerals yet weakly in others. Minerals with loosely bound interlayer cations often contain water between the layers and thus facilitate a link between successive sheets.
An indication of the amount of substitution taking place is gained by measuring the cation exchange capacity (C.E.C.) of the clay. As a rule, the greater the C.E.C. the greater the substitution.

Table 1.1 shows a summary of the main clay groups, including all the properties mentioned above and also an indication of a property known as the basal spacing. If a clay is considered to be capable of extending indefinitely in two directions (the a and b axes) then the c distance is known as the basal spacing and is obtained through measurement of the d_{001} reflection by powder X-ray diffraction (XRD).

TABLE 1.1

GROUP NAME	MINERAL NAME	LAYER STRUCTURE	CHARGE PER UNIT VOLUME (e)	BASAL SPACING (Å)
KANDITE	KAOLIN	DIOCT 1:1	~0	7.15
ILLITE	TALC	TRIOCT 2:1	~0	9.30
	MICA	DIOCT 2:1	~1	9.90
	BRITTLE MICA	DIOCT 2:1	~2	9.90
SMECTITE	MONTMOR ILLONITE	DIOCT 2:1	0.2 - 0.7	14.7
	HECTORITE	TRIOCT 2:1	0.1 - 0.5	14.3
VERMICULITE		TRIOCT 2:1	0.6 - 0.9	14.1
CHLORITE		2:1:1	VARIABLE	14.0

1.3 The Smectite Group

1.3.1 Structure

Comprehensive reviews regarding the smectite clays have been prepared by Ross and Hendricks[5], McEwan[6] and others[1,2,7]. The smectite group minerals consist of saponite, hectorite, montmorillonite, beidellite and nontronite. Table 1.2 shows the idealised structural fomulae of the minerals.

Smectite clays possess a 2:1 silicate layer structure. They can exist as dioctahedral structures, for example montmorillonite (Figure 1.2) or as trioctahedral entities, for example hectorite (Figure 1.3). Isomorphous substitution, generally within the octahedral layer of the clay leads to a layer charge of 0.2 - 0.6 per unit formula. This is balanced usually by sodium or calcium cations in the interlayer. These ions are easily exchangeable and smectite minerals have a C.E.C. in the region of 80 -150 milliequivalents (meq) per 100g of clay.
Bonds between adjacent layers are weak, only dipolar and van der Waal's forces hold the layers together, therefore varying degrees of water can be incorporated into the interlayer region giving the clays their characteristic swelling properties. Basal spacing can vary between 10Å in the dehydrated state up to 20Å when fully hydrated. The arrangement of the layers in smectites tends to be turbostratic, that is, the layers are randomly stacked with respect to the 'a' and 'b' axes of adjoining layers.

Complete dispersion of the crystallites can occur at high relative humidities[8].

1.3.2 Properties of Smectite Clays

The smectite clays possess a combination of swelling, cation exchange and intercalation properties which distinguishes them from other clay mineral groups. Their unique swelling and intercalation properties are primarily derived from their capacity as cation exchangers. This ability to exchange cations and neutral molecules leads to an almost limitless number of possible intercalation compounds. Some properties important to the interlamellar modification of smectite clays are described below.

1.3.2.1 Swelling Properties

The weakness of the forces between successive layers in smectite clays leads to water being incorporated into the interlayer region[2]. The extent of hydration is dependent on the nature of the swelling agent, the interlayer cation, the layer charge and the humidity. The charge and size

TABLE 1.2
The Ideal Structural Formulae for some Smectite Group Minerals.

MINERAL NAME	INTERLAYER CATIONS	OCTAHEDRAL CATIONS	TETRAHEDRAL CATIONS	ANIONS
Saponite	$X_{0.5}^{+1}$	Mg_3	$(Si_{3.5}Al_{0.5})$	$O_{10}(OH)2$
Hectorite	$X_{0.3}^{+1}$	$(Mg_{2.7}Li_{0.3})$	Si_4	$O_{10}(OH)_2$
Montmorillonite	$X_{0.35}^{+1}$	$(Al_{1.65}Mg_{0.35})$	Si_4	$O_{10}(OH)_2$
Beidellite	$X_{0.4}^{+1}$	Al_2	$Si_{3.6}Al_{0.4}$	$O_{10}(OH)_2$
Nontronite	$X_{0.4}^{+1}$	Fe_2^{3+}	$[Si_{3.6}(Al,Fe^{3+})_{0.4}]$	$O_{10}(OH)_2$

N.B. Saponite and Hectorite are trioctahedral minerals, the other three are dioctahedral.

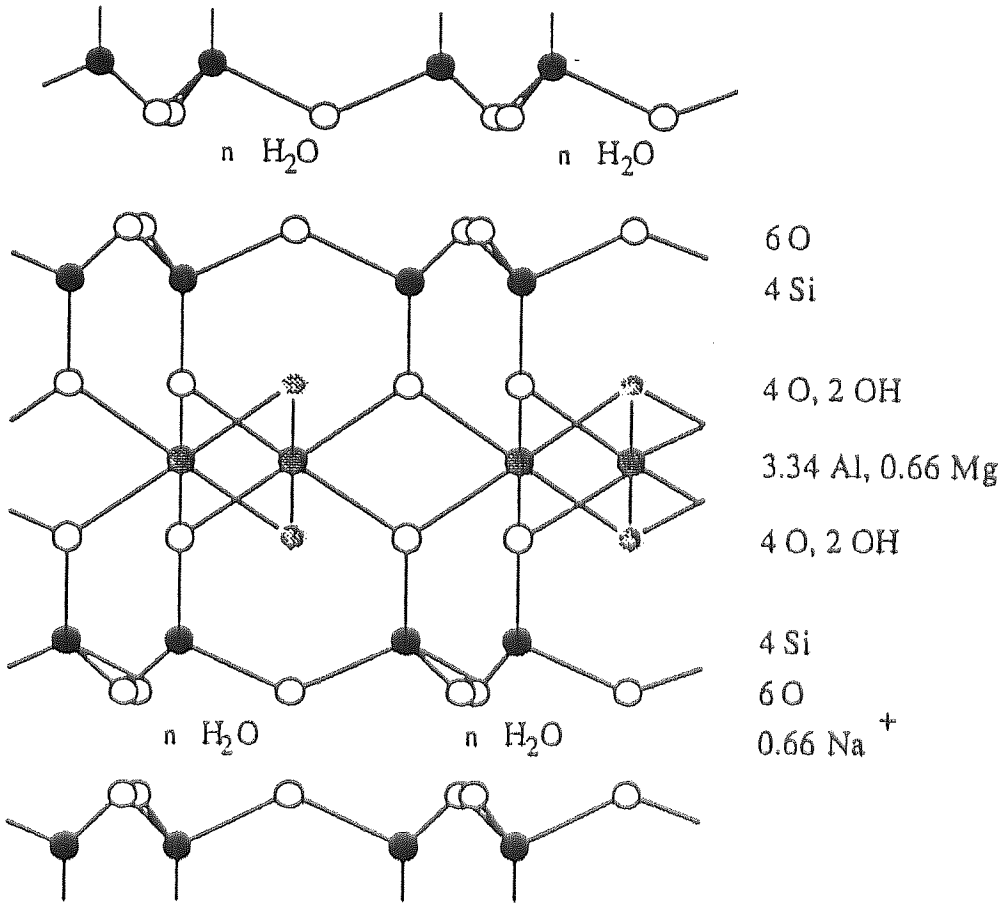

Figure 1.2 The Structure of Montmorillonite - a Dioctahedral Smectite.

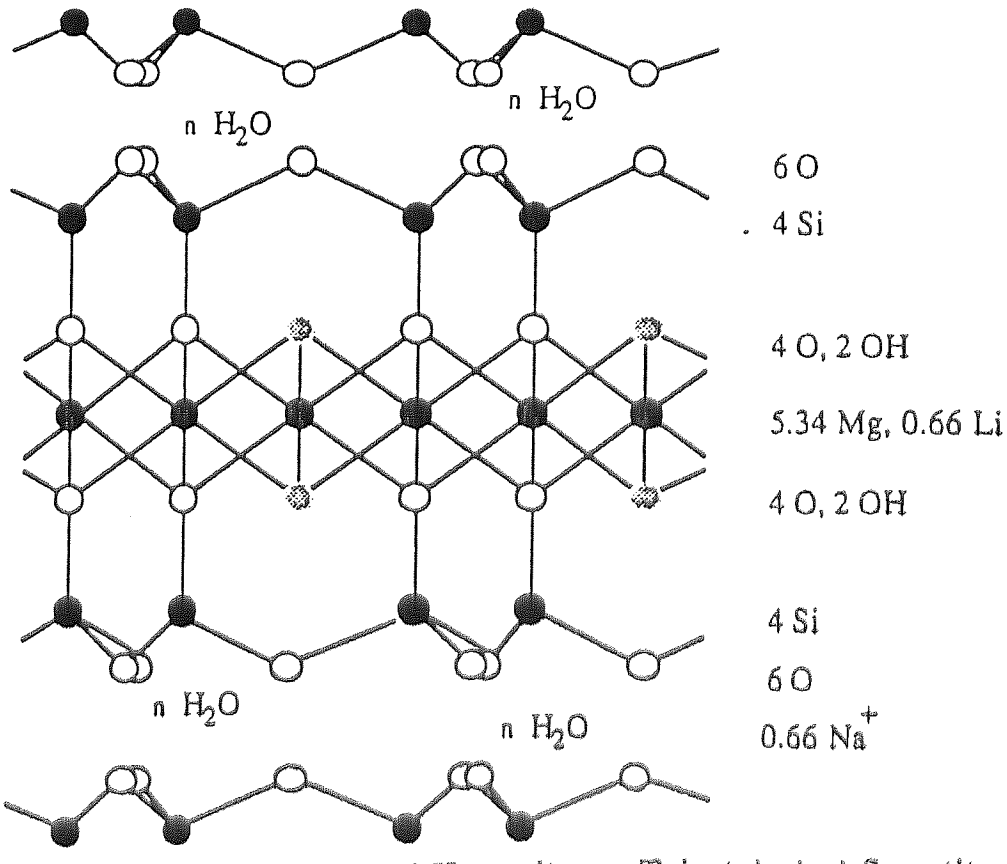

Figure 1.3 The Structure of Hectorite - a Trioctahedral Smectite.

of the cation are important in that the mechanism for hydration is governed by the electrostatic attraction between the polar water molecule and the charge of the interlayer cation.

Li^+ and Na^+ exchange forms are particularly susceptible to hydration [2,15]. Studies of this swelling phenomenon in smectite clays by water has shown that the hydration occurs in a step mechanism. The stepwise water uptake is shown below in Figure 1.4.

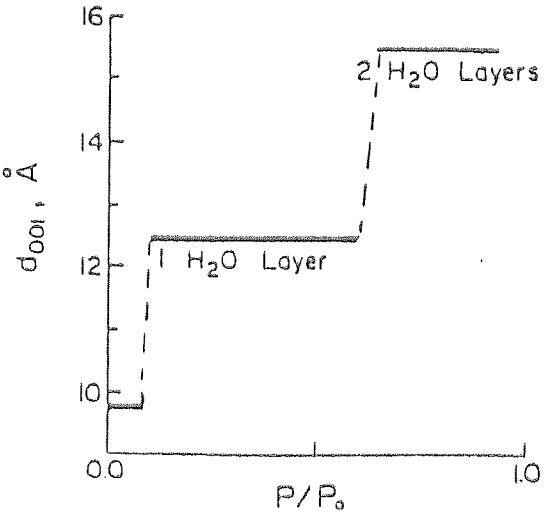

Figure 1.4 Schematic representation of the stepwise uptake of water.

This mechanism was explained by van Olphen in his double layer theory[12]. Up to four layers of water can be absorbed by smectite clays whilst keeping the basic structure intact. Under appropriate conditions (in very dilute aqueous solutions) the silicate layers of Na^+-montmorillonite do in fact disperse completely. The clay is now said to be delaminated. This can lead to gelation which occurs at concentrations of 2% by weight of the clay in water. The cause of gelation is thought to be the result of layer edge-to-face interactions which generate a "house-of-cards" structure[12]. See Figure1.5 below.

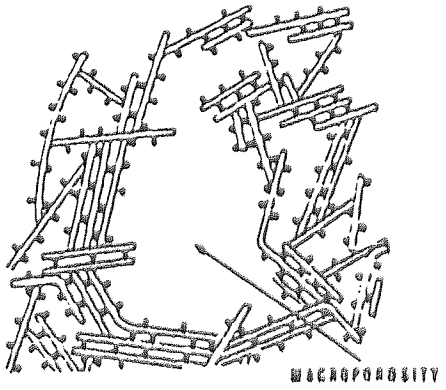

Figure 1.5 "House of cards" structure.

Swelling with other molecules is not as well understood, but several binding mechanisms may operate in the process[4,13]. One important mechanism involves the formation of a complex between the exchangeable cation and the intercalant liquid. An example of this mechanism is seen in the binding of pyridine to Cu^{2+} exchanged forms of smectites.The silicate layers are represented by the horizontal lines in the following illustrations.

$$[Cu(H_2O)_x]^{2+} + \text{pyridine} \xrightarrow{-H_2O} [Cu(py)_4]^{2+}$$

Another possible mechanism is derived from the hydrated interlayer cation behaving as a Brønsted acid[13] and the intercalant functioning as the base. The Brønsted acidity arises from the polarisation and ionisation of water molecules in the interlayer region as illustrated below

$$M(H_2O)_x^{n+} \longrightarrow M(OH)(H_2O)_{x-1}^{(n-1)+} + H^+$$

A study of the uptake of a variety of bases by montmorillonites[14] shows that the uptake is in the sequence ammonia > pyridine > urea.
An example of the mechanism whereby the interlayer cation acts as a Brønsted acid can be seen in the case where ammonia binds as an ammonium ion in Mg^{2+}-montmorillonite.

$$[Mg(H_2O)_x]^{2+} + NH_3 \longrightarrow [Mg(OH)(H_2O)_{x-1}]^+ + NH_4^+$$

Again silicate layers are indicated by horizontal lines.

1.3.2.2 Cation Exchange Capacity (C.E.C.)

The cation exchange capacity of a clay is generally understood to be equal to the layer charge, hence it is considered to be a material constant for each clay material. This value can be measured by various methods well documented in literature[9 - 11]. The layer charge as explained earlier (see section 1.2) is derived from isomorphous substitution and hence incorporation of cations into the interlayer region to balance the charge deficiency. It is these interlayer cations which can be replaced with other cations, usually by treatment with ions in aqueous solution[16]. Common exchangeable cations include Na^+, K^+, H^+, Ca^{2+} and Mg^{2+}.

The C.E.C. is made up of two components[1]. The predominant portion (~80%) is derived from lattice substitution in both the octahedral and to a lesser extent the tetrahedral layers. The remaining 20% is caused by broken bonds around the edges of the clay platelet which produce unsatisfied charges, then balanced by exchangeable cations.

Many factors influence the rate and degree of cationic exchange. For example in smectite clays divalent ions will readily replace monovalent ions. The reverse reaction is not as easily achieved. In cases where ions are of the same valency the important factor is the size of the unhydrated ion. As the ion gets larger so it will more readily replace a smaller ion. Putting these two statements together a series of increasing replacing power is such that

$$Li^+ < Na^+ < K^+ < Mg^{2+} < Ca^{2+}.$$

The concentration of the respective cations is also a factor in any replacement reaction. A dilute solution of the replacing ion will lead to less exchange than if a concentrated solution is used.

Many different ions and complexes can be exchanged into clays, For example tris-bipyridyl metal complexes[17], $[M(bp)_3]^{2+}$, where M = Fe^{2+}, Cu^{2+}, Ru^{2+}, have been shown to replace interlayer sodium ions in hectorite, primarily by an ion exchange reaction and further by intercalation beyond the C.E.C. These complexes have a cage like shape and can open the interlayers up by ~8Å.

Tetra-alkylammonium ions have also been exchanged into lithium and sodium montmorillonites by Mortland and Cementz[18]. Cluster compounds including those of molybdenum containing the $Mo_6Cl_{12}^{n+}$ core[19], and Niobium and Tantalum compounds of the form $M_6Cl_{12}^{n+}$ (where n = 2,3)[20] can be exchanged into smectite clays by the replacement of the interlayer Na^+ ions. Other metals successfully exchanged include Bismuth[21], whereupon interlayer sodium ions

were successfully exchanged by a $[Bi_6(OH)_{16}]^{2+}$ species; Aluminium[22], Nickel[23], Zirconium[24] and Chromium[25].

1.3.2.3 Intercalation

Intercalation is the reversible insertion of a guest molecule or ion into a solid host lattice with the host lattice retaining its major structural features. The host and guest may experience changes in their geometric, optical, electrical and chemical properties.

Compounds such as graphite, MoS_2 and TaS_2 can act as host lattices, but our interest lies in the intercalation of molecules into the interlayer region of clays. Sheet silicate clays possess many features which make them attractive as host molecules. Their ability to incorporate interlamellar water[12] and inorganic/organic species (as neutral molecules or ionised entities)[17-25] is vital to the reaction.

There is an almost infinite number of intercalation compounds which can be produced in order to modify clays and produce the desired properties. Many of the ion exchange reactions described in section 1.3.2.2 can also be classed as intercalation reactions as molecules or ions have been inserted into the interlamellar region. Another form of intercalation reactions are pillaring reactions.

1.3.2.4 Pillaring reactions

In the study of chemically modified clays for use as catalysts, a common problem encountered was that at elevated temperatures (250°C - 300°C) the clay would dehydrate and collapse, therefore destroying the catalytic properties. In order to prevent this collapse it is possible to insert thermally robust molecular pillars which will continue to hold the silicate layers apart at high temperatures.

The first pillared clay was produced using tetra-alkylammonium ions in montmorillonite[26]. Other robust cations have been utilised as pillars in smectite clay chemistry. These include bicyclic amine cations[27] and tris metal chelates[17,28]. These three classes of compounds (Figure 1.6) are not thermally stable and tend to decompose between 250°C and 500°C[29].

A class of pillared clays based on polynuclear hydroxyl metal cations (Figure 1.6) have been prepared which are stable above 500°C.

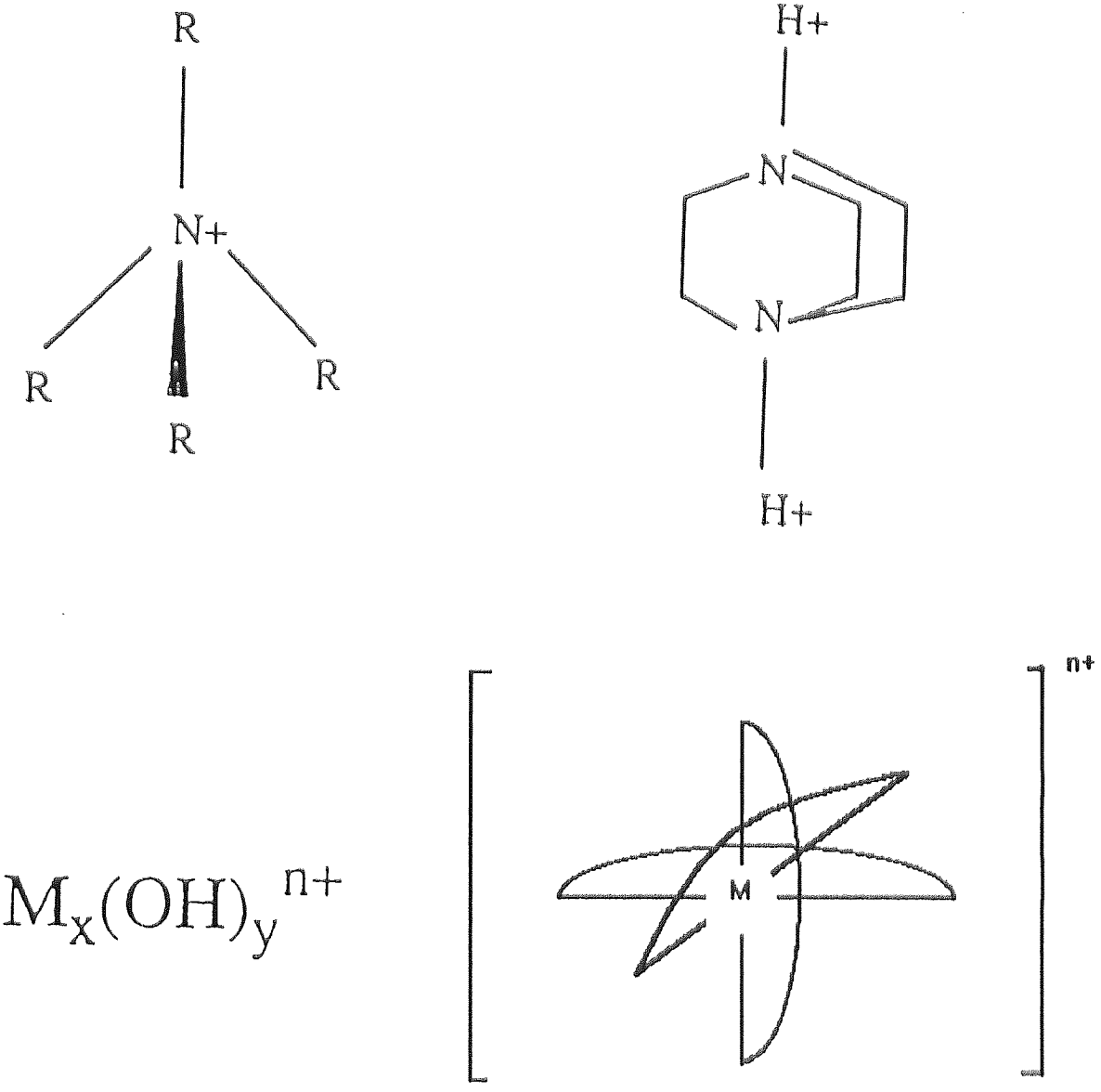

FIGURE 1.6
Various ions used as molecular props / pillaring agents in smectite clays. These include (clockwise from the top) the alkylammonium ion, a bicyclic amine cation, a tris metal chelate (e.g. M = Fe^{2+}, chel = 1,10-phenanthroline or a polynuclear hydroxy metal ion (e.g. $Al_{13}O_4(OH)_{28}^{3+}$).

Clays have been produced using a variety of metals including polycationic species of aluminium[30,31]. These hydroxy-aluminium pillared clays (Figure 1.7) have been found to be stable up to ~700°C, whereupon they sintered and the clay progressively decomposed at temperatures greater than 750°C[32].

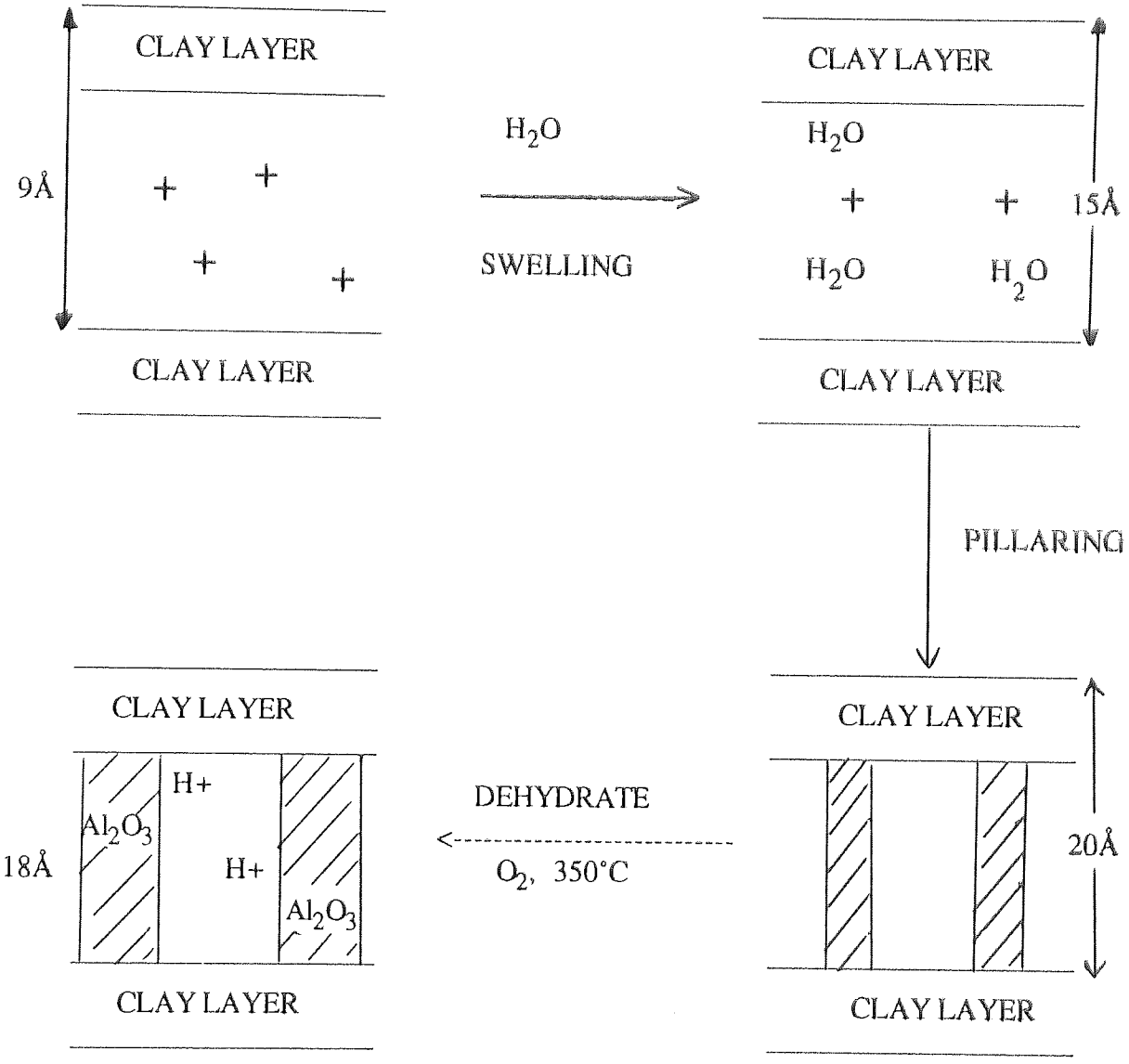

FIGURE 1.7 Diagram to show the process for forming a pillared clay

Titanium polyoxycations also produce pillared clays stable up to ~700°C. Nickel[23], Zirconium[24], Vanadium[36], Silicon[37,38], Magnesium[39], Tin[40], Iron[41] and Niobium[46] clays have all been produced and are all thermally stable to at least 500°C.

Using various pillaring agents it is possible to synthesise pillared clays (Figure 1.8) with pore sizes varying between 2Å and 25Å. This property resulted in the renewed interest in pillared clays because their pore sizes can now be made larger than that of the zeolites (2Å - 8Å), the class of compounds previously favoured as catalysts in hydrocarbon cracking. By varying the size of the pillars or the spacing between the pillars, or both, the pore size can be adjusted to suit a specific application.

In the oil industry pillared clay catalysts, for example Al_{13}- and Zr_4- montmorillonites are utilised as petroleum cracking catalysts. These catalysts give gasoline octane ratings on a par with zeolite catalysts but also have the added advantage of giving higher yields of light-cycle oils such as diesel. Iron-doped pillared laponite is used to catalyse the conversion of syngas into light alkenes[43].

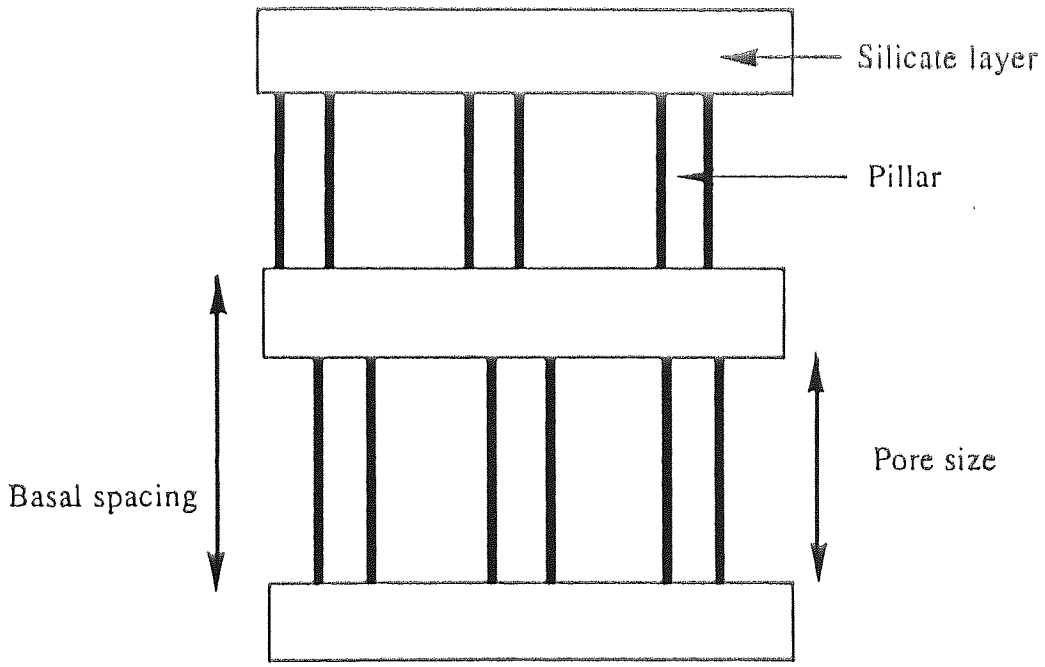

FIGURE 1.8 Schematic representation of a pillared clay.

Relatively little is certain as to the constitution and structure of the clays pillared by polyoxo cations. One possibility is that the cations undergo dehydroxylation at high temperatures to form oxide aggregates which are stable on the interlayer surfaces[44]. Another possible mechanism involves the crosslinking of the pillar to the silicate layers[30].

It is known that smectite clay layers can adopt an ordered lamellar arrangement (Figure 1.9a) or a delaminated ("house-of-cards") structure *via* edge-to-face interactions (Figure 1.9b).

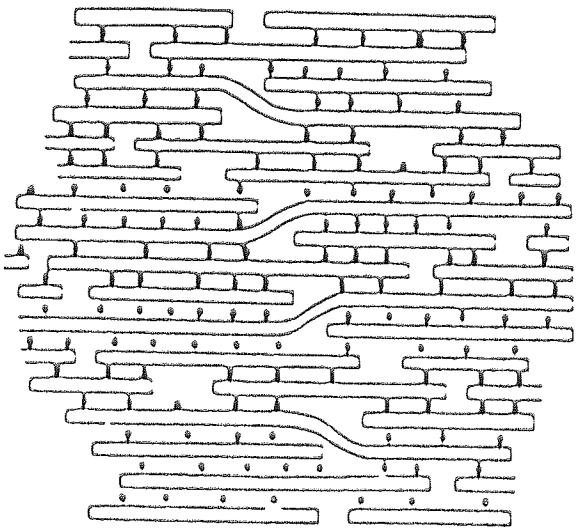

FIGURE 1.9a
Regular ordered clay

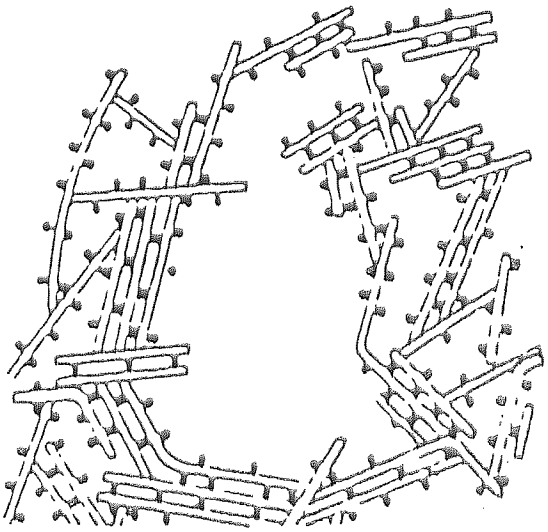

FIGURE 1.9b
Delaminated clay

The question then arises as to whether pillared clays are in part delaminated. If layer delamination accompanies pillaring then the degree of delamination may be as important a factor in determining the pore size as the actual pillaring is.

Recent work has been carried out to extend the pillaring reaction further and produce mixed oxide pillars, again the hope is a greater thermal stability. Gonzalez et al [45,46] prepared mixed Aluminium and Gallium pillared montmorillonite, thermally stable up to 700°C. Sterte[47] has prepared large pore montmorillonite using mixed Lanthanum and Aluminium pillars. This particular clay was reported to have a basal spacing of up to 26Å, as compared to the standard value of 19Å obtained for a conventional Aluminium pillared montmorillonite. Mixed Aluminium and Cerium pillared clays stable above 760°C with basal spacings of between 25Å and 28Å have also been documented[47].

Limitless possibilities exist in the field of mixed oxide clays, much of which remains to be explored, in order to produce clays with large pore sizes and increased thermal stability.

1.4 Uses of Smectite Clays

In terms of annual tonnage used, the major use of smectite clays is in foundry moulding sands. Sand, clay and water are mixed together such that the sand can be moulded around a pattern. The clay is required to give the sand enough strength to keep the mould shape once the pattern is removed and the hot metal is poured in.

Smectite clays used in drilling muds[48] utilises over 2 million tonnes of clay per year. The clay is used to thicken the mud, lubricate and cool the drill heads and protect against corrosion. An added advantage is that they are reuseable.

Large amounts of smectite clays are also used to clarify water, wine, beer, vinegar and fruit juices; to filter and decolourise vegetable oils; and as pet litter and absorbant materials.
Small scale uses include radioactive waste disposal, in paints[48], inks, greases[48], cosmetics, catalysts[49], chromatography[50] and paper coating.

More uses are currently being researched for many specialist applications. The research contained within this thesis hopes to improve the current smectite clay used in the paper industry.

1.4.1 Clay use in the Paper Industry

The first stage of paper manufacture is to transform the wood into pulp. There are three ways of achieving this aim, the method being dependent on the quality of the final paper product required. The cheapest method is to produce mechanical pulp, where basically the whole tree (minus the bark) is ground up therefore giving very little waste. Paper produced by this method is cheap, weak and discolours rapidly in sunlight. A slightly better paper is produced *via* thermomechanical pulp. This is basically mechanical pulp but heat is added which softens lignin 'glue' holding the cellulose fibres together. This paper is slightly stronger but still readily discolours. Paper of these qualities tends to be used in newspaper and paperback book production. The third type of pulp is chemical pulp which uses a process called the 'Kraft' process, involving alkali and sulphate. This is a much more time consuming and expensive process but produces much stronger paper as the fibres are intact rather than cut into pieces (as in the case of the former two methods). The pulp after the Kraft process is dark brown in colour and this unwanted characteristic is removed by bleaching. When the pulp has been produced it must then be turned into paper. Clay can be added at the pulp stage where it acts as a filling agent. This is a cheap alternative to fibre. The clay also has an advantage in that it makes the paper smoother and more opaque, and being white in colour it will enhance the

appearance of the paper. A clay from the Kaolin group of clays called Kaolinite [51] has been used for this purpose for many years. Other additives may be added at this stage including titanium dioxide, dyes, fluorescent whiteners and internal sizing agents. The pulp is then made into paper *via* rollers, presses, drying cylinders and the paper is finally collected on a large reel.

Clays are also employed as surface coating agents. Gloss, opacity, smoothness and brightness are all increased with an increasing coat weight of kaolinite. The coating can be done by a method called blade cutting (Figure 1.10a)

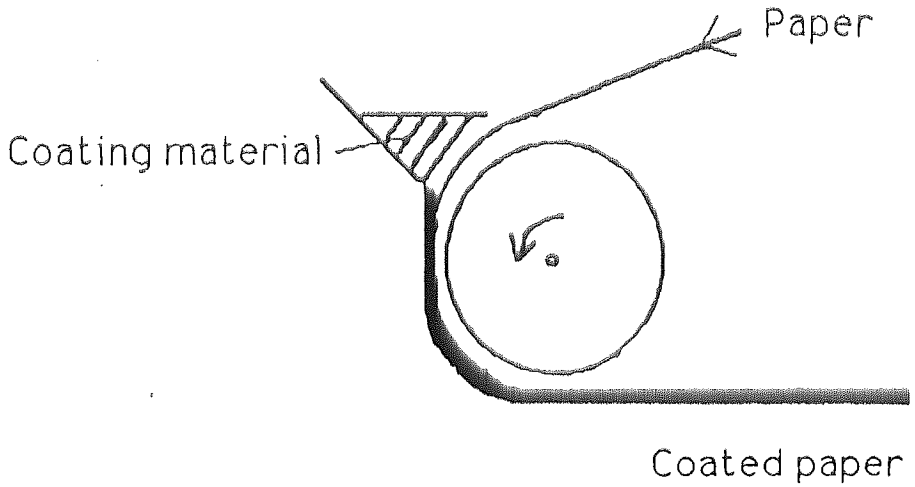

FIGURE 1.10a Schematic representation of the process of blade cutting.

Another slightly different method is seen in Figure 1.10b below. The method is dependent on the orientation of the paper feed.

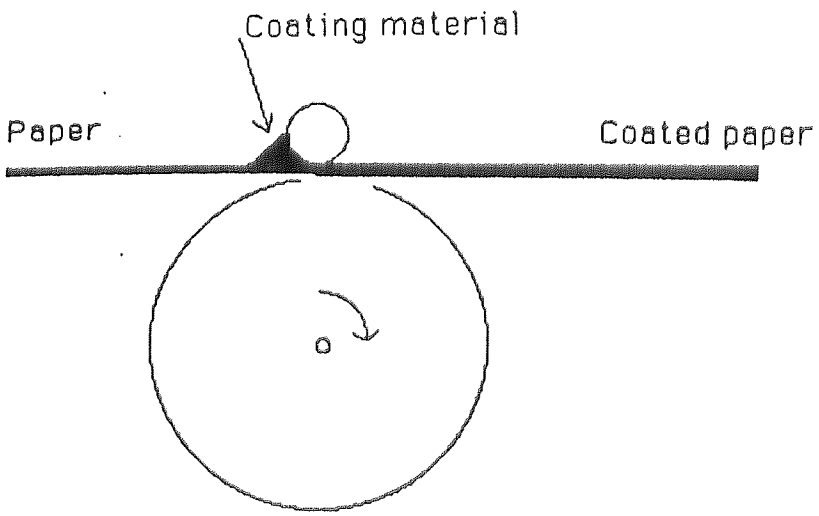

FIGURE 1.10b Schematic diagram of paper coating with clay

These two methods are used on 'dry' paper.

Another alternative is to coat the paper with clay during the paper making process, before it is dried. This can be done by incorporating a piece of equipment called a 'size bath' into the machinery.

Smectite clays are good surface coating agents because of their relatively small crystal size and good film forming properties.

1.4.2 The Use of Clays in Electrographic Paper

Electrographic printers require specialised dielectric paper. This paper is made up of a base paper with a conductive surface coating on each side and a dielectric film on one side only (Figure 1.11). Smectite clays can be used for the conductive surface coating. A highly resistive polymer such as polystyrene or polyvinyl acetate is required for the dielectric component.

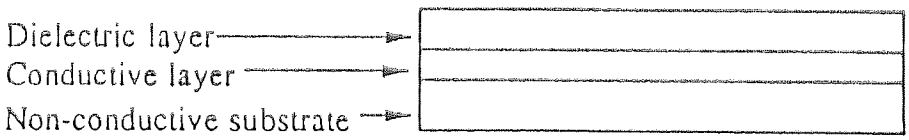

FIGURE 1.11 Schematic representation of Electrographic Paper.

Electrographic printers operate *via* a non-impact printing method often used in automated drawing offices and computer aided design.

Finished dielectric paper works in the following manner: an electrostatic charge is deposited onto a dielectric surface using an electrode system (Figure 1.12). The electrostatic image is made visible by applying a toner which adheres to the charged areas and hence produces the image. The toner becomes fixed to the paper by either pressure, heat or solvent evaporation.
In order to form an electrostatic charge pattern there must be ionic conduction through the air. If two conductors are held very closely together a discharge without a spark is obtained. If then a dielectric material is placed between the conductors, the charge will collect on the dielectric surface. In dielectric printers, the conductors are in the form of stylii and a grounded backing electrode. If a voltage is applied to a stylus a dot of charge is deposited onto the paper. By application of charge to several stylii at one time and by the movement of the paper, characters or images are produced on the paper.

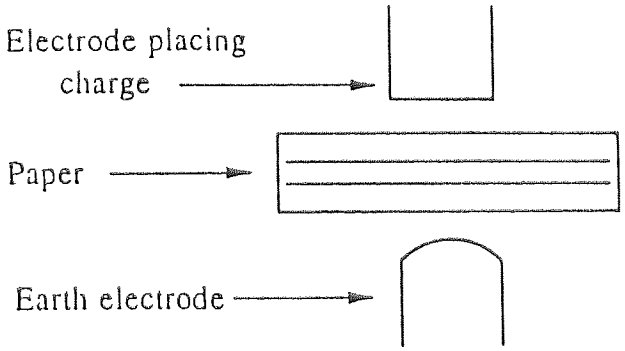

Front grounded electrode system.
The paper must have good conductivity on the top side in order to work effectively.

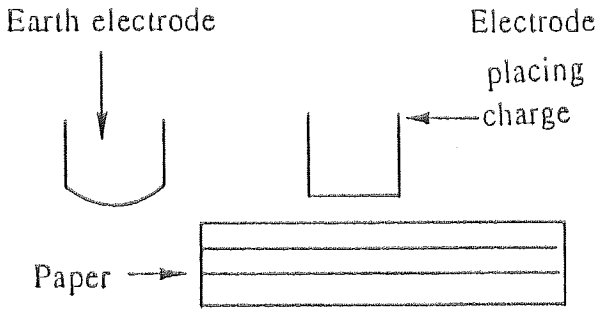

Reverse grounded electrode system.
Paper must have good conductivity on both sides and on the inside.

FIGURE 1.12 Possible electrode systems found in Electrographic Printers.

Producers of electrographic papers include James River Graphics, based at Chartham Paper Mill, the sponsors of this research project. James River Graphics are currently the second largest paper manufacturer in the world. They produce pulp, paper, tracing papers as well as the specialised conductive products.

The mill at Chartham was constructed in 1738 to produce all grades of paper. Until 1939 it continued to be a one machine paper mill making a variety of papers - though mostly high grade writing paper. In 1939 the mill began production of tracing paper in order to break the monopoly the Germans had on the market. The mill now has three machines manufacturing speciality, high quality opaque and tracing papers. It also supplies the conductivised base paper which is transported to the U.S.A. to be dielectrically coated.

1.5 Objectives.

Smectite clays are used in the paper industry as conductive surface coatings on electrographic papers. Market forces demand that this commodity is available cheaply, yet at very high quality. The clay particularly favoured for this use is a synthetic hectorite, laponite[52]. The one

drawback with laponite is a purely economic one; because it is a synthetic clay it costs approximately ten times more to use than would a natural smectite. In the final calculations laponite accounts for 11% of the total cost of the electrographic paper.

If the conductivity of laponite could be increased by chemical modification it would result in less clay being applied to the paper in order to achieve the required conductivity. As well as bringing down the cost of the paper, this action of diluting the clay solution also has the advantage of reducing the probability of the clay forming a gel (see section 1.3.2.1). Laponite has a very small crystal size which is conducive to gel formation. This gel formation if it occurs during the coating of the paper leads to problems in obtaining an even coating.

Another possibility in order to reduce production costs may be to use a different clay with which to coat the paper. If it were possible to significantly increase the conductivity of a natural clay it may lead to a possible solution although to date natural clays do not give papers with a satisfactory appearance and feel.

A final possibility may be to produce new synthetic clays of higher conductivity than laponite and hence coat the paper with a completely new material.

CHAPTER TWO

Physical Methods / Chemical Techniques

CHAPTER TWO
PHYSICAL MEASUREMENTS / CHEMICAL TECHNIQUES.

2.1 Chemicals and Solvents.

The majority of chemicals were obtained from either the Aldrich Chemical Company, British Drug Houses (BDH) or Fluka Chemicals. Laponite RD was obtained from Laporte Industries. Silver epoxy resin and hardner kits were supplied by RS Components. Common solvents were supplied by the Chemistry Department and were dried where necessary and stored over molecular sieves. Analytically pure solvents were used without further purification.

2.2 Atomic Absorption Spectroscopy.

Atomic Absorption measurements were carried out on a Perkin Elmer 360 instrument. Sodium nitrate atomic absorption standard was used for sodium analysis.

2.3 Elemental Analysis.

Micro-elemental analysis for carbon, hydrogen, nitrogen and chlorine were carried out by Medac Ltd, Department of Chemistry, Brunel University.

2.4 Fourier Transform Infra-red Spectroscopy.

Infra-red spectra were recorded on a Perkin Elmer FTIR 1710 spectrophotometer equipped with a D.6300 data station. Either KBr discs or NaCl plates were employed for analysis.

2.5 Gas-Liquid Chromatography.

A Pye Unicam GCD Chromatograph was used for Gas-Liquid Chromatographic analysis.

2.6 Mass Spectroscopy.

Fast Atom Bombardment mass spectra of some compounds were recorded *via* the SERC mass spectroscopy service, University College, Swansea.

2.7 Melting Points.

A Gallenkamp electrically heated melting point apparatus with a mercury thermometer was used to determine all melting points.

2.8 Mossbauer Spectroscopy.

Initial Mossbauer results were obtained at Birmingham University working with Professor F.J. Berry. Subsequent Mossbauer spectra were provided by Professor F.J.Berry, Open University, Milton Keynes.

^{119}Sn Mossbauer spectra were recorded at 77K with a microprocessor controlled Mossbauer spectrometer using a calcium stannate ($Ca^{119m}SnO_3$) source. The drive velocity was calibrated with a natural iron foil absorber. All spectra were computer fitted.

2.9 Nuclear Magnetic Resonance Spectroscopy (NMR).

^{13}C solution spectra were recorded within the Chemistry Department using a Bruker AC-300 MHz instrument. Tetramethylsilane was used as the internal reference.
Solid samples were analysed on the same instrument with a solid state probe. Samples were spun at the magic angle at approximately 5 kHz. Solid state ^{13}C spectra were measured at a frequency of 75.469 MHz.

2.10 Scanning Electron Microscopy (SEM).

A Cambridge instruments Company Sterioscan S90B machine was used for analysis.

2.11 Solid Disc Conductivities.

Full details will be described in chapter 5.

2.12 X-Ray Photoelectron Spectroscopy.

Spectra were recorded on a VG scientific ESCALAB 200-D instrument using MgK (1254eV) radiation. Ph_3SnCl and SnO_2 were used as standard tin compounds. Deconvolution techniques were employed for the $Sn(3d_{5/2})$ spectra. When a satisfactory fit was found the analysis was halted. Tellurium, Antimony and Bismuth spectra of some compounds were examined in the same manner using suitable standards. The standards used for the tellurium analysis were $(p\text{-}CH_3OPh)_2TeCl_2$ and $(p\text{-}CH_3OPh)_2O$, Ph_3Sb was the selected standard for the organoantimony compounds and Ph_3Bi for the organobismuth compounds.

2.13 X-Ray Diffraction (XRD).

Diffraction patterns were obtained from the Department of Geology, Keele University courtesy of Dr Rowbotham..

2.14 X-Ray Fluorescence Spectroscopy (XRF).

Spectra were obtained from the Department of Geology, Keele University courtesy of Dr Rowbotham.

CHAPTER THREE

The Intercalation of laponite RD with Organotin compounds

CHAPTER THREE

The Intercalation of Organotin Compounds into laponite RD

3.1 Introduction

Having established that organometallic molecules can be intercalated into smectite clays[17-26] the effect on the conductivity of such materials was investigated. McWhinnie et al[53] intercalated tetrathiafulvalene (TTF) into sodium montmorillonite, laponite and also clays exchanged with transition metals. TTF was initially chosen as an intercalation agent as it was thought that a charge transfer reaction would occur between the organic molecule and the Fe^{3+} ions in the dioctahedral smectite. This charge transfer was found to occur. The increase in conductivity however was not unique to this system and also occurred in clays containing no structural Fe^{3+} ions. This suggested that the charge transfer is incidental to the increase in conductivity. It was concluded that the intercalation of the large molecule was causing the increased conductivity. The conductivity of the resulting clays were increased by approximately an order of magnitude. Having shown that conductivity can indeed be increased by chemical modification[53], and knowing that clay minerals can intercalate a wide variety of guest molecules[17-26], work began by Bond[54] to gain an increase in the conductivity of laponite for eventual use in the paper industry.

Aryl tin(IV) compounds were the initial choice of precursors for a number of reasons. Firstly they are white in colour and therefore should not affect the colour of the resulting clay. Secondly they are readily available commercially and finally the chemistry of aryl tin(IV) compounds is well documented[55-57].

Another attractive feature was the availability of both ^{119}Sn Mossbauer and Nuclear Magnetic Resonance (N.M.R.) spectroscopies to investigate the nature of the resulting clays. On intercalation by mechanical shaking (see section 3.4.2) and by microwave heating (section 3.4.3) of Ph_3SnCl, Ph_2SnCl_2 and $(Ph_3Sn)_2O$ Bond discovered that 'tin oxide' pillars were forming in the clay interlayers leading to an increase in basal spacing of up to 8Å (from ~14Å to ~21.5Å). It was proposed that hydrolysis of the organotin compound occurred on the clay surface followed by aryl-tin bond breakage *via* proton attack thus leading to the formation of the pillars. The other product produced was benzene and was found to be trapped within the clay lattice (^{13}C MASNMR indicated a peak characteristic of benzene and GLC failed to detect any benzene in the filtrate). The major difference between these clays and the more traditional pillared and intercalated clays is that the interlayer cations are not sacrificed in the course of the reaction. This point is particularly significant in the consideration of the conductivity (to be discussed fully in chapter 5).

3.2 Objectives.

Bond[54] demonstrated that oxide pillars are formed in reactions of laponite with Ph_3SnCl, Ph_2SnCl_2 and $(Ph_3Sn)_2O$ precursors. The conductivity of the clay was found to increase between two and ten times (full details in chapter 5) depending on the precursor, the concentration of the precursor and the method of intercalation. It was decided to continue the organotin investigation using different precursors. A method using an alkyl tin compound was carried out using a commercially obtained compound. Other aryl tin compounds were also considered. Due to the toxic nature of the benzene obtained using the phenyl tin compounds it was preferable to synthesise a precursor which may yield a less harmful other product. The proposed mechanism of pillaring involves electrophilic attack at the tin-carbon bond in the precursor. Presumably using a more 'electron-donating' group would encourage electrophilic attack to occur and consequently the degree of pillaring and hence the conductivity would increase. The choice of ligand was the *p* -methoxyphenyl entity. The methoxy and ethoxy groups possess the property necessary to transfer electrons into the benzene ring in order to facilitate electrophilic attack, yet they are thought to be at a distance far enough from the tin-carbon bond not to cause steric interference.

3.3 Synthesis and characterisation of tetra-*p*-methoxyphenyltin(IV).

A Grignard route of preparation was carried out in which a two stage synthetic route yielded the final product.

$$p\text{-}CH_3OC_6H_4Br + Mg \text{ ----------> } p\text{-}CH_3OC_6H_4MgBr \quad (1)$$

$$4\,p\text{-}CH_3OC_6H_4MgBr + SnCl_4 \text{ ----------> } (p\text{-}CH_3OC_6H_4)_4Sn \quad (2)$$

After several attempts using an ether solvent and a typical 3-4 hours reaction time it was discovered *via* elemental analysis, infra-red spectroscopy and mass spectroscopy that intermediate products were being formed. The synthetic route which achieved the required product was as detailed below.

Freshly degreased magnesium turnings (2.7g) were placed in a 250 cm^3 3-necked round-bottomed flask and covered with HPLC grade tetrahydrofuran(THF). 4-Bromoanisole (14 cm^3) in THF (25 cm^3) were placed in a dropping funnel connected to the round bottomed flask. Nitrogen gas was passed through the system for 20 minutes (to de-aereate the solution) *via* an inlet tube which reached below the surface of the solvent in the reaction vessel. The N_2 gas was then switched off and a crystal of iodine added to the reaction vessel. The hotplate

was set on 20°C and a few drops of the bromoanisole solution added. A heat gun was also required to initiate the reaction. Once the reaction had started the heat sources were removed and the reagent was added at a rate sufficient to keep the reaction going. When the self-sustaining reflux had ended, heat from the hotplate was required and the reaction was refluxed for three hours. The flask contents were cooled to room temperature. Tin tetrachloride (3 cm^3) in dry benzene (50 cm^3) was added with caution over a period of 30 minutes. The contents of the flask were refluxed for ~15 hours. The flask was cooled and the contents poured into a saturated solution of ammonium chloride (150 cm^3). The layers were separated and the organic layer yielded a cream coloured solid. Recrystallisation from xylene yielded a white crystalline solid.

Yield = 3.85g (25.6%). Melting Point = 132-133°C [literature[60,61] = 134.8°C]
Elemental analysis found: C = 62.1%, H = 5.17% [required C = 61.5%, H = 5.17%]

A Fast Atom Bombardment (F.A.B.) Mass Spectrum (see Figure 3.1) revealed characteristic isotope patterns for tin. The required fragments were seen and are presented in table 3.1 below (based on ^{120}Sn, ^{1}H, ^{12}C and ^{16}O).

Fragment	Theory	Found
$(p\text{-}CH_3OC_6H_4)_4Sn^+$	547	547
$(p\text{-}CH_3OC_6H_4)_3Sn^+$	441	441
$(p\text{-}CH_3OC_6H_4)Sn^+$	227	227

Table 3.1 F.A.B. fragment patterns for $(p\text{-}CH_3OC_6H_4)_4Sn$.

There is no fragment corresponding to the $(MeOPh)_2Sn^+$ entity (m/e 333). The following equation may explain the lack of signal at this mass/charge ratio.

$$(p\text{-}CH_3OC_6H_4)_3Sn^+ \xrightarrow{-R_2} (p\text{-}CH_3OC_6H_4)Sn^+$$

A fragment at m/e = 214 can be clearly seen in the spectrum, corresponding to the

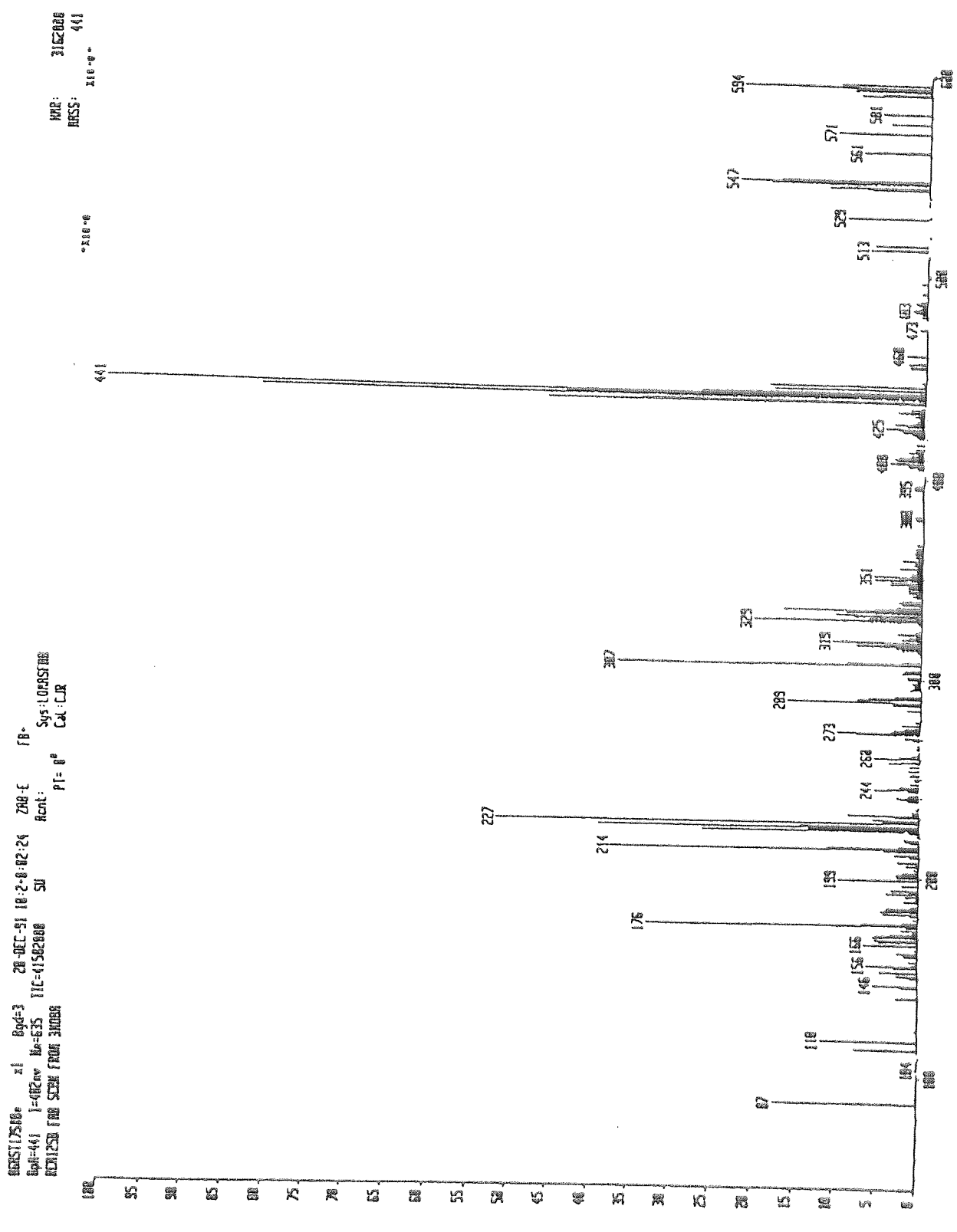

Figure 3.1 F.A.B. Mass Spectrum of $(MeOPh)_4Sn$.

R_2^+ ($H_3COC_6H_4C_6H_4OCH_3$) fragment.

The FTIR spectrum of the (*p*-methoxyphenyl)tin(IV)(Figure 3.2) was consistent with expectations for this compound.

The analogous compound $(p\text{-}H_5C_2OC_6H_4)_4Sn$ was synthesised by the same route.
4-Bromophenetole was the starting reagent in this case. A white crystalline material was obtained in a much lower yield (0.6g). The melting point of the compound was 165°C. [literature[62] = 162-164°C].
Elemental analysis found C = 63.7%, H = 6.08%. [required C = 63.7%, H = 6.01%].

Analysis by F.A.B. Mass spectroscopy produced the spectrum (Figure 3.3) and the following fragments, based on ^{120}Sn, ^{12}C, ^{1}H and ^{16}O, are shown in Table 3.2 below.

Fragment	Theory	Found
$(p\text{-}C_2H_5OC_6H_4)_4Sn^+$	603	603
$(p\text{-}C_2H_5OC_6H_4)_3Sn^+$	483	483
$(p\text{-}C_2H_5OC_6H_4)_2Sn^+$	362	362 (weak)
$(p\text{-}C_2H_5OC_6H_4)Sn^+$	241	241

Table 3.2 F.A.B. Fragment patterns for $(p\text{-}C_2H_5OC_6H_4)_4Sn$

Other noticeable fragments occur at m/e 213 and 333. Possible explanations are shown below:-

$$(p\text{-}C_2H_5OC_6H_4)Sn^+ \xrightarrow{-C_2H_4} HOC_6H_4Sn^+ \quad (m/e = 213)$$

$$(p\text{-}C_2H_5OC_6H_4)_2Sn^+ \xrightarrow{-C_2H_4} (p\text{-}C_2H_5OC_6H_4)SnC_6H_4OH \quad (m/e = 333)$$

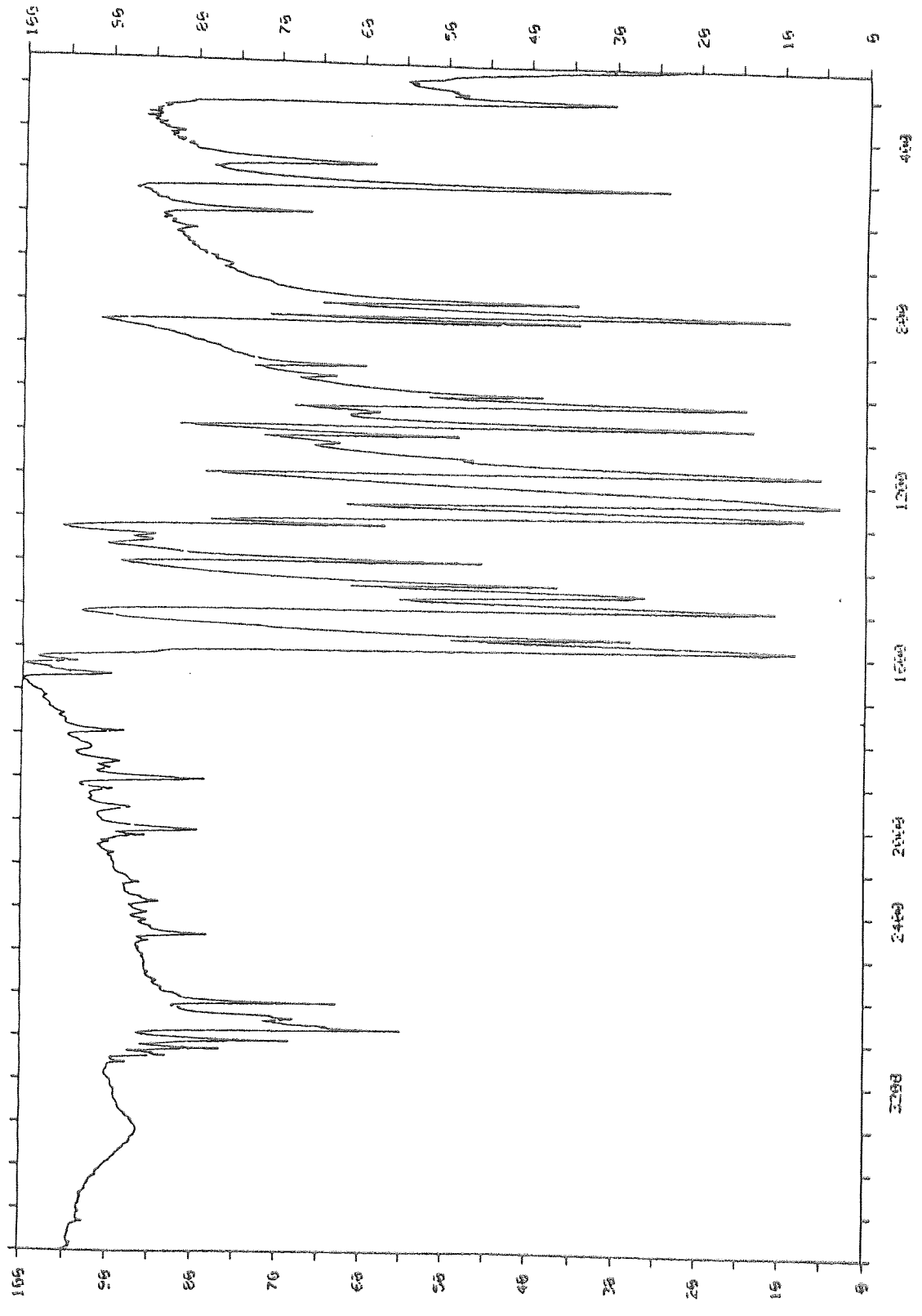

Figure 3.2 F.T.I.R Spectrum of $(MeOPh)_4Sn$.

Figure 3.3 F.A.B. Mass Spectrum of $(EtOPh)_4Sn$.

Both cases are possible as the molecule being lost, ethene, exists as a stable compound.

The FTIR spectrum of the compound (see Figure 3.4) was consistent with expectations.

3.4 Intercalation of Organotin Compounds.

Three methods were utilised for the intercalation of the compounds. The first method used was that of Petridis *et al* [58], described in section 3.4.1. The precursor was dimethyltin(IV) dichloride and the solvent was deionised water. The second and third methods were those developed by Bond[54], these involved mechanical shaking at ambient temperature and microwave heating respectively. In both cases organic solvents were used.

3.4.1 Pillaring by dimethyltin(IV) cationic complexes[58].

Laponite RD (1g) was dispersed in deionised water (50 cm^3). A solution of dimethyltin(IV) dichloride[$(CH_3)_2SnCl_2$] (40mM, 30 cm^3) - with the pH adjusted to between 5.2 and 5.3 with 1M $NaOH_{(aq)}$ - was added to the clay with constant stirring. Flocculation occurred. The mixture was allowed to stand for 30 minutes whereupon the supernatant liquid was removed *via* a pipette and discarded. The solid was centrifuged and washed twice with 50 cm^3 aliquots of deionised water. The above intercalation process was repeated twice. Thereafter the solid was centrifuged and washed with deionised water until the supernatant was free of chloride ions (the silver nitrate test[59] was used). The intercalated clay was dried first at room temperature and then at 50°C. Samples were then calcined at 240°C in the presence of glycerol.

This process produces Tin (IV) oxide pillars but the interlayer cations (Na^+) are sacrificed.

3.4.2. Mechanical Shaker at Ambient Temperatures.

Organotin (1g) was dissolved in dry absolute ethanol (100 cm^3) in a 250 cm^3 quick-fit conical flask. Laponite RD (5g) was added to the solution. The flask was placed on a Gallenkamp mechanical shaker for 1 week, whereupon the clay was gravity filtered and washed with four, 25 cm^3 aliquots of dry absolute ethanol. The filtrate plus washings were analysed by Atomic Absorption Spectroscopy (AA), in some cases by Gas-Liquid Chromatography (GLC) and then evaporated to enable the unreacted organotin compound to be dried and weighed. The uptake of the organotin compound can be expressed in a percentage form as in Table 3.3

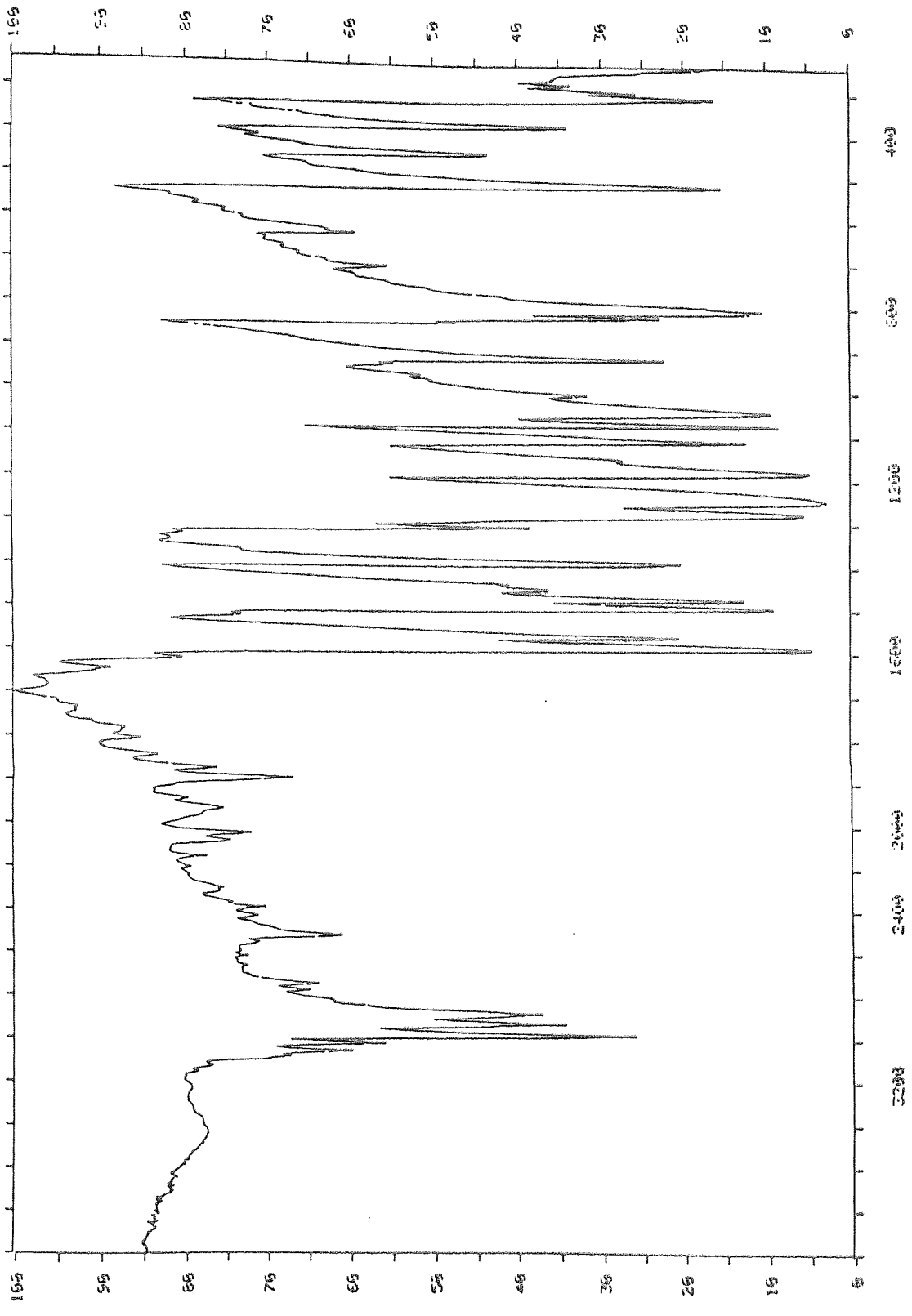

Figure 3.4 F.T.I.R Spectrum of $(EtOPh)_4Sn$.

below.

Precursor	% uptake
Ph_3SnCl	41
Ph_2SnCl_2	33
$(Ph_3Sn)_2O$	8
$(CH_3OC_6H_4)_4Sn$	6
$(C_2H_5OC_6H_4)_4Sn$	5

Table 3.3 Percentage Uptake of Organotin Compounds by Shaking.

3.4.3. Microwave Heating.

Reports in the literature demonstrate that the use of microwave heating can greatly increase reaction rates. Gedye et al [63] found that organic compounds could be synthesised up to 1240 times faster in sealed Teflon vessels in a microwave oven than by conventional techniques. Mingos[63a] showed that although the rate is influenced by the increased pressure within the sealed vessel, this is not the most important factor. Mingos showed this by carrying out microwave reactions in open containers and still achieved a significant increase in the reaction rate. It was found that polar compounds absorb significant amounts of microwave energy. This results in polar compounds with boiling points of < 100°C generally reaching their boiling points within 1 minute[63]. Further work[64] has established that organic solvents in a microwave cavity superheat (see Figure 3.5) by 13-26°C above their conventional boiling points. Layered inorganic materials have also been shown to intercalate greater quantities of guest materials, and at a faster rate when the reaction was carried out in a microwave oven[65]. Bond's results[54] agree with this and show an increased uptake of organotin compounds of between 6% (Ph_2SnCl_2 precursor) and 30% (Ph_3SnCl).

The organotin precursor (0.2g) was dissolved in dry absolute ethanol (10 cm^3). Laponite RD (1g) was added to this solution and sealed in a 120 cm^3 Teflon container with a screw top. The container was placed in a Sharp Carousel 650W domestic microwave oven. The mixture was

subjected to five one minute bursts of microwave radiation on a medium-high setting. The container contents were agitated after each one minute burst of radiation to prevent a pressure build up. The container was then allowed to cool to room temperature before being carefully opened. The clay was gravity filtered and then washed with four 25 cm^3 aliquots of solvent. The combined filtrate and washings were analysed by AA spectroscopy, GLC, and then the liquid was evaporated to leave the unreacted organotin compound which was dried and weighed. Again uptake is expressed in a percentage form in Table 3.4 below.

Organotin pecursor	% uptake
Ph_3SnCl	62
Ph_2SnCl_2	40
$(Ph_3Sn)_2O$	19
$(H_3COC_6H_4)_4Sn$	15
$(H_5C_2OC_6H_4)_4Sn$	12

Table 3.4 Uptake of Organotin Precursors by Microwave Heating.

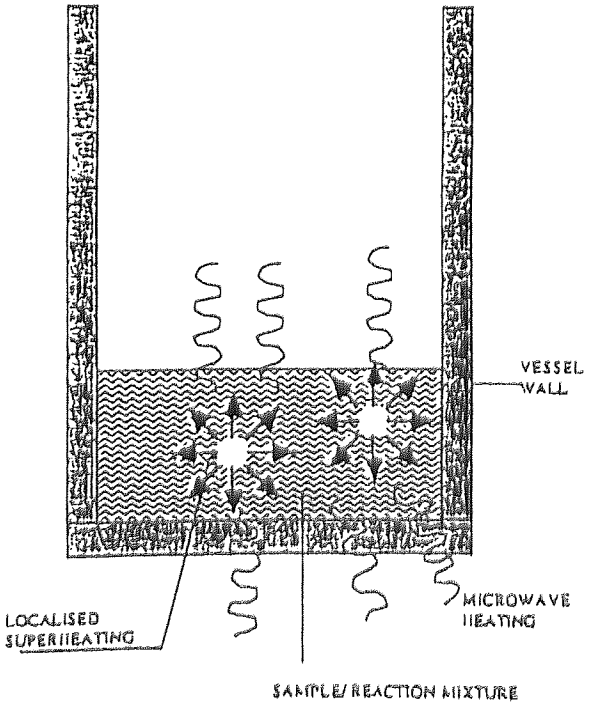

Figure 3.5 Schematic view of Microwave Heating

3.5 Characterisation of the Modified Clays.

Four physical techniques were utilised.

3.5.1 ^{119}Sn Mossbauer Spectroscopy.

^{119}Sn Mossbauer spectroscopy has proved to be a powerful analytical tool.

An absorption at $\delta = 0$ mms^{-1}, using SnO_2[66] as a standard, was seen in the spectra of the intercalation product from the reaction between laponite RD and Ph_3SnCl (see Figure 3.6). This suggests that these tin atoms exist in an "SnO_6" environment. This result was seen with both the shaker and microwave experiments.

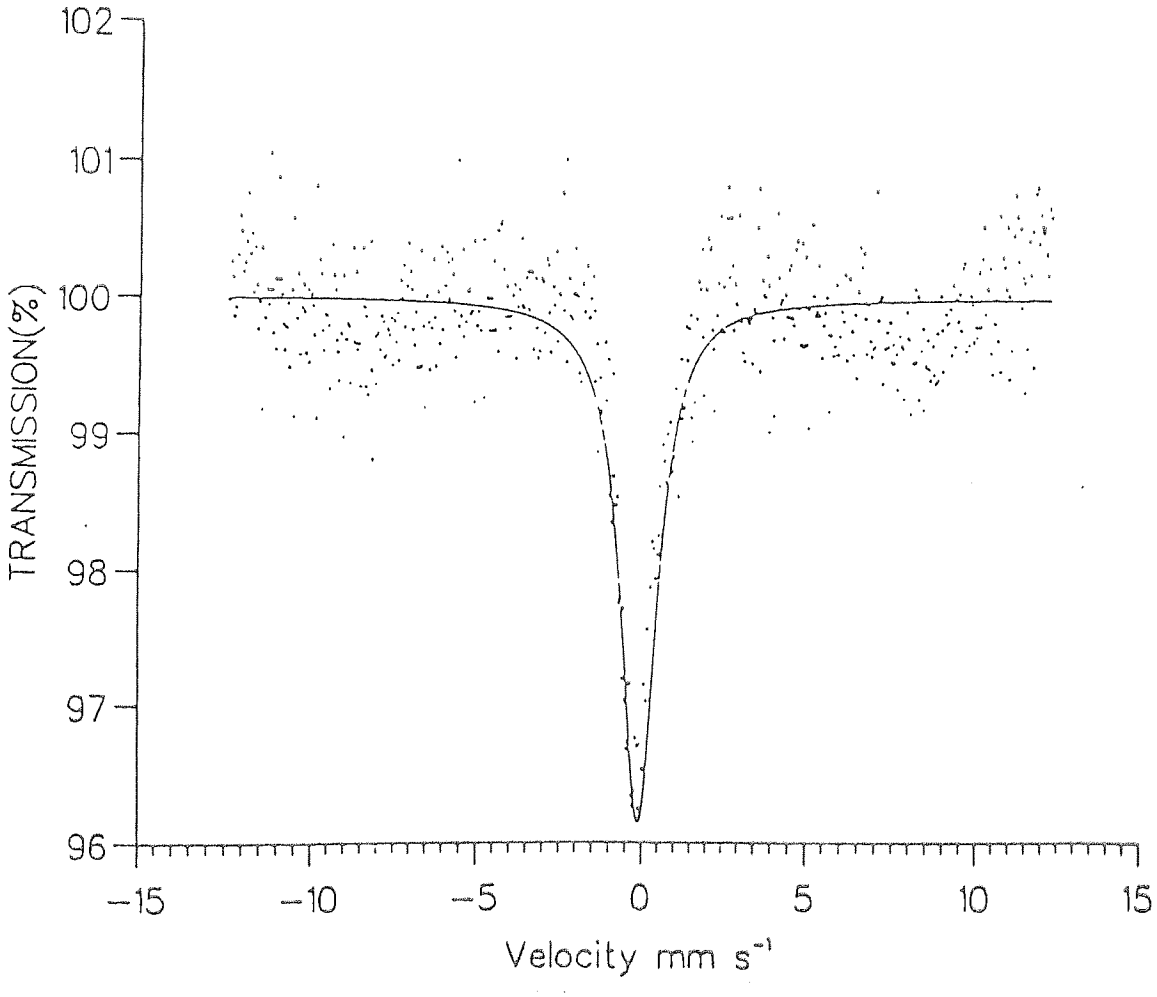

Figure 3.6 ^{119}Sn Mossbauer Spectrum of laponite RD after reaction with Ph_3SnCl

The intercalation product obtained from the reaction between $(CH_3OC_6H_4)_4Sn$ and laponite did not produce any spectrum despite extended data collection. The lack of an absorption at $\delta = 0$ mms^{-1} suggests that there is no pillar formation when this precursor is used.

3.5.2 X-Ray Photoelectron Spectroscopy (XPS).

Analysis by XPS appeared in some cases to show four distinct bands and in other cases just three. Three bands were characterised[67]. These characterisations are shown below in Table 3.5.

Band (eV) ($^+$ 0.2 eV)	Assignment
487.4 - 487.7	Sn - C
485.0 - 485.4	Sn - Cl
486.4 - 486.7	Sn - O

Table 3.5 XPS Characteristic Band Values.

The Sn - C and the Sn - Cl were derived from the Ph_3SnCl or Me_2SnCl_2 precursors. Figures 3.7 - 3.9 show the spectra obtained from reactions between laponite RD and Ph_3SnCl, Me_2SnCl_2 and $(MeOPh)_4Sn$ respectively. The Sn - O band is derived from the "SnO_2" pillars contained within the modified clay. These results were consistent for clays intercalated *via* mechanical shaking, microwave irradiation and also using the method of Petridis[58].

The fourth band appeared randomly within the samples at 483.0 - 483.7 eV. At first it was thought to be an alloy of magnesium and tin (other possible alloys - those of tin-lithium or tin - sodium were eliminated from an energetic viewpoint early in the investigation). The idea of an alloy forming between magnesium and tin is a feasible one as it has been shown that migration of magnesium from trioctahedral to interlamellar regions can occur under microwave irradiation[68]. This phenomenon is not restricted to magnesium. To date it has also been shown that lithium ions can undergo this migration[69].

Figure 3.7 X.P.S. Spectrum of Laponite + Ph_3SnCl.

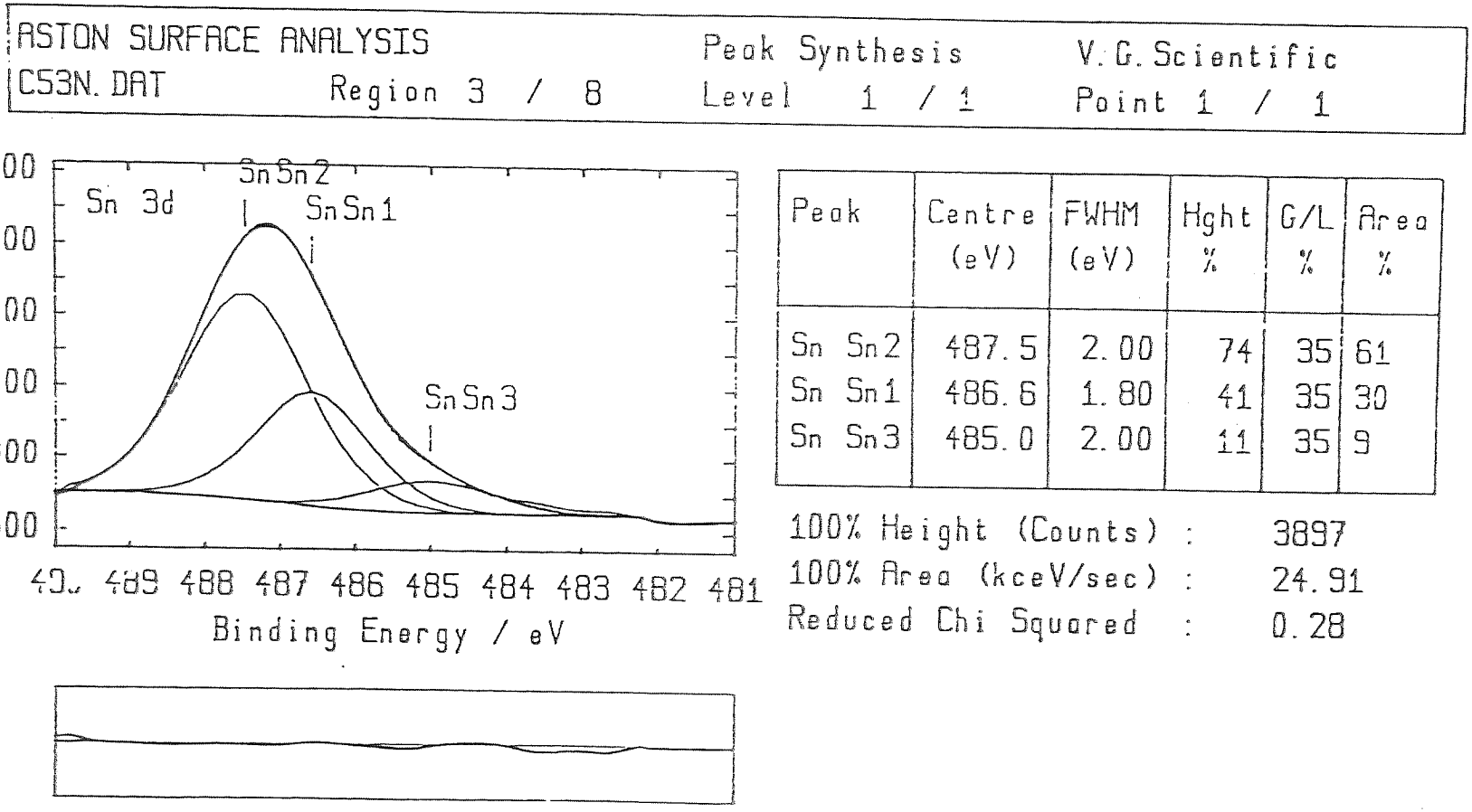

Figure 3.8 X.P.S. Spectrum of Laponite + Me_2SnCl_2.

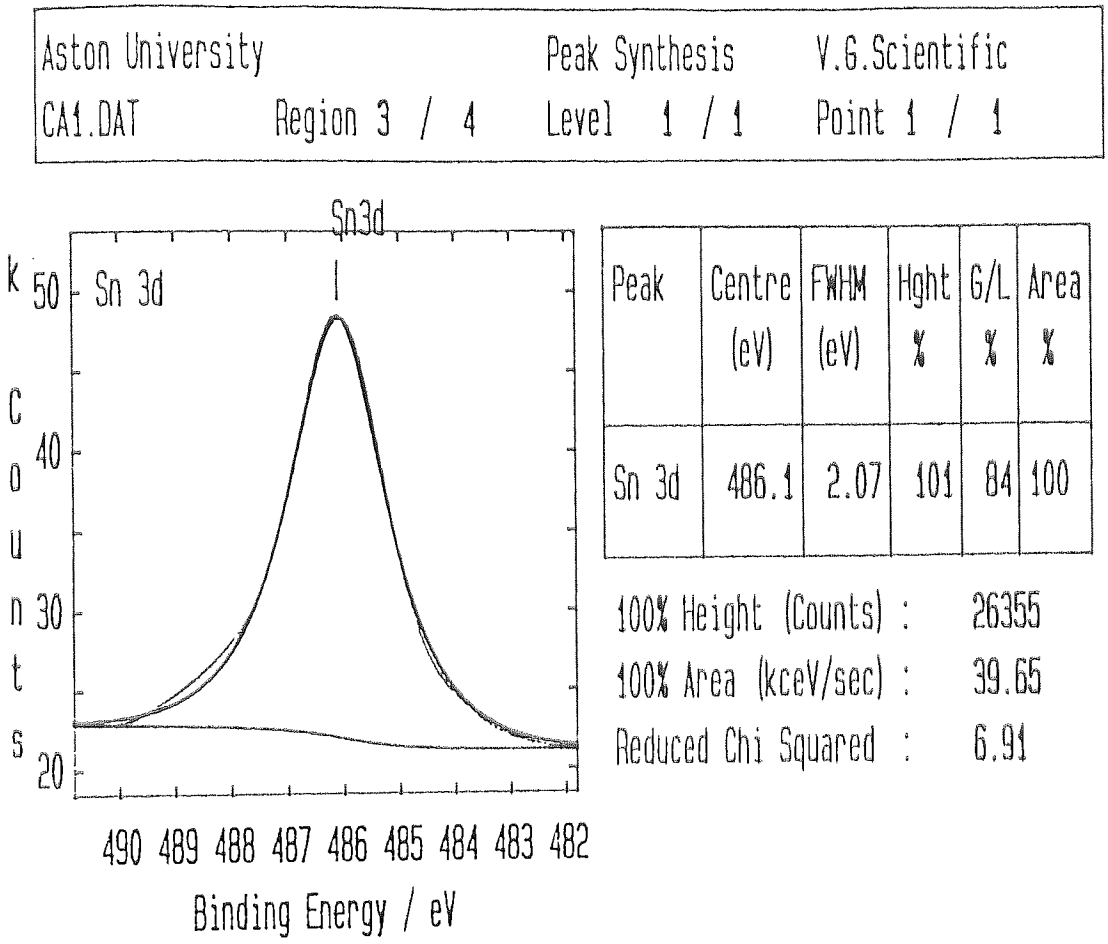

Figure 3.9 The XPS Spectrum of laponite RD reacted with $(p\text{-}CH_3OC_6H_4)_4Sn$

However the random inclusion of this band make this suggestion unlikely. The band was indeed found to be an artefact of the XPS process. The probable explanation is that when under analysis the sample is exposed to energetic X-ray flux or secondary electrons. These observations were later repeated by another worker in the laboratory using organotellurium compounds[70]. Full details are given in chapter 4.

The XPS data thus provides useful qualitative support for the view that the reaction of Ph_3SnCl and Me_2SnCl_2 to a tin-oxygen species does take place on the surface of the clay. The process seems to confirm that pillar formation occurs with both the aryl and alkyl tin halides but does not occur when tetra-(*p*-methoxyphenyl)tin(IV) is used. This therefore lends support to the Mossbauer observations.

3.5.3 Powder X-Ray Diffraction (XRD).

This technique uses the d_{001} reflection of the clay to facilitate calculation of the 'c' or 'basal spacing'. In order for calculations to be carried out the wavelength of the radiation used in the analysis must be known and the d_{001} reflection identified from the diffraction pattern. Bragg's equation, shown below is used for the calculation.

$$n\lambda = 2d\sin\theta$$

The basal spacing shows whether pillaring has occurred to open up the clay layers. Table 3.6 shows the basal spacings obtained for products from intercalation reactions using different tin precursors.

Compound	Basal spacing(Å)
laponite RD	14.25
laponite RD + Ph_3SnCl	17.50
laponite RD + $(CH_3)_2SnCl_2$	18.25
laponite RD + $(CH_3OC_6H_4)_4Sn$	14.15

Table 3.6 Basal spacing of laponite RD modified with Organotin Compounds.

These results show that the basal spacing of the clay is increased when phenyl and methyl tin halides are the precursor. This technique also supports the view that no intercalation or pillaring reaction takes place when the tetra(*p*-methoxyphenyl)tin(IV) is reacted.

3.5.4 Atomic Absorption Spectroscopy (AA).

Analysis of the recovered filtrate and washings were analysed by AA spectroscopy. Bond[54] found that during the intercalation of Ph_3SnCl into Laponite RD that approximately 100 ppm Na^+ ions were released into the filtrate. Results were found to agree well with this observation, with values of between 76.7 and 121.6 ppm being recorded. It is suggested that the cause of this release is a hydrolysis reaction, taking place on the surface of the clay whereupon the following reaction occurs

$$2Ph_3SnCl + H_2O \text{ ----------> } (Ph_3Sn)_2O + 2HCl$$

In solution HCl exists as H^+Cl^-. This acid production allows proton (H^+) exchange to occur with the interlayer sodium ions. The presence of Cl^- ions in the filtrate was confirmed using the silver nitrate test[59]. The clay facilitates this reaction in some way as a blank experiment did not produce such a marked decrease in the pH of the reaction, pH measurements are shown in Table 3.7.

Material	pH
Solvent	7.3
Solvent + Ph_3SnCl	7.0
Solvent + Ph_3SnCl + Clay	6.4
Solvent + Ph_3SnCl + Clay (after irradiation)	4.2

Table 3.7 pH measurements over the course of an intercalation reaction.

Results using the $(CH_3OC_6H_4)_4Sn$ showed that sodium release during the reaction was 19 ppm - only slightly above the blank experiment of laponite + solvent which released 15 ppm. As a consequence the pH is virtually unaltered. These results show that a hydrolysis reaction does not occur with the *p*-methoxyphenyltin(IV) precursor, a not unexpected result.

3.5.5 Gas-Liquid Chromatography (GLC)

A GLC investigation of the filtrate from the reaction of laponite RD with the $(CH_3OC_6H_4)_4Sn$ found no trace of anisole in the filtrate.

3.5.6 ^{13}C MASNMR Spectroscopy

Analysis of the precursor and the resultant clay using this technique revealed almost identical spectra, see Figure 3.10a and 3.10b respectively. This observation again lends support to the hypothesis that no reaction is occurring between the $(CH_3OC_6H_4)_4Sn$ precursor and laponite.

3.5.7 Summary

Collecting these results together it can be seen that Ph_3SnCl is a much more efficient precursor in the reaction to form tin (IV) oxide pillars in laponite than the other organotin compounds.

The formation of the pillars stems from an initial hydrolysis reaction on the clay surface. As a result acid is released which facilitates proton exchange with the interlayer sodium ions. The pillars lead to an increase in basal spacing. Results using the $(CH_3OC_6H_4)_4Sn$ precursor were disappointing. It was thought that the $(CH_3OC_6H_4)$- group would prove to be a better 'leaving group' than the phenyl and hence would increase the rate of electrophilic attack and thus the degree of pillaring. This was found not to be the case. It is suggested that steric factors hindered the molecule in the respect that it cannot fit into the lattice of the clay as benzene from Ph_3SnCl appears to do. (Bond[54] showed by GLC that the other expected product, benzene, from Ph_3SnCl was not found in the filtrate but ^{13}C MASNMR revealed a single resonance at 128 ppm, characteristic of benzene suggesting that benzene is tenaciously held within the lattice.)
However steric considerations may be inconsequential as if the initial hydrolysis reaction does not take place then it is unlikely that there will be breakage of the tin - carbon bond in order to produce the postulated other product, anisole. (The importance of the hydrolysis reaction will be discussed in depth in chapter 4.)
This together with only a small uptake of the organometallic , a minimal sodium release and no increase in the basal spacing of the clay suggest that little if any reaction is taking place.

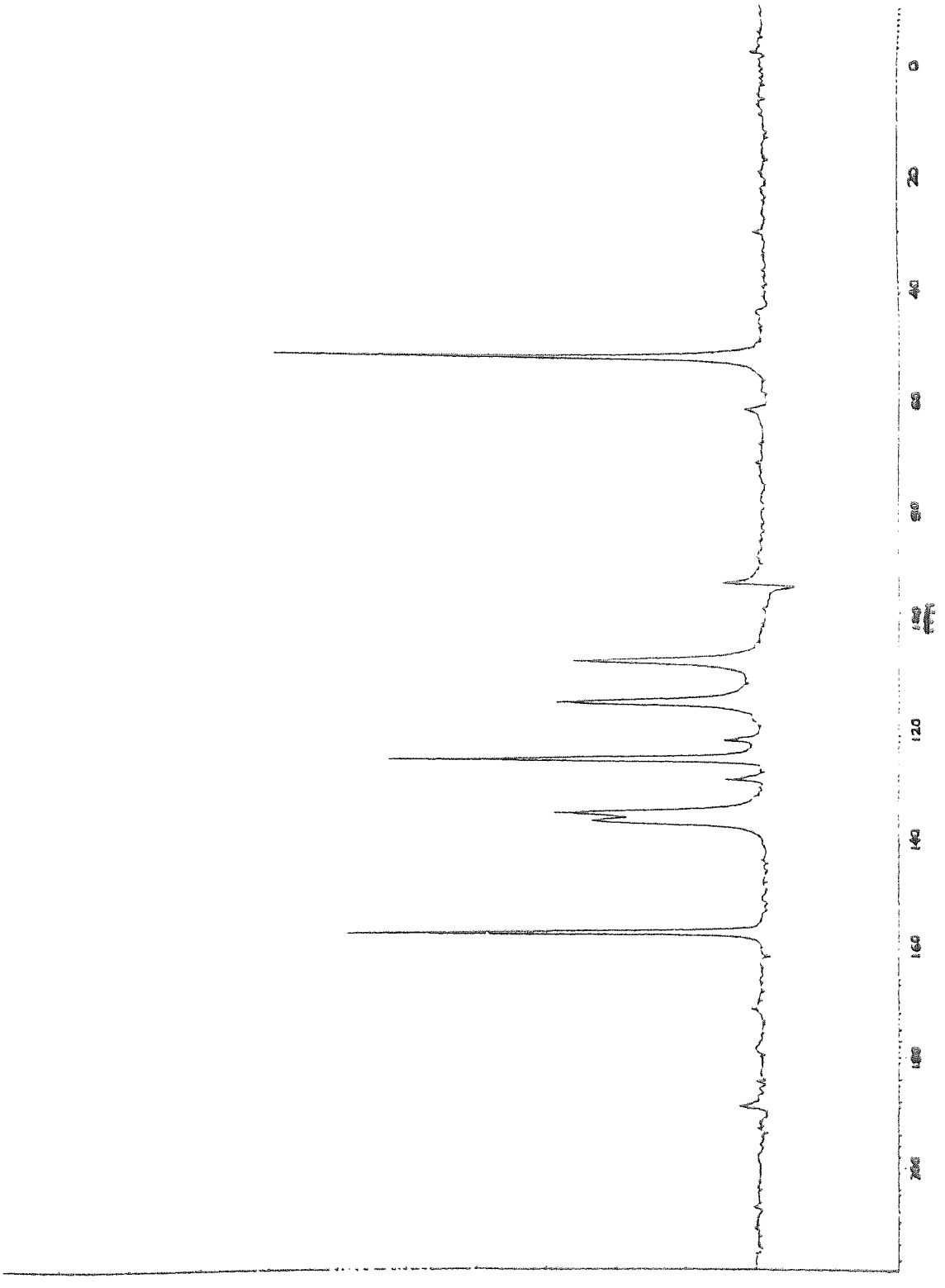

3.10a ^{13}C MASNMR Spectrum of $(MeOPh)_4Sn$.

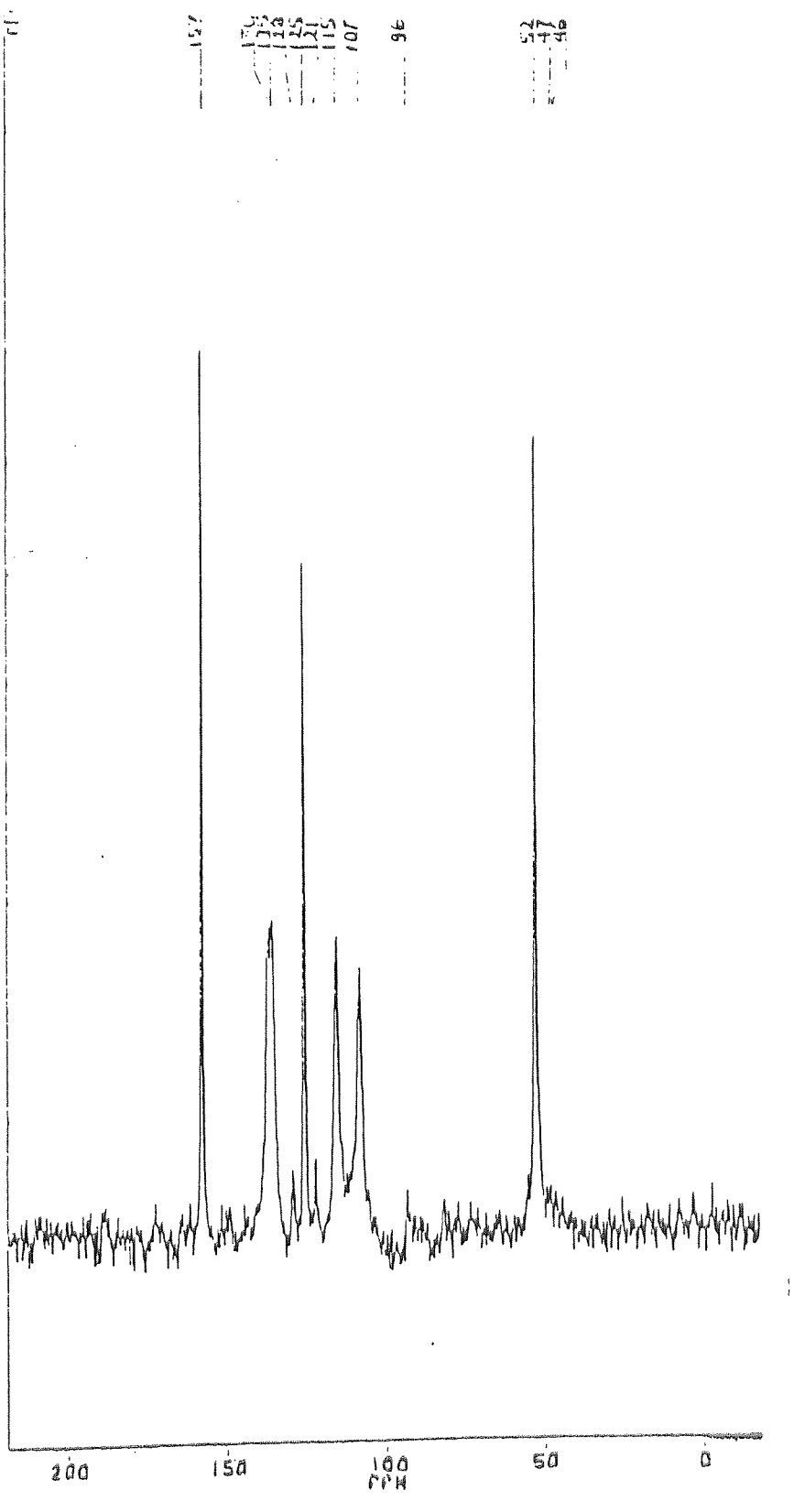

3.10b ^{13}C MASNMR Spectrum of laponite RD reacted with $(MeOPh)_4Sn$.

CHAPTER FOUR
The Intercalation of laponite RD with Organometallic Compounds

CHAPTER FOUR

The Intercalation of laponite RD with Organometallic Compounds

4.1 Introduction

A wide variety of organometallics are known to react with clays[17-26]. It was decided to expand the investigation beyond that of organotin compounds. Having established in chapter 3 that organotin compounds have the ability to produce tin (IV) oxide pillars within the clay *via* a hydrolysis reaction yet other organometallics[20-23] merely ion-exchange or incorporate themselves within the layers as added, it was apparent that there were several avenues to explore.

Triphenylsilyl and germanium halides were investigated by Phillips[71]. Intercalation experiments using both the mechanical shaker and the microwave oven were carried out as described in sections 3.4.2 and 3.4.3 respectively. In the case of the triphenylsilylchloride no increase in basal spacing was found and it was suggested that moisture in the solvents caused an immediate hydrolysis of the organometallic as shown below.

$$Ph_3SiCl \xrightarrow{EtOH/H_2O} Ph_3SiOH + HCl$$

This resulted in no reaction of any kind with the clay.

Experiments with triphenylgermanium(IV) chloride showed that a hydrolysis reaction occurred.

$$2Ph_3GeCl \xrightarrow{H_2O} (Ph_3Ge)_2O + 2HCl$$

Little or no increase was found in the basal spacing *via* powder XRD. XPS analysis on the microwave samples showed that no germanium was present within the clay sample. Samples prepared *via* the mechanical shaker had a germanium content of less than 1% making characterisation, beyond stating that there was a Ge(IV) species present, difficult.

It was felt from these initial investigations that neither of these organometallic precursors were as effective as tin and hence would not be pursued in a more detailed study.

4.2 Bismuth Intercalation.

Bismuth compounds are attractive as intercalation agents. Generally bismuth containing materials are non-toxic and have been used industrially without major toxicological problems. To date the main uses of bismuth[72] are in pharmaceuticals, fusible alloys and metallurgical additives. The knowledge of organobismuth chemistry is very well documented. An excellent review was published by Freedman and Doak[72]. Triaryl bismuth compounds have also been reviewed comprehensively[73]. It was decided to use aryl bismuth derivatives as these molecules were of a relatively large size and if successfully intercalated into the laponite should increase basal spacing regardless of whether there was pillar formation.

4.2.1 Triphenylbismuth (Ph_3Bi)

A variety of preparative routes are available to synthesise triphenylbismuth in the laboratory. Challenger and Allpress[74] found that triphenylbismuth can be prepared in almost quantitative yield by the reaction of bismuth tribromide and diphenylmercury in ether. Early methods also included heating a mixture of diphenylmercury and bismuth metal in a stream of hydrogen gas at 250°C for ten minutes[73]. However the high toxicity, and the expense of using mercury compounds have discouraged the use of these materials in synthetic work if other routes can be found.

The use of organolithium compounds to produce triphenylbismuth has been successful[75] as has a route involving the treatment of a hydrochloric acid solution of bismuth trichloride and phenylhydrazine with cupric and ferric chlorides[73]. This reaction probably involves the intermediate formation of a diazonium salt.

The favoured method of preparation is to use the Grignard reaction. The use of Grignard reagents in the formation of the carbon-bismuth bond was first demonstrated in 1904 by Pfeiffer and Pietsch[76].

$$3RMgX + BiX_3 \text{ ----------> } R_3Bi + 3MgX_2$$

Adaptations of this method have since been documented using organobismuth chlorides[77].

$$RBiCl_2 + 2R'MgX \text{ ----------> } RR_2'Bi + 2MgXCl$$

$$R_2BiCl + R'MgX \text{ ----------> } R_2R'Bi + MgXCl$$

Triphenylbismuth was therefore synthesised *via* a Grignard reaction. The two stage reaction outlined overleaf was followed.

$$C_6H_5Br + Mg \text{ ----------> } C_6H_5MgBr$$

$$3C_6H_5MgBr + BiCl_3 \text{ ----------> } (C_6H_5)_3Bi + 3MgBrCl$$

Experimentally the following procedure was undertaken.

Magnesium turnings (10g) were placed in a 1.5 litre round-bottomed-3-necked flask fitted with a dinitrogen inlet tube and reflux condenser. The magnesium was covered with dry ether (50 cm^3). A mixture of bromobenzene (75 cm^3) and ether (200 cm^3) was placed in a dropping funnel and connected to the flask. A small amount of the bromobenzene/ether mixture was added together with a crystal of iodine to initiate the reaction. Once the reaction was engaged in a self-sustaining reflux the remainder of the bromobenzene/ether was added at a rate great enough to keep the reflux going. A hot plate was later employed to sustain the reflux for three hours.

On cooling to room temperature, bismuth trichloride (50g) in ether (150 cm^3) was added slowly and the flask contents refluxed for a further 3 hours.

The flask was then allowed to cool before the contents of the flask were poured slowly into 2 litres of ice/water with stirring. The ether layer was separated. The water layer was washed three times with ether (100 cm^3) and the residue discarded. The ether portions were combined and on evaporation yielded a pale yellow solid. This yielded a white crystalline solid upon recrystallisation from petroleum ether (60 - 80°C).

Yield = 60%. Melting Point = 76.5 - 77.5°C (literature[78] = 77.6°C).
Elemental Analysis C = 48.8%, H = 3.64%. (Required for Ph_3Bi, C = 49.1%, H = 3.41%).

The FTIR spectrum of the synthesised compound (Figure 4.1) compares favourably with that of reference spectra in literature[102,103].

Triphenylbismuth was intercalated into laponite *via* mechanical shaking and microwave irradiation (as described in sections 3.4.2 and 3.4.3 respectively). The uptake of Ph_3Bi (determined by mass balance) was 20% in the case of the mechanical shaker and 32% using the microwave heating. XPS data however suggested that there was no bismuth in the compound and AA spectroscopy revealed a very low release of sodium ions, only 14ppm, into the filtrate. Combining these data suggests that if any reaction has occurred then it is a simple insertion of the Ph_3Bi molecule between the layers and not a hydrolysis and subsequent pillaring reaction as seen in the case of Ph_3SnCl. However analysis of the data obtained from XRD suggests a basal spacing of 13.6 - 14.0Å which is in fact smaller than that of the laponite.

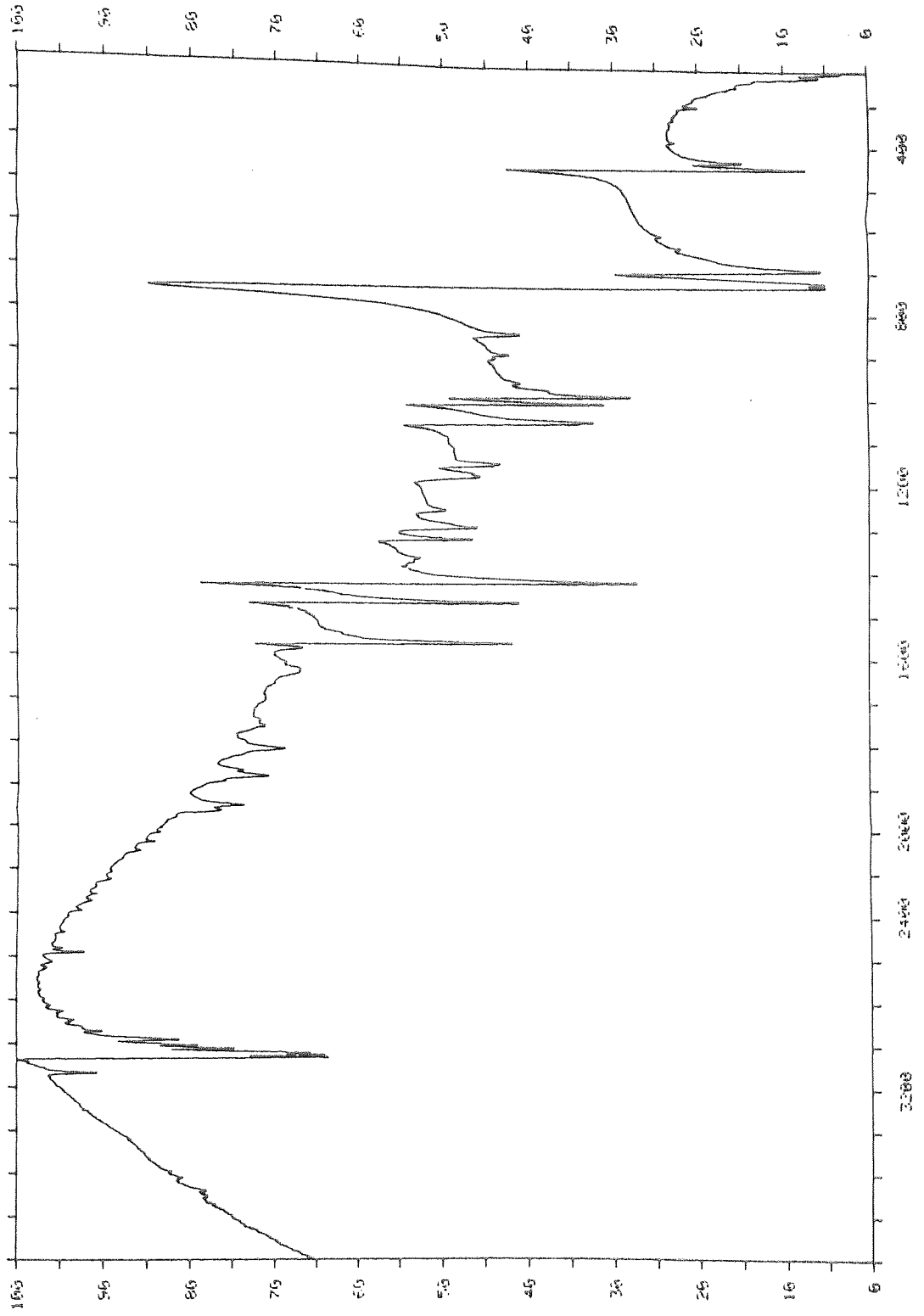

Figure 4.1 FTIR Spectrum of Ph_3Bi.

4.2.2 Diphenylbismuth(III) chloride (Ph_2BiCl).

The replacement by a halogen ion of one of the phenyl groups to give diphenylbismuth(III) chloride was the next stage. There are a number of methods available which produce the required product. Solomakhina[79] refluxed triphenylbismuth, copper(II)chloride and mercury(II)chloride in chloroform for 5 hours with success.

$$Ph_3Bi \xrightarrow{CuCl_2 + HgCl_2} Ph_2BiCl$$

The reaction of triphenylbismuth with antimony trichloride ($SbCl_3$) in ether yields diphenylbismuth(III) chloride and triphenylantimony(V) dichloride[80].

$$Ph_3Bi + SbCl_3 \longrightarrow Ph_2BiCl + Ph_3SbCl_2$$

Many reactions of this type, reacting Ph_3Bi with inorganic metal or metalloid halides[72] can successfully yield the required compound as the principal product.

Two routes of preparation were actually carried out in the laboratory.

(a) Ph_3Bi (2g) and $CuCl_2.2H_2O$ (1.55g)[80] in absolute ethanol (30 cm^3) were placed in a 100 cm^3 volumetric flask and vigorously shaken for 20 minutes. A colour change of dark green to white occurred during this time. The mixture was filtered and the filtrate then evaporated. A white crystalline solid was obtained.

Yield = 66%. Melting Point = 180°C (literature[81] = 184-185°C).
Elemental analysis found C = 35.4%, H = 2.48%. (Required for Ph_2BiCl, C = 36.2%, H = 2.53%).

(b) Ph_3Bi (4.45g) and $BiCl_3$(1.6g) in xylene (21.75g) were refluxed for 30 minutes with stirring. The flask was cooled and vacuum filtered. A white solid product was obtained.

Yield = 59%. Melting Point = 183-184°C (literature[81] = 184-185°C.)
Elemental analysis found C = 34.4%, H = 2.58%. (Required for Ph_2BiCl, C = 36.2%, H = 2.53%).

The Ph_2BiCl was intercalated *via* microwave irradiation (see section 3.4.3). By mass balance the uptake of the bismuth compound was calculated to be 39%. XPS data identified a band at

159.4 eV, this confirmed that the bismuth compound had reacted with the clay in some way (unlike the Ph_3Bi). Data books[67] suggest that the band found is characteristic of a Bi-O bond in a Bi_2O_3 arrangement, however the concentration of bismuth compound in this sample (~0.08%) makes absolute characterisation very difficult. Analysis of the filtrate by AA spectroscopy indicated a sodium release of 30 ppm, about double that of laponite alone. XRD data revealed a basal spacing of 15.2Å, implying that intercalation may have occurred with this compound.

4.2.3 Triphenylbismuth(V) dibromide (Ph_3BiBr_2).

A wide range of preparative methods are available for the synthesis of this compound. These include oxidative halogenation with Br_2 and Cl_2 of triphenylbismuth carried out in an organic solvent [75,82,83]. This is the most common method for converting triarylbismuthines to the corresponding dibromide or dichloride. However other chlorinating agents can be utilised. Sulphur dichloride, sulphur monochloride and thionyl chloride[84,85] will all produce triphenylbismuth(V) dichloride. The disadvantage of using these reagents is that the yields are much lower.

Triphenylbismuth(V) bromide was prepared using the above mentioned method of oxidative halogenation.

Ph_3Bi (1g) in chloroform (25 cm^3) was placed in a round-bottomed flask and bromine liquid in excess was added with stirring. The reaction yielded yellow needle-like crystals.

Yield = 78%. Melting point = 115-116°C. (literature[86] = 118°C.)
Elemental analysis found C = 35.8%, H = 2.58%. (Required, C = 36.1%, H = 2.53%).

An FTIR spectrum (Figure 4.2) compared well to that reported by Jensen[103]. The absorptions correlating to those reported are all caused by the phenyl ring vibrations. It is suggested that the carbon-bismuth vibration is found below 400 cm^{-1}. Significant absorption bands can be seen in this spectrum at both 238 and 225 cm^{-1}.

The Ph_3BiBr_2 was intercalated into laponite *via* microwave irradiation (see section 3.4.3). The uptake of Triphenylbismuth dibromide was 61%. Analysis of the final material by XPS revealed a band at 159.2 eV, which is in the range reported for Bi_2O_3(158.6-159.8)[67]. The small concentration of bismuth compound (0.09%) within this clay sample makes confident characterisation unlikely.

Analysis of the filtrate by AA spectroscopy showed that the sodium ion release was 58ppm, a three fold increase over that of laponite. A basal spacing of 15.4Å was revealed *via* powder

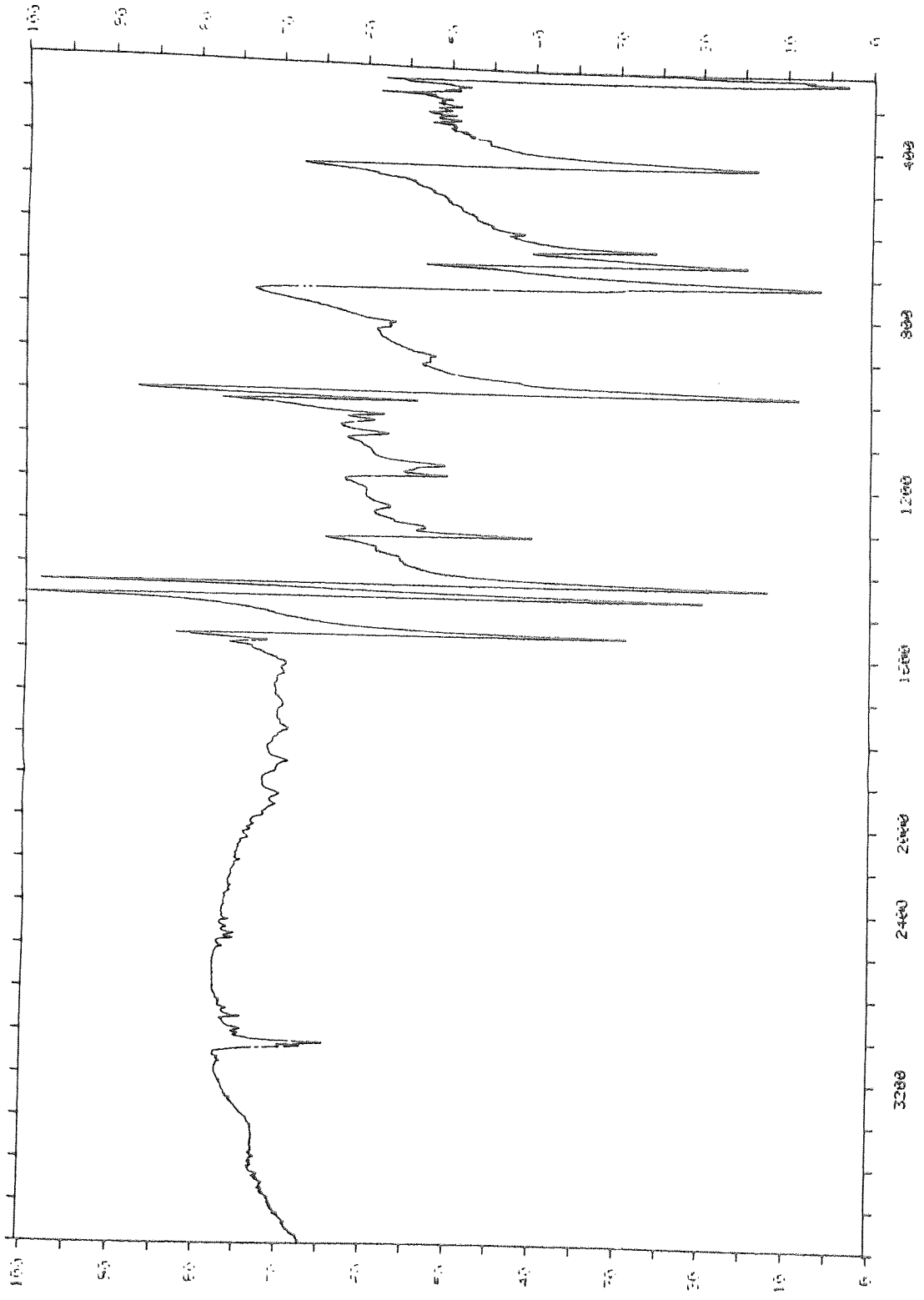

Figure 4.2 FTIR Spectrum of Ph_3BiBr_2.

XRD. This suggested that a reaction had taken place between this organobismuth compound and laponite.

The results of the intercalation of organobismuth compounds can be summarised. Of the three organobismuth compounds intercalated with laponite, triphenylbismuth appears to be the least receptive to the reaction. The organobismuth compounds containing one or two halogen atoms are more successful. This agrees with the findings for the organotin compounds, triphenyltin(IV) chloride and tetra-(*p*-methoxypheny)ltin. It is tentatively suggested that at least one halogen atom is required in the organometallic precursor in order for the hydrolysis and/or intercalation reaction to occur.

4.3 Antimony Intercalation.

The ultimate aim in the choice of the antimony organometallics as possible intercalation agents was to produce a clay containing mixed oxide pillars of tin and antimony. However before that investigation was started it seemed prudent to test antimony in its own right as an intercalation guest molecule. The general chemistry of antimony is well known. Excellent accounts of the chemistry have been presented by Doak and Freedman[73], Aylett[87] and Cotton and Wilkinson[88].

Antimony has many industrial uses both in the form of alloys and chemical compounds[89].

Major metallurgical uses include batteries, bearings and cable sheathings. Alloys[90] in use include antimony-sodium, -silver, -gold, -tin, -tellurium and -bismuth. Chemical uses of antimony and its compounds include mordants, fire-proofing of fabrics and interestingly antimony trioxide[91] is used in enamels and paints to improve the opacity and the "whiteness" of the materials.

A number of compounds were synthesised for use in intercalation reactions. The Bart[92] reaction and its modifications provide the essential means for the synthesis of a wide variety of organoantimony compounds.

4.3.1 Triphenylantimony (Ph_3Sb).

Triphenylantimony has been synthesised in many ways. The Grignard method[93,94] is the most convenient to date. Triphenylantimony is also formed in very good yield from antimonytrichloride ($SbCl_3$), bromobenzene and sodium, using toluene and benzene as solvents[95]. Other methods include preparation by the decomposition of diazonium chloride - zinc chloride complexes by antimony[96]; by the addition of a solution of lithium tetraphenyl aluminate ($LiAlPh_4$) in iodobenzene to finely divided antimony in an autoclave followed by

consequent heating to 110°C for 4 hours[97]; the cleavage reaction of tetraphenylantimony-bromide with Lithium Aluminium Hydride ($LiAlH_4$)[98]; the thermal disproportionation of stibosobenzene at 180-200°C[99] and *via* a reaction between Phenylsilicontrifluoride ($PhSiF_3$), Ammoniumantimonypentafluoride [$(NH_4)_2SbF_5$] and Ammonium Fluoride[100].

The Grignard reaction was employed to synthesise triphenylantimony[93].

As with all Grignard reactions methods were followed to purge the system of air before the experiment was carried out (using a dinitrogen inlet tube).
Bromobenzene (62.8g) was placed in a dropping funnel. A few drops were added to the magnesium turnings (9.6g) in dry ether (20 cm^3) contained in the reaction flask to initiate the reaction. Once the reaction had begun the remaining bromobenzene was added over approximately 30 minutes. The contents of the flask were then refluxed for 2 hours. A solution of antimonytrichloride (22.8g) in ether (50 cm^3) was added slowly *via* the dropping funnel. The flask contents were then refluxed for 3 hours. After cooling to room temperature the reaction mixture was slowly poured into an aqueous saturated ammonium chloride solution (200 cm^3)[101]. The product was extracted with ether and dried.

Yield = 61%. Melting Point = 49-51°C. (literature[83] = 48-53°C).
Elemental analysis found C = 74.8%, H = 5.25%. (Required, C = 76.6%, H = 5.32%)

An FTIR spectrum (Figure 4.3) was compared with those reviewed in literature[102-104]. Saliant features included strong absorptions at 695, 728 and 1432 cm^{-1} plus other weaker vibrations between 454 and 1575 cm^{-1}. These are all characterised as phenyl ring vibrations and match the literature values well. No confident characterisation is made of the C-Sb vibration, although Jensen[103] suggests it will be found below 400 cm^{-1}.

Triphenylantimony was intercalated into laponite *via* mechanical shaking (see section 3.4.2) and by microwave heating (see section 3.4.3). The uptake of Ph_3Sb by the above methods was 15% and 28% respectively. Analysis of the filtrate by AA spectroscopy indicated that there was little additional sodium release (16ppm) to that obtained from laponite alone. XPS data suggested that there was no antimony contained in the clay. XRD spectroscopy indicated a basal spacing of 14.31Å, approximately that of laponite. All these factors suggest that little if no reaction has occurred with this precursor. Results are analogous with those obtained using triphenylbismuth as the organometallic precursor.

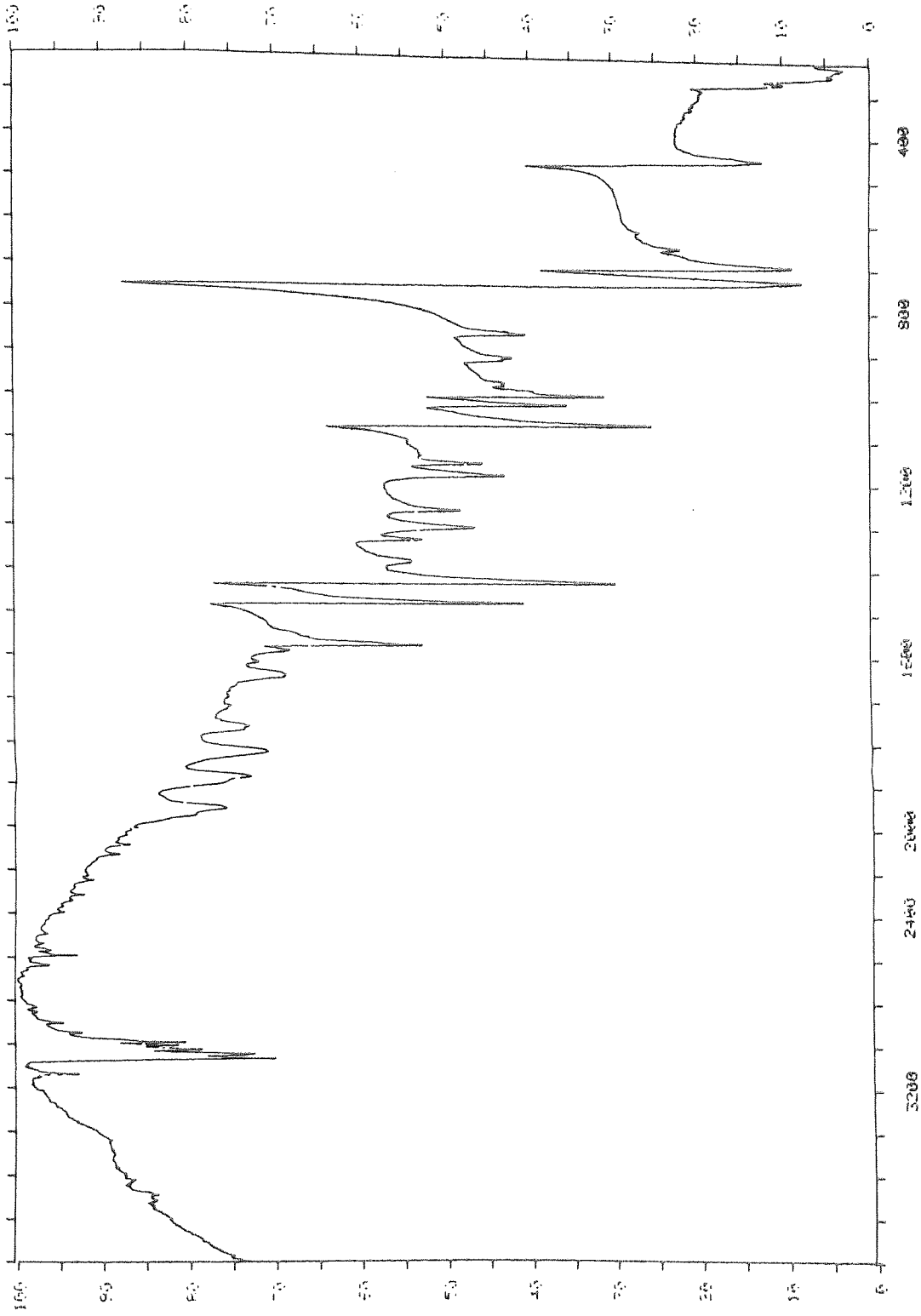

Figure 4.3 FTIR Spectrum of Ph_3Sb.

4.3.2 Diphenylantimony(III) chloride (Ph_2SbCl).

This compound has been synthesised in a number of ways. Boiling methanolic hydrochloric acid displaces a phenyl group from triphenylantimony[87] but produces the carcinogenic bi-product benzene.

$$Ph_3Sb + HCl \text{ ----------> } Ph_2SbCl + C_6H_6$$

Ph_2SbCl can also be obtained using diphenylmercury or tetraphenyllead with antimony trichloride[87]. From an environmental viewpoint though it is not favourable to use mercury or lead compounds as both are extremely toxic. Other methods include refluxing stoichiometric amounts of triphenylantimony and antimony trichloride in an inert hydrocarbon solvent; the reaction of triphenylbismuth with antimony trichloride under carbon dioxide[79]; Manulkin[106] successfully prepared diphenylantimony(III) chloride using tetraphenyltin and antimony trichloride; another route is to proceed *via* diphenylstibonic acid[107].

The method chosen for the preparation of Ph_2SbCl was that of Leonard[105].

Ph_3Sb (8.8g) and $SbCl_3$ (2.9g) were mixed in dichloromethane (50 cm^3). This mixture was heated and refluxed for 64 hours.

Yield 82%. Melting Point = 63-64°C (literature[105] = 61-65°C).
Elemental analysis found C = 45.7%, H = 3.14%. (Required, C = 46.2%, H = 3.21%).

Upon intercalation by the method of microwave irradiation (see section 3.4.3) the uptake was calculated to be 20%, yet again the XPS analysis detected no antimony in the clay. Atomic absorption spectroscopy revealed a very low sodium release, only 8ppm. The basal spacing was found to be approximately equal to that of laponite.

4.3.3 Triphenylantimony(V) dichloride/dibromide (Ph_3SbCl_2/Ph_3SbBr_2).

The dihalides are very stable molecules and can be formed by direct addition of halogen to triphenylantimony[108],

e.g. $$Ph_3Sb + X_2 \text{ ----------> } Ph_3SbX_2$$

or by the Grignard route using antimony pentachloride[94],

e.g. $3PhMgBr + SbCl_5 \text{ ----------> } Ph_3SbCl_2 + 3MgBrCl$

Other methods include the reaction of triphenylantimony with S_2Cl_2 or SCl_2[85]; use of diazonium salts[109-110]; interaction of organometallic compounds with inorganic halogen derivatives[80,111]. These can all be successfully utilised to prepare the required product.

The method producing the best product was that of organometallic interaction with inorganic halides[80].

Ph_3Sb (3.53g) and $CuCl_2.2H_2O$ (1.70g) were vigorously shaken in dry ether (30 cm^3). The solution decolourised as the reaction took place.

$$Ph_3Sb + 2CuCl_2 \text{ ----------> } Ph_3SbCl_2 + 2CuCl$$

A white crystalline material was obtained.

Yield = 67%. Melting point = 142-143°C, (literature[80] = 142°C).
Elemental analysis found C = 51.1%, H = 3.56%. (Required, C = 51.0%, H = 3.57%).

The FTIR spectrum (Figure 4.4) agreed well with values quoted in the literature[103,104]. A range of strong to weak absorptions betwee 455 and 3090 cm^{-1} were characteristic of phenyl ring vibrations in Ph_3SbCl_2.

Intercalation results followed the same pattern as for the previous antimony compounds. Mass balance calculations suggested an uptake of 15-20%, there was no detection of antimony by XPS methodology, a small sodium release into the filtrate (9ppm) and a basal spacing of 13.83Å, less than that of laponite . All indications point to no reaction taking place.

The triphenylantimony(V) dibromide derivative was synthesised by direct halogenation[108].

Ph_3Sb (5g) was dissolved in chloroform (50 cm^3). An excess of Br_2 liquid was added in a fume cupboard and the mixture continually stirred. A pale yellow crystalline material was obtained as the residue.

Yield = 77%. Melting point = 215°C (literature[112a] = 217-218°C).
Elemental analysis found C = 42.2%, H = 2.97%. Required, C = 42.9%, H = 2.98%.

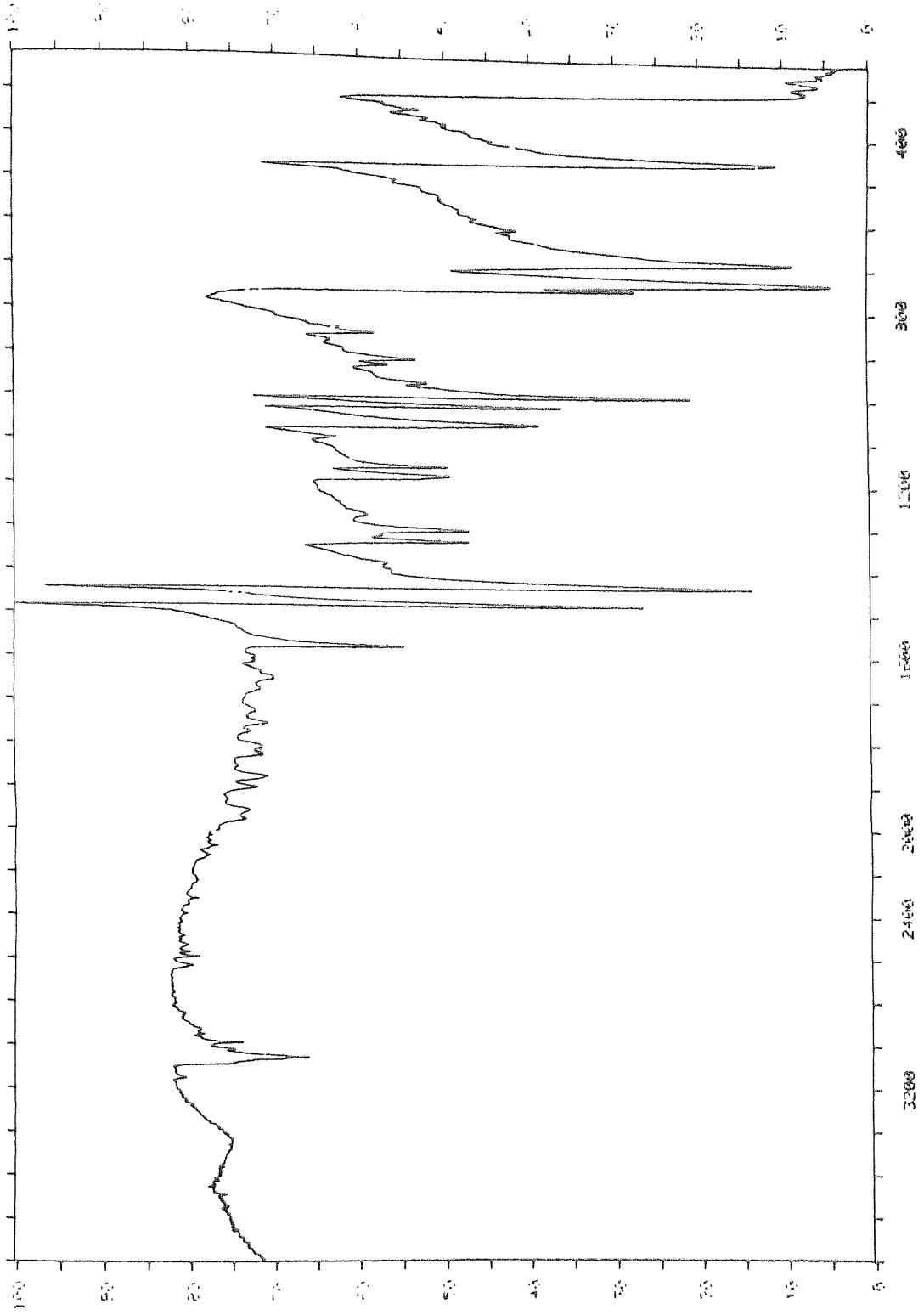

Figure 4.4 FTIR Spectrum of Ph_3SbCl_2.

The FTIR spectrum (Figure 4.5) agreed with reference spectra and values in literature[103,104]. Strong vibrations were noted at 682 and 729 cm^{-1}. A range of other vibrations between 455 and 3060 cm^{-1} created the spectrum characteristic of Ph_3SbBr_2.

Intercalation with laponite produced analogous results with respect to the other antimony compounds. The uptake was calculated to be ~12%, XPS methods could detect no antimony within the sample, AA spectroscopy showed a sodium release of 6ppm and the basal spacing was found to be 13.92Å by powder XRD.

Intercalation with all the organoantimony compounds produced the same results and implied that no reaction had taken place between the organometallics and laponite. This conclusion was derived from a combination of data from three techniques which are summarised below:

1. XPS investigations could detect no antimony within the clay.
2. AA spectroscopy indicated a very low sodium ion release.
3. Powder XRD revealed basal spacings approximately equal to that of laponite.

4.4 Preparation of mixed Tin and Antimony Oxide Clays by Intercalation.

Having established that tin can indeed be successfully intercalated into laponite (see chapter 3), but with a question mark as to what happens to the antimony compounds, it was decided to carry on with the target of achieving a mixed tin oxide and antimony oxide pillared clay. There appeared to be two separate approaches to the problem.

1. To use a precursor containing a tin-antimony bond in order to produce a clay containing tin and antimony in the same pillar.
2. To use separate tin and antimony precursors to produce a clay with two oxide pillar types.

4.4.1 Attempted synthesis of an organometallic molecule containing a tin-antimony bond.

Details of organometallic compounds containing a tin-arsenic or a tin-antimony bond were recorded by Campbell *et al*[113] mirroring work done previously on the formation of species containing a tin-phosphorus bond[114].
One method successfully employed was that shown in the equation below,

$$R_3SnX + Ph_2ANa \text{ ----------> } R_3Sn.APh_2 + NaX$$

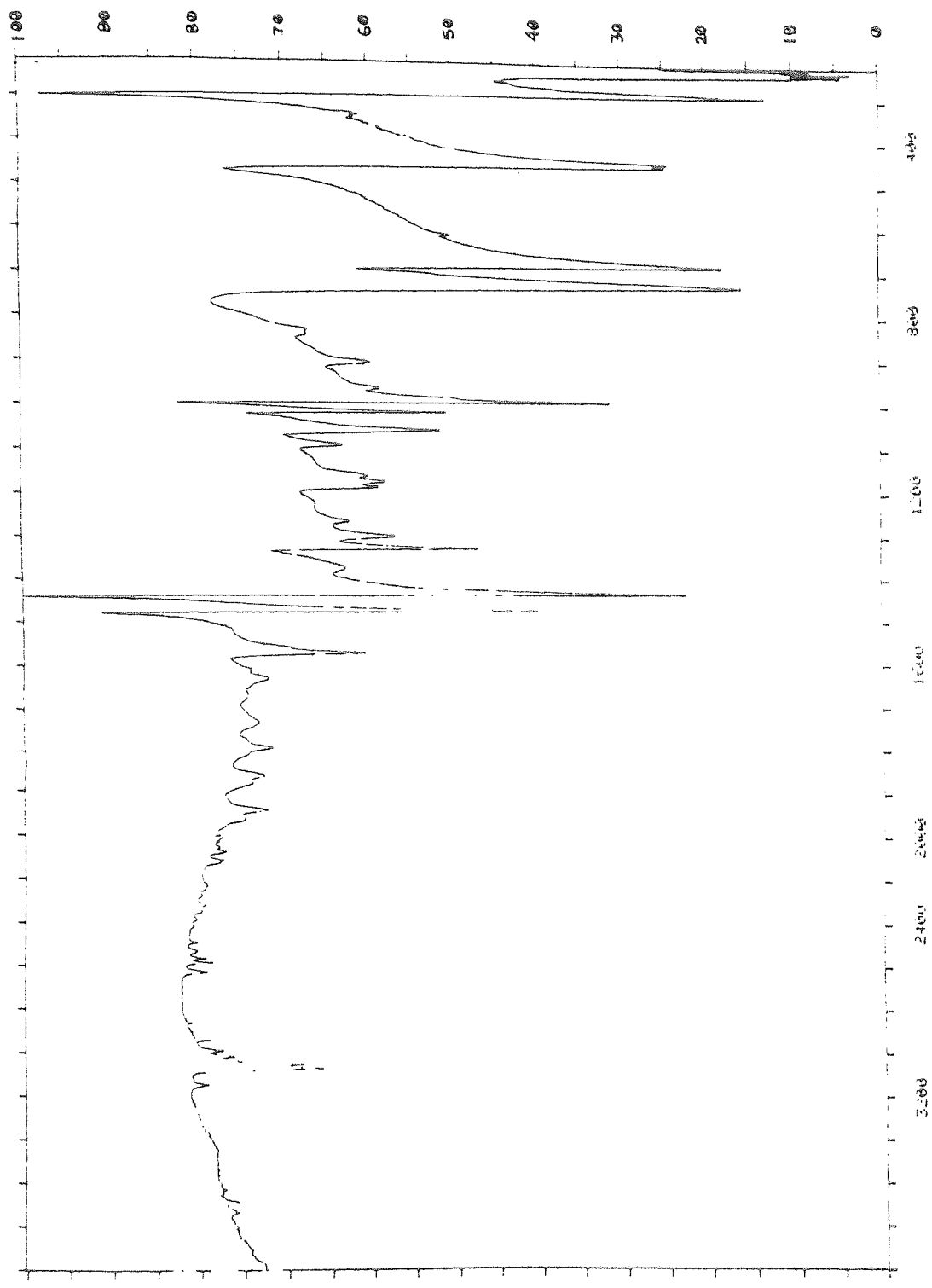

Figure 4.5 FTIR Spectrum of Ph_3SbBr_2.

where X is a halogen and A is either arsenic or antimony.
The sodium derivatives were prepared from the triphenylantimony (or triphenylarsenic) by reaction with sodium in liquid ammonia[115]. Reactions of triphenyltinlithium with diphenylantimony(III) chloride in tetrahydrofuran (THF) as shown in the equation below have also been reported[116].

$$n\ Ph_3SnLi + Ph_{3-n}SbCl_n \xrightarrow[(n=1,2,3)]{} [Ph_3Sn]_nSbPh_{(3-n)} + nLiCl$$

Another method to produce the tin-antimony bond was to react diphenylantimonymagnesium-bromide with triphenyltin(IV) chloride in an ether-benzene solvent[114]. Schumann and others[117] found that the reaction of sodium-diphenylantimony with organotin halides and tin tetrachloride in liquid ammonia forms a number of compounds containing the tin-antimony bond; as does the reaction between lithium-triphenyltin(IV), diphenylantimony(III) dichloride and antimony trichloride in a THF solvent under an inert atmosphere.

The method selected to synthesise $Ph_3Sn.SbPh_2$ was *via* a Grignard reaction.

Diphenylantimony(III) chloride (5.3g, 0.022 moles) was added under nitrogen gas to a solution of phenylmagnesiumbromide, prepared from bromobenzene (3.9g, 0.025 moles), magnesium turnings(0.6g) and ether (20 cm^3). The solution was refluxed for 30 minutes. Triphenyltin(IV) chloride (8.45g, 0.022 moles) in benzene (20 cm^3) was slowly added and the mixture was refluxed for a further 3 hours. The resulting solution was filtered. The filtrate yielded a small amount of white solid. The isolated product was washed with ether and benzene.
The melting point was recorded and found to be 240°C. The literature value for the required product is 116°C[117]. Elemental analysis confirmed that the $Ph_3Sn.SbPh_2$ had not been synthesised. It is suggested that a hydrolysis reaction on either the organotin or the organoantimony compound or both occurred before a reaction between the two could take place.

After a number of unsuccessful reactions it was decided to concentrate on the alternative route to producing a clay containing both tin and antimony, i.e. to use separate precursors.

4.4.2 Intercalation with two precursors.

Reports of clays containing mixed oxide pillars are relatively recent. Gonzalez *et al* have prepared Aluminium-Gallium pillared clays[45,46], and Sterte has reported the preparation of mixed Lanthanum-Aluminium and Cerium-Aluminium pillars[47]. No literature to date has suggested a method by which a clay containing tin-antimony pillars may be prepared. Three approaches were made, two utilised the methods of Bond (see section 3.4.2 and 3.4.3), the third was a modification of the process used by Gonzalez[46] in the preparation of Al-Ga pillared clays.

4.4.2.1 Addition of Two Precursors Simultaneously.

(a) By Mechanical Shaking.

Triphenyltin(IV) chloride (1g) and Triphenylantimony (1g) were placed in a 250 cm^3 conical flask. Absolute ethanol (100 cm^3) was added and the organometallic material was dissolved. Laponite RD (5g) was added and the flask sealed and placed on a mechanical shaker for 7 days. The contents were filtered, the clay dried and the filtrate analysed by AA spectroscopy and then evaporated. This experiment was repeated substituting the Ph_3Sb for two other precursors, Ph_3SbCl_2 and $SbCl_3$. The results of the intercalation reactions are shown in table 4.1 below.

Tin Precursor	Antimony Precursor	Na^+ release	Total Organometallic Uptake (%)
Ph_3SnCl	Ph_3Sb	102	26
Ph_3SnCl	Ph_3SbCl_2	114	30
Ph_3SnCl	$SbCl_3$	98	27

Table 4.1 Results of the intercalation using two precursors simultaneously on a Mechanical Shaker.

It can be seen from the above results that the sodium release is no greater than that seen when the triphenyltin(IV) chloride alone is intercalated into laponite.
Analysis by XPS revealed that no antimony was detected in the clay. The tin XPS spectrum indicated that the results were the same as when just the organotin precursor was used. XRD analysis showed an increase in the basal spacing when compared to laponite equivalent to that obtained *via* intercalation with Ph_3SnCl alone.

(b) By Microwave Heating.

Triphenyltin(IV) chloride (0.2g) and the antimony precursor (0.2g) were dissolved in absolute ethanol (10 cm^3) in a Teflon container. Laponite RD (1g) was added and the container tightly sealed. The reaction mixture was subjected to five 1 minute bursts of microwave radiation. The contents were cooled and filtered. Analysis proceeded as outlined in the previous section. Results of organometallic uptake and Na^+ release are shown in table 4.2 below.

Tin Precursor	Antimony Precursor	Na^+ release	Total Organometallic Uptake (%)
Ph_3SnCl	Ph_3Sb	108	34
Ph_3SnCl	Ph_3SbCl_2	105	31
Ph_3SnCl	$SbCl_3$	93	25

Table 4.2 Results of intercalation using two precursors simultaneously by microwave heating.

Results from both the shaker and microwave experiments correlated well.
Analysis by Mossbauer spectroscopy ,using a SnO_2 standard, (see figure 4.6) clearly shows an absorption at $\delta = 0$, hence characteristic of tin oxide (SnO_2). On careful examination a second smaller absorption centred at ~1.2 mms^{-1} is apparent. This is derived from the Sn-Cl bond in the Ph_3SnCl precursor, some of which may not have reacted with the laponite. XRD measurements detail a basal spacing of ~15Å. These results show that addition of the antimony

compounds does not impede the reaction of the triphenyltin(IV) chloride with laponite nor alter it in any way.

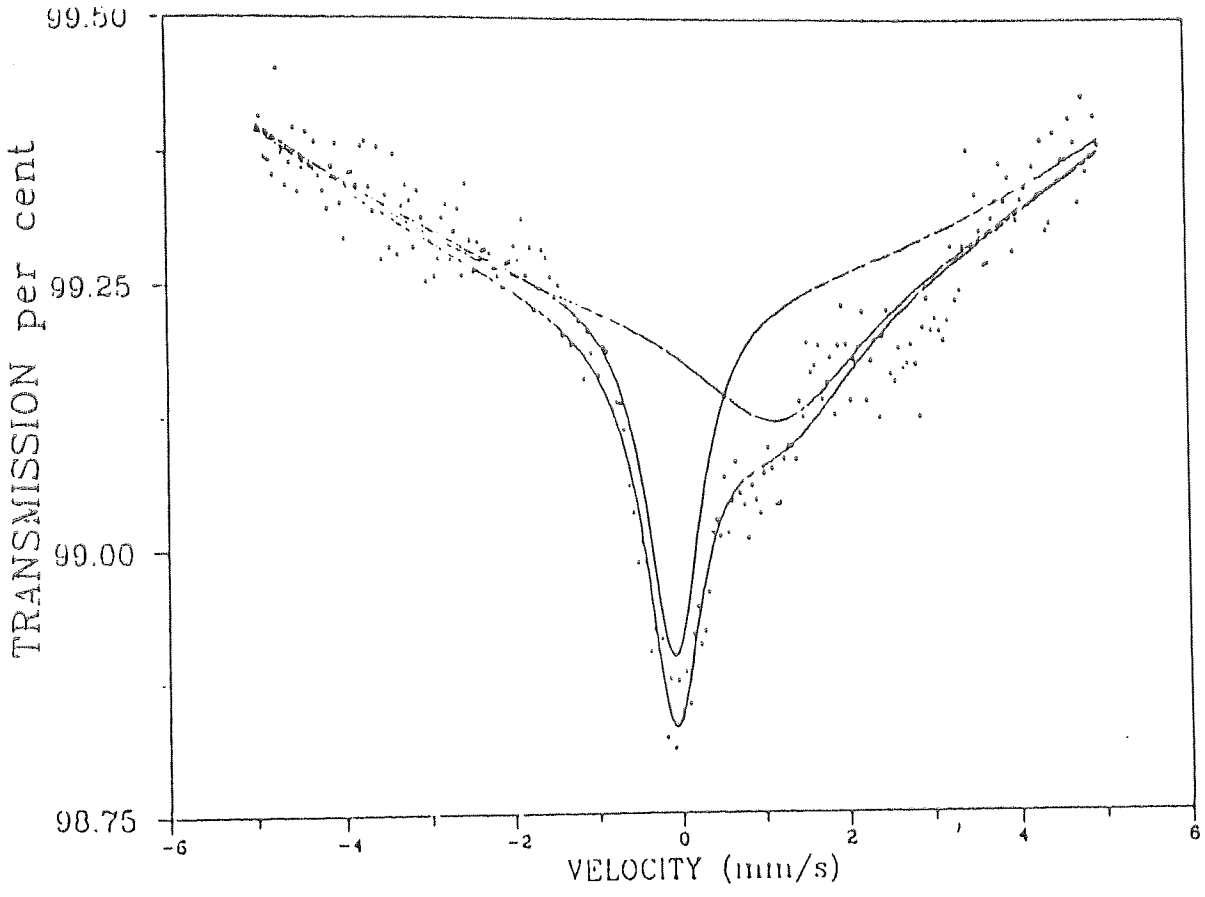

Figure 4.6 The ^{119}Sn Mossbauer spectrum from a clay intercalated with a tin and antimony precursor simultaneously.

4.4.2.2 Intercalation by two precursors consecutively.

(a) By Mechanical Shaker

Triphenyltin(IV) chloride (1g) was reacted as described in section 3.4.2. After 7 days the flask was removed from the shaker and the antimony precursor (1g) was added to the flask. The flask was then replaced and shaken for a further 7 days. The uptake of organometallic and the release of sodium are shown in table 4.3.

Tin Precursor	Antimony Precursor	Na^+ release	Total Organometallic Uptake (%)
Ph_3SnCl	Ph_3Sb	148	42
Ph_3SnCl	Ph_3SbCl_2	162	36
Ph_3SnCl	$SbCl_3$	103	27

Table 4.3 The results of intercalation of two consecutive precursors using the Mechanical Shaker.

The microwave preparation was modified in a similar way and results were analogous to those of the shaker. Results are shown below in table 4.4.

Tin Precursor	Antimony Precursor	Na^+ release	Total Organometallic Uptake (%)
Ph_3SnCl	Ph_3Sb	129	40
Ph_3SnCl	Ph_3SbCl_2	134	32
Ph_3SnCl	$SbCl_3$	94	24

Table 4.4 The results of intercalation of two consecutive precursors using the Microwave Oven.

Analysis by XPS suggested that antimony was present in the clay in a very small quantity (0.9%). The band at 540.2 eV (see figure 4.7a) fits that expected for Sb_2O_5, although the very small quantity of antimony in the sample makes characterisation difficult.
The tin analysis by XPS (see figure 4.7b) was particularly interesting as it revealed only one

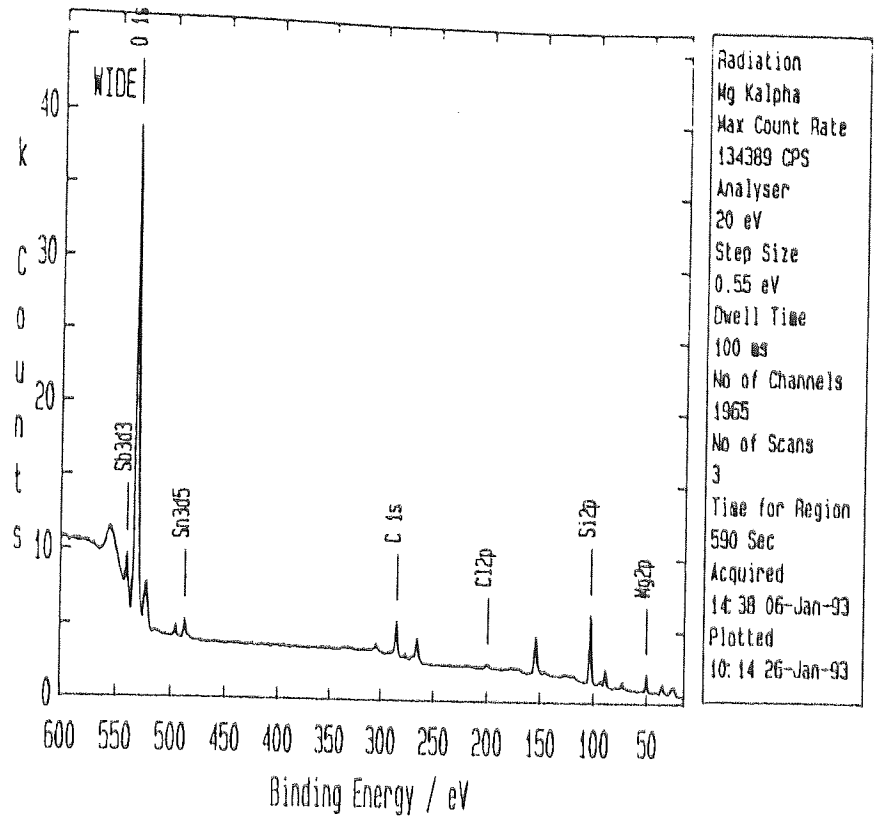

Figure 4.7a Antimony XPS Spectrum of laponite reacted with Ph_3SnCl then Ph_3Sb.

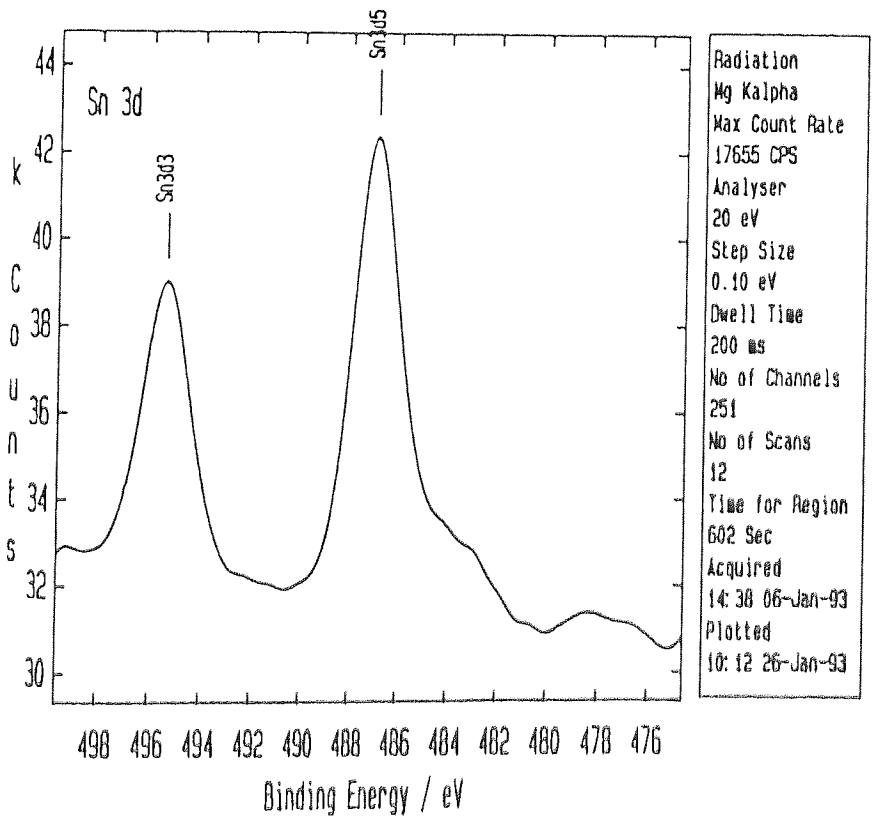

Figure 4.7b Tin XPS Spectrum of laponite reacted with Ph_3SnCl then Ph_3Sb.

band at 486.8 eV, the region suggested for a tin-oxygen bond. No bands were seen for Sn-Cl and Sn-C from the precursor. This suggests that all the organotin compound absorbed by the clay has been converted to the tin oxide.
The introduction of the phenylantimony compound after the initial reaction of the organotin with the clay appears to facilitate the hydrolysis of any unreacted tin compound to form pillars.

Analysis by powder XRD showed a basal spacing of 15.45Å.

Addition of the antimony precursor followed by the tin precursor did not produce the same results. In this case results were consistent with addition of the tin compound alone.

4.4.2.3 Intercalation by the method of polyoxycations[46].

Gonzalez[46] reported the successful preparation of clays containing aluminium-gallium pillars. The method of preparation involved the use of ethanolic solutions of aluminium and gallium polyoxycations. A modified procedure aimed to incorporate tin and antimony into laponite was carried out.

Ethanolic solutions of $SnCl_4.5H_2O$ and $SbCl_3$ were made up to various ratios (see table 4.5).

No	$SnCl_4.5H_2O$	$SbCl_3$
1	5.265g (0.15M)	1.1425g (0.05M)
2	3.510g (0.10M)	2.2850g (0.10M)
3	1.755g (0.05M)	3.4275g (0.15M)

N.B. All weights are per 100 cm^3 solvent. Corresponding quantities of $NaOH_{(alc)}$ (11.34g per litre, 0.2835 mole) were added to give a metal : OH ratio of 1 : 2.

Table 4.5 Ratios of precursors for intercalation *via* the method of polyoxycations.

In practice 50 cm^3 $SnCl_4.5H_2O/SbCl_3$ solution was added to 50 cm^3 $NaOH_{(alc)}$ in a 250 cm^3 conical flask. Laponite RD (2.5g) was added and the flask placed on a mechanical shaker for 3 days.

On a scale of $10cm^3$: 10 cm^3 : 1g the reactions were repeated in the microwave oven for five 1 minute bursts of microwave irradiation.
Results of sodium release are shown below in Table 4.6.

Reagents	Na^+ release (ppm)
0.15M $SnCl_4.5H_2O$ 0.05M $SbCl_3$	51
0.10M $SnCl_4.5H_2O$ 0.10M $SbCl_3$	47
0.05M $SnCl_4.5H_2O$ 0.15M $SbCl_3$	32

Table 4.6 Sodium release from laponite when intercalating by the method of polyoxycations[46].

The sodium release was lower than that when a Ph_3SnCl is used as the precursor (~100ppm), yet higher than the release from the clay alone (~15ppm).

Analysis by powder XRD showed a basal spacing of 13.8 - 14.4Å. This is approximately the same value that is obtained for laponite RD.

XPS analysis (Figures 4.8a and 4.8b) revealed that both the tin and antimony were present in the clay and in much larger quantities than previously measured. Tin represented 4.5% of the sample and antimony 3.7%. The tin peak was centred on 486.7 eV, a value expected for a Sn-O bond. The antimony peak is found at 540.2 eV, this value is in the range characteristic of an Sb-O bond in an Sb_2O_5 arrangement[67].

4.5 Tellurium Intercalation.

Over the past three decades, work carried out within the research laboratory at Aston has made a significant contribution to present day knowledge on the chemistry of organotellurium compounds.

The intercalation of organotellurium compounds into smectite clays has not to date been reported. However it is known that organotellurium(II) compounds can be used as donors in

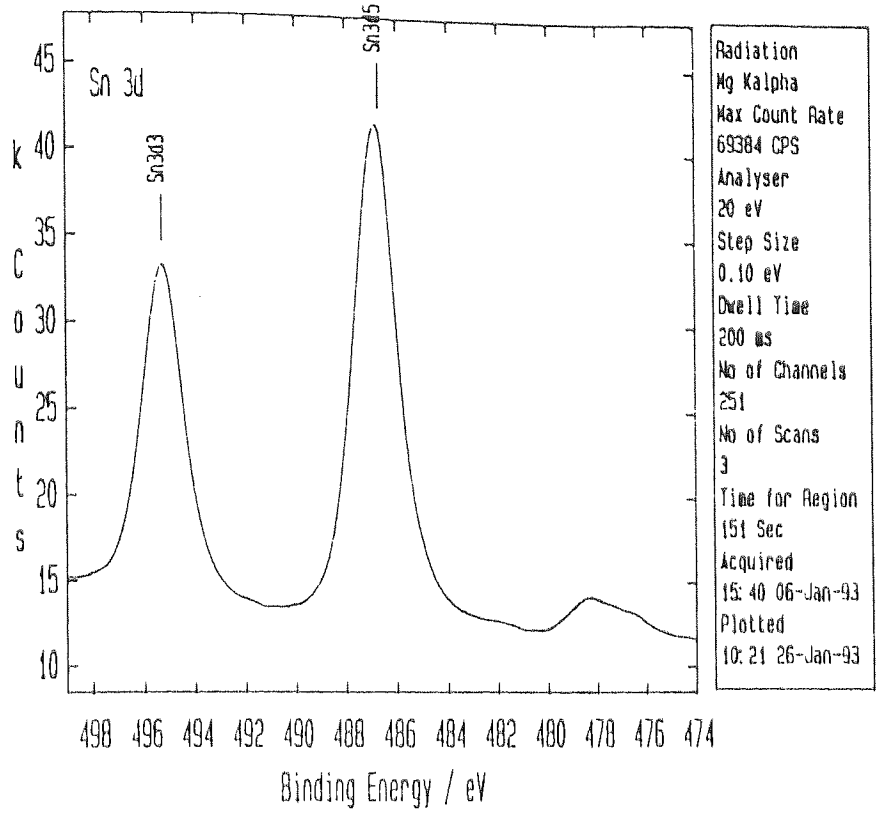

Figure 4.8a Tin XPS Spectrum of laponite after intercalation with polyoxycations.

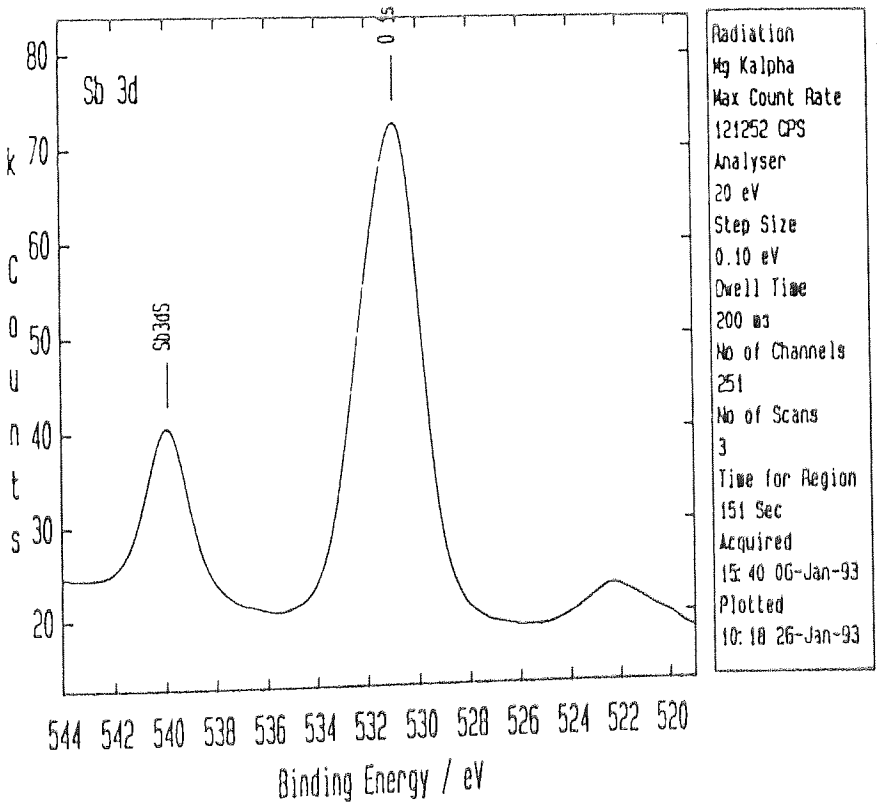

Figure 4.8b Antimony XPS Spectrum of laponite after intercalation with polyoxycations.

the formation of donor-acceptor complexes with 7,7,8,8-tetracyano-*p*-quinodimethane (tcnq)[118,119]. Some complexes were reported to show semiconducting properties[118] with conductivity values varying over an order of magnitude.

The initial organotellurium compound used for the intercalation investigation was 1,1'-Diiodo-1-telluracyclopentane. The compound was synthesised in the laboratory by standard literature methods[120]. All intercalation reactions using organotellurium compounds were executed in the microwave oven alone.

4.5.1 Intercalation of 1,1'-Diiodo-1-telluracyclopentane.

The initial investigation proceeded with an intercalation reaction using microwave irradiation (see section 3.4.3) whereupon 0.2g organotellurium compound was dissolved as far as possible in absolute ethanol (10 cm^3). The 1,1'-Diiodo-1-telluracyclopentane is a red crystalline solid[120] and when dissolved in absolute ethanol produces a bright yellow solution. Excess red solid was filtered off before the addition of laponite RD (1g) to the teflon container. After subjecting the reagents to five 1 minute bursts of microwave irradiation the flask was cooled and the contents filtered. A white clay and clear filtrate were obtained.

The decolourisation of the solvent was thus investigated. To show that it was not an artefact of the microwave radiation a blank experiment consisting of the organotellurium compound in the ethanol solvent was microwaved for five minutes. The solution remained a bright yellow colour. A portion of the original clear filtrate was tested with acidified silver nitrate solution[59]. This revealed a positive result for I^- ions in the solution (a yellow precipitate). It would appear that the clay facilitates a hydrolysis reaction of the organotellurium compound in a way analogous to that seen in the case of triphenyltin(IV) chloride (see chapter 3).

Although investigation *via* XPS appeared to show that no tellurium was present in the clay and XRD revealed a basal spacing of only 14.41Å, approximately equal to that of laponite RD, the fact that a hydrolysis reaction took place gave enough encouragement for a more detailed evaluation of a wider range of organotellurium compounds as intercalation agents.

A range of organotellurium compounds including $(MeOPh)_2TeCl_2$, $(MeOPh)_2TeBr_2$, $(EtOPh)_2TeCl_2$, $(EtOPh)_2TeBr_2$, $EtOPhTeCl_3$ and $(EtOPh)_2Te$ were subsequently synthesised and reacted with laponite RD.

4.5.2 Intercalation of *Bis* (*p*-methoxyphenyl)tellurium(IV) dichloride.

4.5.2.1 Synthesis of $(MeOPh)_2TeCl_2$.

Most synthetic routes leading to the preparation of biaryls require halogen substituted aromatic starting materials (as in the case of the Grignard reaction[121a,121b] and Ullmann coupling [122]). However a better method involves the use of tellurium tetrachloride as an electrophile[123]. In this case the aromatic compound must contain activating components (for example RO- or R_2N-) to produce aryltellurium trichlorides or *bis* (aryl)tellurium dichlorides as shown below.

$$CH_3OC_6H_5 + TeCl_4 \xrightarrow[1\text{ hour}]{60\text{-}80^\circ C} CH_3OC_6H_4TeCl_3 + HCl$$

$$CH_3OC_6H_5 + CH_3OC_6H_4TeCl_3 \xrightarrow[6\text{ hours}]{145\text{-}160^\circ C} (CH_3OC_6H_4)_2TeCl_2 + HCl$$

This method is very simple and gives excellent yields.

Quantitatively the synthesis was carried out as follows. Tellurium tetrachloride (7.5g) and anisole (15g) were refluxed for 6 hours at ~160°C. On cooling, the solution solidified. The final material crystallised from acetonitrile and was recrystallised in methanol. White crystals were obtained.

Yield = 9.5g, 83%. Melting point = 181-182°C (literature[123,124] = 181-183°C).
Elemental analysis found C = 40.6%, H = 3.30%. (Required C = 40.7%, H = 3.42%.)

An FTIR spectrum (Figure 4.9) showed the characteristic C-C and C-O vibrations from the organic part of the molecule at values between 1000 and 1600 cm^{-1}. The absorptions at the lower end of the spectrum, 600-300 cm^{-1} may be caused by the C-Te or possibly the Te-Cl bond within the molecule.

A ^{13}C solution N.M.R. spectrum (Figure 4.10) whereupon the compound was dissolved in $CDCl_3$ has also been characterised as shown in Table 4.7. It should be noted that the signals have been shifted upfield. The triplet centred at ~ 83.5ppm is derived from the solvent $CDCl_3$, however the correct value associated with this signal is 77ppm. The same phenomenon is seen with the pentet at 44.5ppm, attributable to the $DMSOD_6$. Consequently each signal on the spectrum must be decreased by 7 ppm to get true values.

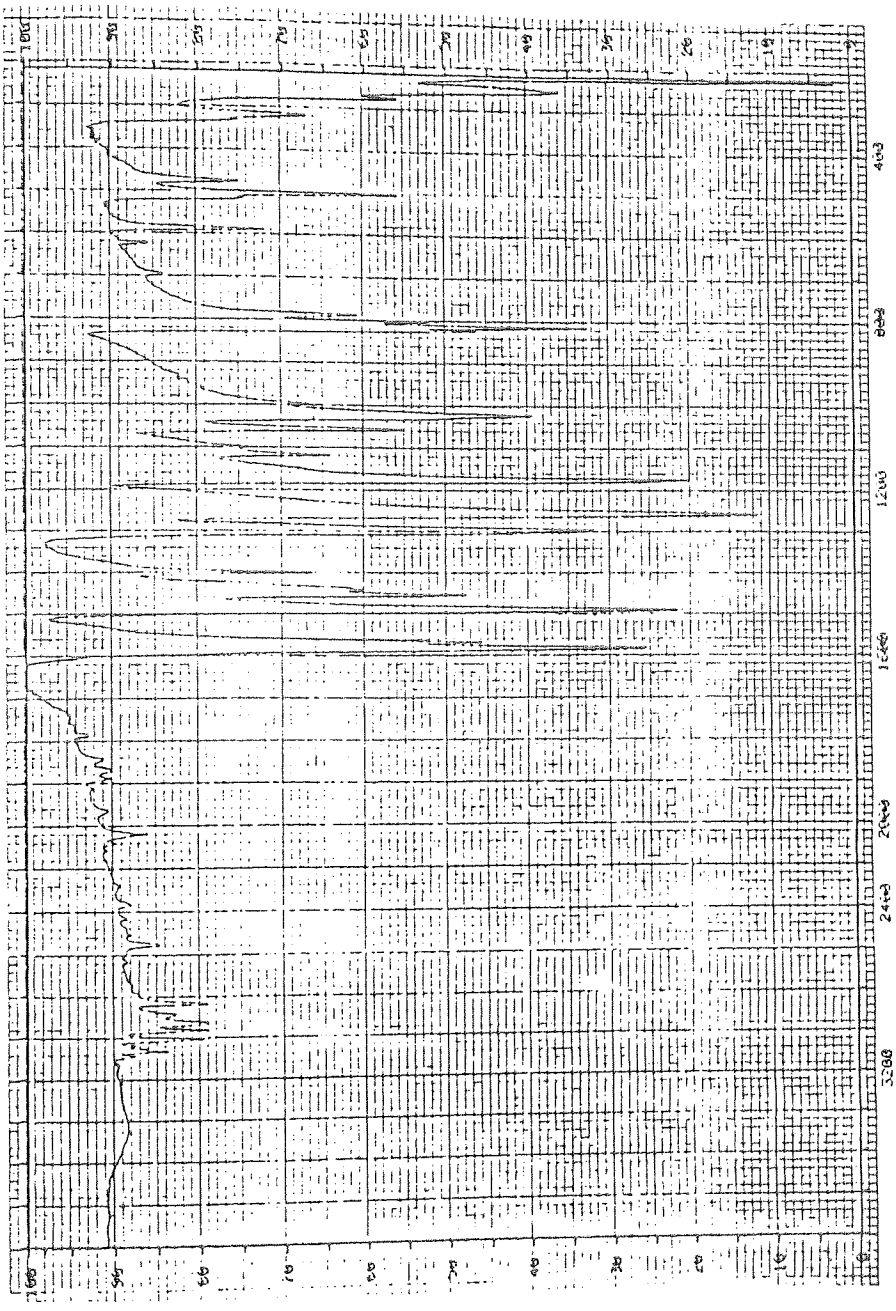

Figure 4.9 FTIR Spectrum of $(MeOPh)_2TeCl_2$.

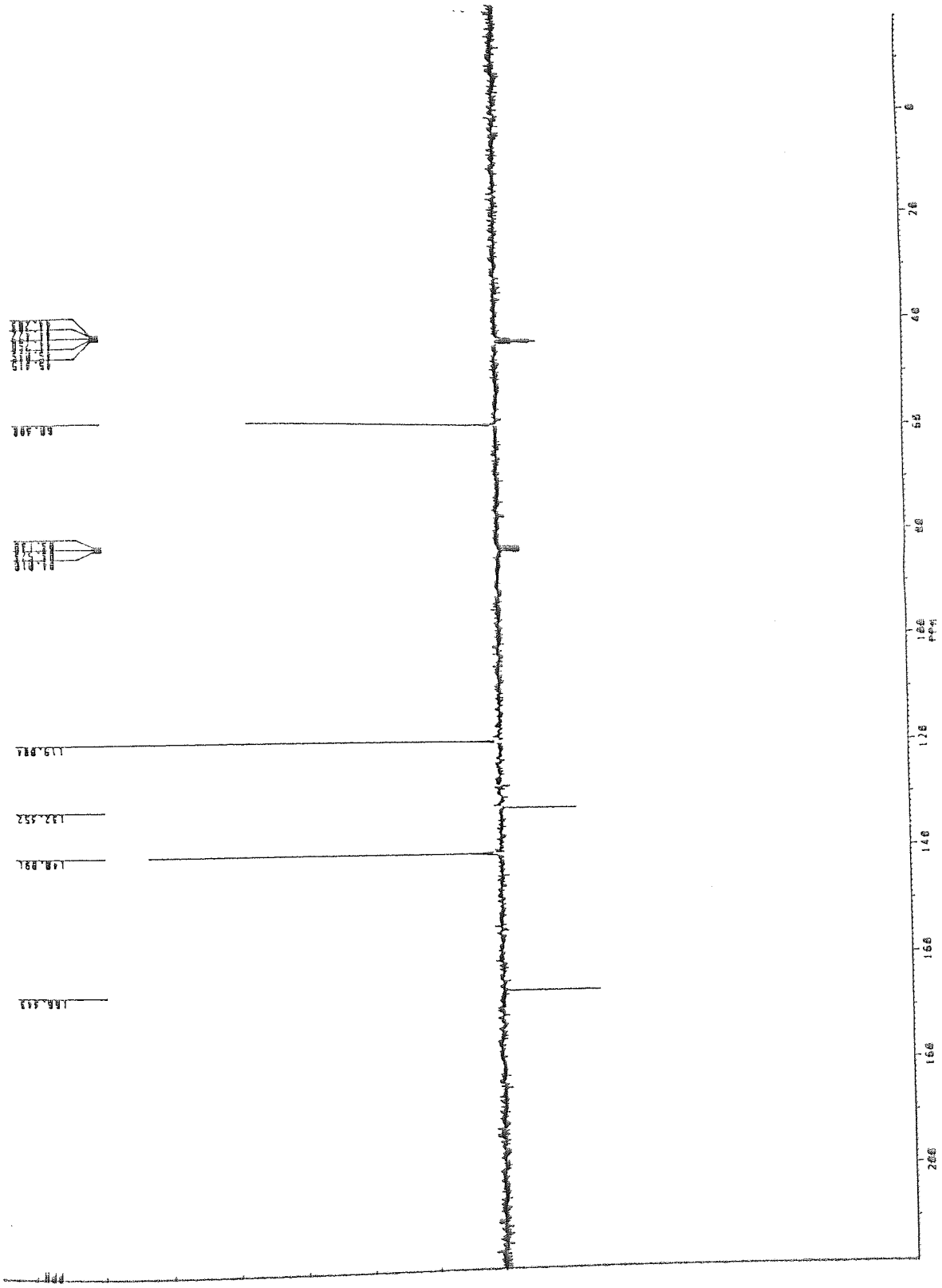

Figure 4.10 ^{13}C Solution NMR of $(MeOPh)_2TeCl_2$.

Signal Value (ppm)	Carbon assignment
53.4	5
112.8	3
125.4	1
133.9	2
159.3	4

NB. Carbon numbering is shown in the structure below:

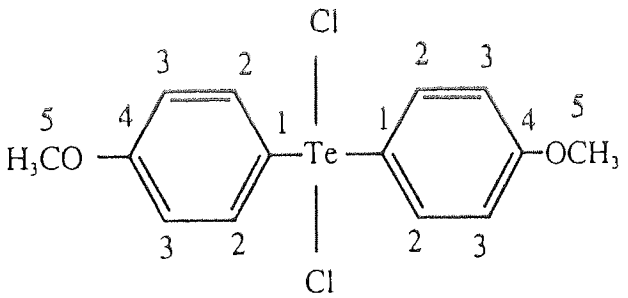

Table 4.7 ^{13}C N.M.R. characterisation of $(MeOPh)_2TeCl_2$.

4.5.2.2 Intercalation.

The intercalation was carried out using the microwave method (see section 3.4.3). After filtration a white clay was produced.

Analysis of the filtrate with silver nitrate solution[59] revealed the presence of Cl^- ions in the solution, suggesting that a hydrolysis reaction has taken place. Hydrolysis reactions of diaryltellurium(IV) dihalides are documented[125] whereupon *bis-p*-anisyltellurium oxychloride or *bis-(p*-anisyl)telluroxide can be formed under suitable conditions. By virtue of the fact that the Cl^- ions are found in the filtrate it is suggested in this case that the telluroxide (R_2TeO) is formed.

Analysis by GLC seems to confirm that the tellurium-carbon bond remains intact as no trace of anisole or possible decomposition products (benzene or methanol) were found in the filtrate.

Atomic absorption spectroscopy revealed a release of sodium ions in the region of 428ppm (compared with 100ppm for Ph_3SnCl and 15ppm for laponite RD). This could indicate that a far greater degree of hydrolysis is occurring with the organotellurium precursor.

Analysis of the product clay began with an XPS evaluation (see Figure 4.11). This confirmed the presence of tellurium in the clay shown by three bands. The lowest band, that at 573.9 eV is an artefact of the XPS experiment[70]. The other bands at slightly higher eV values, 575.1 and 576.7 cannot be confidently quantified, (although 576.7 eV is within the range listed for a Te-O bond), because of the very low concentration of tellurium within the clay (0.22%).

The XPS band found at 573.9eV in this sample suggests the presence of a low oxidation state of the metal, tellurium. This low oxidation state band has been found randomly throughout the organometallic samples (including organotin, organoantimony and organobismuth compounds) examined using XPS. It was the random nature of this feature which first suggested it may be an artefact of the XPS experiment.

The observations are certainly not without precedent since, for example, similar reduction of Co^{2+}[131] and Ni^{2+}[132] have been observed on clay surfaces on exposure to the x-ray flux; however to date there have been no reports of the phenomenon for organometallic compounds sorbed on clay surfaces.

In order to show that the presence of the low oxidation state peak is caused by the XPS and not by the intercalation reaction between the organometallic compound and the clay the following experiment was carried out.

Attention was directed to samples where the clay surfaces had been exposed to tellurium (IV) compounds i.e. $TeBr_4$ or $Br_3Te.C_6H_4.CH{=}N.CH_2CH_2N{=}CH.C_6H_4.TeBr_3$, (I),

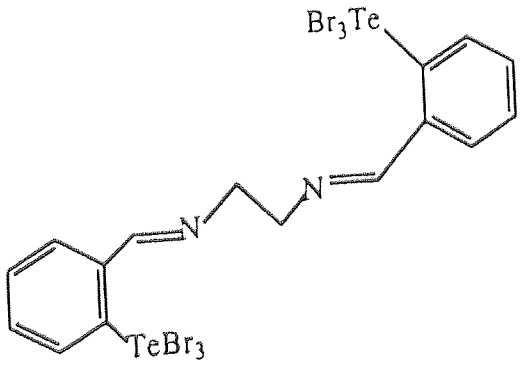

Compound I

since separation of the $3d_{5/2}$ photopeak energies for Te(IV) and Te(0) was likely to be better resolved[133]. It can be seen from Figure 4.12 that the XPS experiment showed two photopeaks with binding energies consistent with Te(IV) and Te(0). The XPS spectrum of compound (I) sorbed onto cetylpyridinium exchanged montmorillonite was then evaluated as a

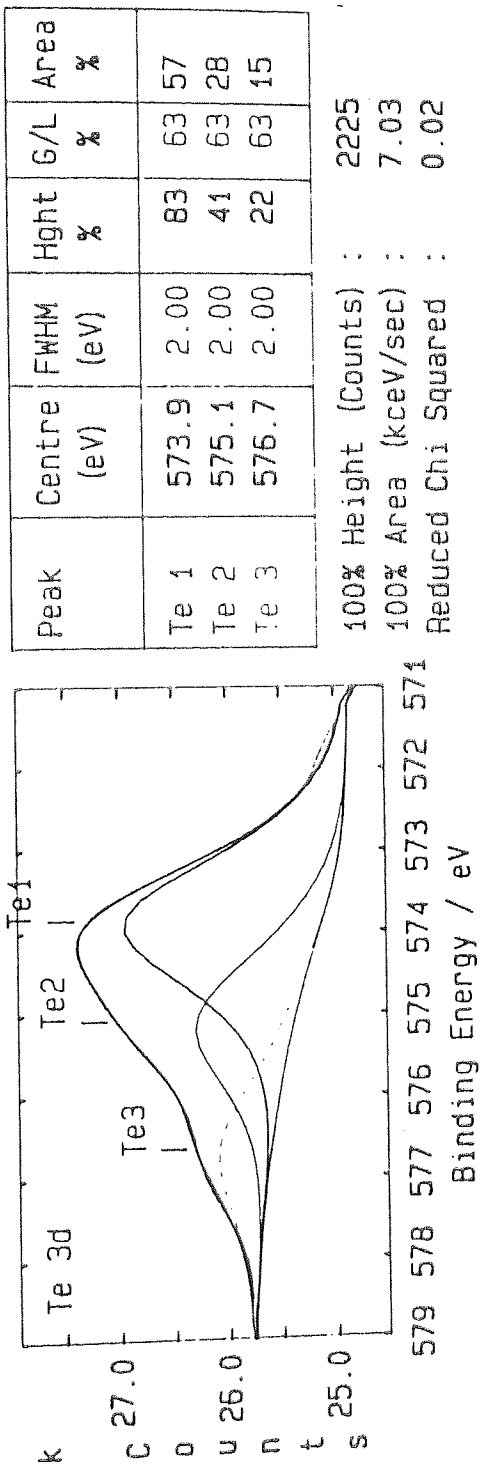

Figure 4.11 Tellurium XPS Spectrum of laponite reacted with $(MeOPh)_2TeCl_2$.

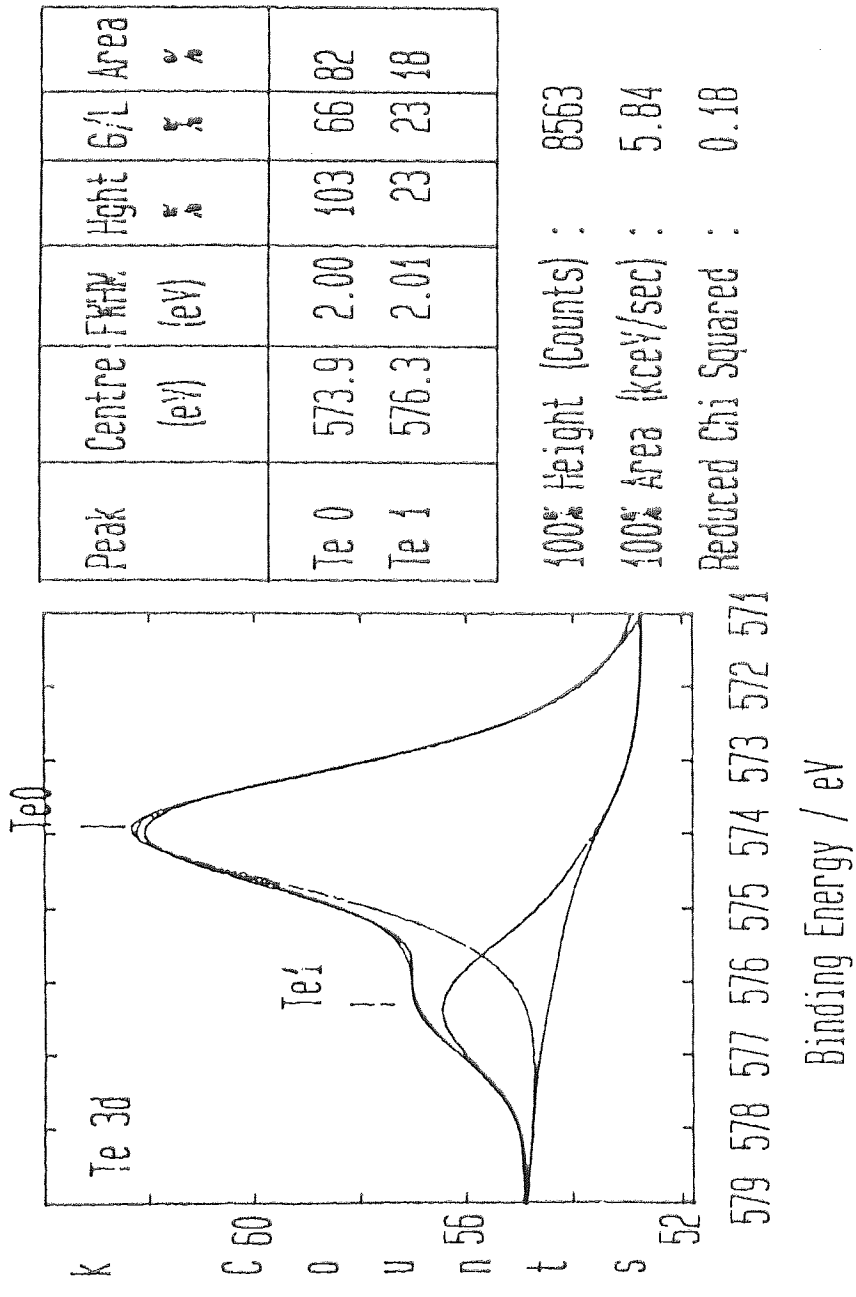

Figure 4.12 Tellurium XPS Spectrum of laponite reacted with $TeBr_4$.

function of time. The data are displayed graphically in Figures 4.13 and 4.14. It is clear that the Te(0) photopeak (573.5 eV) grows in intensity at the expense of the Te(IV) photopeak (576.0 eV) as the time of exposure of the surface to the X-ray flux increases. It therefore follows that XPS data obtained from clay sorbed organometallics needs to be interpreted with care.

An FTIR spectrum (Figure 4.15) reveals absorptions, although partially masked by the broad absorptions from the clay, in the region 1000-1600 cm^{-1}. These absorptions are caused by the C-O and C-C vibrations from the benzene ring. This confirms that the organic groups of the molecule are attached to the surface of the clay.

A ^{13}C MASNMR spectrum (Figure 4.16) when compared with that of the ^{13}C solution N.M.R. spectra of the organometallic precursor and a reference solution spectrum of a possible other product anisole (Figure 4.17), shows the same pattern of bands as the organometallic precursor, rather than that of anisole (illustrated in Table 4.8). This shows that the bulk of the precursor is present on the surface of the clay and that this system is behaving in an entirely different way to that described by Bond[54] for Ph_3SnCl. It is suggested that the Te-C bond remains intact unlike the Ph_3SnCl system where there is breakage of the Sn-C bond.

Carbon assignment	^{13}C solution signal in anisole	^{13}C solution signal in $(MeOPh)_2TeCl_2$	^{13}C m.a.s.n.m.r. signal from clay
1	120.8	125.4	124.5
2	129.7	133.9	134.7
3	114.1	112.8	114.0
4	159.8	159.3	161.2
5	55.0	53.4	52.6

NB. Carbon assignments as outlined with table 4.7

Table 4.8 ^{13}C solution and ^{13}C MASNMR signals for $(MeOPh)_2TeCl_2$, anisole and laponite RD intercalated with $(MeOPh)_2TeCl_2$.

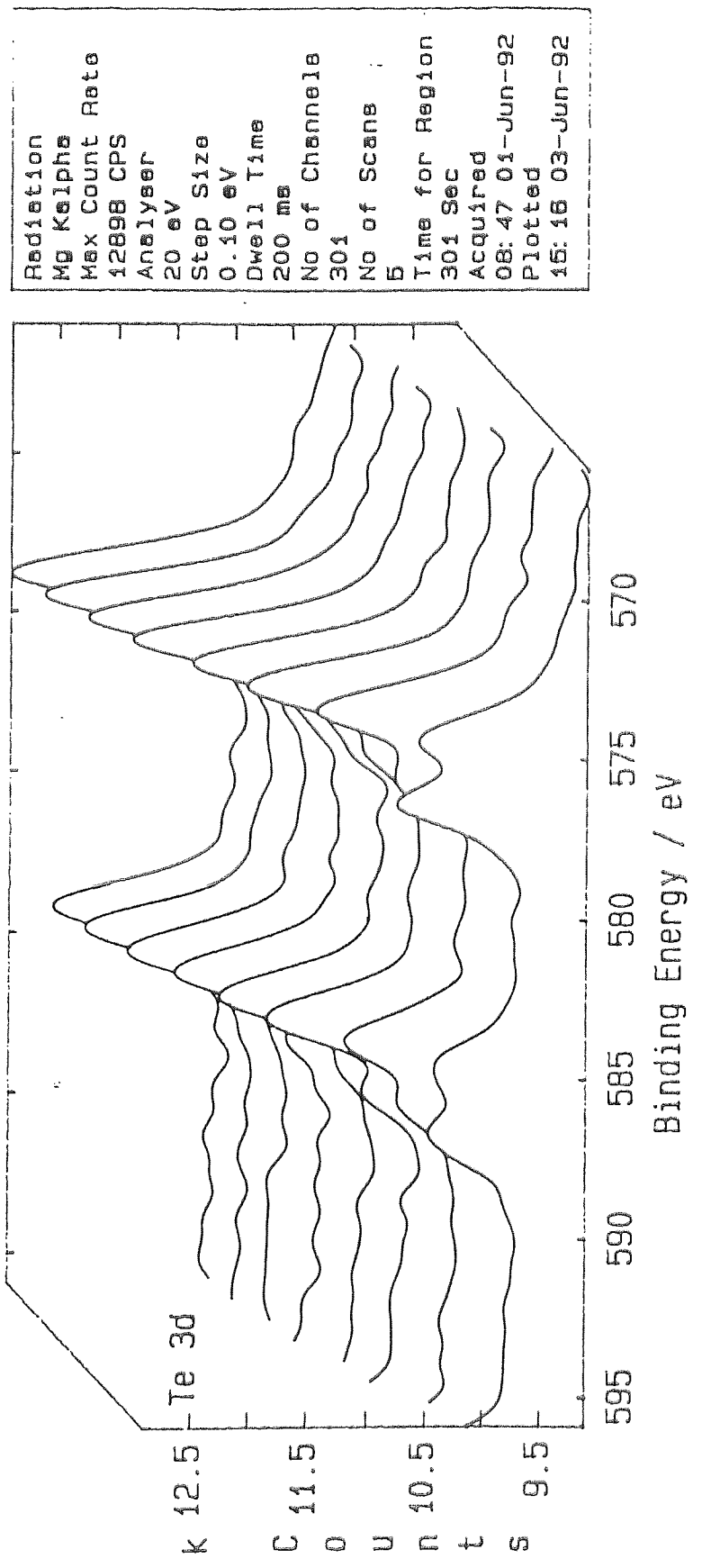

Figure 4.13 Tellurium XPS Spectrum of montmorillonite reacted with compound (I) with respect to time.

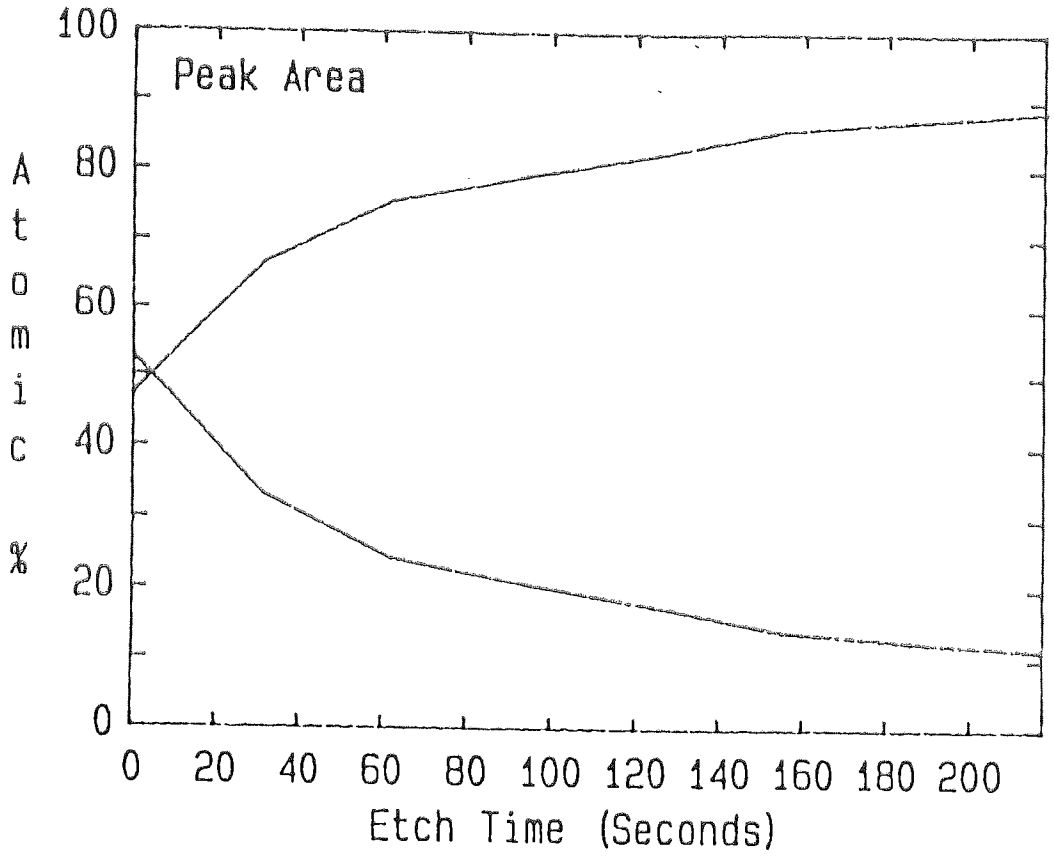

Figure 4.14 Plot showing the growth of the Te(0) photopeak at the expense of the Te(IV) photopeak with increasing exposure to x-ray flux.

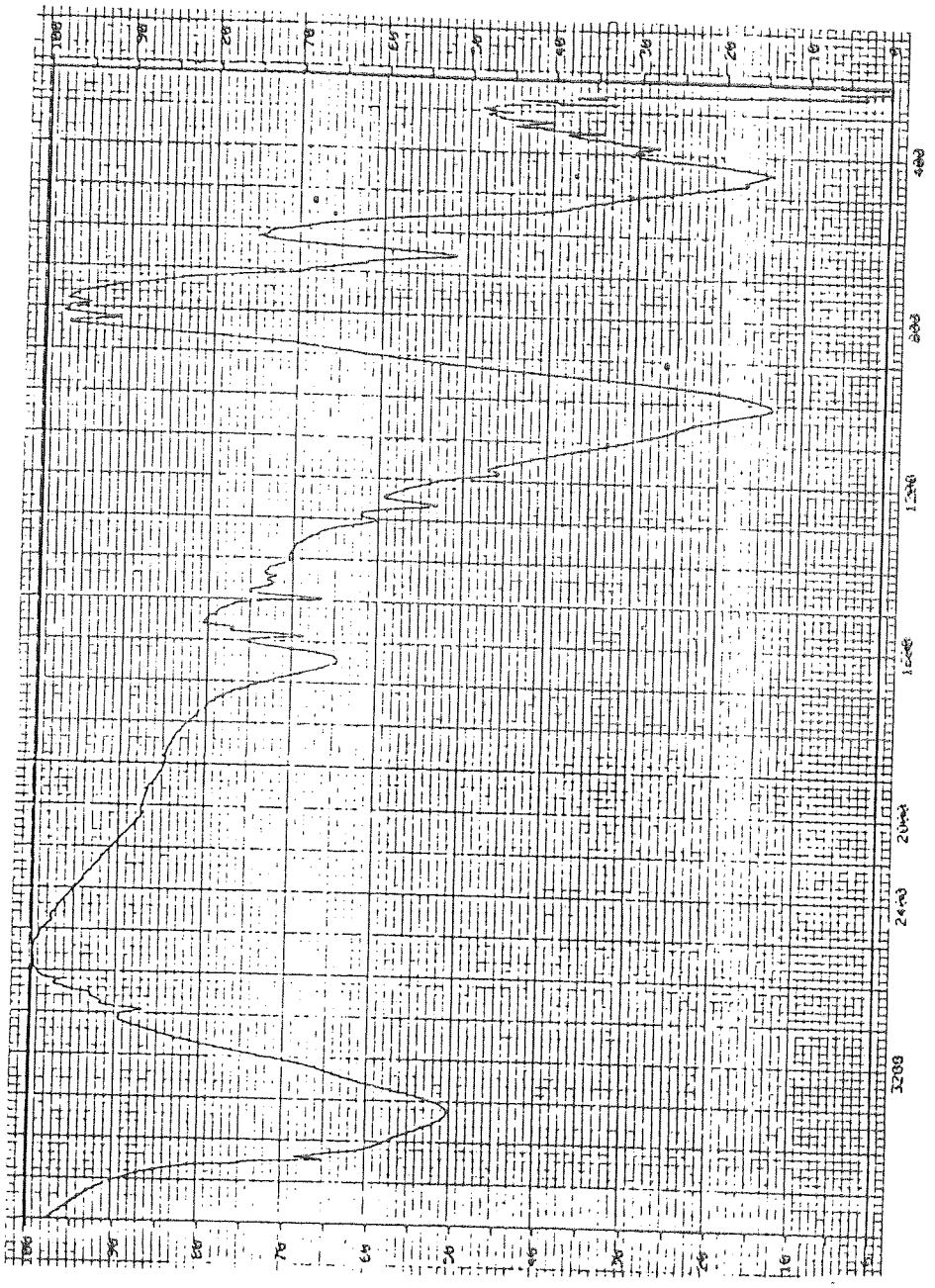

Figure 4.15 FTIR Spectrum of laponite RD reacted with $(MeOPh)_2TeCl_2$

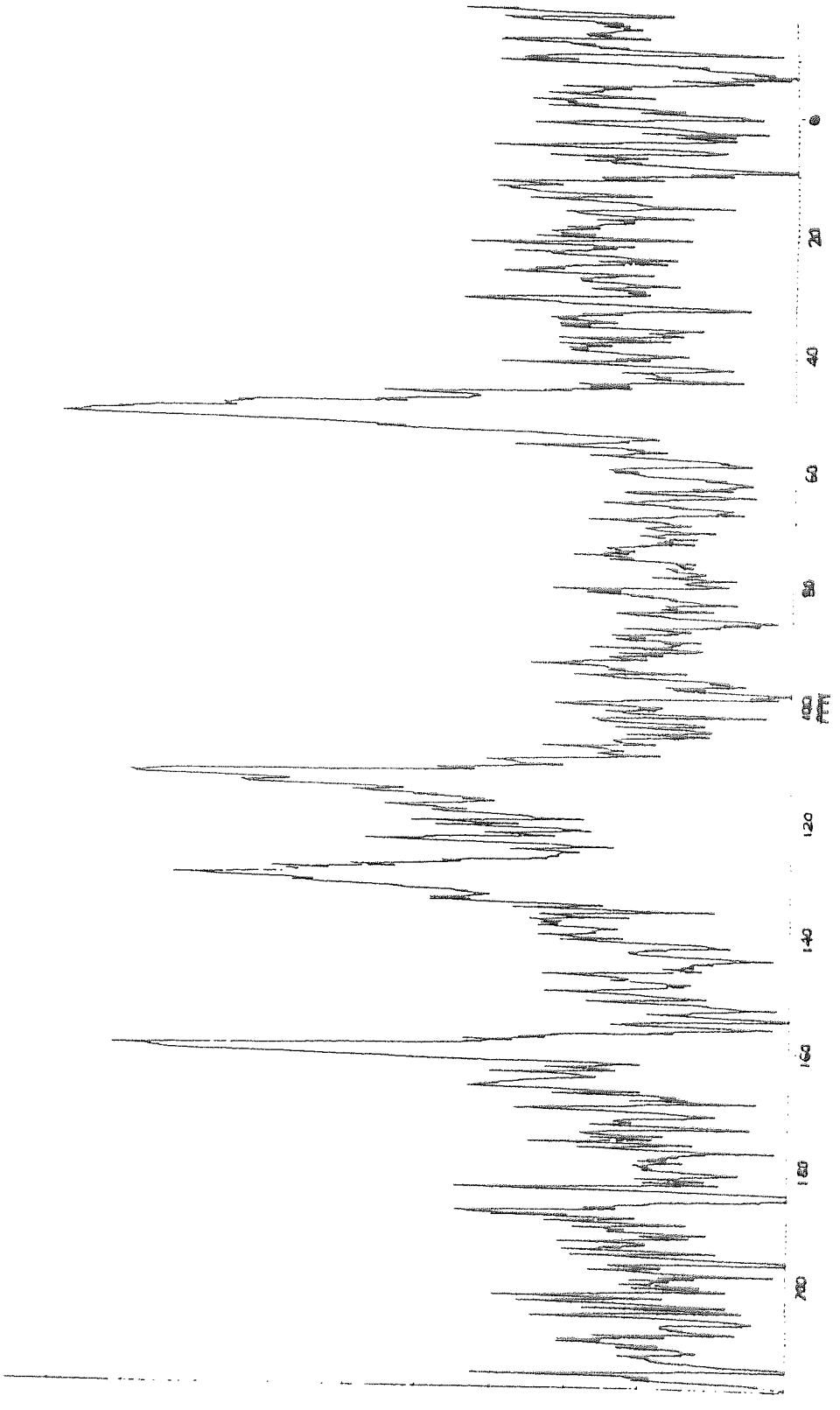

Figure 4.16 ^{13}C MASNMR Spectrum of laponite RD reacted with $(MeOPh)_2TeCl_2$.

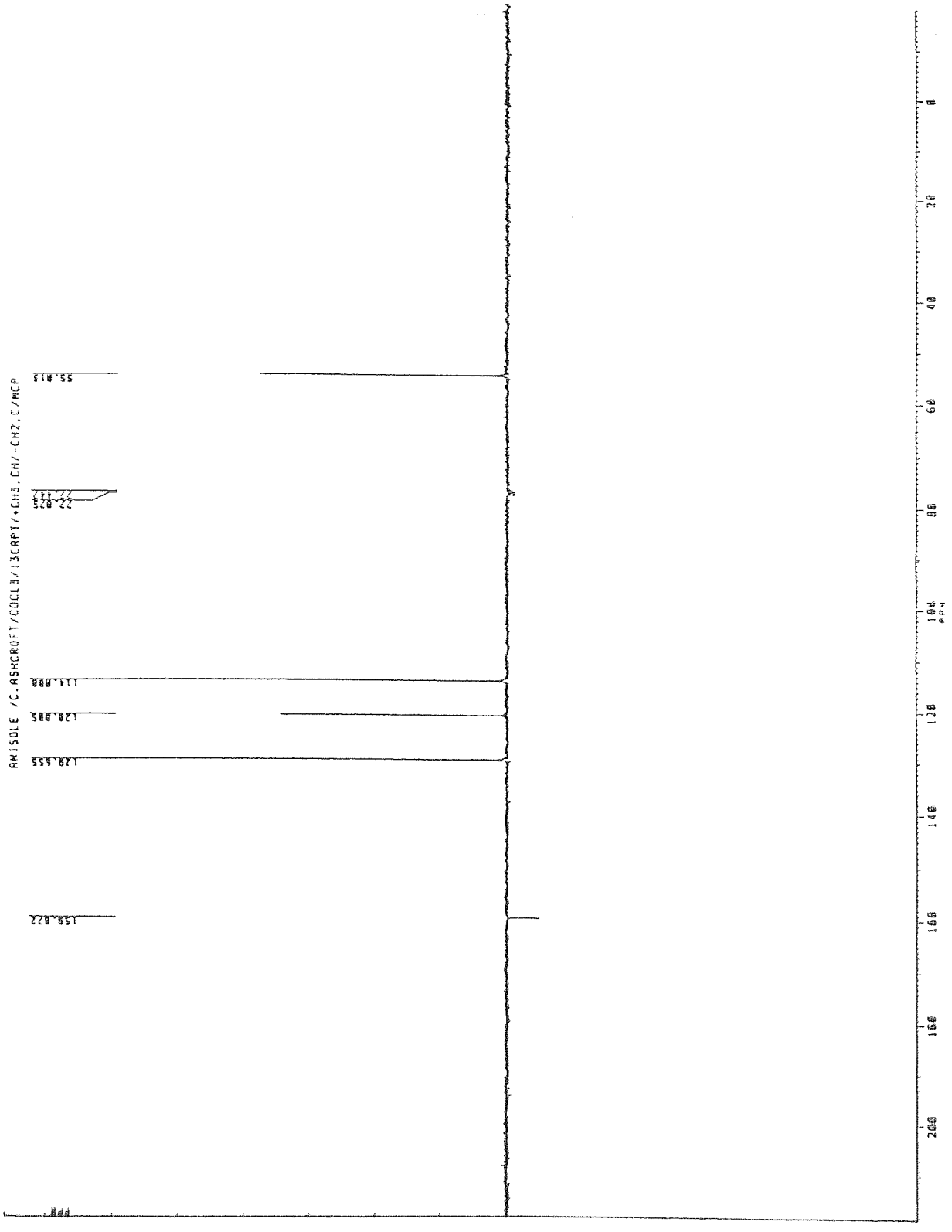

Figure 4.17 ^{13}C Solution NMR Spectrum of Anisole.

The complexity of the ^{13}C MASNMR spectrum obtained from the reaction of laponite RD with $(MeOPh)_2TeCl_2$ suggests that the tellurium compound on the clay surface may be present in more than one chemical form. This is consistent with the idea that a hydrolysis reaction is taking place, hence the original precursor and the hydrolysis product may be present.

X-ray powder diffraction studies indicated a basal spacing of 13.7Å, which was less than that of laponite RD (~14.5Å). This would suggest that it is not an intercalation or pillaring reaction that is taking place with this precursor.

In summary, with the precursor $(MeOPh)_2TeCl_2$ it appears that a substantial hydrolysis reaction takes place on reaction with the laponite RD. This assumption is derived from the very high sodium release measured by AA spectroscopy and the positive identification of chloride ions in the filtrate. The sodium ions are released from the interlayer of the laponite and replaced by acid protons. This exchange is facilitated by the release of hydrochloric acid following a hydrolysis reaction on the clay surface whereupon the following steps occur.

$$R_2TeCl_2 \xrightarrow{\text{Clay / } H_2O} R_2TeO + 2H^+Cl^-$$

$$Na^+\text{-Laponite} + HCl \longrightarrow H^+\text{-Laponite} + NaCl$$

Other spectroscopic methods (XPS, NMR and FTIR) show that both the tellurium and the organic part of the molecule are contained within the final clay (probably on the surface as there appears to be no increase in the basal spacing).

4.5.3 Dimethoxyphenyltellurium(IV) dibromide.

In order to confirm visually that a hydrolysis reaction on the clay surface was occurring the dibromide derivative (a bright yellow crystalline material) was synthesised. If this compound undergoes hydrolysis on the clay surface then the solution would lose the yellow colour (the telluroxide formed is a colourless compound).

4.5.3.1 Synthesis of $(MeOPh)_2TeBr_2$.

To $(MeOPh)_2TeCl_2$ (1g) in absolute ethanol (50 cm^3) was added sodium bromide (NaBr)(2g). The solution was refluxed for two hours. Filtration yielded a yellow crystalline material which was recrystallised in absolute ethanol.

Yield = 80%. Melting point = 194-195°C (literature[126] = 190°C)
Elemental analysis found C = 33.7%, H = 2.93%. (Required C = 33.5%, H = 2.93%)

An FTIR spectrum (Figure 4.18) showed the characteristic vibrations between 1000 and 1600 cm^{-1} of the organic C-C and C-O vibrations. The lack of a broad absorption at 3400 cm^{-1} showed that the compound had not hydrolysed. Absorptions lower than 600 cm^{-1} may be derived from the Te-C and the Te-Cl vibrations.

4.5.3.2 Intercalation

Intercalation was carried out *via* the method of microwave heating. On filtration it was noted that the solution had decolourised (as with the 1,1'-Diiodo-1-telluracyclopentane in section 4.5.1). [A blank experiment of $(MeOPh)_2TeBr_2$ in ethanol was subjected to five 1 minute bursts of microwave radiation and remained yellow, thus ruling out an artefact of the microwave energy.] Testing the filtrate with silver nitrate solution[59] confirmed the presence of Br^- ions in the solution (a cream coloured precipitate was formed).
Analysis of the filtrate by AA spectroscopy revealed a large Na^+ release of 297ppm.

XPS (see Figure 4.19) indicated the presence of tellurium within the clay with a band seen at 575.8 eV, but beyond stating that a tellurium(IV) compound is present further characterisation is not possible due to the small quantity of tellurium contained within the clay (<1%).

FTIR spectroscopy (see Figure 4.20) shows the organic C-C and C-O vibrations between 1000 and 1600 cm^{-1}, again partially masked by the broad absorptions of the laponite. This therefore shows that the organic part of the molecule is attached to the clay surface.

A basal spacing of 14.9Å was obtained by XRD. This is slightly larger than that of laponite, although not by a significant amount. This may suggest as with the dichloride derivative that little or no intercalation/pillaring is taking place.

4.5.4 Diethoxyphenyltellurium(IV) dihalide.

Preparation of the diethoxytelluriumdichloride and dibromide are well documented in the literature[124,126]. Preparative routes include the addition of chlorine to a solution of diethoxyphenyltelluride $[(EtOPh)_2Te]$ in tetrachloromethane; by heating *bis*(*p*-ethoxyphenyl)telluritrichloride with excess phenetole at 180-190°C[127] or by heating tellurium tetrachloride with phenetole at 180-190°C (the analogous preparation to the one used to

Figure 4.18 FTIR Spectrum of $(MeOPh)_2TeCl_2$.

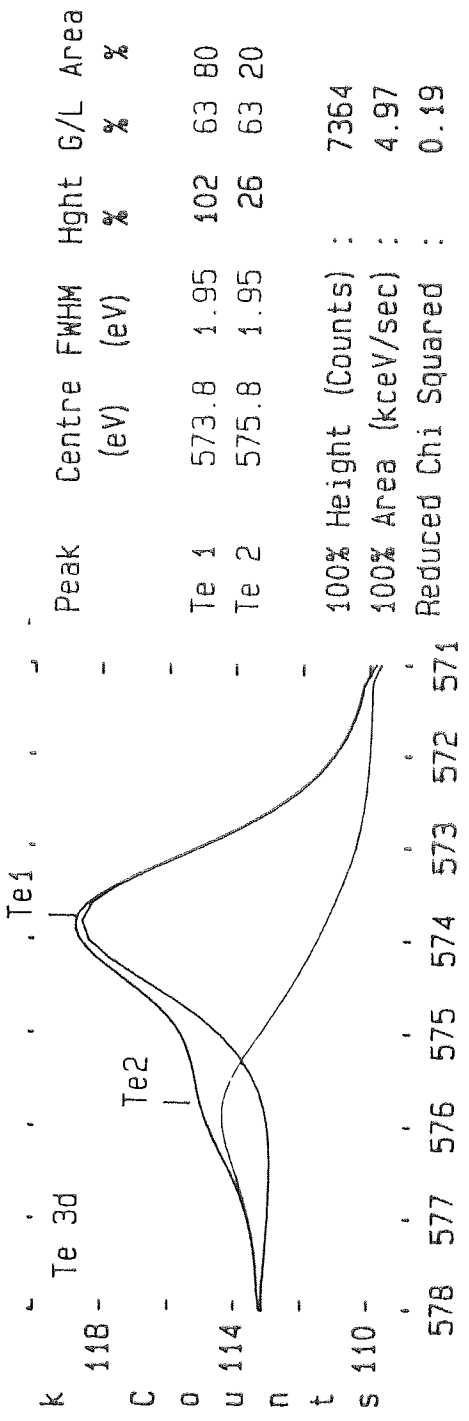

Figure 4.19 Tellurium XPS Spectrum of laponite reacted with $(MeOPh)_2TeCl_2$.

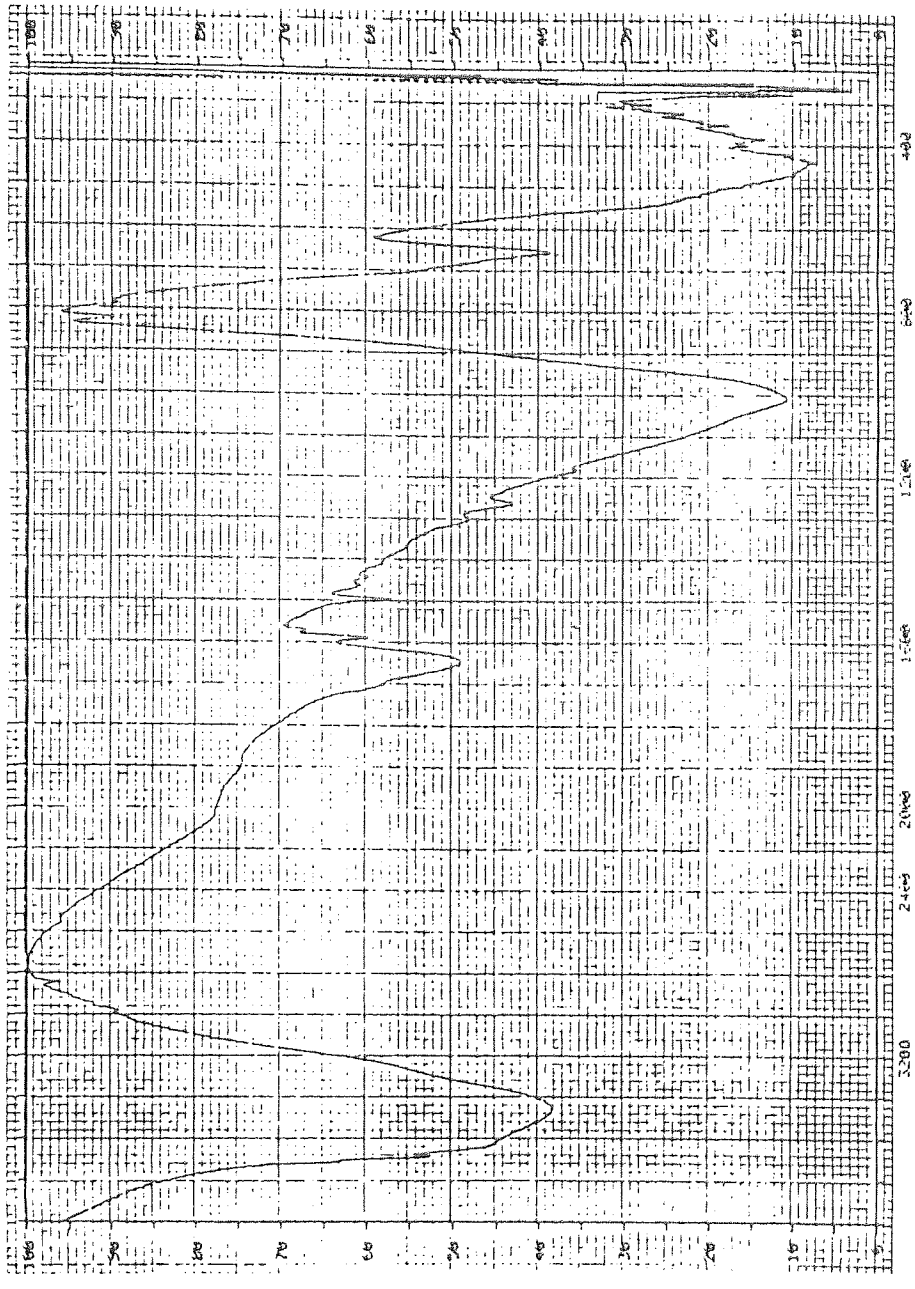

Figure 4.20 FTIR Spectrum of laponite reacted with $(MeOPh)_2TeCl_2$.

successfully prepare the methoxy derivative). It was this route that was taken to synthesise the required precursor.

4.5.4.1 Synthesis.

Tellurium tetrachloride (7.5g) and phenetole (15g) were refluxed for 6 hours at 180°C. The solution on cooling solidified and the product was obtained from acetonitrile and recrystallised from absolute ethanol. White crystals were obtained.

Yield = 90%. Melting point = 105-106°C (literature[125] = 108°C).
Elemental analysis found C = 43.7%, H = 4.01%. (Required, C = 43.6%, H = 4.12%).

An FTIR spectrum (see Figure 4.21) showed all the features expected with this compound.

A ^{13}C solution N.M.R. spectrum is shown in Figure 4.22 and characterised in Table 4.9. The numbering of the carbon atoms is shown below:

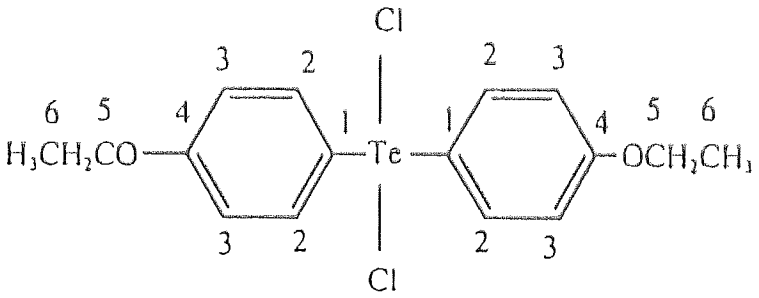

Signal Value (ppm)	Carbon assignment
14.6	6
63.8	5
115.9	3
124.9	1
135.4	2
161.5	4

Table 4.9 ^{13}C solution N.M.R. characterisation of $(EtOPh)_2TeCl_2$.

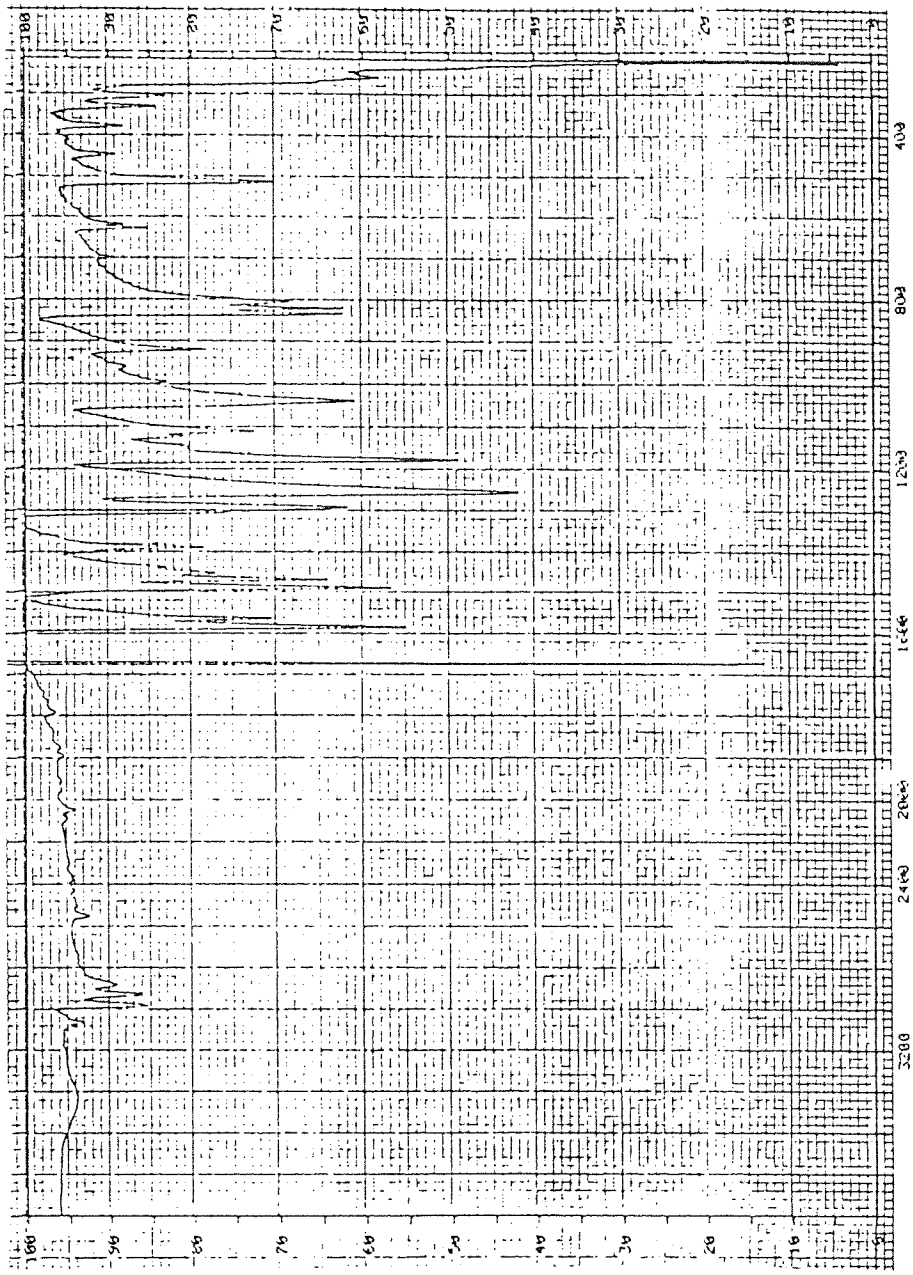

Figure 4.21 FTIR Spectrum of $(EtOPh)_2TeCl_2$.

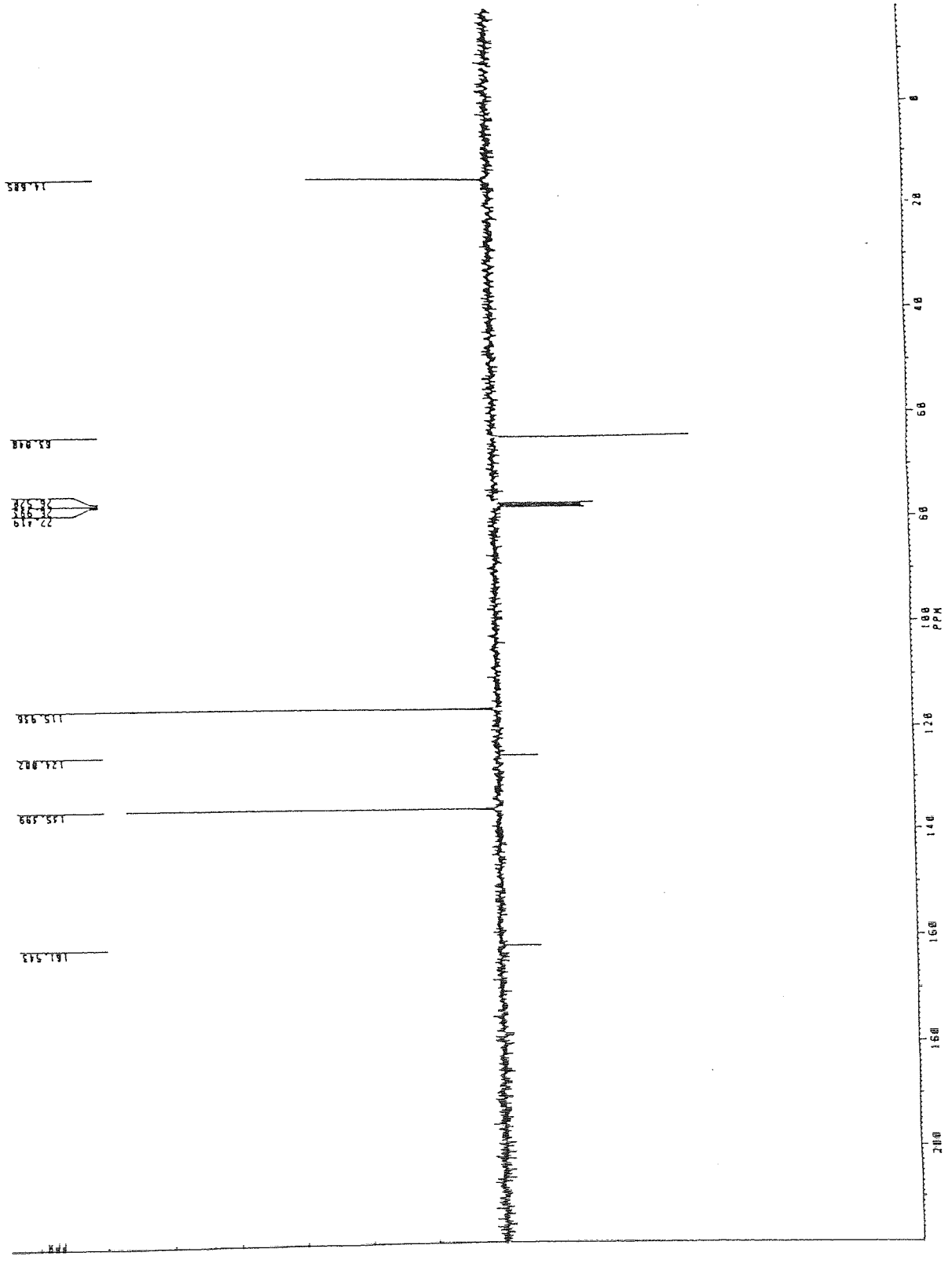

Figure 4.22 ^{13}C Solution NMR of $(EtOPh)_2TeCl_2$.

4.5.4.2 Intercalation

Microwave heating was utilised to facilitate the reaction and procedures followed were those outlined previously.

Analysis of the filtrate by AA spectroscopy showed a Na^+ release of 242ppm; GLC studies revealed no trace of phenetole in the filtrate hence suggesting that the Te-C bond is preserved within the clay. The filtrate when tested with silver nitrate solution[59] confirmed the presence of Cl^- ions by the appearance of a white precipitate.

XPS (see figure 4.23) confirmed the presence of tellurium within the sample with a band at 575.5 eV but characterisation beyond that of a tellurium (IV) compound was not possible due to the low concentration of tellurium in the clay (less than 1%).

An FTIR spectrum (Figure 4.24) showed the absorptions associated with the organic part of the molecule, although masked once again by the clay bands.

A ^{13}C MASNMR spectrum (Figure 4.25) was compared with the ^{13}C solution spectrum of the precursor (Figure 4.22) and that of phenetole (Figure 4.26) a possible other product from the intercalation reaction. The characterisation is shown in Table 4.10.

Carbon assignment	^{13}C solution signal in phenetole	^{13}C solution signal in $(EtOPh)_2TeCl_2$	^{13}C MASNMR signal from clay
1	120.7	124.9	
2	129.6	135.4	130.1
3	114.6	115.9	114.5
4	159.2	161.5	159.4
5	63.3	63.8	55.5 60.9
6	15.0	14.6	10.8 13.9

Table 4.10 ^{13}C solution and ^{13}C m.a.s.n.m.r. signals for $(EtOPh)_2TeCl_2$, phenetole and laponite RD intercalated with $(EtOPh)_2TeCl_2$.

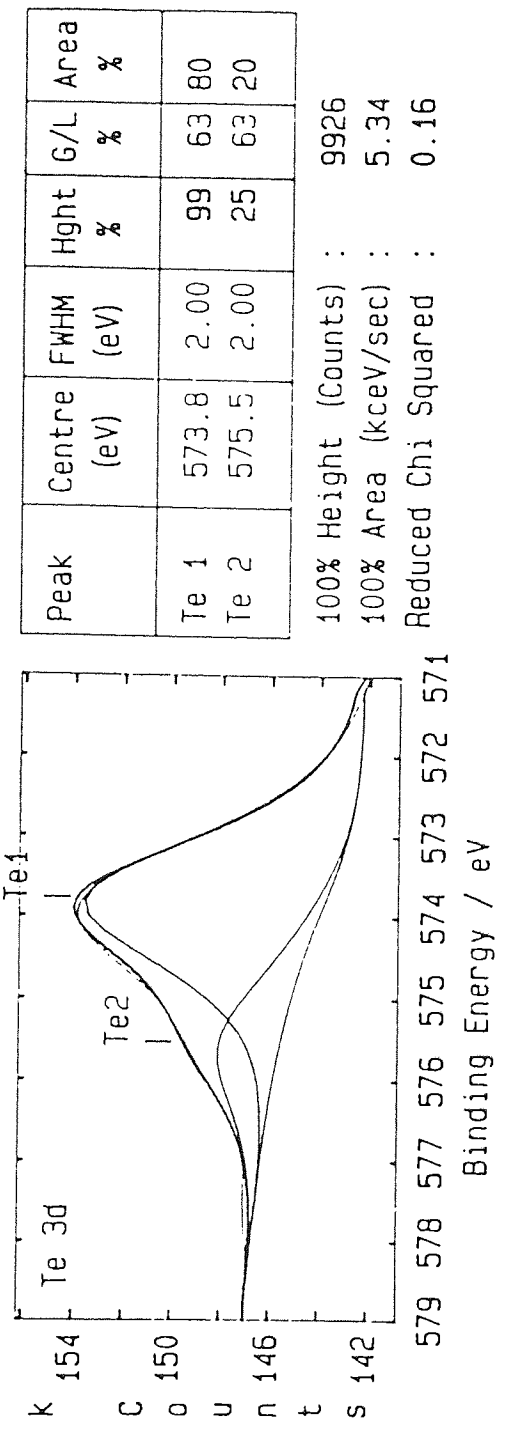

Figure 4.23 Tellurium XPS Spectrum of laponite reacted with $(EtOPh)_2TeCl_2$

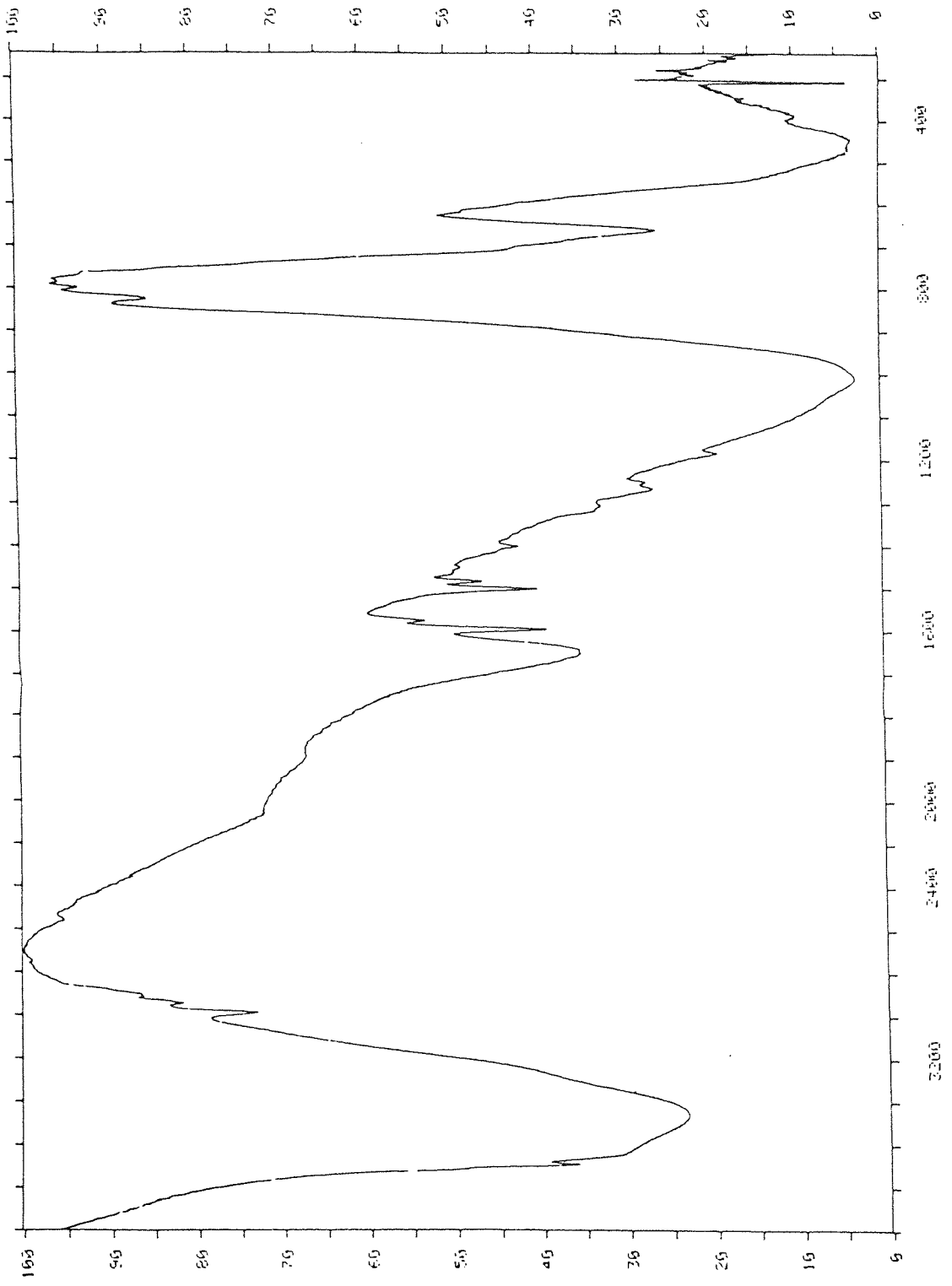

Figure 4.24 FTIR Spectrum of laponite reacted with $(EtOPh)_2TeCl_2$.

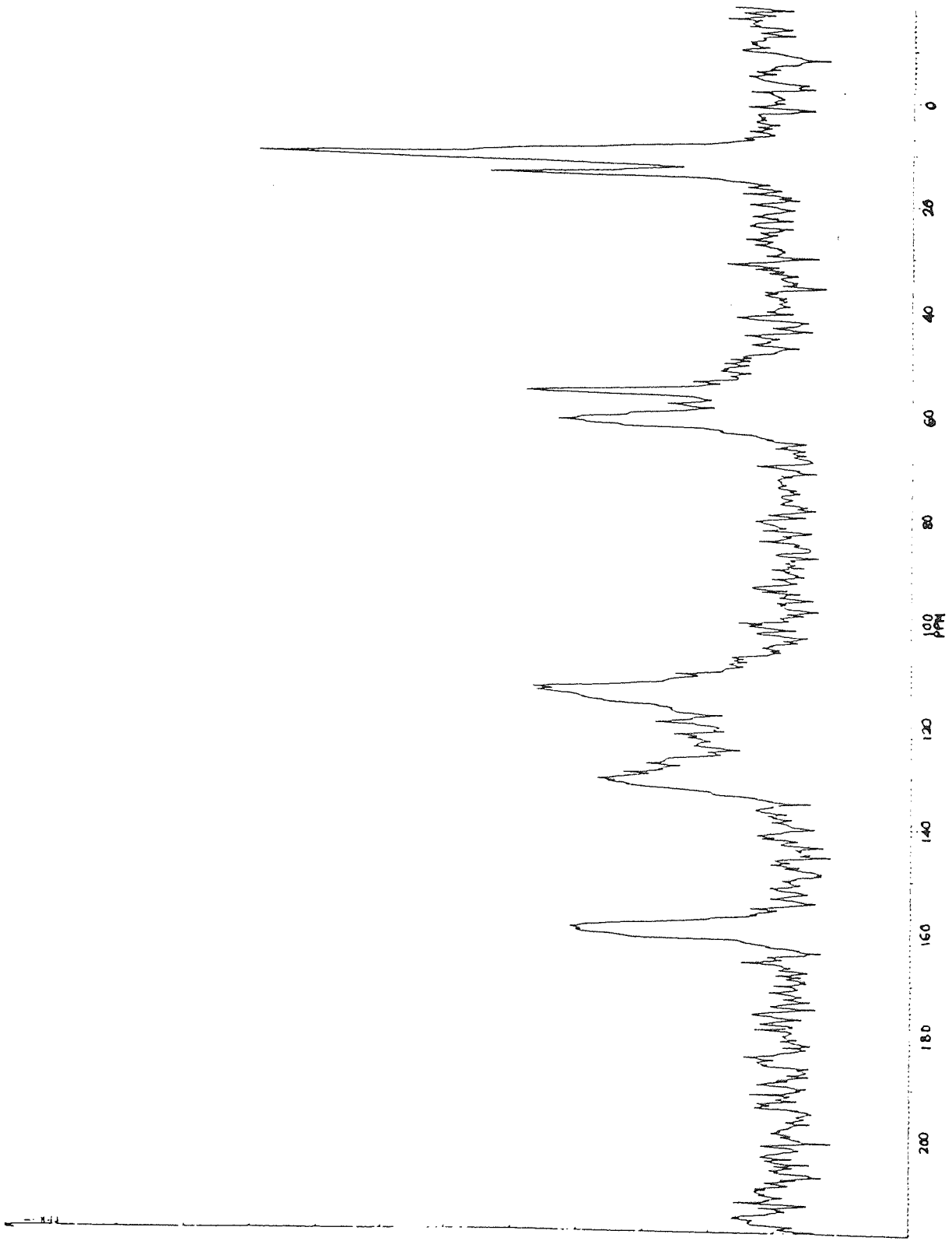

Figure 4.25 ^{13}C MASNMR Spectrum of laponite RD reacted with $(EtOPh)_2TeCl_2$.

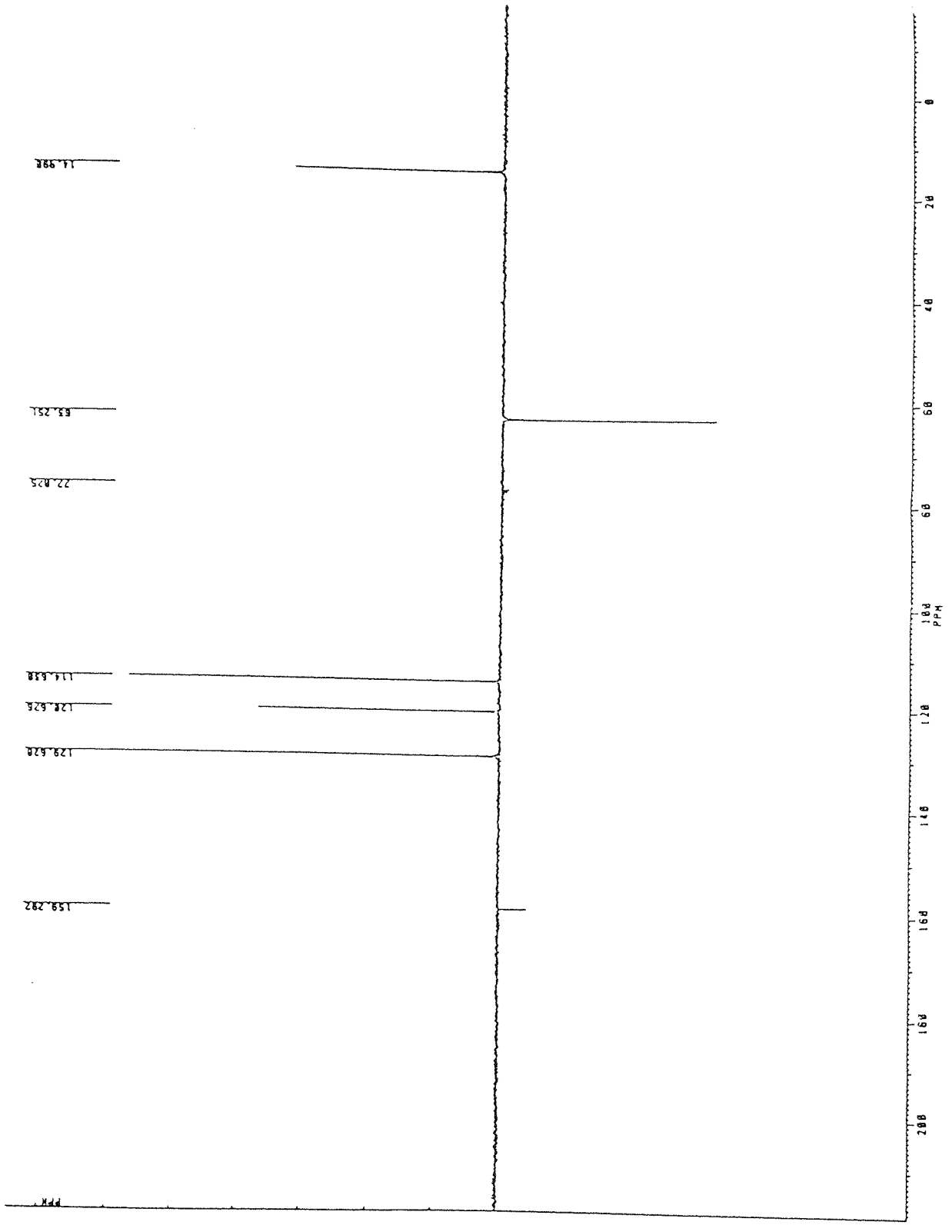

Figure 4.26 ^{13}C Solution NMR Spectrum of Phenetole.

The definite doublet for the two alkyl carbons show that they are present in two different chemical environments.

XRD revealed a basal spacing of 14.97Å, again slightly above that of laponite.

All indications point towards a hydrolysis reaction leading to the organotellurium compound being incorporated into the surface of the clay and not the pillaring reaction seen with the Ph_3SnCl system.

4.5.5 *Bis*(*p*-ethoxyphenyl)tellurium(IV) dibromide

4.5.5.1 Synthesis

Synthesis was *via* halogen replacement as shown below:

$$(EtOPh)_2TeCl_2 + 2NaBr \text{ ----------> } (EtOPh)_2TeBr_2 + NaCl$$

The $(EtOPh)_2TeCl_2$ (1g) and NaBr (2g) in absolute ethanol (50 cm^3) were refluxed for 2 hours. After cooling, filtration yielded a white solid and yellow filtrate. The white solid proved to be an inorganic material, the FTIR spectrum showed no organic absorptions. The filtrate on evaporation yielded yellow needle-like crystals.

Yield = 66%. Melting point = 114-115°C (literature[125] = 127°C).
Elemental analysis found C = 36.5%, H = 3.35%. (Required C = 36.3%, H = 3.42%).

An FTIR spectrum (Figure 4.27) showed all the features characteristic of this molecule.

4.5.5.2 Intercalation.

The microwave method of intercalation was utilised. On filtration it was seen that the solution had decolourised suggesting that the hydrolysis reaction seen in the previous organotellurium reagents also proceeds with this precursor. The positive result for Br^- ions in the filtrate *via* the silver nitrate test[59]; the lack of phenetole in the filtrate analysed by GLC; and the large Na^+ release (182ppm) all followed the pattern seen previously with other organotellurium species.

Analysis of the resultant clay by XPS (Figure 4.28) confirmed the presence of a tellurium (IV)

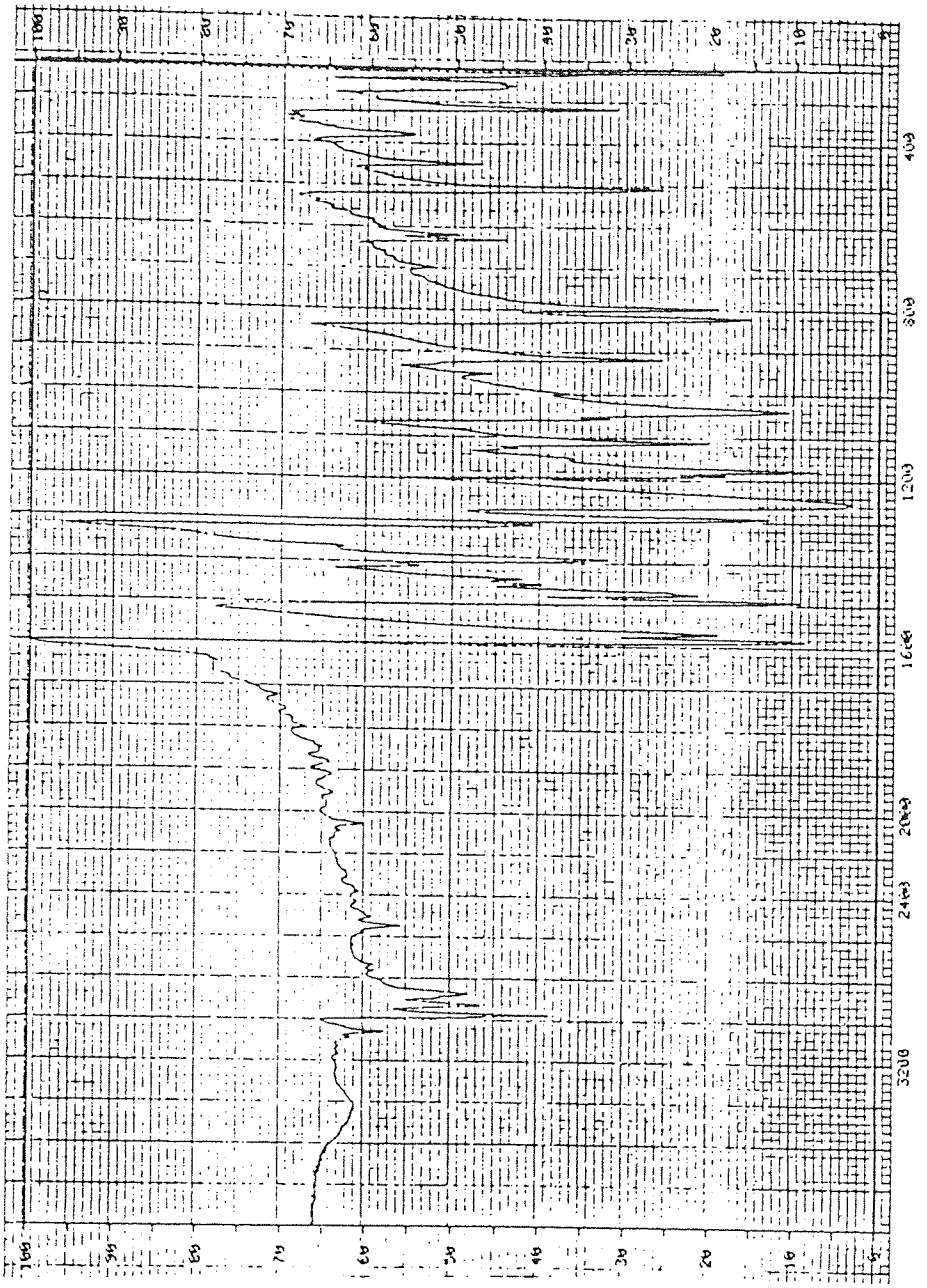

Figure 4.27 FTIR Spectrum of $(EtOPh)_2TeBr_2$.

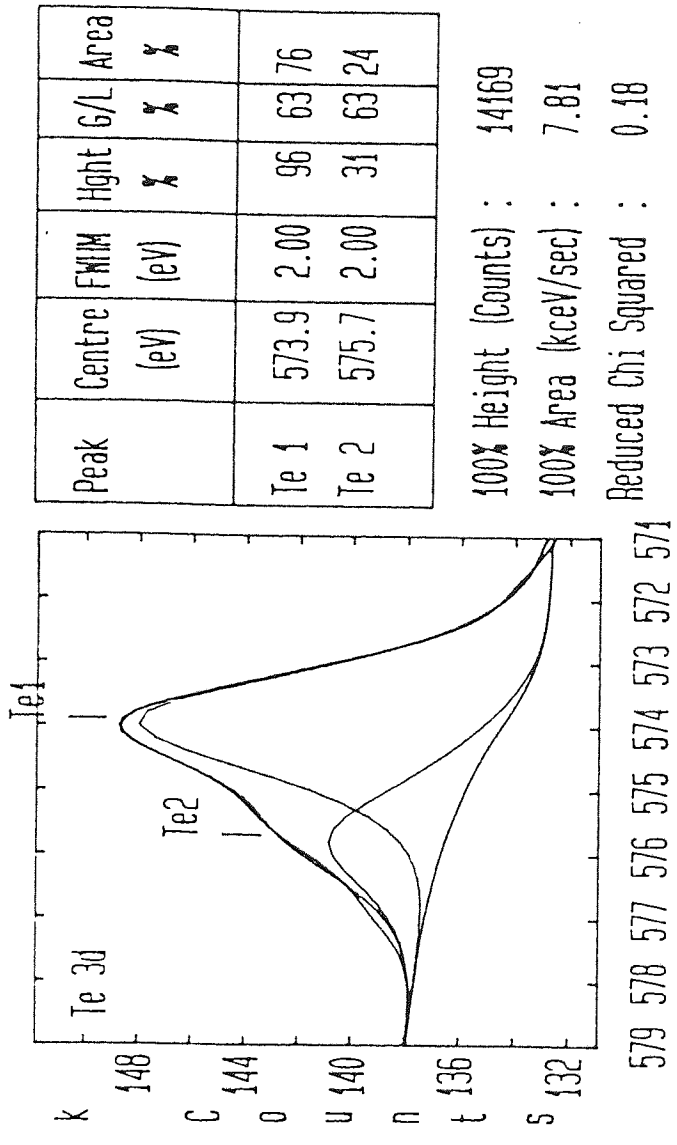

Figure 4.28 Tellurium XPS Spectrum of laponite reacted with $(EtOPh)_2TeBr_2$.

compound in the clay.

The FTIR spectrum showed that the organic absorptions from the organometallic molecule were still visible and distinguishable from the broad absorptions caused by the clay, thus indicating that the organic groups of the precursor are incorporated into the clay.

XRD gave a basal spacing of 14.83Å. Slightly above that of laponite.

4.5.6 (*p*-Ethoxyphenyl)tellurium(IV) trichloride

4.5.6.1 Synthesis

The action of tellurium tetrachloride as an electrophile[123] was utilised for this synthesis, although modified reaction conditions are necessary.
Tellurium tetrachloride (7.5g) and phenetole (7.5g) were heated at 60-80°C for 1 hour. The trichloride derivative crystallised from acetonitrile. Yellow crystals were obtained.

Yield = 55%. Melting point = 179-182°C (literature[128] = 182-183°C).A red/brown liquid was produced on melting the solid which agreed with observations in the literature[128].
Elemental analysis found C = 26.3%, H = 2.43%.(Required C = 27.0%, H = 2.53%).

4.5.6.2 Intercalation

The microwave method was used for the intercalation reaction. Analysis of the filtrate by AA spectroscopy determined a Na^+ release of 155 ppm. The silver nitrate test[59] proved positive for the presence of Cl^- ions.

The resultant clay was analysed by XPS (see Figure 4.29) and the spectrum revealed three bands. One was discounted as an artefact of the XPS process[70]. The other bands at 575.4 and 577.2 eV are in the region denoting tellurium (IV) compounds. Characterisation to a further degree is difficult as the clay contains only 1.4% tellurium. It is however feasible that the predominant peak at 575.4 eV is characteristic of a Te-O bond.
The FTIR spectrum revealed that the organic group absorptions were visible despite the broad bands of the clay.
XRD determined the basal spacing as 14.7Å, slightly greater than that of laponite.

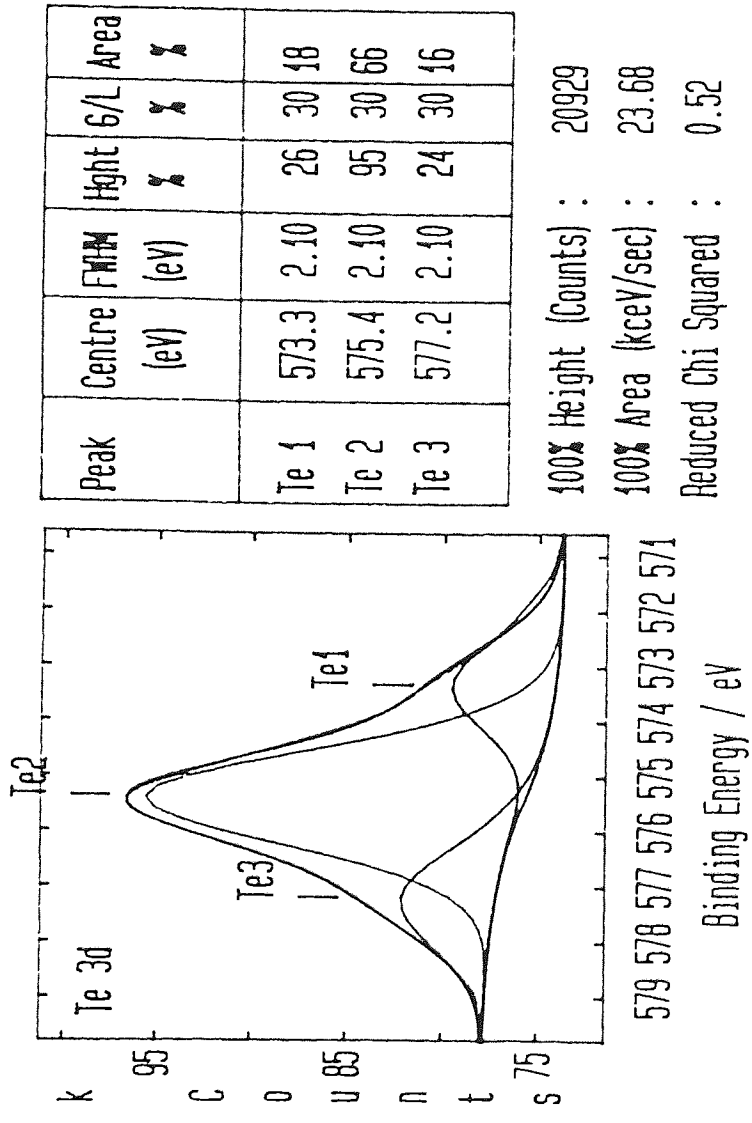

Figure 4.29 Tellurium XPS Spectrum of laponite reacted with $EtOPhTeCl_3$.

4.5.7 Diethoxyphenyltelluride

4.5.7.1 Synthesis

In literature there are many reports of successful syntheses of the compound $(EtOPh)_2Te$. Reduction of *bis*(aryl)tellurium(IV)di- and trichlorides by zinc[124,125]; preparation *via* the Grignard method[125]; reduction with $KHSO_3$[126] and water all produce the required product in high yield. This compound was prepared by another member of the laboratory[120].

The colourless crystals supplied were found to melt at 62-63°C (literature[125] = 64°C).
Elemental analysis found C = 51.8%, H = 4.86%. (Required, C = 51.9%, H = 4.86%).

4.5.7.2 Intercalation

A clay prepared by the microwave method was analysed by XPS, The technique suggested that no tellurium was present in the clay.
An FTIR spectrum also showed an absence of absorptions caused by C-C and C-O vibrations from the organic part of the molecule.
XRD revealed a basal spacing of 14.09Å, smaller than that of laponite.

Analysis of the filtrate showed a comparitively low sodium release of 38 ppm compared with the other organotellurium compounds.

The combination of these results suggest that no hydrolysis or intercalation reaction is taking place between the telluride and the laponite. This again leads towards the conclusion that a halide molecule within the organometallic precursor is necessary in order for the hydrolysis reaction to occur.

CHAPTER FIVE
The Electrical Conductivity Properties of Modified laponite RD

CHAPTER 5

Electrical Conductivity Properties of Chemically Modified laponite RD.

5.1 Introduction

Studies have shown that many smectite clays, including laponite, act as electrical conductors[53,119]. Both McWhinnie[53] and van Damme[119] suggest that the mechanism of conductivity is ionic. A more detailed study was conducted by Bond[54] utilising alternating current (a.c.) rather than direct current (d.c.) used in previous studies. The study showed that the a.c. conductivity of the clay samples had two components. The major component of the conductivity is ionic and the minor component is termed reactive. The ratio of the two components is found to be related to the electrode system used to meaure the conductivity of the sample. The method used to obtain measures of conductivity is outlined below.

Approximately 0.25g of the sample was pressed into a solid disc using a hydraulic press, usually reserved for the manufacture of KBr discs for infra-red analysis. Discs were produced by pressing at 10 tonnes for 3 minutes. A disc with a diameter of 13mm and a thickness of approximately 1mm was produced. An accurate measurement of thickness (to 1/100th mm) was made using a dial micrometer. Silver loaded epoxy resin, obtained from RS Components, was used to attach freshly stripped enamelled copper wire (0.7mm diameter) to both surfaces of the disc. Care was taken to cover the surfaces completely but to avoid the disc edges. The resin was allowed to dry for one week before measurement. All samples were measured in duplicate at least. The resistance and capacitance of the samples were measured using a Genrad impedence Digibridge and hence the conductivity of the sample calculated (see section 5.2).

The Digibridge considers the clay sample to be an ideal resistor and ideal capacitor in parallel.

When an ideal resistor is subjected to A.C. it obeys Ohm's law;

$$R = V/I \qquad \text{equation 5.1}$$

where R = resistance, V = voltage and I = current.

The clay sample hence has a resistance which is independent of the applied frequency.
An ideal capacitor allows the passage of alternating current *via* a displacement current flow (caused by changes in the potential difference). Electrical conductivity arises from the movement of electrons or ions.

This leads to the simplistic test configuration illustrated in Figure 5.1.

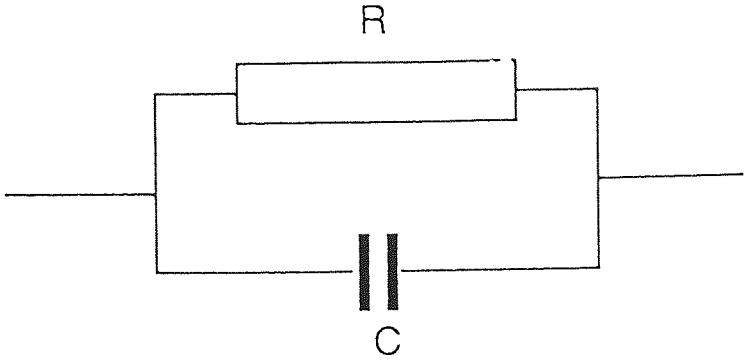

Figure 5.1 Digibridge Test Configuration.

The Digibridge calculates values of resistance and capacitance based on a frequency input. These data are based on the test configuration behaving in an ideal manner. In reality we actually get two capacitive and two resistive phases, one from the sample and one from the electrode system. Differing results gained by Bond[54] using different electrode systems can be attributed to differences in the electrode-sample interface. Bond[54] initially utilised two electrode systems to measure the conductivity of 13mm diameter clay discs. These systems were a silver loaded epoxy resin and an aluminium sputtered electrode system. The conductivity plots were found to differ in their general shape. This observation was due to the different natures of the sample-electrode interfaces influencing the shape of the curve. Bond found that the electrode contact using the silver-paste system was highly ohmic and therefore current passed as alternating current was observed to be frequency dependent. The aluminium sputtered electrode showed much less frequency dependence.
Data from the two systems are illustrated in Figure 5.2.

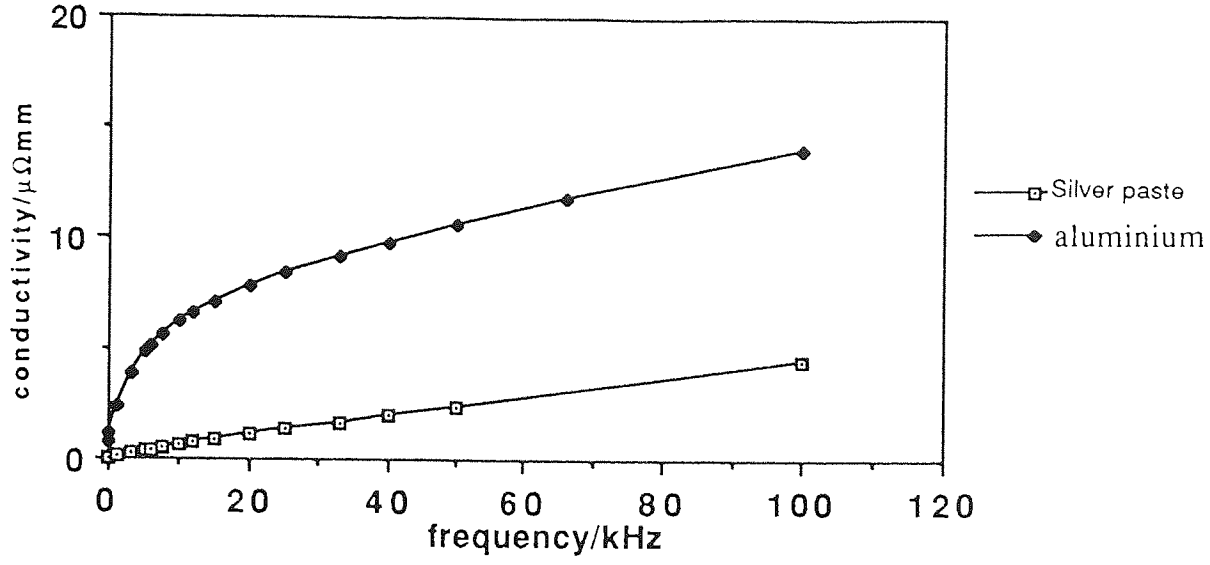

Figure 5.2 The Conductivity of laponite RD measured on Silver-paste and Aluminium Sputtered Electrode Systems.

5.2 Method of Calculation.

The digibridge measures values of resistance (R) and capacitance (C). From the values of capacitance the capacitive reactance (Xc) can be determined using equation 5.2.

$$Xc = \frac{1}{2\pi fc} \qquad \text{equation 5.2}$$

where f = frequency (k/Hz) and c = capacitance.

The property of capacitive reactance (Xc) together with the measured resistance (R) give the total impedance (Z) caused by the sample using the following equation:

$$(1/Z)^2 = (1/Xc)^2 + (1/R)^2 \qquad \text{equation 5.3}$$

This equation can thus be rearranged;

$$Z = 1/\sqrt{[(1/Xc)^2 + (1/R)^2]} \qquad \text{equation 5.4}$$

By plotting the reciprocals of Z, Xc and R against frequency it can be seen to what extent the a.c. conductivity is reactive against ionic. Bond[54] found this relationship to be dependent on the electrode system employed for the measurement. Using the silver paste electrode system (see section 5.1) he found that the reactive component accounts for the majority of the impedance (see Figure 5.3) caused by the laponite RD sample. This was caused by the ohmic nature of the silver paste system.

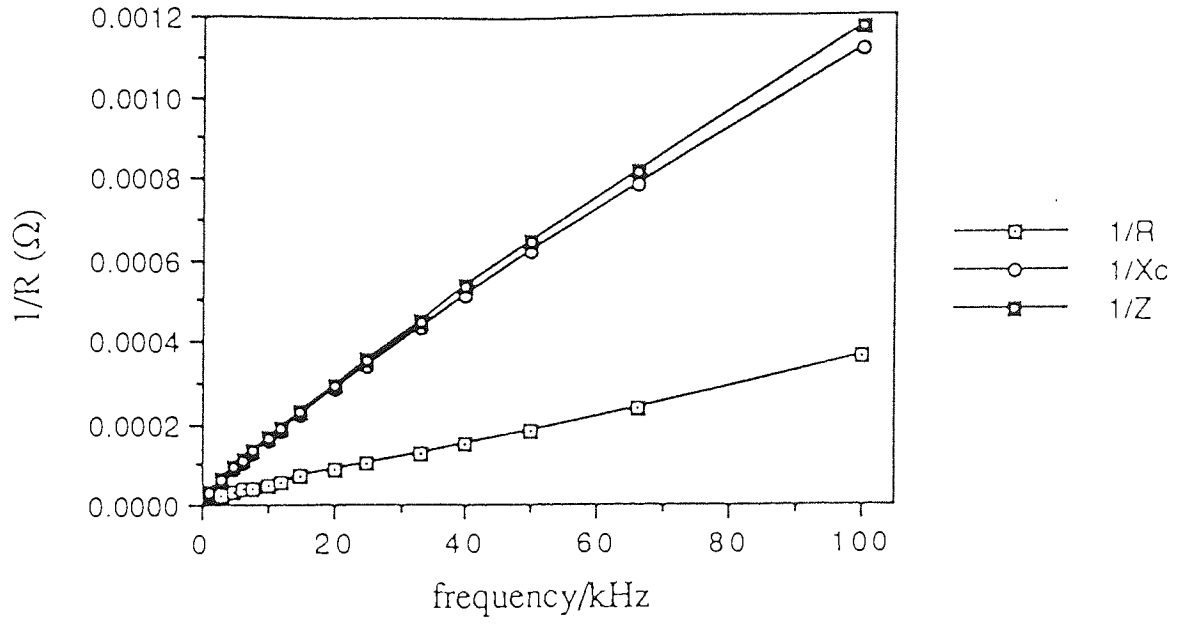

Figure 5.3 Components of Impedance using the Silver Paste System.

Use of a stainless steel electrode system, as described overleaf, produced a different result. The equipment (see Figure 5.3) utilised for the stainless steel system was a stainless steel die for pressing solid discs. The die produces discs with a 17mm diameter. The die plunger was insulated from the die by a Teflon sleeve.

1g of clay was required to make a disc. A pressure of 5 tonnes was applied for 3 minutes. During measurement a pressure of 0.5 tonnes was maintained to ensure good contact between the sample and the electrodes. The positive electrode was the raised bottom of the die, the negative electrode was the base of the plunger. Electrical contacts were made to the plunger and to the barrel of the die.

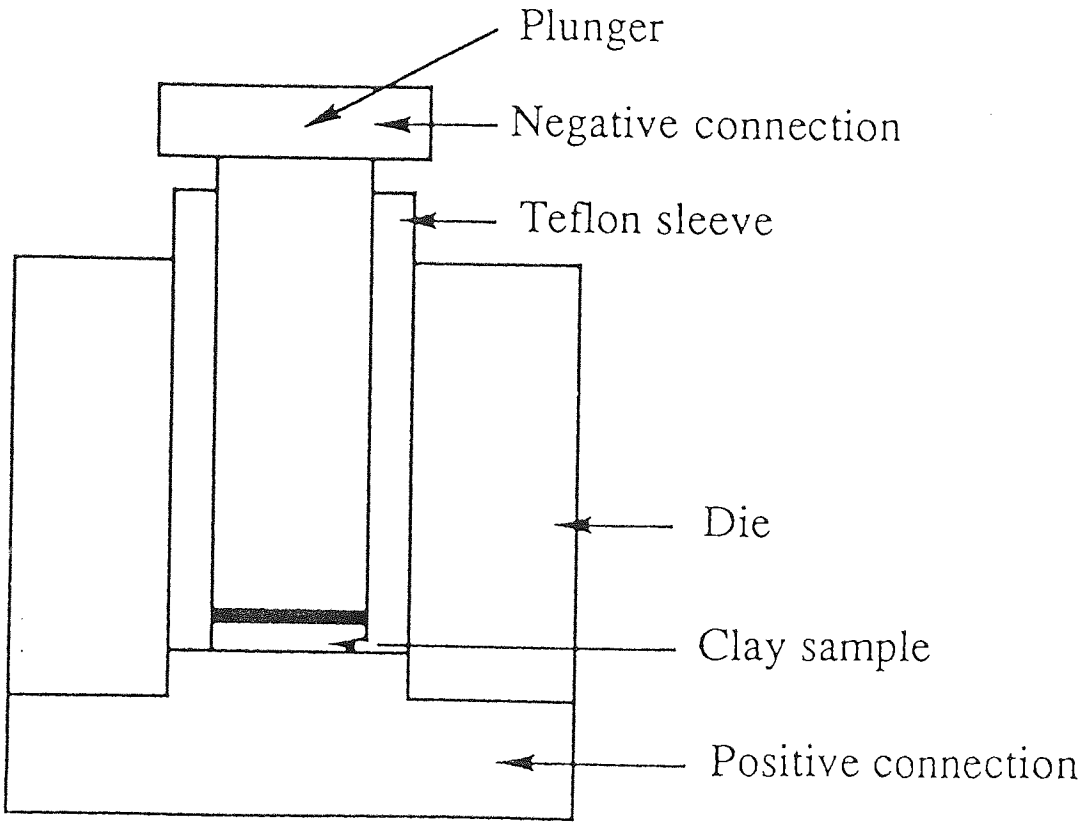

Figure 5.4 Schematic representation of the Stainless Steel Electrode System.

Measurement using this system reveals conductivity graphs similar to those obtained by Bond[54] using the aluminium sputtered system. At frequencies above 10kHz the conductivity was largely independent of the frequency, i.e. the ionic component was dominant over the reactive. The differences between the silver paste electrode and the stainless steel electrode is believed to be caused by several factors. As suggested previously, the silver paste-clay interface may be providing a high ohmic resistance and/or preventing the discharge of ions and hence causing polarisation at the electrodes. The latter point would produce an increase in the total resistivity of the clay sample. Using a stainless steel electrode under pressure may enhance particle-particle or electrode-particle interaction and hence increase the conductivity. Bond[54] showed that the value of conductivity calculated is dependent upon the pressure exerted, see Figure 5.5.

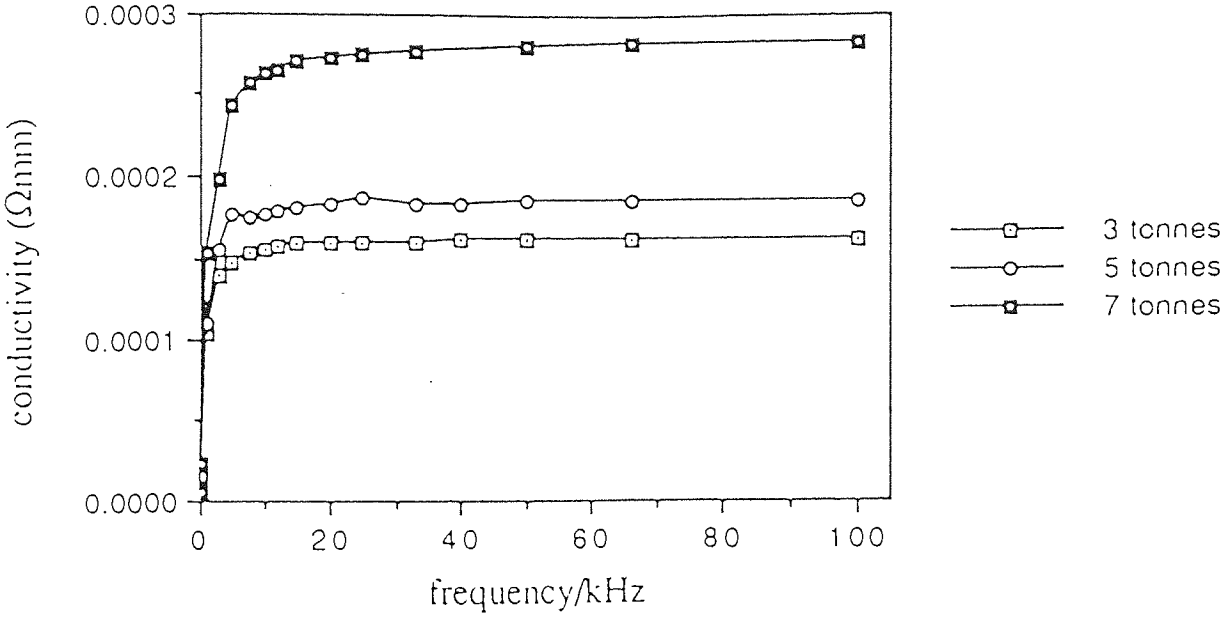

Figure 5.5 Pressure dependence on electrical conductivity.

As a consequence, results using different electrode systems and conditions cannot be directly compared.

Conductivity values for the samples were calculated from values of R or Z, depending on whether the reactive capacitance (Xc) was a significant factor, using the following equations.

$$\delta = 1/RA \qquad \text{equation 5.5}$$

$$\delta = 1/R\pi r^2 \qquad \text{equation 5.6}$$

where δ = conductivity, l = thickness of the disc in mm, R = resistance in ohms and r = radius of the disc.

Bond[54] demonstrated that although the observed conductivity using the silver paste electrode was dominated by the reactive component, and hence was influenced by the frequency, the method did provide measurements effective in determining whether a compound was more or less conductive than another compound. Hence the conductivity of modified samples could be measured relative to laponite RD. For this reason initial conductivity measurements on the chemically modified laponites (see chapter 3 and 4) were carried out using the silver paste electrode system. This system utilises a simple procedure to obtain consistent results. Each sample was measured at least in duplicate.

5.3 Conductivity Evaluation of Chemically Modified Clays.

The aim of this work was to increase the electrical conductivity of the synthetic clay laponite for use in the paper industry.

5.3.1. Laponite modified with Organotin Compounds.

The hypothesis used in reacting laponite with organotin compounds (see chapter 3) was that opening up the clay layers would lead to an increase in the mobility of the interlayer ions. These interlayer ions are thought to act as electrical charge carriers. Increasing the mobility of these ions would result in the charge being carried more efficiently hence giving an increase in the conductivity.

Pillared tin clays were produced both with and without the sacrifice of the interlayer cations (see sections 3.4.2 and 3.4.1 respectively). In the production of the clay containing tin (IV) oxide pillars and interlayer cations (from the Ph_3SnCl precursor) a hydrolysis reaction on the clay surface was found to be the initial stage of the reaction. A clay was also produced using $(MeOPh)_4Sn$ as the precursor. This clay showed no evidence of pillaring but a slight degree of intercalation may have occurred.
The conductivity results are shown graphically in Figure 5.6. The silver paste electrode system was used.

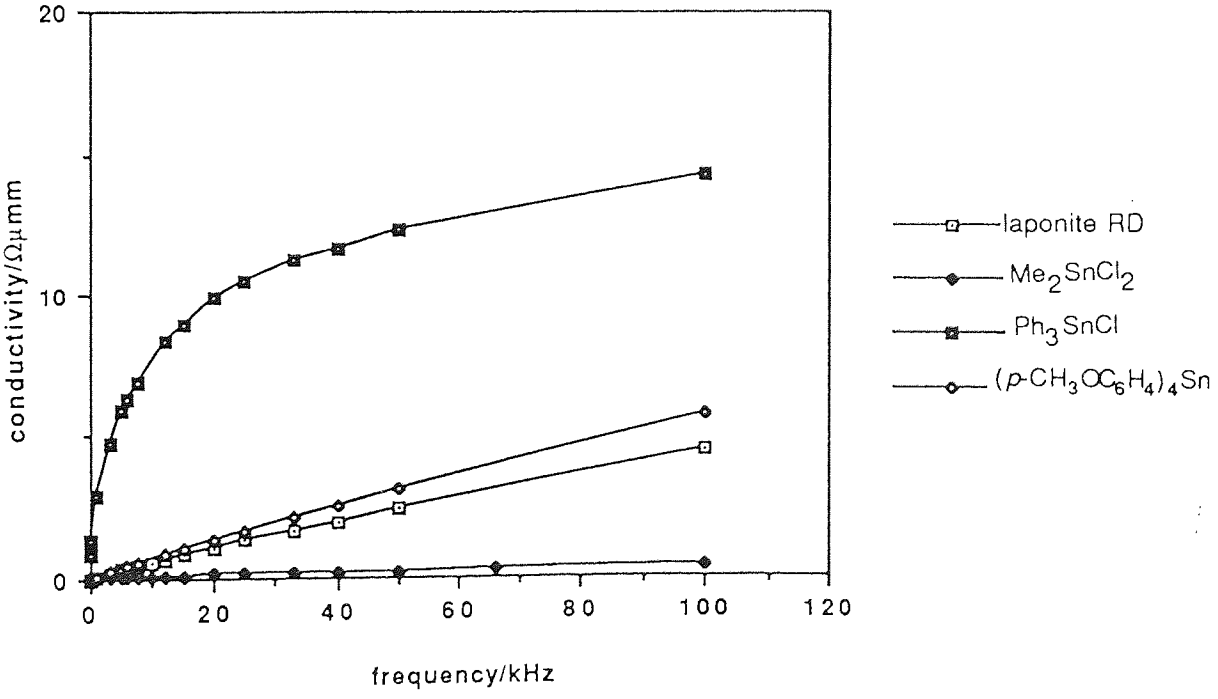

Figure 5.6 The Electrical Conductivity of Organotin modified laponite.

It can be seen that the order of conductivity is

laponite + Ph_3SnCl > laponite + $(CH_3OC_6H_4)_4Sn$ > laponite RD > laponite + $(CH_3)_2SnCl_2$

The pillared clay formed without the sacrifice of the interlayer ions (Ph_3SnCl precursor) showed the largest increase in the conductivity, suggesting that both the pillars (shown by an increase in the basal spacing and Mossbauer evidence) and the mobile interlayer cations contribute to the conductivity mechanism. Lack of either of these features is seen to be detrimental to the electrical conductivity. Evidence in chapter three suggests that the clay produced using $(CH_3OC_6H_4)_4Sn$ contains no oxide pillars and that the clay produced with the Me_2SnCl_2 precursor contains no interlayer cations.

The shape of the curve for the clay intercalated with Ph_3SnCl, shown in Figure 5.6 suggests that the conductivity contains a noteable ionic component. Calculation of the resistive (R) and reactive (Xc) contributions to the impedance (Z) of the most conductive pillared clay, shown in Table 5.1 confirm this observation. The reactive component is large compared with the resistive force. This suggests a dominant ionic component in the conductivity when using the silver paste electrode system for this compound.

Frequency / kHz	Resistance / Ω	Reactance / Ω	Impedance / Ω
100	782	1619	704
33	1006	1904	890
20	1170	2003	1010
5	2104	2883	1670
1	4200	5793	3400

Table 5.1 The Components of Impedance for laponite RD reacted with Ph_3SnCl.

It is suggested that interlayer sodium ions act as charge carriers and that the increased basal spacing aids the mobility of the interlayer ions. Analysis of the resistive and reactive contributions in the clays produced using $(CH_3OC_6H_4)_4Sn$ and Me_2SnCl_2 reveal that the resistive component of impedance is large compared with the reactive component. Using the silver paste electrode system this suggests that there is a build up of ohmic resistance and prevention of ion discharge leading to a polarisation effect at the sample-electrode interface. These factors cause an increase in the resistance of the clay to the charge. It is apparent from the graphical data (Figure 5.6) that the conductivities of these samples are dependent on the frequency thus suggesting that the reactive component is the dominant force in the conductivity.

5.3.2. Modification of laponite RD with Organobismuth compounds.

The strategy involved in the choice of organobismuth compounds as intercalation agents was that the large molecules would slip between the clay layers and hence act as pillars thus aiding the mobility of the interlayer cations. This increase in the mobility of the ions should in theory lead to an increase in the electrical conductivity of the clay.
Conductivity measurements of clays produced using Ph_3Bi and Ph_3BiBr_2 precursors were made. Conductivity results are shown graphically in Figure 5.7.

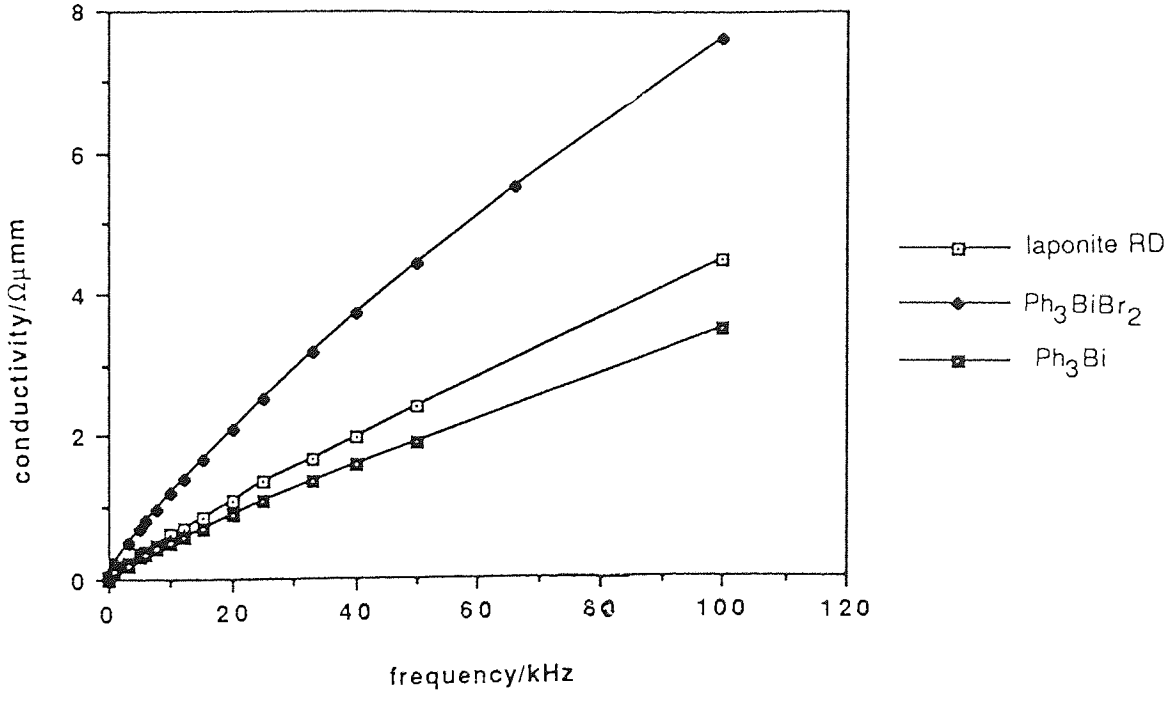

Figure 5.7. The Electrical Conductivity of laponite reacted with organobismuth compounds.

Clays modified using organobismuth precursors show only a small change in conductivity over that of laponite RD. In some cases the conductivity was slightly increased but in others it was calculated to be less than that of laponite RD. This was expected, after analysis of the final products (see section 4.2), as there was no noticeable increase in the basal spacing of the modified samples and only very small amounts, if any, of bismuth were detected within the samples.
The shapes of the curves and the analysis of the impedance components suggested that using the silver paste electrode system results in the resistive element being the dominant component of impedance and hence the reactive component of conductivity being dominant over the ionic component.

5.3.3. Modification of laponite RD with Organoantimony Compounds.

Organoantimony compounds were chosen as intercalation agents primarily with the objective of producing tin oxide pillared clays doped with antimony. Doping tin(IV) oxide with antimony is known to increase it's conductivity several times[130]. The first stage however was to ascertain how organoantimony compounds alone affected the conductivity of laponite RD.
The results of the conductivity measurements on laponite reacted with Ph_3Sb and Ph_3SbBr_2 are illustrated graphically in Figure 5.8.

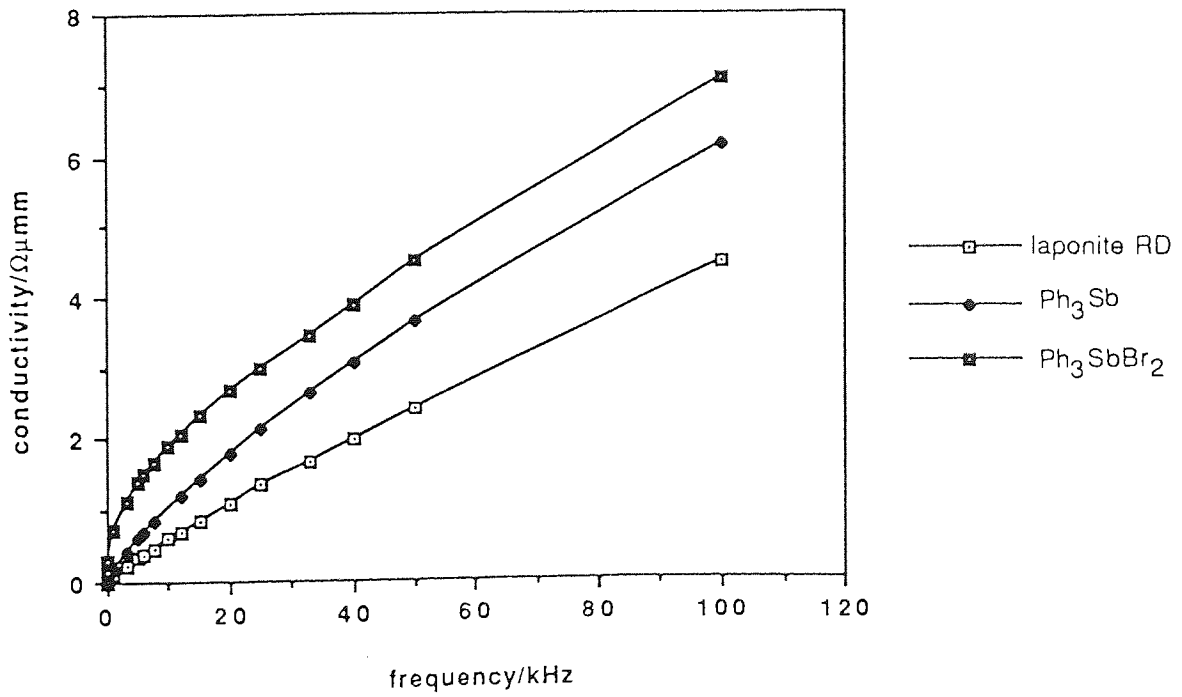

Figure 5.8 The Electrical Conductivity of laponite modified with Organoantimony compounds.

The increase in the conductivity is not significant and in some cases the addition of the organoantimony compound led to a decrease in the conductivity. The shape of the conductivity plots and analysis of the components of impedance suggest that the conductivity value is frequency dependent. The resistive component of impedance is dominant over the reactive and consequently the reactive component of conductivity is larger than the ionic component.

5.3.4. Modification of laponite RD with Organotin and Organoantimony compounds.

Incorporation of both tin and antimony into laponite RD was attempted *via* a number of routes outlined in chapter 4. The measurement of the conductivities of these clay samples revealed that the degree of conductivity was dependent on the method of preparation used. The results are illustrated in Figure 5.9.

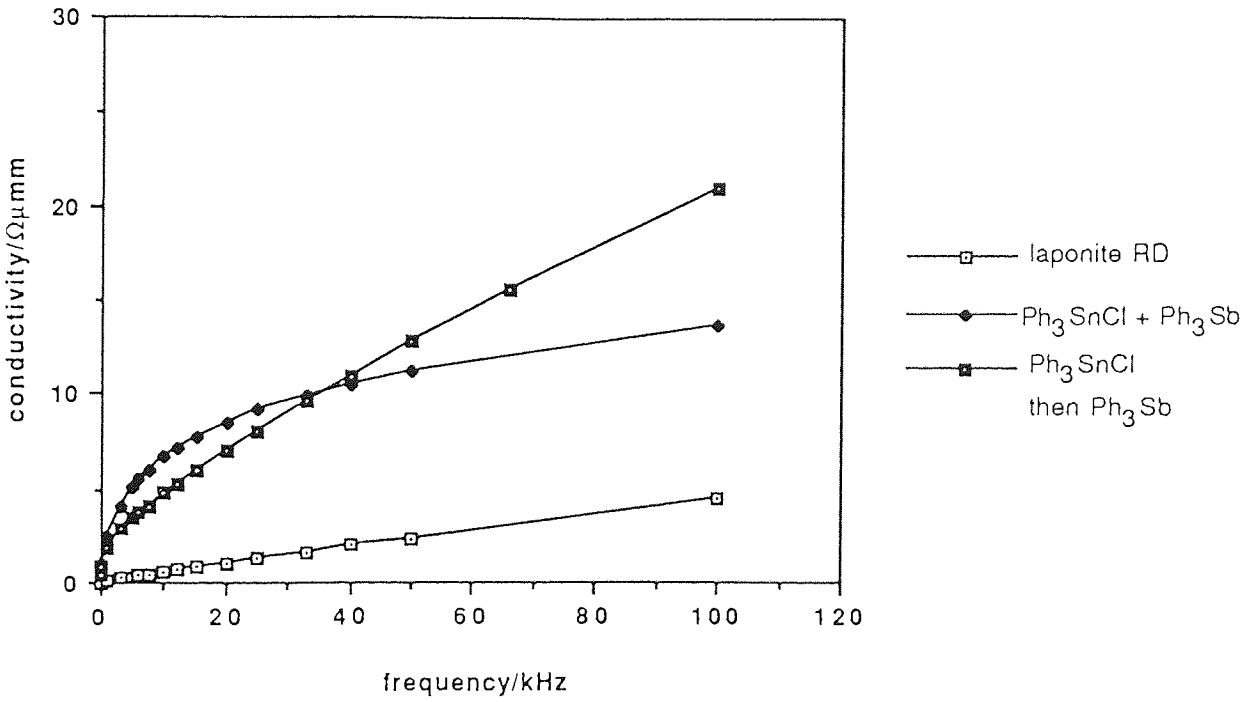

Figure 5.9 The Electrical Conductivity of laponite modified with Organotin and Organoantimony Compounds.

The clays prepared *via* simultaneous addition of the organotin and organoantimony precursors exhibited a conductivity analogous to that of a clay prepared with the organotin precursor alone. The preparation involving consecutive addition of the organotin and organoantimony compounds (in that order) showed a noticeable increase in the conductivity of the clay. Bond[54] noted that increasing the amount of Ph_3SnCl precursor would increase the conductivity of the clay. He suggested that increased pillaring was beneficial to the mobility of the charge carrying interlayer cations thus increasing the amount of precursor would increase the quantity of pillars formed. XPS data relating to the clay prepared by the consecutive addition of the precursors (see section 4.4.2.) showed that all the tin precursor had been converted to Sn-O species. It is therefore suggested that addition of the antimony compound after the initial reaction of the organotin precursor facilitates complete reaction of the organotin precursor to tin(IV) oxide pillars. These additional pillars may lead to an additional increase in the conductivity of the sample.
It can be observed from the graphical data and is supported by analysis of the components of impedance that the conductivity is dominated by the ionic component in both cases.

5.3.5. Modification of laponite RD with Organotellurium compounds.

It was found that all the organotellurium halide compounds on reaction with laponite RD underwent a hydrolysis reaction in the same manner as Ph_3SnCl. In the case of organotellurium compounds however there is no evidence for the consequent formation of oxide pillars. Measurement of the conductivity of the resultant clays is shown graphically in Figure 5.10.

The increase in conductivity using organotellurium precursors was the greatest seen in all the compounds used. The greatest increase within the range of organotellurium precursors was with $(CH_3OC_6H_4)_2TeCl_2$. This increase could not be attributed to increasing the mobility of the sodium interlayer cations as the basal spacing had not been increased. These observations cast doubt over whether the pillars were actually a significant factor in the conductivity mechanism.
A breakdown of the impedance components is shown in Table 5.2.

It can be noted from these data that the reactive component of impedance is the larger factor. This suggests that the ionic component of the conductivity is dominant over the reactive when the silver paste electrode system is in use. The shape of the conductivity plot (Figure 5.10) would lend support to this hypothesis.

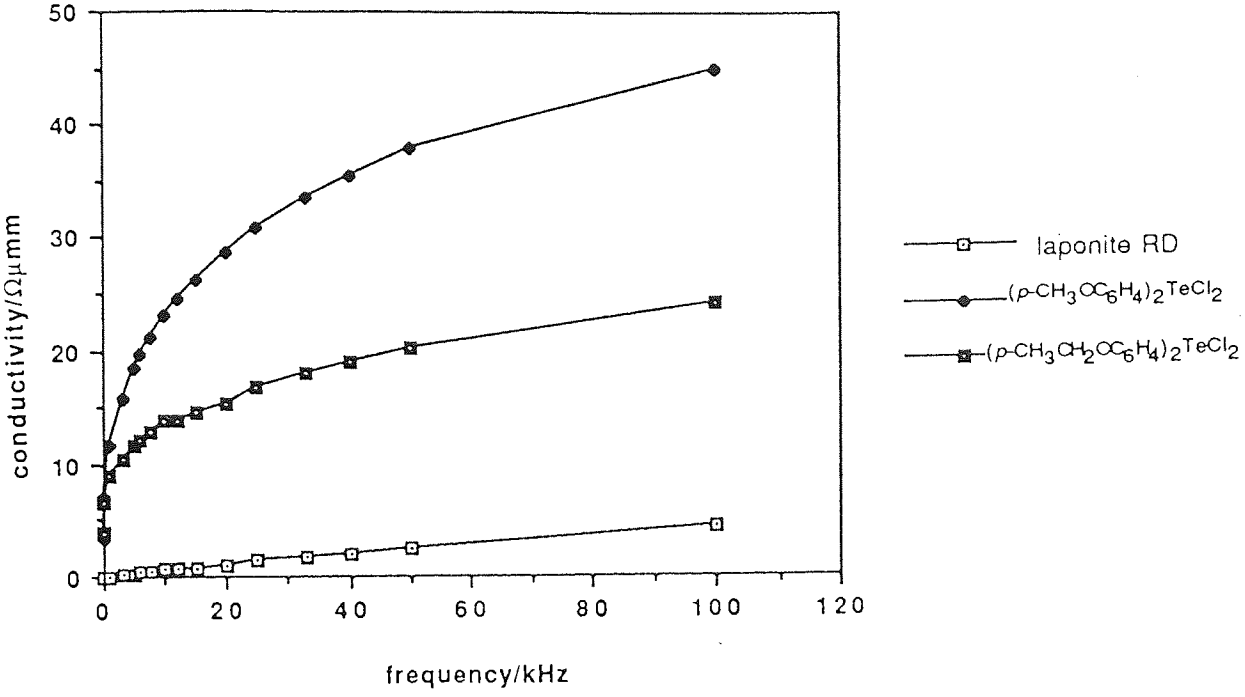

Figure 5.10 The Electrical Conductivity of laponite modified with Organotellurium Compounds.

Frequency / kHz	Resistance / Ω	Reactance / Ω	Impedance / Ω
100	228	629	215
33	315	713	288
20	373	770	336
12	444	865	395
5	591	1132	524

Table 5.2 Components of Impedance for laponite RD reacted with a $(CH_3OC_6H_4)_2TeCl_2$ precursor.

5.4 Discussion

A wide variety of organometallic molecules were reacted with laponite. Interestingly across the range a pattern does appear to emerge with respect to the level of conductivity and the dominant component of conductivity. In the case of the less conductive clays, produced from precursors including organobismuth, organoantimony and tetra (*p*-methoxyphenyl)tin(IV), the majority of the conductivity is derived from the reactive component. Conversely it was seen that in clays produced *via* reaction with Ph_3SnCl, consecutive addition of organotin and organoantimony compounds and with organotellurium precursors the clays possessed a conductivity dominant in the ionic part.
It is suggested that the two 'groups' of clays undergo different reactions with laponite.
Taking the case of the most conductive clay, that prepared using $(CH_3OC_6H_4)_2TeCl_2$, the salient points are:

1. There is a hydrolysis reaction on the surface of the clay.
2. There is a large release of interlayer sodium cations.
3. The tellurium - carbon bond remains intact.
4. There is no significant increase in the basal spacing.

The complementary feature between Ph_3SnCl and the organotellurium precursor is the hydrolysis reaction on the clay surface, leading to the release of a substantial amount of interlayer sodium cations. The less conductive clays do not undergo this reaction.
A comparison of interlayer sodium release is shown in Table 5.3.

Precursor	Na^+ release(ppm)
$(CH_3OC_6H_4)_2TeCl_2$	428
Ph_3SnCl	120
Organobismuth	4 - 20
Organoantimony	10 - 20

Table 5.3 Interlayer Sodium Release on Reaction with laponite RD.

The release of the sodium ions occurs as a result of acid release on hydrolysis (see chapter 4). The acid protons exchange with interlayer sodium ions resulting in H^+ ions becoming part of the interlamellar structure of the clay. The H^+ ions have the potential to act as more efficient charge carriers than the Na^+ ions due to their greater mobility. This factor could be causing the observed increase in the conductivity of the clays produced with Ph_3SnCl and organotellurium precursors.

The involvement of the oxide pillars in the conductivity mechanism is brought into question following the impressive conductivity increase in the case of the organotellurium halide precursors. Evidence from the analysis of these clays (see chapter 4) shows that there is no formation of oxide pillars.

Previous work by Bond[54] implied that the pillars, although not behaving as semi-conductors themselves, were instrumental in the improved conductivity by aiding the mobility of the charge carrying interlayer cations.

The hypothesis that the incorporation of protons into the interlayer region is the significant factor seemed feasible. This led to an investigation whereupon laponite RD was acidified to various degrees of its cation exchange capacity and the conductivity measured.

5.5. Acid exchange of laponite RD

The hypothesis that the exchange of acid protons for interlayer sodium ions in the laponite was the reason for the enhanced conductivity was investigated. Laponite RD was exchanged with an ethanolic hydrochloric acid (HCl) solution up to 100% ion exchange capacity (it was found that using an aqueous solution caused the laponite to form a gel) in the microwave oven. The samples were subjected to five 1 minute bursts of microwave radiation. The quantity of acid required in order to facilitate exchange was calculated using the following equation.

$$\text{Weight of acid required} = \frac{\text{Meq clay/100g x Wt of clay used(in Kg) x RMM acid}}{\text{Activity (acid) x Valency (acid)}}$$

The activity must be between 0-100 and is the degree of exchange required. The valency is taken from the charge on the ions of the acid in solution, in the case of HCl the valency is 1. The cation exchange capacity (C.E.C.) of the laponite is 73 meq/100g[9].

After irradiation in the microwave the acidified laponite was filtered and allowed to dry in air. The filtrate was collected and analysed by AA spectroscopy to determine the quantity of sodium ion release. The results are presented in Table 5.4.

H^+ exchanged laponite	Na^+release (ppm)
100%	74
70%	32
50%	30
30%	27

Table 5.4 Sodium Ion release on Acidification of laponite RD.

The values of sodium ion release obtained from this investigation when compared with those given in Table 5.3 from the organometallic modified clays were a little surprising. The sodium release for laponite RD after reaction with *Bis* (*p*-methoxyphenyl)tellurium(IV) dichloride was 428ppm. That obtained from the sample of laponite RD reacted with enough HCl to theoretically give 100% cation exchange was just 74ppm.

Calculation of the total theoretical amount of interlayer sodium ions in 1g of laponite RD, based on a theoretical formula[9] of

$$\{Si_8(Mg_{5.3}Li_{0.7})O_{20}(OH)_4\}Na^+_{0.7}$$

revealed a value of 0.0211g. The actual release on acidification, 74ppm, is equivalent to a release of 0.000074g. It is therefore apparent that there is not full exchange of the interlayer sodium cations by acid protons when a sample of laponite RD is subjected to hydrochloric acid. The actual release is only 0.35%. Further attempts to gain greater exchange by acidification did not produce significantly improved data.

The conductivities of the samples were measured using the silver paste electrode system. It was found that the conductivities of the samples were very similar to one another despite the difference in the attempted amount of acid exchange. The conductivity of the samples (Figure 5.11) was found to be above that of laponite RD yet had not improved to the levels achieved *via* reaction with organotellurium compounds. A comparison of the conductivities is illustrated graphically in Figure 5.11. It was therefore suggested that the factor of incorporation of protons into the lattice alone did not account for the large rise in conductivity obtained through reaction with the organotellurium compounds. The conductivity increase found in the acidified clays was lower than that produced using Ph_3SnCl as the precursor with the level of sodium ion release also lower, yet in the same order (100-120ppm for the organotin modified clay

compared with 70-90ppm with the acidified clays).This may suggest that the incorporation of the protons is an important factor in the conductivity, but that it is not the only factor influencing the conductivity.

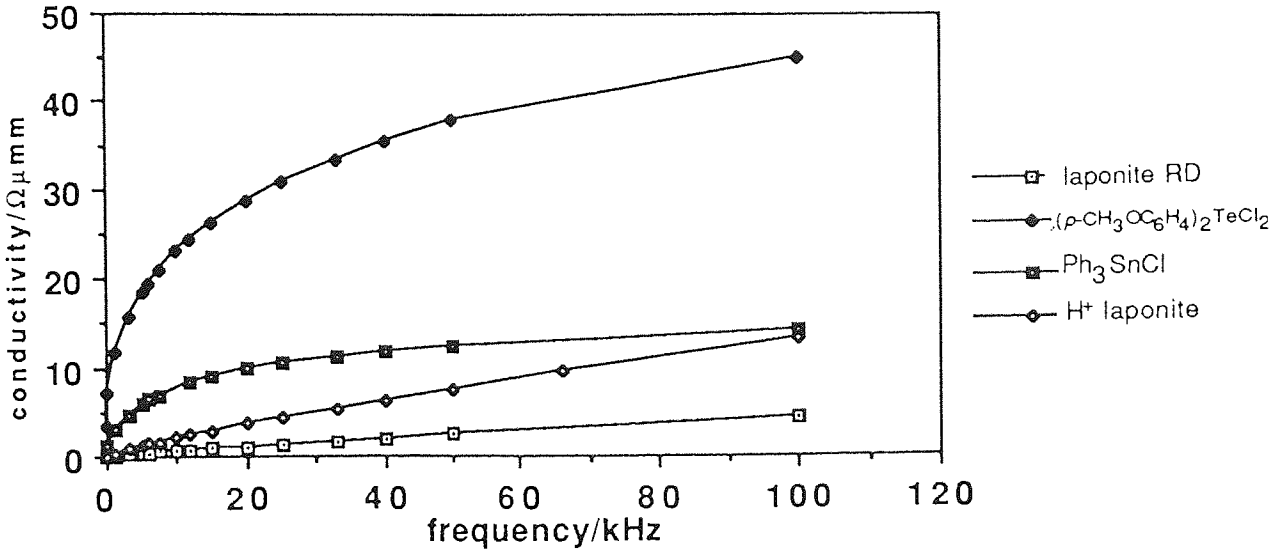

Figure 5.11 The Conductivity graph of Acidified laponite RD compared with laponite RD and laponite modified with Ph_3SnCl and organotellurium compounds.

5.6 Investigation of Conductivity using a Stainless Steel Electrode System.

A stainless steel electrode system as illustrated in Figure 5.4 was used to gain additional conductivity data. The design of the equipment necessitates measurement being recorded under a pressure of 0.5 tonnes. All samples were pressed for 3 minutes at 5 tonnes pressure prior to measurement.

5.6.1 Conductivity Measurement of laponite RD.

Comparison of results gained from this electrode system cannot be compared directly with those obtained using the silver paste system for a number of reasons. The sample-electrode interface will be different thus affecting the measure of conductivity and the A.C. conductivity is pressure dependent (see Figure 5.5). The graph obtained on measuring the conductivity over a range of frequencies is shown in Figure 5.12.

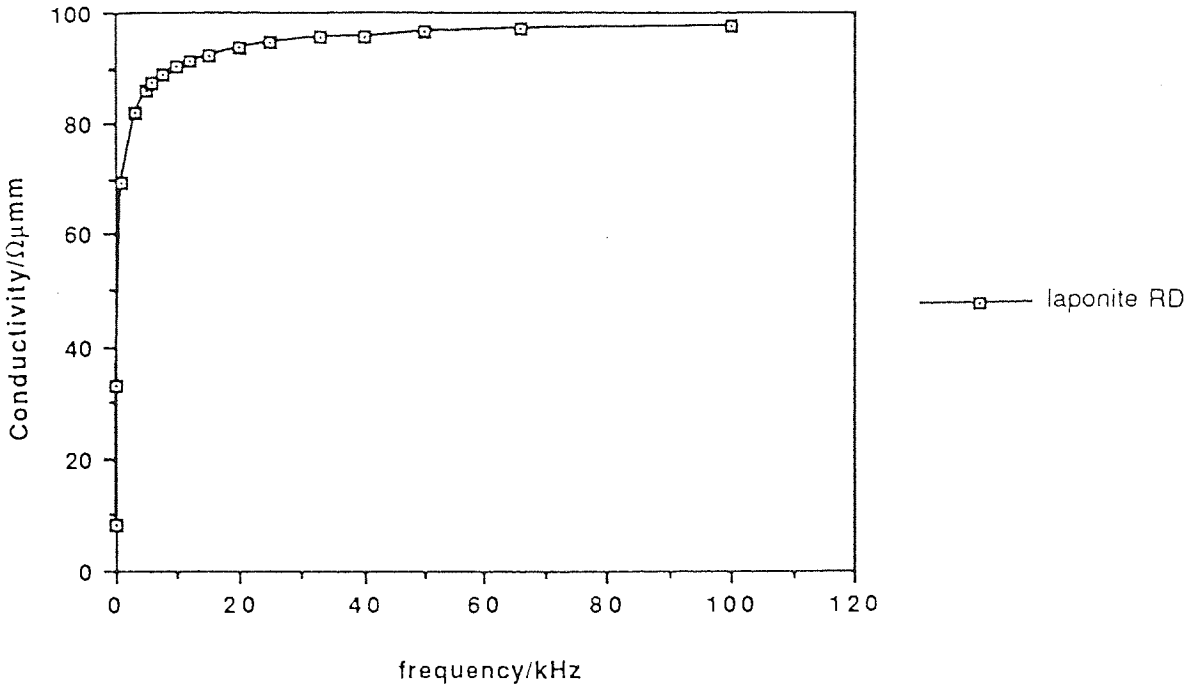

Figure 5.12 The Conductivity of laponite RD measured using the Stainless Steel Electrode System.

An interesting feature of the conductivity plot is that the shape of the curve is different to that obtained using the silver paste electrode system (see Figure 5.6). If the components of impedance are analysed, as shown in Table 5.5, it can be seen that the reactive component (Xc) is larger than the resistive (R) suggesting that the dominant component of conductivity is ionic. The graph shows little dependence on frequency between 10 and 100kHz. The slight slope between these values can be attributed to the small reactive component of the conductivity. The values calculated for R and Z are very close suggesting that there is little capacitive effect using the stainless steel system.

The second interesting observation is that the A.C. conductivity of laponite RD is approximately two orders of magnitude higher than when measured using the silver paste electrode. This could be attributed to the fact that applying pressure to the clay increases the electrode-particle and/or the particle-particle contact thus increasing the total conductivity.

Frequency / kHz	Resistance / Ω	Reactance / Ω	Impedance / Ω
100	62.6	730	62.4
33	63.9	742	63.7
20	65.2	652	64.9
12	67.1	553	66.6
5	71.8	398	70.6

Table 5.5 Components of Impedance for laponite RD measured using a Stainless Steel Electrode System.

5.6.2 Measurement of laponite RD modified with Organometallic Molecules.

Data were collected under the conditions described in section 5.6. It had been expected at the start of this investigation that the order of conductivity would follow that determined *via* the silver paste electrode system. However the two order of magnitude increase in the conductivity seen with laponite RD between electrode systems was not seen with the organometallic modified clays. In general it was noted that the clays with the highest conductivity values obtained using the silver paste electrode system remained in the same order of magnitude when measured using the stainless steel electrode system. Those showing lower conductivities under the silver paste conditions (i.e. the organobismuth and antimony clays) showed increases of between one and two orders of magnitude.

The results are illustrated graphically in Figures 5.13a and 5.13b.

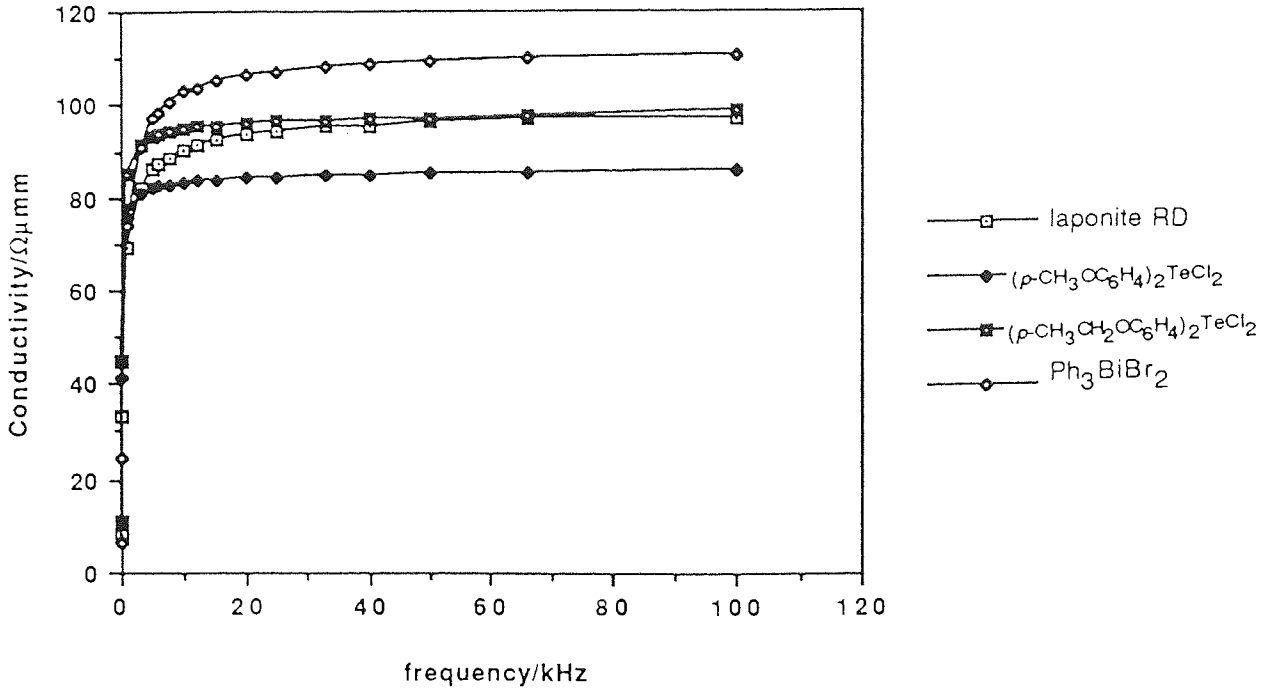

Figure 5.13a Conductivity of Modified laponite using Stainless Steel System.

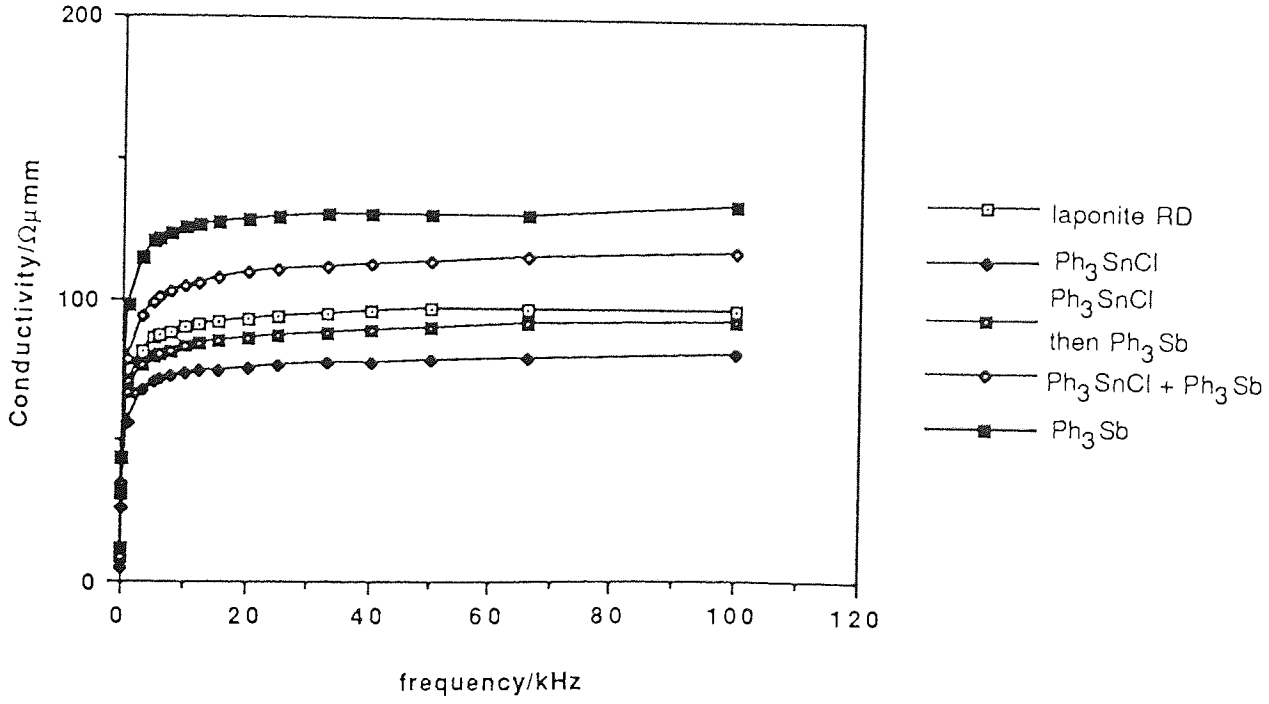

Figure 5.13b Conductivity of modified laponite measured on the Stainless Steel Electrode.

The curves for all the organometallic modified clays were of the same general shape using this electrode system, indicating that ionic conductivity was the dominant component of the total conductivity. The gradual slope of many of the graphs between 10 - 100 kHz is attributed to the small reactive component.

5.6.3. Discussion.

The two order magnitude increase in the conductivity of laponite RD between electrode systems against the variable change found in the organometallic modified laponites raises an important question as to the mechanism of the conductivity. Bond[54] also reported this phenomenon in laponite RD. Further examination of data produced by him indicate that a significant increase in the conductivity of organotin modified clays in the same order to that of laponite RD was not seen. These results were not commented upon by Bond, although the data are available in his thesis. Bond[54] showed that increasing the pressure under which the sample is pressed leads to an increase in the total conductivity of the clay through improved particle-particle and/or particle-electrode interaction. As a significant increase between electrode systems is not seen in the most conductive clay (under silver paste conditions), it is suggested that good particle-particle interaction is already present before pressure is applied. Similarly in the other modified clays if particle-particle interaction has been increased due to a reaction between the organometallic compound and laponite then the increase in conductivity when the sample is measured under pressure will be less noteable than with laponite RD.

5.7. Investigation of the clay surface by Scanning Electron Microscopy (SEM).

5.7.1 Introduction

The suggestion that particle-particle contact may be an important factor in the conductivity consideration led to the use of SEM to examine the clay surface under powerful magnification. A number of regions were observed under the microscope. Images shown are representative of the sample as a whole.

5.7.2. Sample Preparation

Samples of laponite RD and the modified clays were prepared in the following manner: The samples were ground thoroughly. The clay to be analysed was mounted on a sample holder and sputtered with gold particles under vacuum in order to enhance the image. Samples were observed at magnifications between 3190 and 7760. Thermal images and photographs were

taken of the samples.

5.7.3. Results

Examination of the clay surface of laponite RD and the modified clays provided some very interesting observations, laponite RD was examined as a standard sample. The clay had a particulate appearance as shown in Figure 5.14.

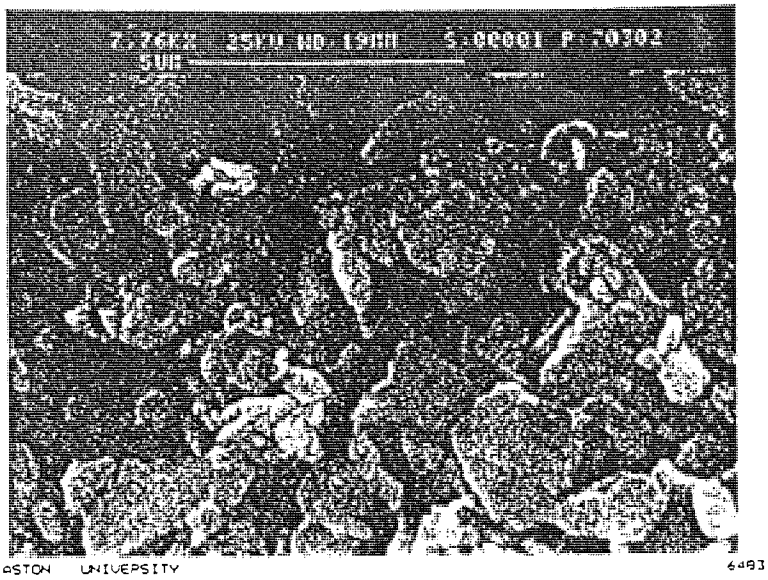

Figure 5.14 SEM Image of laponite RD.

It was shown in earlier sections that when laponite RD is intercalated with organometallic molecules the electrical conductivity is increased by varying degrees. The SEM investigation revealed some interesting differences in the appearance of the modified clays.
Examining those clays with the lower conductivities (under the silver paste electrode system) first and then moving to those with the higher conductivities gave the following results.

5.7.3.1. Modification of laponite RD with Organobismuth Compounds.

The conductivity increase using these precursors was found to be minimal (see Figure 5.7). Examination of the clay surface, where laponite RD had been reacted with Ph_3Bi, at a magnification of 3630 (see Figure 5.15) showed that the sample had a surface appearance which was obviously particulate much the same as the laponite RD.
Examination of laponite RD after intercalation with Ph_3BiBr_2 (see Figure 5.16) showed a surface less particulate and slightly "smoother" in appearance, although particles were still very much in evidence.

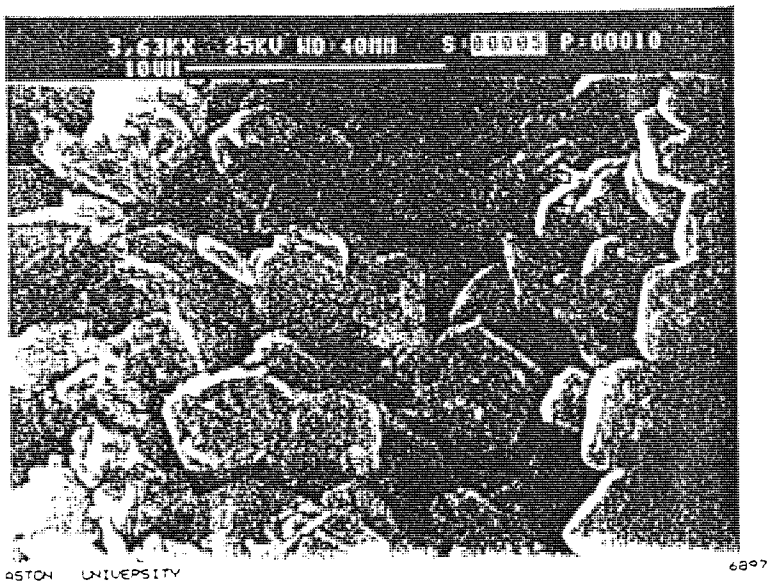

Figure 5.15 SEM Image of laponite RD intercalated with Ph_3Bi.

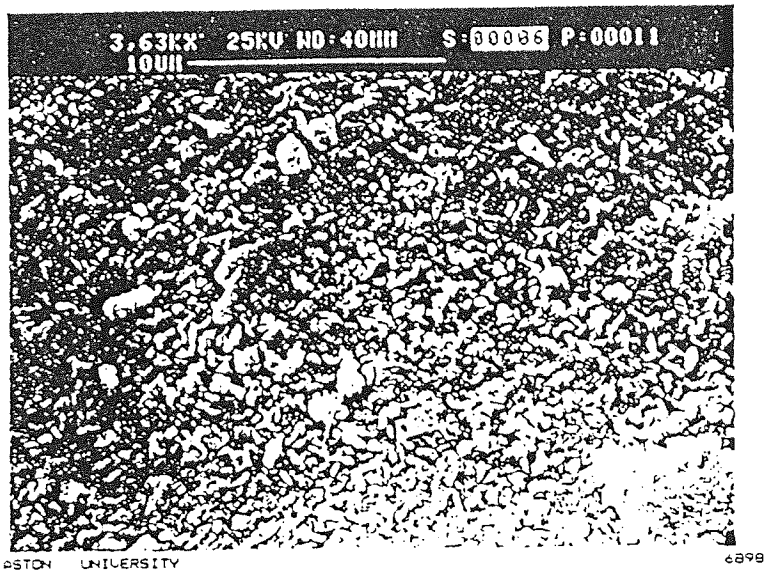

Figure 5.16 SEM Image of laponite RD after Intercalation with Ph_3BiBr_2.

5.7.3.2. Modification of laponite RD with Organoantimony Compounds.

Conductivity investigations on laponite RD modified with organoantimony compounds revealed that the conductivity was approximately that of laponite RD (see Figure 5.8).
Examination by SEM at a magnification of 7210 indicated that the same pattern as the organobismuth compounds had emerged. The clay surface had a particulate appearance as shown in Figure 5.17.

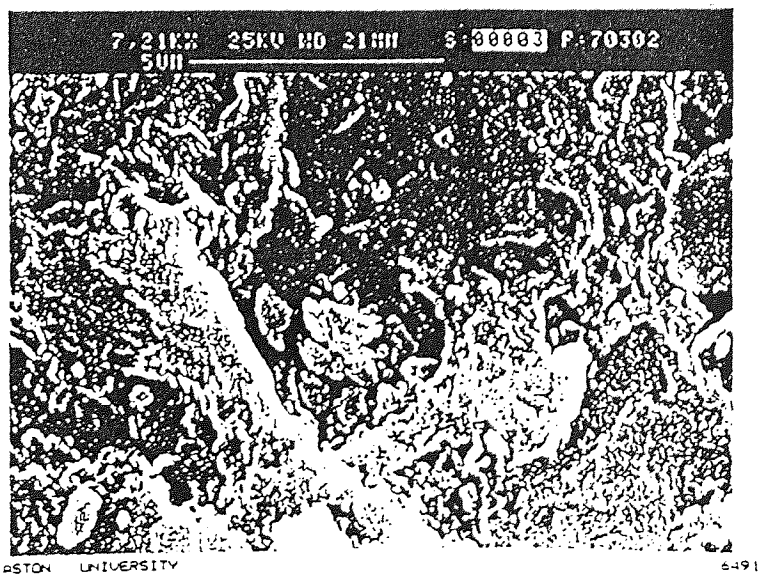

Figure 5.17 SEM Image of laponite RD after Intercalation with Ph_3SbBr_2.

5.7.3.3. Modification of laponite RD with $(p\text{-}CH_3OC_6H_4)_4Sn$.

The conductivity increase was found to be minimal on intercalation with this precursor (see Figure 5.6). Examination of the clay surface at a magnification of 3630 (see Figure 5.18) showed a particulate surface similar to that of laponite RD.

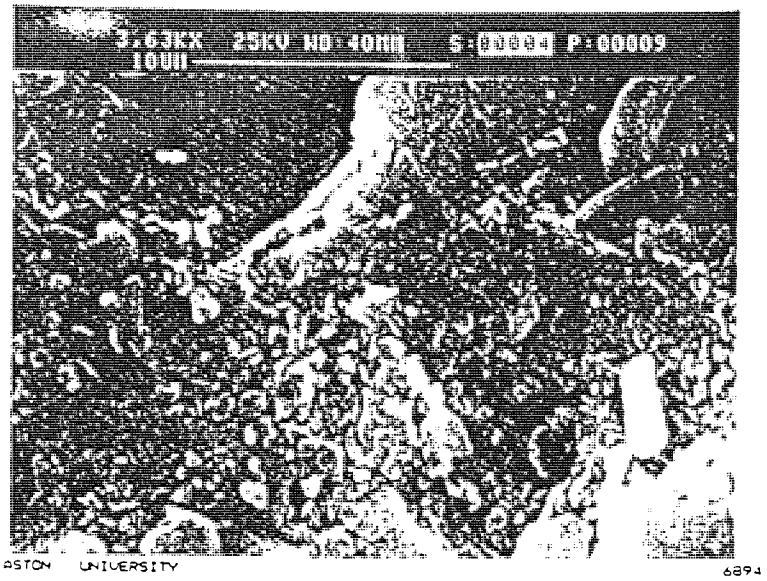

Figure 5.18 SEM Image of laponite RD after Intercalation with $(p\text{-}CH_3OC_6H_4)_4Sn$.

Decreasing the magnification to 110 (see Figure 5.19) revealed that the sample was in fact a mixture of laponite RD and the organotin precursor. This supports the earlier suggestion (see section 3.5) that little if any reaction occurs between laponite RD and $(p\text{-}CH_3OC_6H_4)_4Sn$.

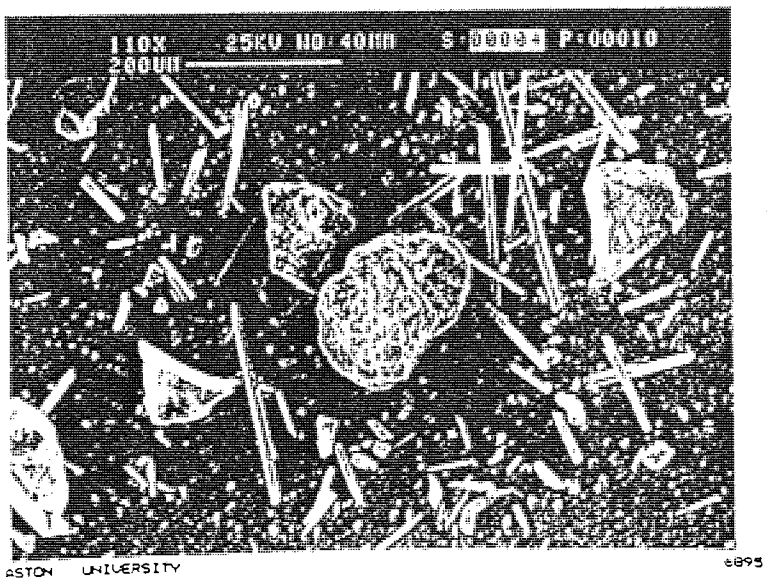

Figure 5.19 SEM Image showing a mixture of laponite RD and the $(p\text{-}CH_3OC_6H_4)_4Sn$

5.7.3.4. Modification of laponite RD with Ph_3SnCl.

The conductivity measurement of the clay produced by reaction of laponite RD with Ph_3SnCl showed a good increase above that of laponite (see Figure 5.6). Examination of the surface by SEM at a magnification of 7760 revealed a change in the appearance of the clay compared to previous samples. The individual particles were no longer visible and the surface had a much smoother appearance as shown in Figure 5.20.

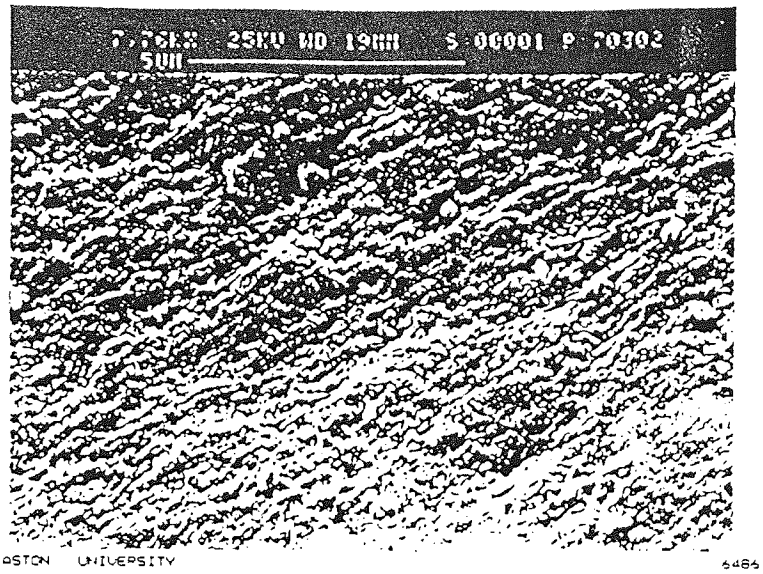

Figure 5.20 SEM Image of laponite RD after Intercalation with Ph_3SnCl.

Examination of the surface of laponite RD after reaction with Ph_3SnCl followed by addition of an organoantimony compound (see Figure 5.21) revealed that the surface had taken on a smooth appearance. The particulate surface found when organoantimony compounds alone were used was not in evidence.

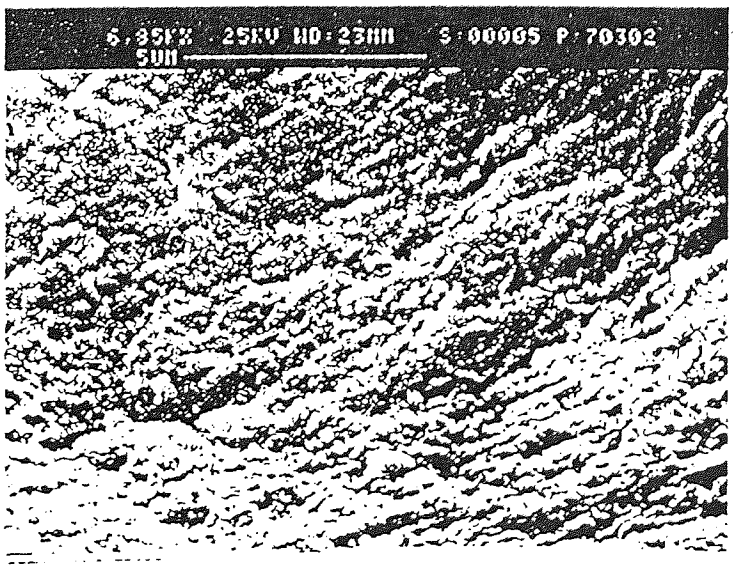

Figure 5.21 SEM Image of clay after intercalation with Ph_3SnCl then Ph_3Sb.

5.7.3.5 Modification of laponite RD with Organotellurium Compounds.

The greatest increase in the electrical conductivity of laponite RD was produced by reacting the clay with organotellurium compounds (see Figure 5.10). Examination of clays produced in this way at a magnification of 3750 revealed that the surface appearance was smooth (see Figure 5.22).

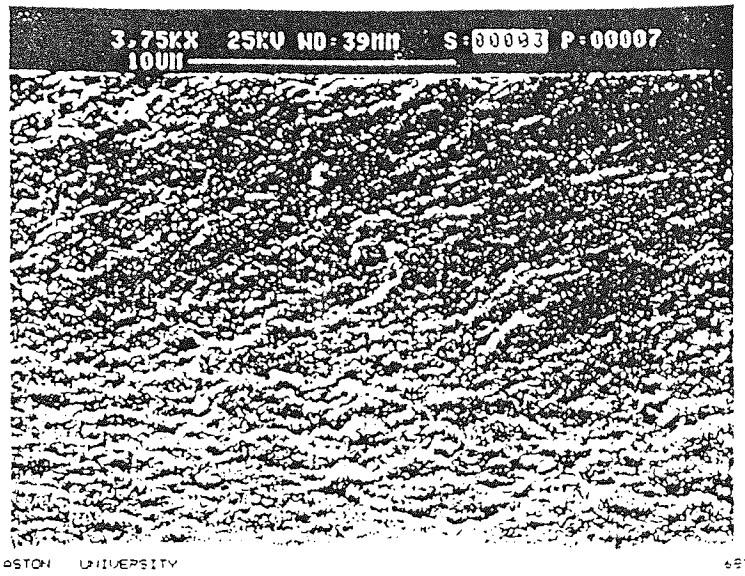

Figure 5.22 SEM Image of laponite RD after Intercalation with $(p\text{-}CH_3OC_6H_4)_4TeCl_2$.

5.7.4. Discussion

The SEM investigation proved very useful and provided more evidence to suggest that the hydrolysis reaction on the clay surface is very important in order to achieve a conductive sample. The clays with improved conductivities were found to undergo an initial hydrolysis reaction on the surface of the laponite RD, followed by acid release and consequent proton exchange for interlayer sodium ions. The release of interlayer sodium ions may be a significant factor in the improvement of the conductivity of clay samples. To date the greater the release of sodium then the greater the conductivity of the final clay. However in the case of the laponite modified with Ph_3SnCl the release of sodium ions is very similar to that obtained when laponite is in part converted from Na^+-laponite into H^+-laponite. The increase in the conductivity (using the silver paste system) of both samples is of the same order (see Figure

5.11) although the organotin clay was slightly superior. This may suggest that there are several factors influencing the conductivity of the clay, the incorporation of protons into the interlayer being one of them. Measurement of the conductivity of the acidified laponite using the stainless steel electrode system showed that an increase in the order of the conductivity analogous to the laponite RD was seen (Figure 5.23). This result when combined with the silver paste electrode results, would appear to suggest that both the incorporation of protons and the improvement of particle-particle contact are important in the total conductivity of a clay sample.

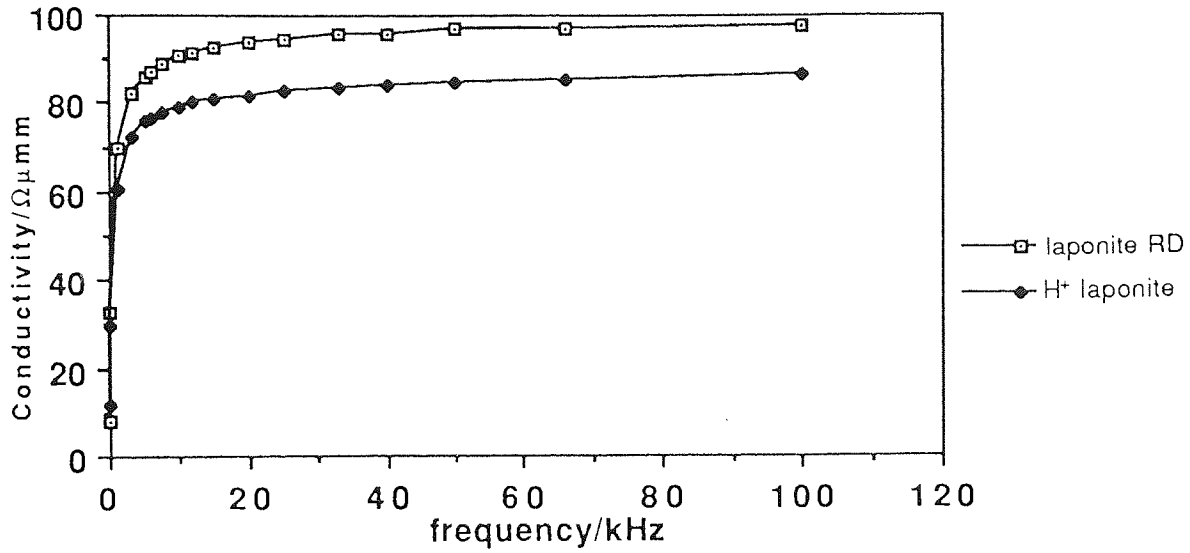

Figure 5.23 The conductivity of acidified laponite measured on the Stainless Steel Electrode.

The smooth appearance of the surface in the conductive samples, produced from reaction of laponite RD with organotellurium compounds and with Ph_3SnCl suggested that the particle-particle interaction had been improved by the organometallic molecule behaving as some sort of 'glue' within the clay. In the case of the Ph_3SnCl there is formation of oxide pillars, yet with the better conducting organotellurium compounds there is no oxide pillar formation, perhaps suggesting that pillar formation is not essential in the conductivity mechanism. The variable increase in the conductivity observed with the stainless steel electrode system suggests that in the more conductive clays, where particle-particle contact is good that the pressing of the clay has little effect. However by measuring laponite RD under pressure there is vastly improved particle-particle contact and hence a much improved conductivity. The significant factor in the conductivity consideration therefore appears to be the efficiency of the particle-particle contact within the clay.

CHAPTER SIX
Synthetic Clays

CHAPTER SIX

Synthetic Clays

6.1 Introduction.

The aim of this research was to improve the electrical conductivity of laponite, the clay material used for the coating of high technology electrographic paper. In chapter five it was shown that the conductivity of some organometallic modified laponites, whose production is outlined in chapters three and four, had improved the electrical conductivity of laponite.
Unfortunately the organometallic reaction with laponite produced a change in the rheological properties of the final materials when compared with the original clay. Laponite has the ability to swell when added to water and also has the ability to form a gel. This property is essential for use in the paper industry, where the clay is used in the form of a 13% aqueous suspension. The inability of the organometallic modified clays to swell in water effectively eliminates them from this industrial application.
Previous experiments (see chapter 5) indicated that the interlayer cations are important in the consideration of conductivity. The organometallic study with organotellurium compounds suggested that the formation of pillars, initially thought to improve cation mobility and hence conductivity, is not an important consideration. This together with the necessity of the clay to swell in water contributed to the formation of an alternative strategy. This being to modify the nature of or to increase the concentration of the interlayer ions. Bond[54] suggested that the dominant component of clay conductivity was ionic, therefore by increasing the concentration of ions in the clay structure it was hoped that an increase in the overall conductivity would be seen.

6.2 Modification of the nature of the interlayer cation.

Laponite RD is synthesised with sodium (Na^+) interlayer cations. Previous work by Bond[54] involving the substitution of the interlayer Na^+ ion by the other Group I ions showed that the potassium (K^+) ion led to a four fold increase in the conductivity of the clay. The other alkali metals had little significant effect. These conductivity results are illustrated graphically in Figure 6.1. Unfortunately the lesser hydration properties of the K^+ cation resulted in a change in the rheological properties of the clay. When the K^+-exchanged clay is added to water it does not swell readily and unlike its sodium counterpart does not form a gel. This gelling property is essential for use in the paper industry.

Following the work carried out by Bond[54] in exchanging interlayer sodium ions with the other alkali metals it was deemed prudent to widen the investigation using a divalent ion. The

ion selected was the copper (Cu^{2+}) ion. The copper ion was chosen following the synthesis of a copper containing fluorohectorite (described in detail in section 6.3.2.2). This clay was produced such that the copper was found in the lattice structure rather than the interlayer region. After examining the conductivity of the synthesised fluorohectorite it was logical to investigate the effect on the conductivity of laponite containing Cu^{2+} ions in the interlayer region in case there had been cation migration from the lattice into the interlayer in the fluorohectorite clay.

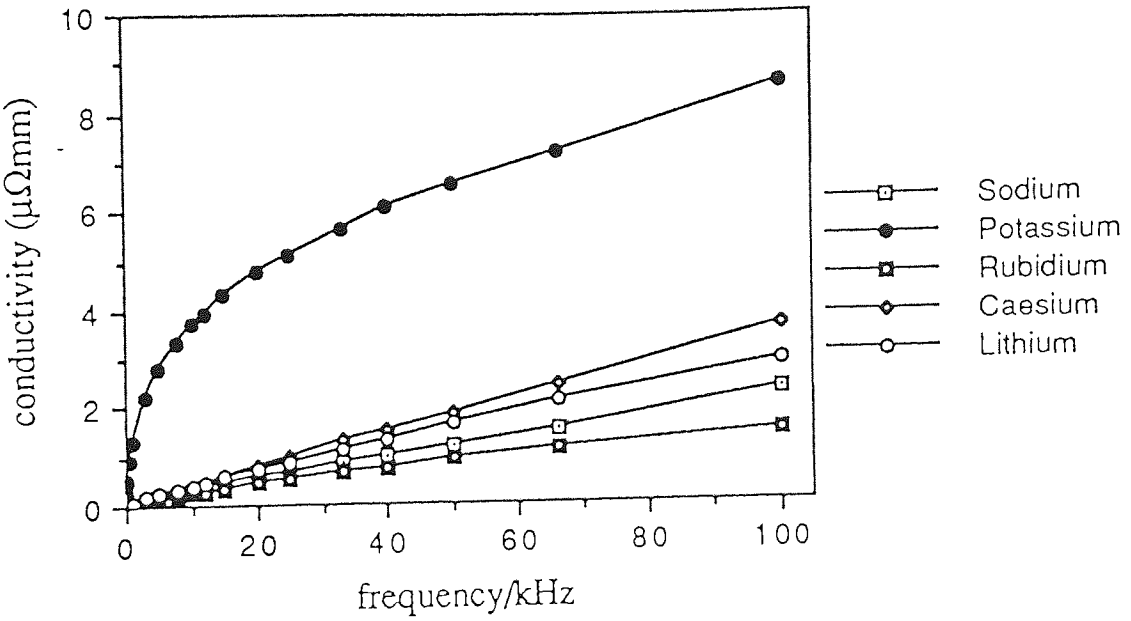

Figure 6.1 The effect on the conductivity of laponite RD by substituting the interlayer sodium ions for the other Group I metals.

6.2.1. Ion Exchange using a Divalent Cation.

6.2.1.1. Experimental Methods.

In order to convert laponite RD from the sodium (Na^+) form into a clay containing Cu^{2+} interlayer cations a method developed by Posner and Quirk[16] was used.

Laponite RD (5g) was washed with a 1M solution of copper(II) chloride ($CuCl_2$) and separated by decantation. This procedure was repeated five times. The clay was then suspended in 1M aqueous solution of $CuCl_2$ at pH 3 (adjusted with 1M hydrochloric acid) and allowed to settle

before decantation. This procedure was repeated three times. The clay was resuspended in $CuCl_2$, pH 3, and stirred for 36 hours. After standing, the clay was recovered and dialysed with deionised water until no chloride ions were observed in the water using the acidified silver nitrate test[59].

6.2.2 Results.

The resultant clay was an inferior electrical conductor (see Figure 6.2) than laponite RD. This was expected as Cu^{2+} ions are strongly hydrated, forming a $[Cu(H_2O)_6]^{2+}$ species. Pinnavaia *et al*[143] reported *via* electron spin resonance (ESR) that the $[Cu(H_2O)_6]^{2+}$ species contained within Cu^{2+}-exchanged hectorite were orientated as opposed to free tumbling. This suggests that the larger charge on the interlayer ion gives it a greater affinity for the negative charge on the sheet silicate and hence it is less mobile than a monovalent ion. This observation was also reported *via* tests within the paper industry[129]. Reports indicate that smectite clays containing monovalent cations are better electrical conductors than those with group II metals (and hence divalent cations). Metals tested included calcium (Ca^{2+}) and magnesium (Mg^{2+}).

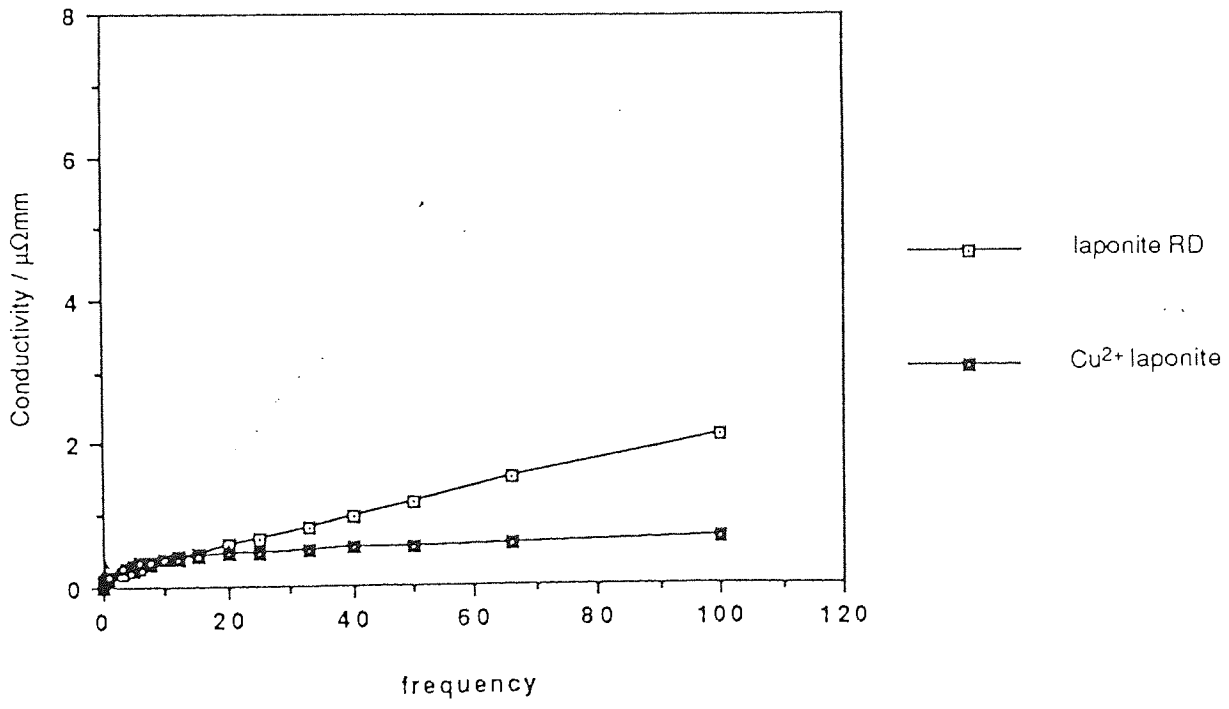

Figure 6.2 The effect of a divalent interlayer cation on the conductivity of laponite.

6.3 The Modification of the concentration of interlayer cations.

6.3.1 The Structure of laponite RD.

The synthetic hectorite, laponite RD (see Figure 6.3) is a trioctahedral clay containing sodium as the interlayer cation. The idealised formula[134] of the clay is given as

$$\{Si_8(Mg_{5.34}Li_{0.66})O_{20}(OH)_4\}Na^+_{0.66}$$

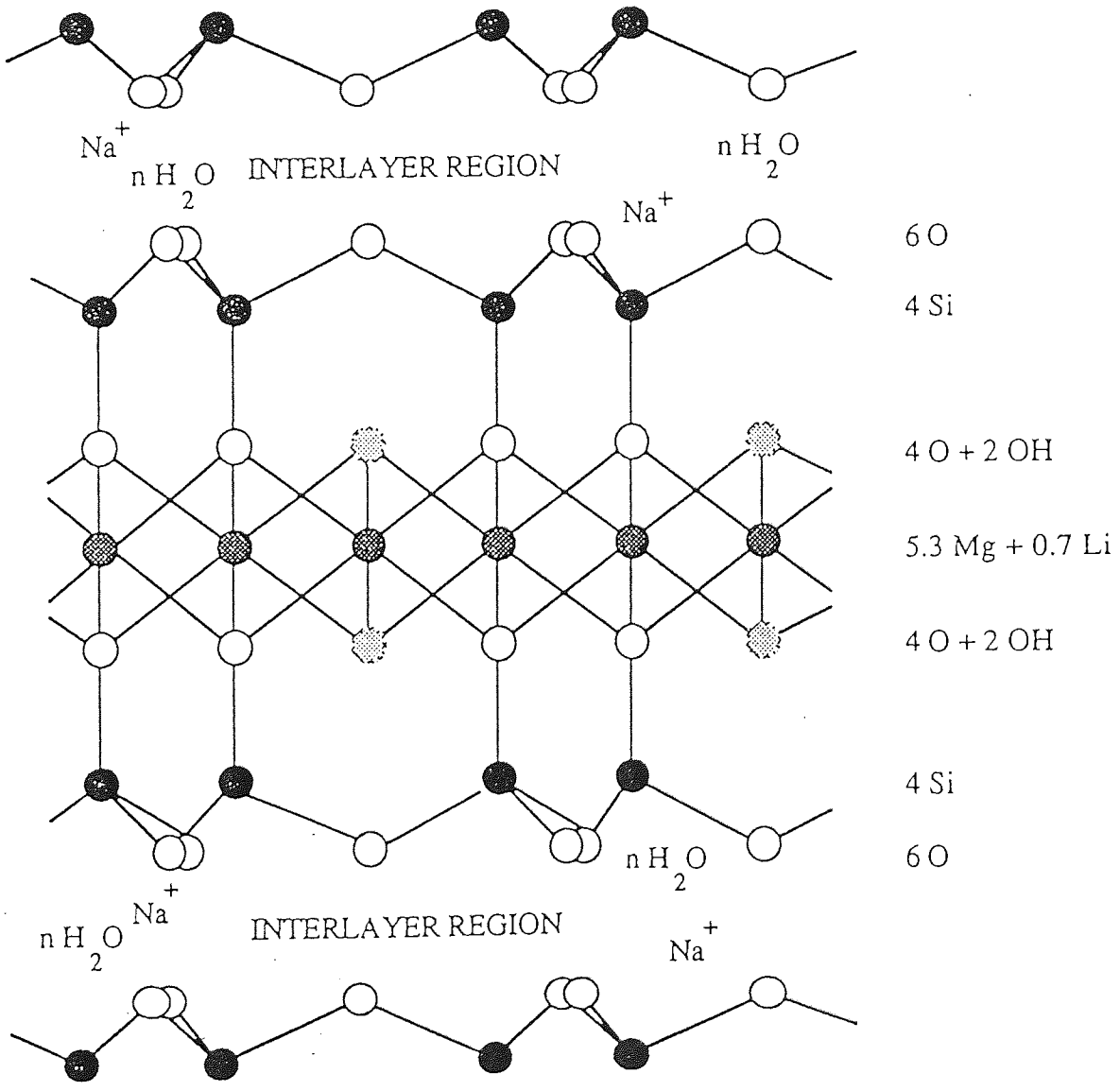

Figure 6.3 The Structure of laponite RD.

It was suggested that if the concentration of sodium ions within the interlayer could be increased then there is the potential for more electrical charge to be carried.

In order to increase the concentration of the interlayer sodium ions it is necessary to manipulate the magnesium to lithium ratio within the structural lattice. The sodium ions contained in the interlayer fulfill the function of balancing charge defects caused by the trioctahedral substitution of lithium (Li^+) ions for magnesium (Mg^{2+}) ions. Each time a lithium ion replaces a magnesium ion in the structure there is a loss of one positive charge, hence resulting in a net negative charge imbalance. The interlayer sodium ions balance this charge, therefore the concentration of the sodium ions must be approximately equal to the concentration of the lithium structural ions. Logic suggests that if the concentration of lithium ions in the structure is increased at the expense of the magnesium ions then the concentration of sodium ions incorporated within the interlayer region will also increase so that the negative charge excess may be balanced.

To achieve this objective it was necessary to synthesise the clay materials from their component parts.

6.3.2 Synthesis of Clay Minerals.

6.3.2.1 Introduction

Historically in order to synthesise clay minerals, high temperatures and/or pressures together with specialised apparatus have been necessary. In order to synthesise fluorine micas[135] it was necessary to produce a melt at temperatures of between 1200 and 1500°C or carry out a solid state reaction at 900-1200°C. Tateyama *et al* [136] reported the synthesis of micas by the solid state reaction of talc with alkali fluorosilicates (Na_2SiF_6 and K_2SiF_6) at temperatures between 700 and 900°C.

Lithium-smectites[137] were synthesised in the solid state at 800°C within 24 hours, or *via* melts at 850°C within 2 hours.

Granquist and Pollack[138] synthesised a montmorillonite from a slurry of diatomite and bayerite. In this case the reaction was caried out at 300°C using a superpressure bomb.

Another procedure for the preparation of clay minerals is known as the co-precipitated gel method[139]. This method is dependent on at least one of the constituent materials forming a gel structure. The non-gel-forming constituents are then held within the framework of the gel. Materials are fired at ~800°C.

Zeolites can also be synthesised. A review of the synthesis of these compounds was presented by Davis and Lobo[140]. The majority of methods for zeolite synthesis presented in the literature[140, 141] require the constituent mixture to be calcined at temperatures greater than 500°C.

The necessity of high temperatures and in some cases high pressures made preparation, in the laboratory at Aston, of these materials unattractive. However a recent report by Luca *et al* [142] suggested a route of synthesis *via* a sol-gel method which could be readily carried out in the laboratory. The method was a simple but time consuming one, taking several weeks, but it reached temperatures of less than 100°C (high enough to carry out a reflux reaction of the constituents in an ethanol/water solvent) and the apparatus required was simple quickfit glassware and a heating mantle. The method also afforded better control over the manipulation of the elemental ratios within the material being prepared.

6.3.2.2 Experimental Procedure.

The method of Luca[142] was followed in order to synthesise a Copper(II)-substituted fluorohectorite with composition given by

$$\{Si_8(Mg_{4.98}Cu_{0.02}Li_{1.0})O_{20}F_4\}Na^+_{1.0}$$

The synthesis is outlined below:
Tetraethylorthosilicate (41.66 g) was added to ethanol (100 cm^3) and stirred at 60°C for 3 hours. To this solution was added $MgCl_2.6H_2O$ (21.31 g) and $CuCl_2.2H_2O$ (0.085 g) dissolved in deionised water (200 cm^3). This ethanol/water solution was stirred for 4 hours. Aqueous NaOH solution was added until a pH of 9.5 was achieved. The solution was stirred for 12 hours. The Mg/Si precipitate was filtered and washed. The solid was resuspended in deionised water whereupon LiF (0.648 g) and NaF (~3g) were added. This solution was stirred for 12 hours and subsequently refluxed for 7 days. The product was treated with an ethylenediamine tetraacetic acid (EDTA) / sodium acetate pH = 5.5 buffer solution. This procedure removes possible exchangeable Cu(II) or surface bound Cu(II) which are not part of the structural lattice. The hectorite suspension was filtered and dialysed to remove any excess cations. The sol remaining after dialysis was allowed to stand for one week in a beaker. When it was apparent that no particulate material had collected at the bottom of the beaker it was concluded that the suspension consisted of pure smectite, The clay was dried over silica gel.

This clay will be assigned as synthetic clay I in subsequent pages of this thesis.

A series of synthetic clays was produced *via* this method, each one with the constituent materials ($MgCl_2.2H_2O$ and LiF) modified in quantity in an attempt to alter the Mg:Li ratio in the octahedral layer. Table 6.1 lists the molar quantities and hence grams of material used for each clay. The calculated quantities of materials were designed to produce clays containing 90, 80, 75 and 50% of the original magnesium content (that seen in synthetic clay I). The code assigned to each preparation will be used throughout this chapter for simplicity.

In the preparations of synthetic clays II-VI inclusive, the EDTA/sodium acetate buffer stage was deemed unnecessary as no $CuCl_2.H_2O$ was added to the reaction flask (the purpose of the buffer solution is to remove any Cu^{2+} not forming part of the octahedral lattice).

Synthetic Clay code	% original Mg	$MgCl_2.2H_2O$	LiF
I	100	0.015 mole, 21.35g	0.025 mole, 0.65g
II	100	0.105 mole, 21.35g	0.025 mole, 0.65g
III	90	0.0945 mole, 19.18g	0.0355 mole, 0.92g
IV	80	0.084 mole, 17.08g	0.046mole, 1.19g
V	75	0.0788 mole, 15.99g	0.051 mole, 1.33g
VI	50	0.053 mole, 10.67g	0.0775 mole, 2.01g

Table 6.1 Quantities of $MgCl_2.2H_2O$ and LiF used in the preparation of Synthetic Clays.

6.3.3 Characterisation and Analysis of the Synthetic Clays.

It was preferable to obtain analytical data on these new materials. X-ray fluorescence spectroscopy is widely used by geologists in order to obtain an elemental analysis of the clay mineral. Unfortunately low molecular weight elements, including lithium and fluorine cannot be detected using this technique. However for our purposes a ratio of Si : Mg : Na provides very useful information. Samples were sent to Keele University for analysis. Data were received in the form of elemental oxides. The technique also measures the loss of weight on ignition which was given as between 5 and 12% over the range of samples.

6.3.3.1. Synthetic Clay I.

According to Luca[142] the composition of the final product clay - Synthetic clay I - is given by

$$\{Si_8(Mg_{4.98}Cu_{0.02}Li_{1.0})O_{20}F_4\}Na^+_{1.0}$$

As the literature preparation had been duplicated it was expected that the composition would be very similar to that suggested by Luca[142]. X-ray fluorescence spectroscopy (XRF) data and calculated elemental ratio are presented in Table 6.2.

Oxide	% composition
SiO_2	63.99
MgO	23.04
Na_2O	2.64
Elemental Ratio	$Si_8 : Mg_{5.16} : Na_{0.92}$

Table 6.2 XRF Analysis of Synthetic Clay I.

Manipulation of these figures yielded a ratio of Si : Mg : Na. The lithium content is assumed to be equal to that calculated for the sodium (for reasons outlined in section 6.3.1). A formula derived for the clay and expressed below.

$$\{Si_8(Mg_{5.16}Li_{0.92}Cu_x)O_yF_z\}Na^+_{0.92}$$

The presence of copper within the clay was confirmed by scanning electron microscopy (SEM) whereupon a peak in the copper 'window' was observed. Examining the elements we have figures for and comparing these to the literature preparation, see Table 6.2 it can be seen that the ratio of Si : Mg : Na is comparable with that expected.

The basal spacing of the clay was found to be 13.55Å, a value comparable to that reported for laponite RD[9].

6.3.3.2. Synthetic Clays II-VI.

X-ray fluorescence, calculated formulae and basal spacing results are presented in tabular form. Table 6.3 shows the data obtained from analysis by x-ray fluorescence spectroscopy.

Oxide	Synthetic II	Synthetic III	Synthetic IV	Synthetic V	Synthetic VI
SiO_2	62.71	59.86	79.81	65.16	78.33
MgO	23.88	22.84	10.69	19.39	13.48
Na_2O	2.98	7.30	1.73	2.22	0.96

Table 6.3 XRF Analysis for Synthetic Clays II-VI.

The figures were manipulated to produce a ratio of elements. These results are presented in Table 6.4. The theoretical figures are shown in brackets. In all cases ratios were calculated relative to Si_8.

Oxide	Synthetic II	Synthetic III	Synthetic IV	Synthetic V	Synthetic VI
SiO_2	8.0	8.0	8.0	8.0	8.0
MgO	5.65 (5.0)	5.47 (4.50)	1.92 (4.0)	2.26 (3.75)	2.43 (2.50)
Na_2O	0.88 (1.0)	2.20 (1.50)	0.40 (2.0)	0.64 (2.25)	0.22 (3.50)

Table 6.4 Theoretical and Found Elemental Ratios for Synthetic Clays II-VI.

Powder XRD was employed in order to derive the basal spacings of the new clays. These data are presented in Table 6.5.

Clay Sample	Basal spacing (Å)
II	13.59
III	14.31
IV	11.30
V	4.49
VI	4.47

Table 6.5 The "basal" spacings of Synthetic Materials II-VI.
(i.e. d spacing corresponding to the lowest 2θ value)

6.3.4 Discussion.

The samples, synthetic clays I-II were in good agreement with the theoretical calculations. The aim of increasing the sodium content above that of laponite RD had been achieved with these samples. The comparison of sodium ion content per unit structure is illustrated in Table 6.6.

Clay	Na^+ content per unit structure
laponite RD	0.66
synthetic I	0.92
synthetic II	0.88

Table 6.6 A Comparison of sodium ion content per unit structure.

Solid state ^{6}Li and ^{29}Si MASNMR studies were carried out on synthetic clays I and II.

6.3.4.1 ^{6}Li MASNMR

The ^{6}Li rather than the more abundant ^{7}Li nucleus (92.5%) was utilised in this study. McWhinnie *et al*[69] reported that the use of this nucleus is profitable, as the quadropole moment is significantly lower than that of ^{7}Li and hence the spectral peaks are much narrower. This enables resonances of similar frequency to be resolved more efficiently.

The ^{6}Li MASNMR spectrum of laponite RD is shown in Figure 6.4 as a reference spectrum. A signal at 0.65 ppm is clearly seen. The ^{6}Li spectrum of synthetic clay I (Figure 6.5) shows a doublet at 0.71 ppm. The presence of a doublet indicates that lithium is present in two different chemical environments. This would be expected in this sample as the lithium can be found adjacent to both magnesium and copper ions within the trioctahedral layer. The ^{6}Li spectrum of synthetic clay II (Figure 6.6) reveals one band, at 0.75 ppm. In all these spectra the signal is found at comparable values (within 0.1 ppm). A slight drift in the absolute number of the signal may be expected due to the fact that the apparatus had no lock during this run of experiments. These spectra show that all the clays contain lithium and that the structures are very similar. The number of pulses used in these analyses were of the same order and the intensity of the resultant signals were comparable suggesting that the lithium content within each sample is very similar.

6.3.4.2 ^{29}Si MASNMR

The chemical environment of the silicon within the clay samples I and II was investigated.

A ^{29}Si spectrum of laponite RD (Figure 6.7) was in agreement with that reported in the literature[144]. Two signals are seen at -94.4 and -85.4 ppm respectively. The dominant signal (-94.4 ppm) is derived from the Q^3 silicon content - that is those silicon atoms bonded to three adjacent oxygen atoms - found in the bulk of the clay. The smaller signal at 85.4 ppm is caused by the Q^2 silicon - those at the edge sites on the clay and hence bonded to only two adjacent oxygen atoms. This component is visible with laponite RD because of the very small particle size of the clay, and hence a significant proportion of edge sites.

Examination of synthetic clay I (Figure 6.8) revealed three signals. The Q^3 band at -94.1 ppm is the dominant component of the silicon content. The Q^2 peak at -85.4 ppm indicates that synthetic clay I has a particle size comparable to that of laponite RD. A third signal is apparent at -110.6 ppm, this feature is characteristic of a silicon in a Q^4 environment and is caused in this case by an impurity within the clay of amorphous silica.

Analysis of the ^{29}Si spectrum of synthetic clay II (Figure 6.9) showed two peaks; the Q^3 environment (-93.7 ppm) and a smaller Q^2 band (86.2 ppm). From these spectra it can be concluded that the synthetic clays I and II are lithium containing laponite species, with a relatively small particle size, a sensible basal spacing and a concentration of sodium ions above that of laponite RD.

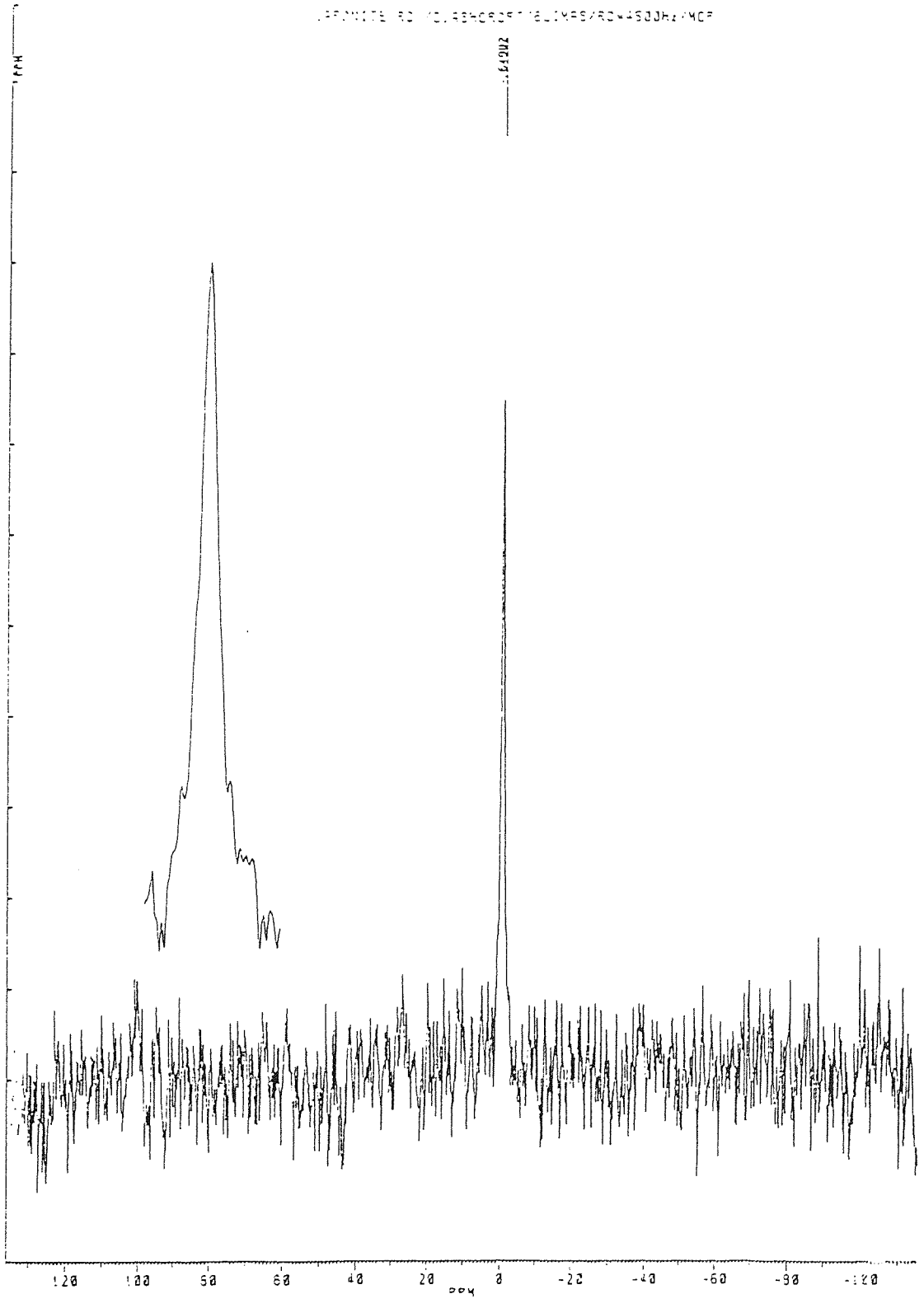

Figure 6.4 ^{6}Li MASNMR spectrum of laponite RD

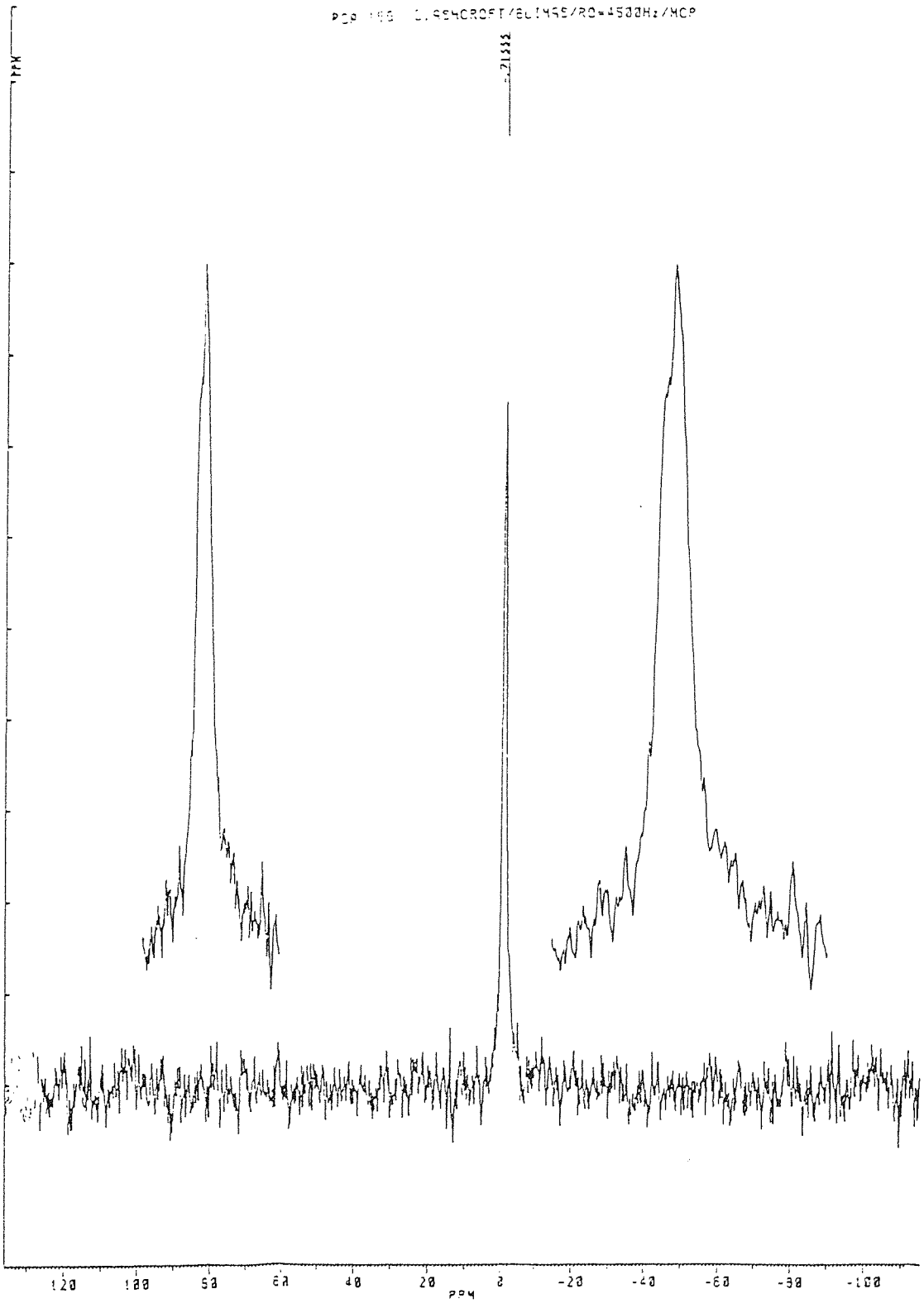

Figure 6.5 ^{6}Li MASNMR spectrum of Synthetic clay I

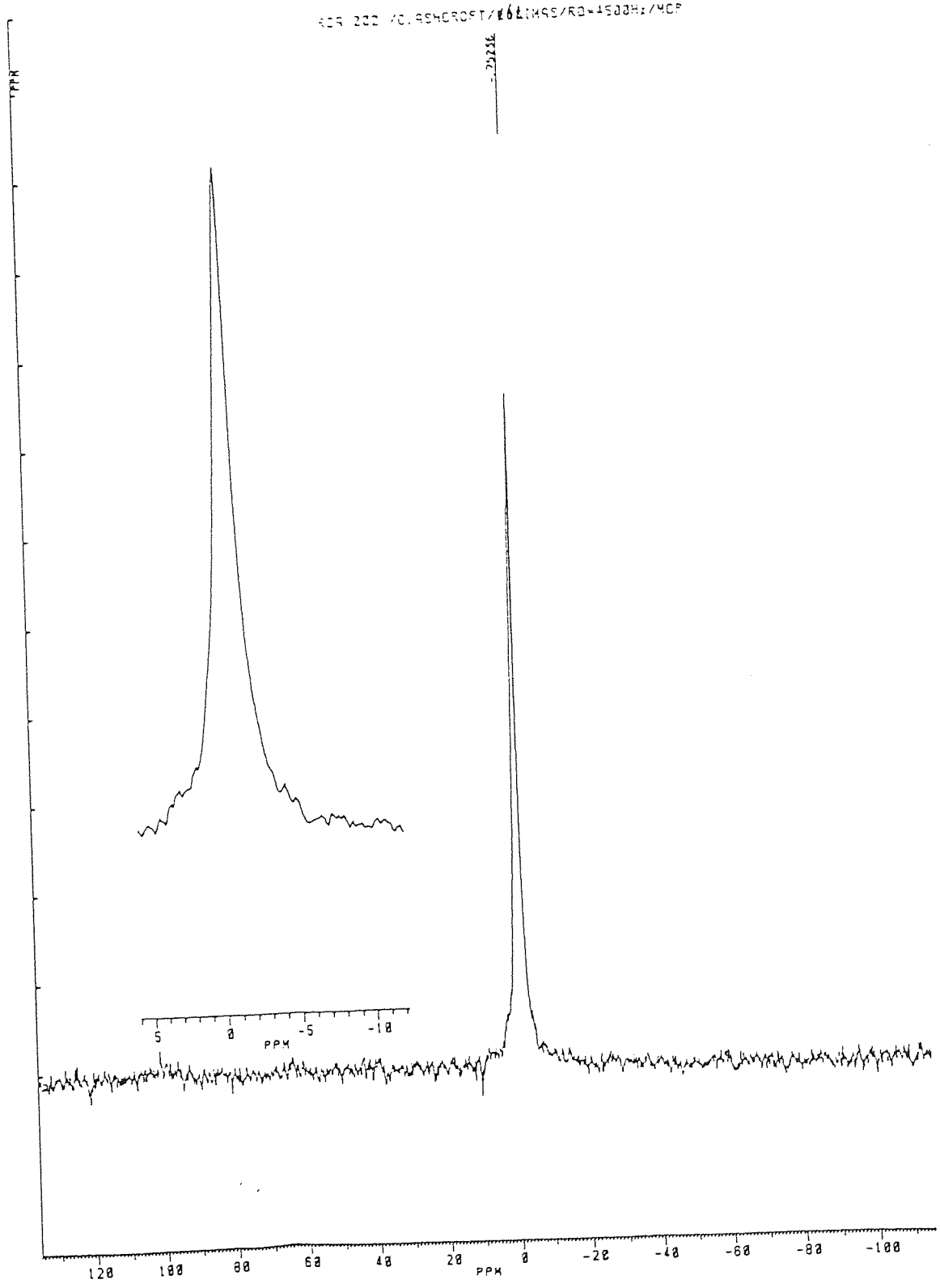

Figure 6.6 ^{6}Li MASNMR spectrum of Synthetic clay II

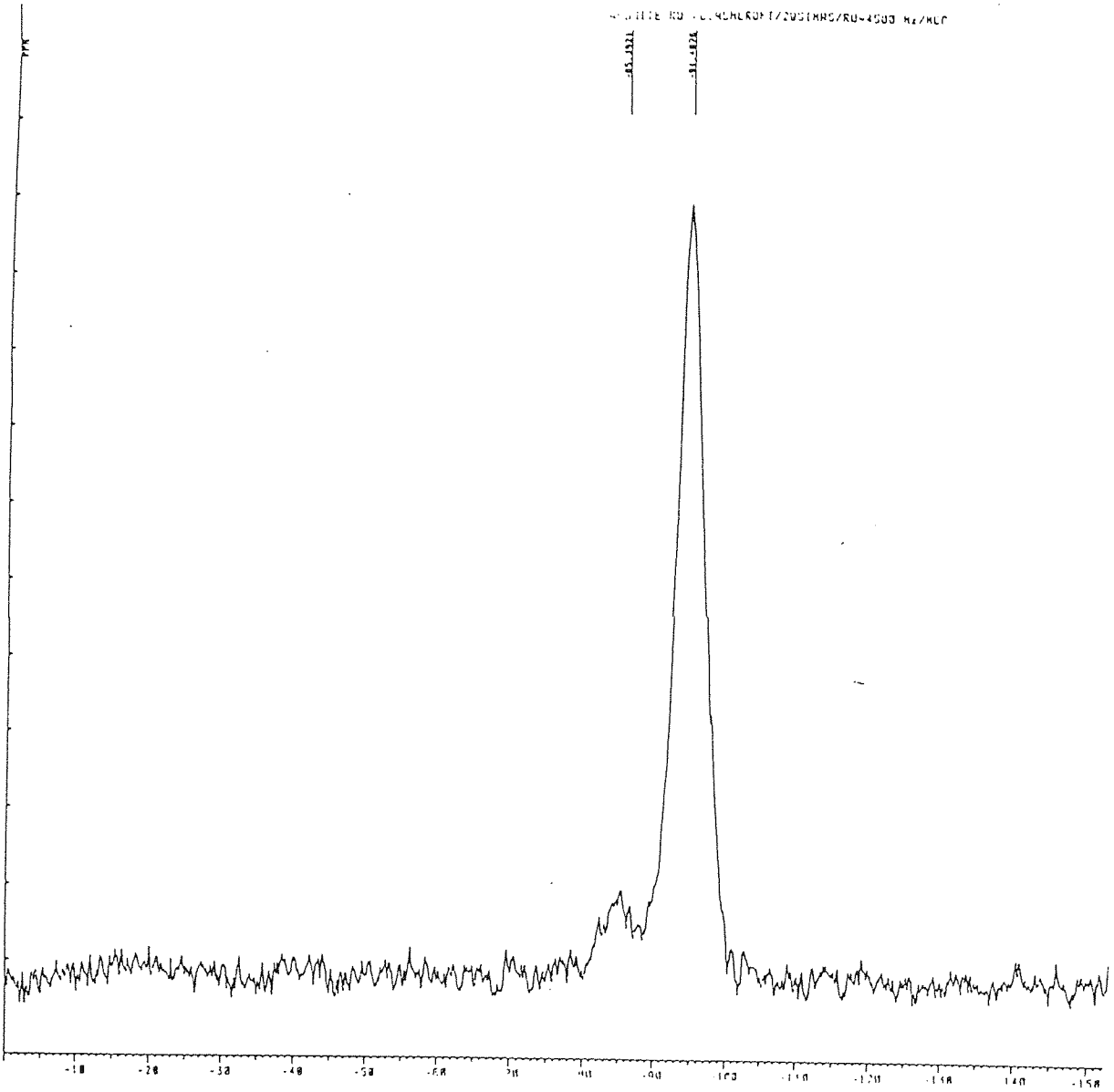

Figure 6.7 ^{29}Si MASNMR Spectrum of laponite RD

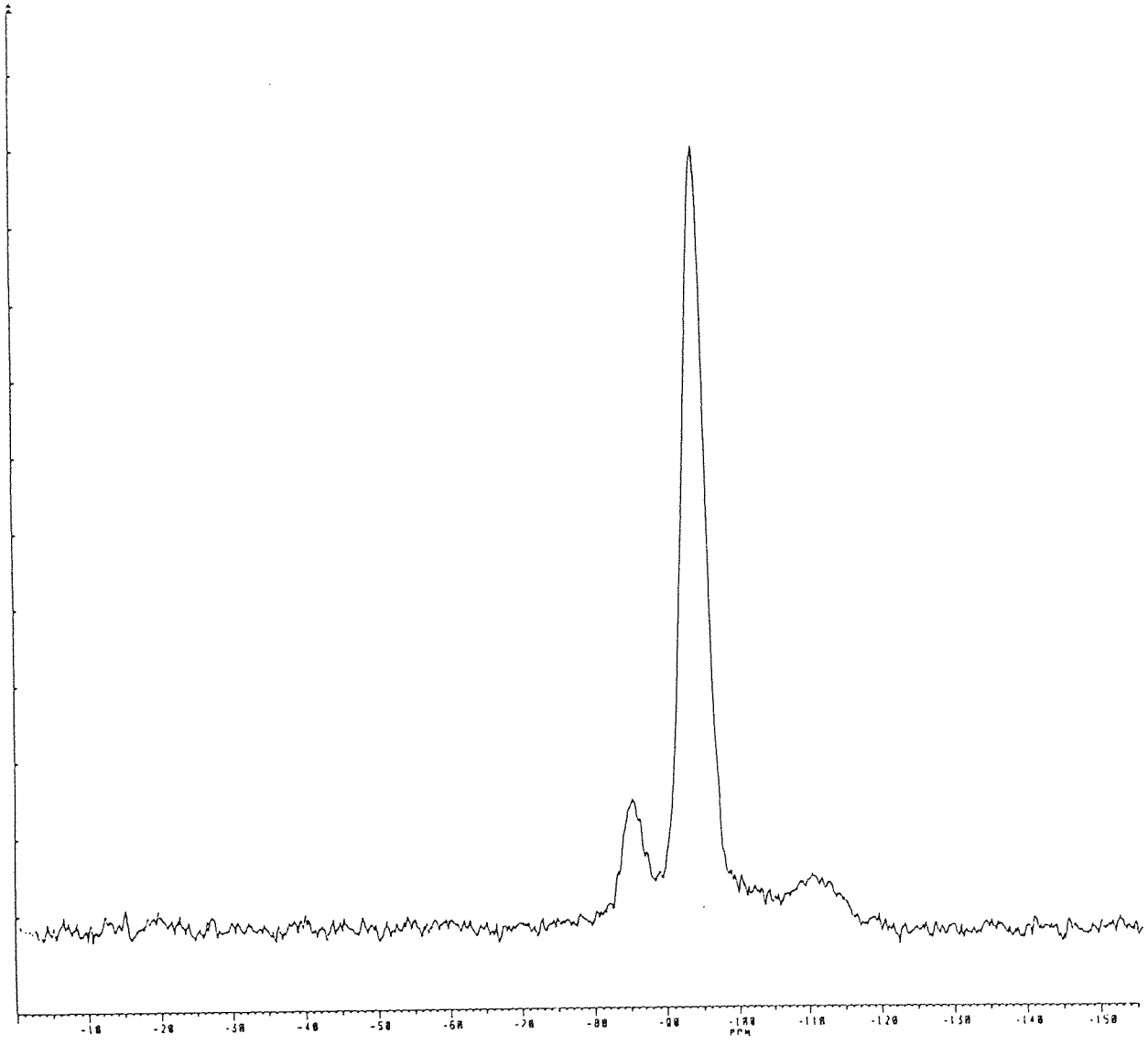

Figure 6.8 ^{29}Si MASNMR Spectrum Synthetic clay I

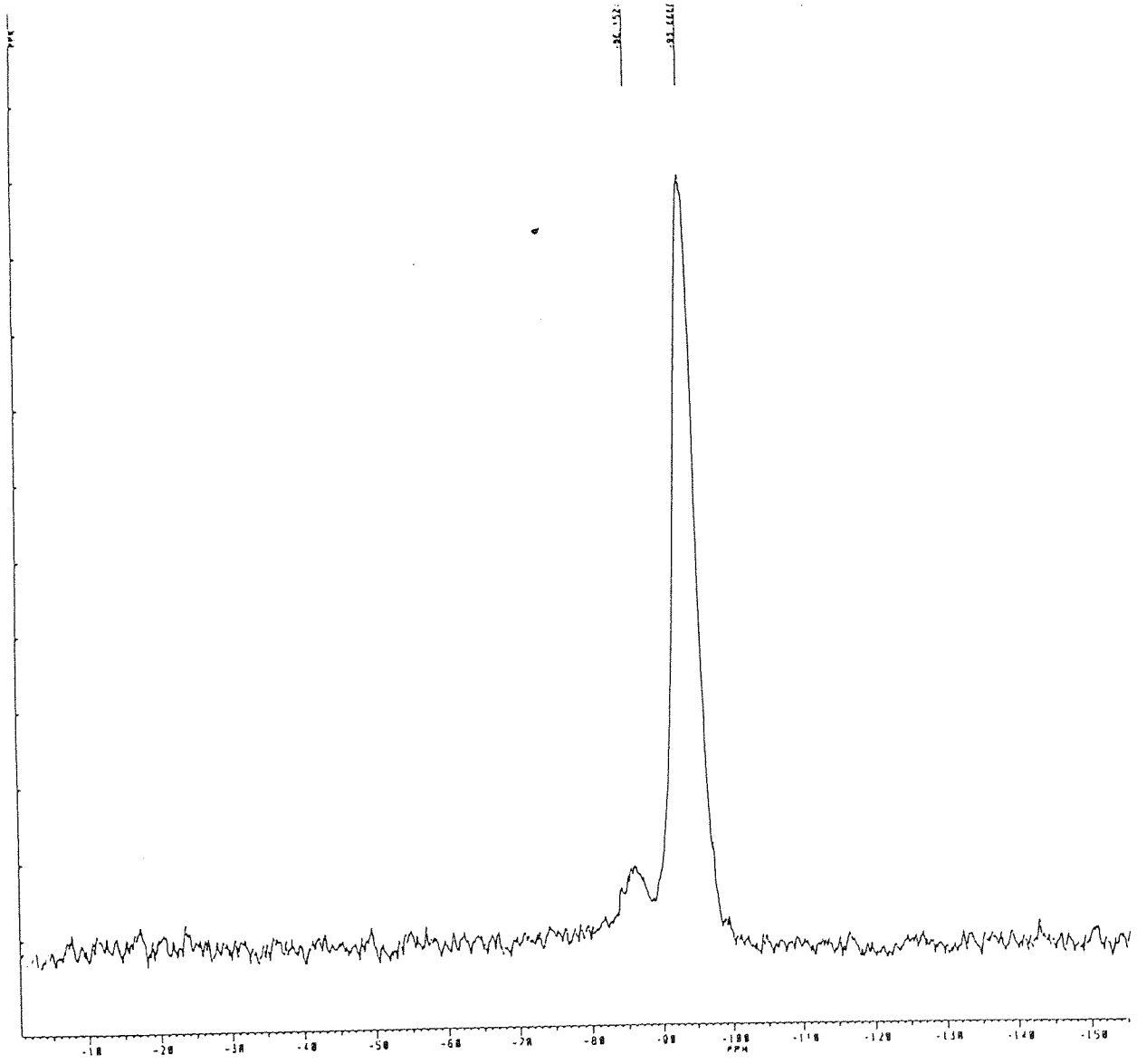

Figure 6.9 ^{29}Si MASNMR Spectrum Synthetic clay II

The remaining synthetic clays III-VI inclusive, in which attempts were made to further increase the sodium content, results were disappointing. The sodium ion content in Synthetic clay III was greater than that found in laponite RD but was out of proportion to that calculated. The 'basal' spacing was also rather low for the material to be considered as a laponite type clay. In the Synthetic materials IV to VI the sodium content was low compared to the theoretical values calculated and also lower than laponite RD itself. The appearance of these samples also cast doubt on whether they were the same class of compound as Synthetic clays I and II. In these samples, and in particular in synthetic materials IV and VI, the elemental analyses (see Table 6.3) reveal that the percentage of silicon in each clay is very high (15 - 20% greater than in the first three samples). The magnesium content is also depleted by 40-50% of the synthetic I-II values. The magnesium depletion was largely in line with that calculated (see Table 6.4), unfortunately the depletion was not made up by lithium (and hence sodium) as was hoped but was replaced by silicon. The d spacings for materials IV to VI were low and not consistent with that expected from laponite type materials. These factors suggest that a different class of material is being produced when attempts are made to raise the sodium content beyond a critical point. The physical appearance of the two sets of clays (I-III and IV-VI) were obviously different to the naked eye. The first three synthetic clays dried to a dense opaque material which required concerted grinding to produce a powder. Synthetic clays IV- VI were much less dense, were white in colour, and had a physical state analogous to soft chalk.
These samples were consequently of little interest in the context of this chapter, however SEM analysis and conductivity measurements were carried out in case these compounds were of interest to future workers. Further characterisation beyond that of XRF and XRD was deemed unneccesary at this stage.

6.4 Investigation of the clay surface using Scanning Electron Microscopy (SEM).

The interesting physical differences in the appearances of the clays were examined in more detail under powerful magnification. Samples were prepared as described in section 5.7.2.

6.4.1 Examination of Synthetic Clay I using SEM.

Observation of the clay surface at a magnification of 3960 (Figure 6.10) revealed a surface unlike that of laponite RD (see Figure 5.14). The surface of synthetic clay I did not appear to be individually particulate but had a predominantly smooth surface. This appearance was similar to that seen when organotellurium compounds had been reacted with laponite RD. This observation suggests that there may be better particle-particle contact or larger particles in this synthetic clay than in laponite RD.

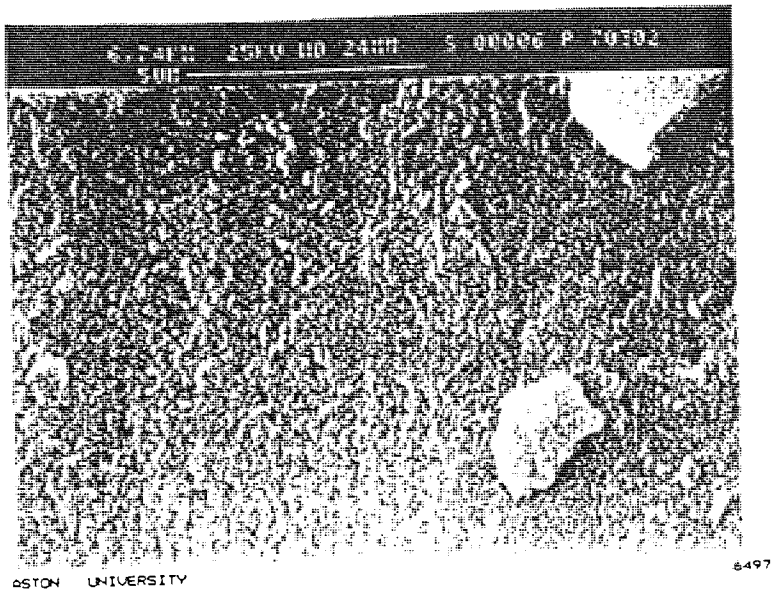

Figure 6.10 SEM image of Synthetic Clay I.

6.4.2 Examination of Synthetic Clay II using SEM.

After examination of synthetic clay I it was expected that synthetic clay II would have the same appearance (the preparation of both were identical apart from the exclusion of the $CuCl_2.2H_2O$ in the second clay). Examination of the surface at a magnification of 6740 (Figure 6.11) showed that there was better particle-particle contact / larger particle size as expected.

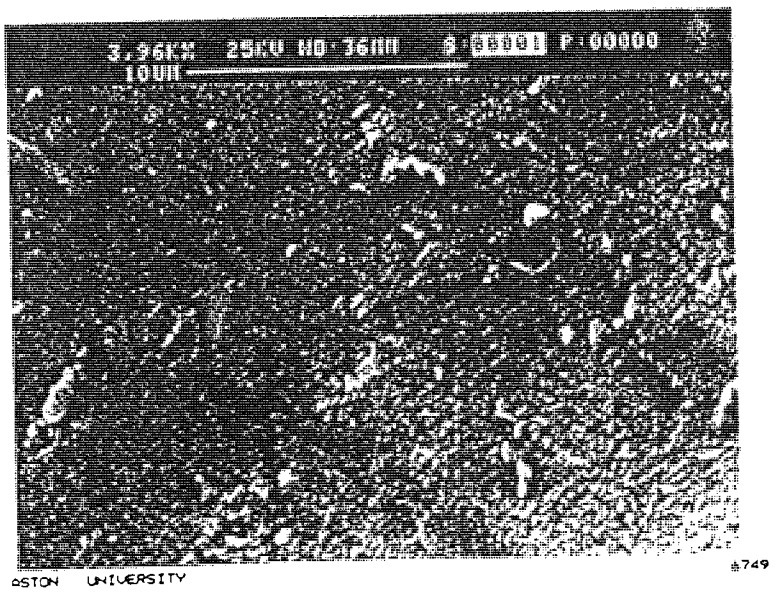

Figure 6.11 SEM Image of Synthetic Clay II.

6.4.3 Examination of Synthetic Clay III using SEM.

Examination of the clay surface at a magnification of 3900 (Figure 6.12) showed a surface analogous to synthetic clays I and II.

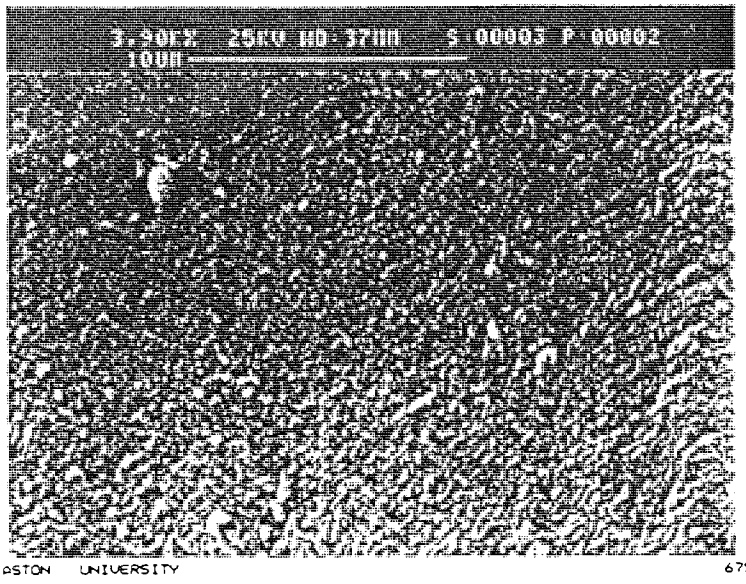

Figure 6.12 SEM Image of Synthetic Clay III.

6.4.4 Examination of Synthetic Clay IV using SEM.

This sample was different in appearance when compared with synthetic clays I-III. This difference was visible to the naked eye and was confirmed by examination under a magnification of 3820. The image, shown in Figure 6.13, has the appearance of a 'sponge-like' material.

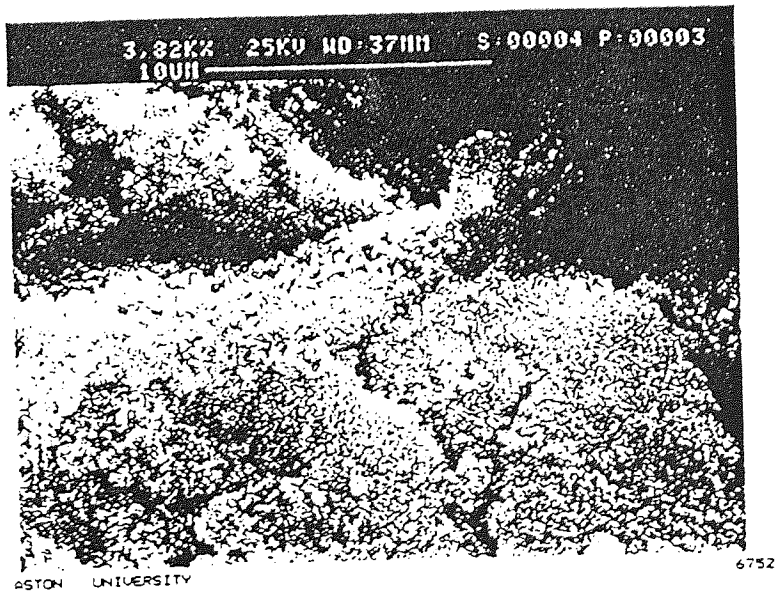

Figure 6.13 SEM Image of Synthetic Clay IV.

6.4.5 Examination of Synthetic Clays V and VI using SEM.

Examination of the surface of Synthetic Clay V using a magnification of 3960, (Figure 6.14) revealed a surface similar to that of synthetic clay IV.

The appearance of synthetic clay VI was similar to that of synthetic clays IV and V.

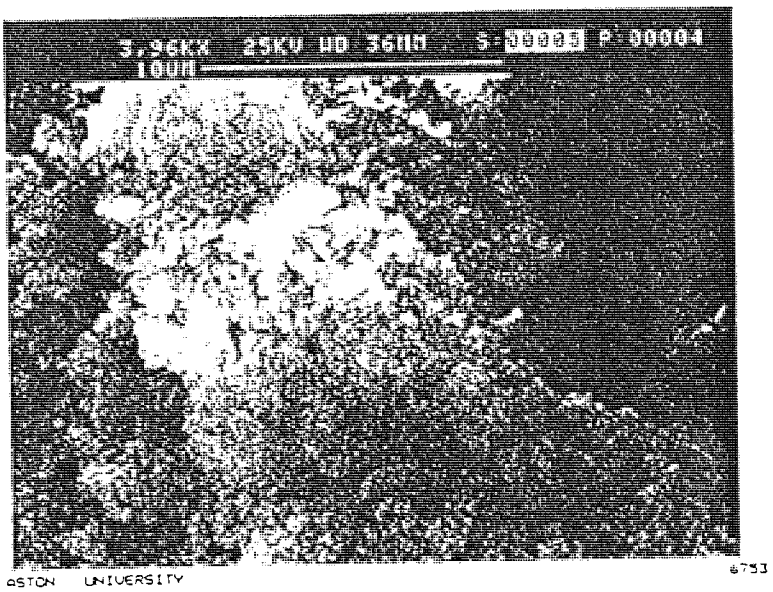

Figure 6.14 SEM Image of Synthetic Clay V.

6.4.6 Discussion

The SEM investigation of the clay surfaces suggested that the synthetic clays could be divided into two sets of compounds (I-III and IV-VI respectively). Synthetic clays I and II resemble laponite RD in composition, but not in surface appearance. Synthetic material III is a little questionable in its structure although the SEM suggests that the particle-particle contact or the size of the particles has been improved. The latter set are primarily silicate materials with much smaller basal spacing measurements than clays I-III. Synthetic clays V and VI in particular are observed to have a basal spacing of ~4.5Å (the basal spacing for laponite RD is ~14Å[9]).

6.5 Conductivity evaluation of the Synthetic Clays.

The initial hypothesis behind the synthesis of new materials was to increase the concentration of interlayer sodium ions. Analysis of the six synthetic clays suggests that this target has been achieved in three of the six cases. Initial conductivity measurements were carried out using the silver paste electrode system in order to gain an indication of the conductivities relative to laponite RD.

6.5.1 Conductivity evaluation of Synthetic Clays I and II.

Synthetic clay I was synthesised according to Luca[142] and hence contained a quantity of Cu^{2+} ions within the octahedral layer. Synthetic clay II was synthesised to theoretically be of the same composition as synthetic clay I but without the copper. The conductivity of both samples is illustrated, relative to the conductivity of laponite RD, in Figure 6.15.

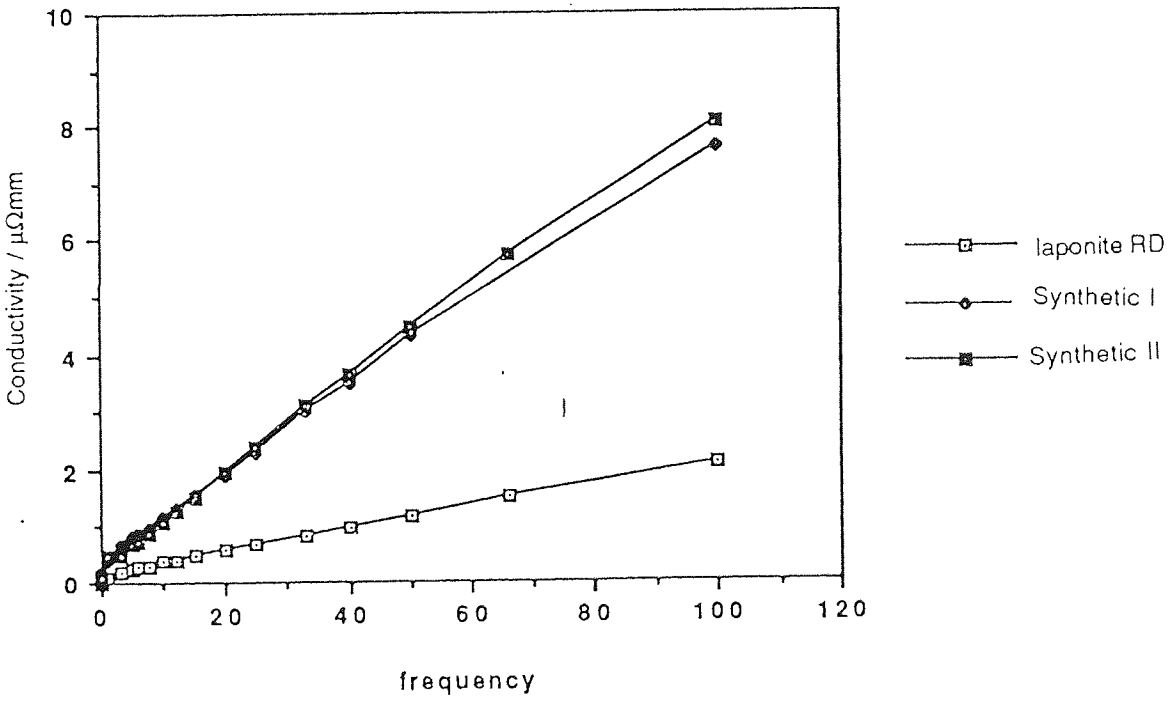

Figure 6.15 The conductivity of synthetic clays I and II in relation to laponite.

It can be seen that the conductivity graphs of the two synthesised samples are very similar, both in numerical value and shape. They also exhibit approximately a three to four fold increase in the electrical conductivity compared with that of laponite RD.

The conductivity of the copper containing synthetic clay, (I), was compared with the Cu^{2+}-exchanged laponite (Figure 6.16) prepared *via* a method described in section 6.2.1.1. The

Cu^{2+} ions contained within the two samples are found in different areas of the clays. In synthetic clay I the copper is found as part of the octahedral layer in the lattice structure. In the Cu^{2+}-exchanged laponite it is the interlayer region which contains the copper.

The results suggest that there is no migration of copper(II) ions from the lattice into the interlayer region as Cu^{2+} interlayer ions cause a decrease in the conductivity of the clay (see section 6.2.2). This decrease is not seen in synthetic clay I when compared with synthetic clay II (see Figure 6.15).

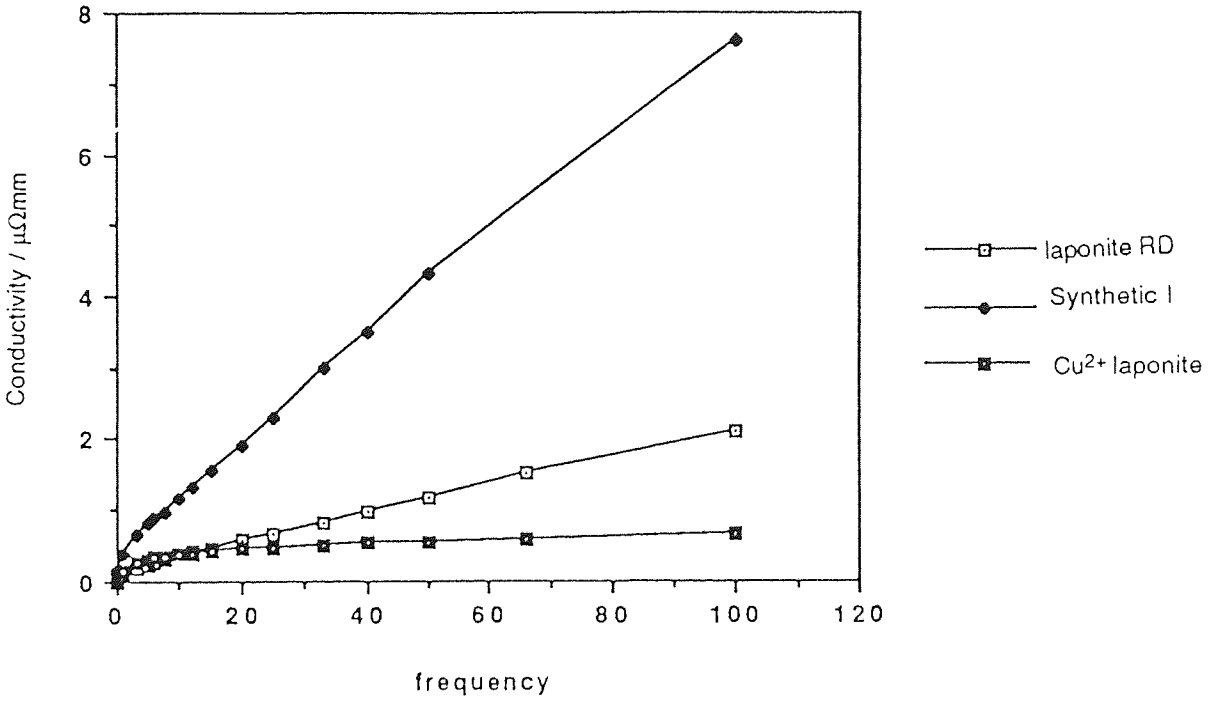

Figure 6.16 Comparison of the conductivity of clay containing Cu^{2+} ions in the interlayer and the lattice.

6.5.2 Conductivity evaluation of Synthetic Clay III.

Synthetic clay III was calculated to possess the highest concentration of sodium ions in all the clays prepared. The conductivity was measured using the silver-paste electrode system. The conductivity result is illustrated graphically in Figure 6.17.

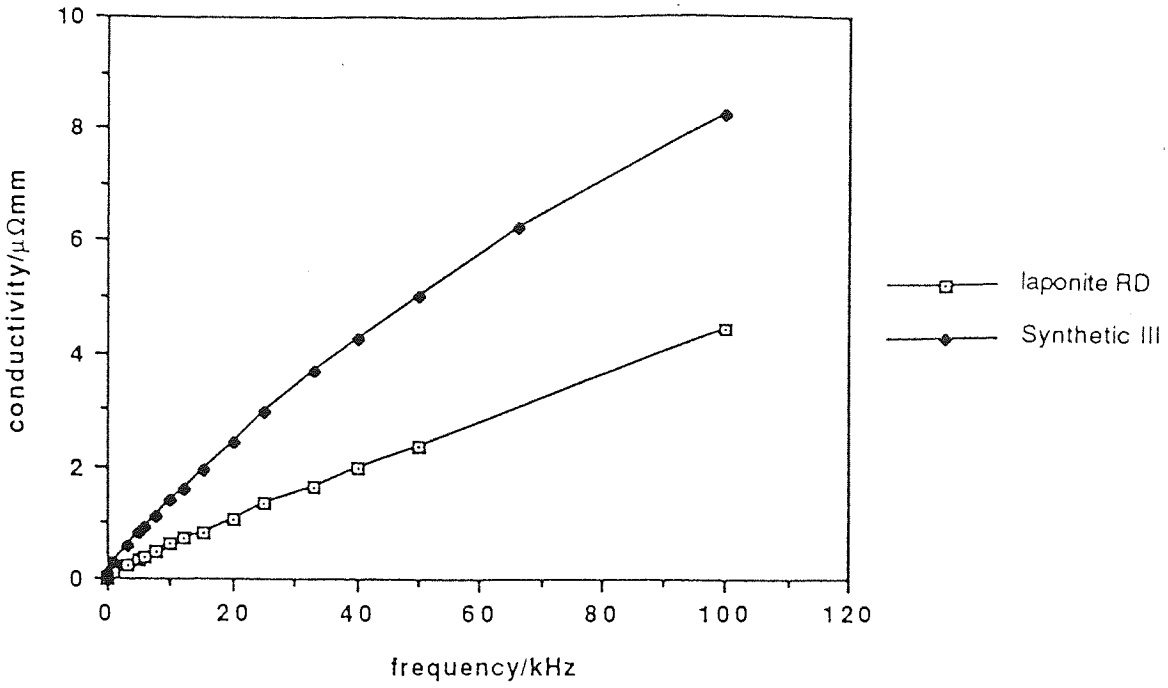

Figure 6.17 The Conductivity of Synthetic clay III.

It can be observed that the recorded conductivity is slightly improved over that of synthetic clays I and II. A four fold increase in the conductivity compared with laponite RD is seen.

6.5.3 Conductivity Evaluation of Synthetic Clays IV and V.

The synthetic samples were simplistically silicate material. The concentration of the interlayer sodium ions was very low and as expected the conductivity of these samples was inferior to that of laponite RD. Conductivity results are illustrated graphically in Figure 6.18.

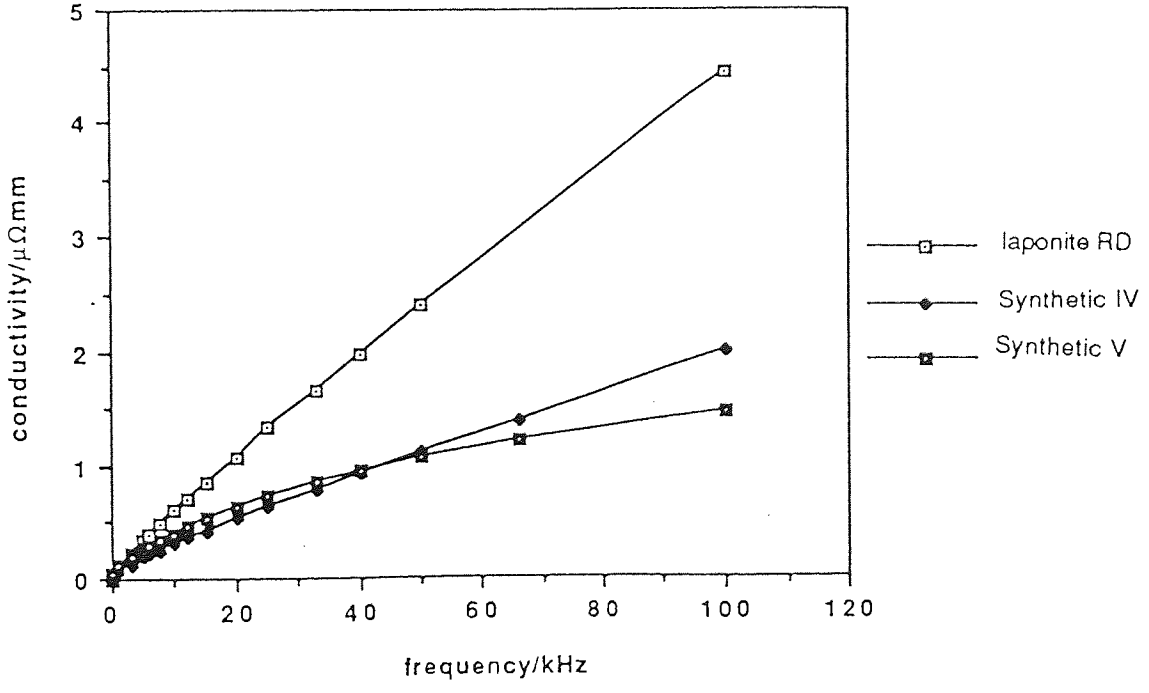

Figure 6.18 The Conductivity of Synthetic clays IV and V.

6.5.4 Discussion

The results of the conductivity evaluation show that by increasing the sodium ion concenration, the electrical conductivity also increases. An increase in the ion concentration of 0.66 to ~1.0 per unit structure facilitates an increase in the conductivity of three to four times that of laponite RD. Attempts to further increase the concentration of sodium ions within the interlayer resulted in the preparation of clays containing mainly silicate material and very little sodium. The resultant conductivities were lower than that found for laponite RD. This is further indication that the concentration of the interlayer ions is an important factor in the conductivity mechanism.

An investigation of the conductivity of the synthetic clays I-II using the stainless steel electrode (see Figure 6.19) indicated that there was no significant increase in the order of magnitude of the conductivity as seen with laponite RD. This together with the SEM images suggests that synthetic clays I-II have better particle-particle contact than laponite RD. It was suggested that increasing the particle size may be improving the conductivity rather than purely a better contact between the particles, however the ^{29}Si MASNMR evidence suggests that synthetic clays I and II have particle sizes still small enough for the edge (Q^2) silicon sites to be differentiated in the spectrum, unlike montmorillonite for example, yet the clays have conductivities at ambient pressure three times greater than that of laponite.

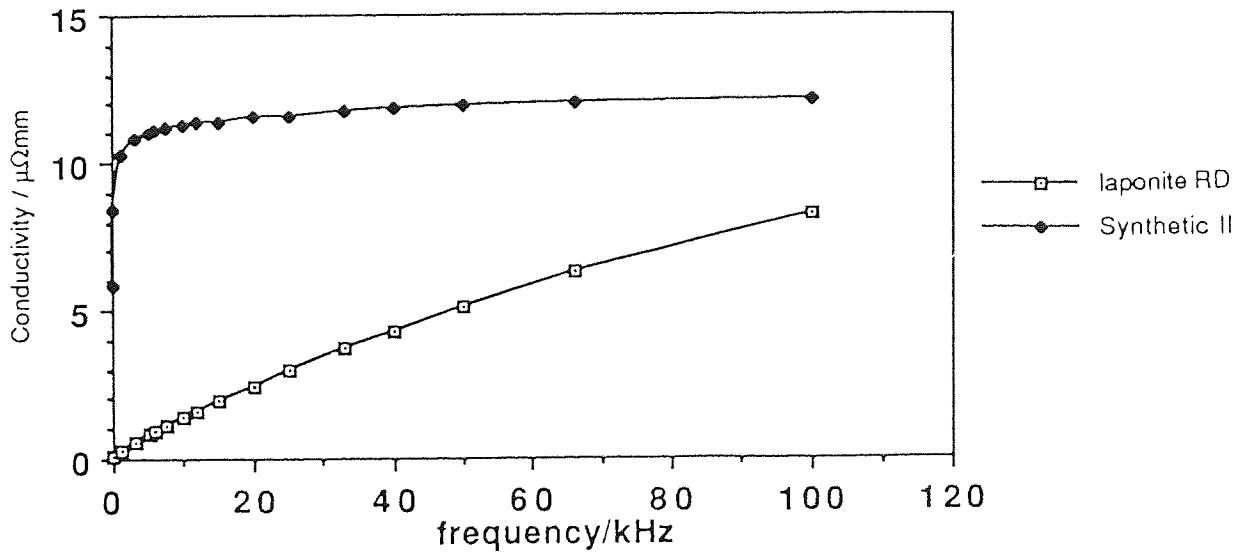

Figure 6.19 The conductivity of synthetic clay II measured on the stainless steel electrode.

These synthetic clays with the increased conductivities have potential for use in the paper industry as they not only have better conductivities than laponite RD but importantly they retain the property to swell in water and form a gel.

Overall Summary

The aim of this research was to try and increase the electrical conductivity of a smectite clay for use in the production of electrographic paper.

Previous research had shown that increasing the temperature led to an increase in the conductivity of laponite, however this avenue of exploration is impractical in terms of the eventual use of the clay. Exposing pillared laponites to increasing humidity produced negligable changes in basal spacing and consequently only small changes in the conductivity. Producing clays containing oxide pillars had been successful in obtaining an increase in conductivity and it was this path that was therefore taken.
In the modification of laponite with organometallic compounds a pattern was seen to emege in respect of any increase in the conductivity. It was found that in order for a significant reaction to occur with the clay the precursor must contain a halide content. In the case of Ph_3SnCl and the organotellurium precursors a hydrolysis reaction was seen to occur on the surface of the laponite. This hydrolysis led to the release of hydrochloric acid. The acid protons then underwent exchange with the interlayer sodium ions within the clay. This incorporation of hydrogen ions within the interlayer appears to be an important consideration in the overall conductivity. The other important factor appears to be the improvement in the particle-particle contact within the modified clays. SEM investigations revealed that the more conductive clays had a less particulate appearance than laponite RD. Conductivity measurements under pressure also suggested that an improvement in the particle-particle contact increased the conductivity.
Modification of the concentration of the interlayer cations *via* the synthesis of new materials suggested that increasing the concentration of the ions did in fact increase the conductivity but attempts to push the sodium content beyond a certain level led to the formation of a different class of materials. The modification of the clay by this method also left the rheology of the clay unchanged and hence this method of increasing the conductivity is the one most apt for eventual use in the paper industry.

Further work

The manipulation of the synthesis of new materials could be further refined to give a greater degree of control over the final products.
Synthesis of the clays by the sol-gel method is a time consuming one, it may be profitable to attempt to carry out these syntheses in a microwave oven as in many cases the microwave medium can increase a reaction rate by many times.

REFERENCES

REFERENCES

1. R.E. Grim. Clay Mineralogy. McGraw-Hill. New York, 1968.
2. G.W .Brindley and G. Brown. Crystal Structures of Clay Minerals and their X-ray Identification. Mineralogical Society. London, 1984.
3. J.B. Dixon and S.B. Weed. Minerals in the Soil Environment. Soil Science Society, America. Madison, 1977.
4. B.K.G. Theng. The Chemistry of Clay-Organic Reactions. Adam Hilger. London, 1974.
5. C.S. Ross and S.B. Hendricks. Minerals of the Montmorillonite Group; their origin and relation to soils and clays. U.S.Geol. Survey Prof. Paper 205-B, pp23-79, 1945.
6. D.M.C. McEwan. Montmorillonite Minerals. Chapter 4 in The X-ray Identification and Crystal Structures of Clay Minerals. G. Brown (ed). Mineralogical Society. London, 1961.
7. N. Guven. Smectites. Chapter 3 in Reviews in Mineralogy, Vol. 19, Hydrous Phyllosilicates. Mineralogical Society of America.
8. I.E. Odom. Smectite Clay Minerals: Properties and Uses. *Phil. Trans. R. Soc. Lond.* 1984, **A311**, 391-409.
9. H. van Olphen and J.J. Fripiat. Data handbook for clay materials and other non-metallic minerals. OECD and the Clay Minerals Society. Pergamon Press. New York, 1979.
10. G. Rytwo, C. Serban, S. Nir and L. Margulies. Use of Methylene Blue and Crystal Violet for Determination of Exchangeable Cations in Montmorillonite. *Clays and Clay Minerals*, 1991, **39(5)**, 551-555.
11. G.W. Brindley and P.T. Hang. Methylene Blue Adsorption by Clay Minerals. Determination of Surface Areas and Cation Exchange Capacity. *Clays and Clay Minerals*, 1970, **18**, 203-212.
12. H. van Olphen. An Introduction to Clay Colloid Chemistry. Wiley. New York, 1977.
13. M.M. Mortland. *9th Inter. Cong. Soil Sci. Trans.* 1968, **1**, 691.
14. A.P. Legrand and S. Flandrois. Chemical Physics of Intercalation. Nato ASI Series B: Physics, Vol. 172, p. 239.
15. H. Suquet, C. de la Calle and H. Pezerat. Swelling and Structural Organisation of Saponite. *Clays and Clay Minerals*, 1975, **23**, 1-9.
16. A.M. Posner and J.P. Quirk. The Absorption of Water from Concentrated Electrolyte Solutions by Montmorillonite and Illite. *Proc. R. Soc. Lond.*, 1964, **A278**, 35-56.
17. Sister M.F. Traynor, F.S.E., M.M. Mortland and T.J. Pinnavaia. Ion Exchange and Intersalation Reactions of Hectorite with Tris-Bipyridyl Metal Complexes. *Clays and Clay Minerals*, 1978, **26(5)**, 318-26.
18. D.M. Clementz and M.M. Mortland. Properties of Reduced Charge Montmorillonite: Tetra-alkylammonium Ion Exchange Forms. *Clays and Clay Minerals*, 1974, **22**, 223-229.

19. S.P. Christiano and T.J. Pinnavaia. Intercalation in Montmorillonite of Molybdenum Cations Containing the Mo_6Cl_8 Cluster Core. *Journal of Solid State Chemistry*, 1986, **64**, 232-239.

20. S.P. Christiano, T.J. Pinnavaia and J. Wang. Intercalation of Niobium and Tantalum $M_6Cl_{12}^{n+}$ Cluster Cations of Montmorillonites: A New Route to Pillared Clays. *Inorg. Chem.*, 1985, **24**, 1222.

21. S. Yamanaka, G. Yamashita and M. Hattori. Reaction of Hydroxy-Bismuth Polycations with Montmorillonite. *Clays and Clay Minerals*, 1980, **28(4)**, 281-284.

22. G.W. Brindley and R.E. Sempels. Preparation and Properties of some Hydroxy-Aluminium Beidellites. *Clay Minerals*, 1977, **12**, 229.

23. S. Yamanaka and G.W. Brindley. Hydroxy-Nickel Interlayering in Montmorillonite by Titration Method. *Clays and Clay Minerals*, 1978, **26(1)**, 21-24.

24. S. Yamanaka and G.W. Brindley. High Surface Area Solids obtained by Reaction of Montmorillonite with Zirconyl Chloride. *Clays and Clay Minerals*, 1979, **27(2)**, 119-124.

25. G.W. Brindley and S. Yamanaka. A Study of Hydroxy-Chromium Montmorillonites and the form of the Hydroxy-Chromium Polymers. *Amer. Mineral.*, 1979, **64**, 830-835.

26. R.M. Barrer and D.M. MacLeod. Activation of Montmorillonite by Ion Exchange and Sorption Complexes of Tetra-Alkyl Ammonium Montmorillonites. *Trans. Far. Soc.*, 1955, **51**, 1290-1300.

27. M.M. Mortland and V.E. Berkheiser. Triethylene Diamine-Clay Complexes as Matrices for Absorption and Catalytic Reactions. *Clays and Clay Minerals*, 1976, **24**, 60.

28. V.E. Berkheiser and M.M. Mortland. Hectorite Complexes with Cu(II) and Fe(II)-1,10-Phenanthroline Chelates. *Clays and Clay Minerals*, 1977, **25**, 105.

29. R.H. Loeppert, M.M. Mortland and T.J. Pinnavaia. Synthesis and Properties of Heat Stable Expanded Smectite and Vermiculite. *Clays and Clay Minerals*, 1979, **27(3)**, 201-208.

30. N. Lahav, U. Shani and J. Shabtai. Cross-linked Smectites.I. Synthesis and Properties of Hydroxy-Aluminium-Montmorillonite. *Clays and Clay Minerals* , 1978, **26(2)**, 107-115.

31. M.L. Ocelli and R.M. Tindwa. Physicochemical Properties of Montmorillonite interlayered with Cationic Oxyaluminium Pillars. *Clays and Clay Minerals*, 1983, **31(1)**, 22-28.

32. D. Tichit, F. Fajula, F. Figueras, B. Ducourant, G. Mascherpa, C. Gueguen and J. Bousquet. Sintering of Montmorillonites Pillared by Hydroxy-Aluminium Species. *Clays and Clay Minerals* , 1988, **36(4)**, 369-375.

33. J. Sterte. Synthesis and Properties of Titanium Oxide Cross-linked Montmorillonite. *Clays and Clay Minerals*, 1986, **34(6)**, 658-664.

34. A. Carrado, S.L. Suib, N.D. Skoularikis and R.W. Coughlin. Chromium-(III)-Doped Pillared Clays (PILC's). *Inorg. Chem.*, 1986, **25**, 4217-4221.

35. T.J. Pinnavaia, M-S. Tzou and S.D. Landau. New Chromia Pillared Clay Catalysts. *J. Amer. Chem. Soc*, 1985, **107**, 4783-4785.
36. B.M. Choudray and V.L.K. Valli. A Novel Vanadium Pillared Montmorillonite Catalyst for Molecular Recognition of Benzyl Alcohols. *J.Chem. Soc. Chem. Commun.*, 1990, 1115.
37. T. Endo, M.M. Mortland and T.J. Pinnavaia. Properties of Silica-Intercalated Hectorite. *Clays and Clay Minerals*, 1981, **29(2)**, 153-156.
38. T. Endo, M.M. Mortland and T.J. Pinnavaia. Intercalation of Silica in Smectite. *Clays and Clay Minerals*, 1980, **28(2)**, 105-110.
39. G.W. Brindley and C-C. Kao. Formation, Composition and Properties of Hydroxy-Al- and Hydroxy-Mg- Montmorillonite. *Clays and Clay Minerals*, 1980, **28**, 435-442.
40. A. Simipoulos, D. Petridis, A. Kostikas and N.H. Gangas. Intercalation of Dimethyltin(IV) Cationic Complexes in Montmorillonite. *Hyperfine Interactions*, 1988, **41**, 843-846.
41. S. Yamanaka, T. Doi, S. Saka and M. Hattori. High Surface Area Solids Obtained by Intercalation of Iron Oxide Pillars in Montmorillonite. *Mat. Res. Bull.*, 1984, **19**, 161.
42. See reference 14, p 489.
43. J. Barrault, C. Zivkov, F. Bergaya, L. Gatineau, N. Hassoun, H. Van Damme and D. Mari. Iron-doped Pillared Laponites as Catalysts for the Selective Conversion of Syngas into Light Alkenes. *J. Chem. Soc. Chem. Commun.*, 1988, 1403.
44. D.E.W. Vaughan and R.J.Lussier. Prepr. 5th Int. Conf. Zeolites, Naples, 1980.
45. F. Gonzalez, C. Pesquera, I. Benito and S. Mendioroz. Aluminium-Gallium Pillared Montmorillonite with High Thermal Stability. *J. Chem. Soc. Chem. Commun.*, 1991, 587.
46. F. Gonzalez, C. Pesquera, C. Bianco, I. Benito and S. Mendioroz. Synthesis and Characterisation of Al-Ga Pillared Clays with High Thermal and Hydrothermal Stability. *Inorg. Chem.*, 1992, **31**, 727-731.
47. J. Sterte. Preparation and Properties of Large-pore La-Al-Pillared Montmorillonite. *Clay Minerals*, 1991, **39(2)**, 167-173.
48. T.R. Jones. The Properties and Uses of Clays which Swell in Organic Solvents. *Clay Minerals*, 1983, **18**, 399-410.
49. M.I. Attalla, L.A. Bruce, S.I. Hodgson, T.W. Turney, M.A. Wilson and B.D. Batts, Reactions of Coal Liquids with Cross-linked Smectite Catalysts.1. Effects of Pillaring Materials and Recycling. *Fuel*, 1990, **69**, 725-734.
50. L.H. Klemm, J. Shabtai and K.C.Bodily. Gas Chromatography of some Alkenyl- and Cyclo-alkenyl-naphthalenes on Bentone 34, Silicone Fluid DC 550 and Apiezon L Phases. *J. Chromat.*, 1980, **198**, 1-6.
51. W.B. Jepson. Kaolins: Their Properties and Uses. *Phil. Trans. R. Soc. Lond.*, 1984, **A311**, 411-432.
52. K.W. Barr and V.D.Royston. Aqueous Conductivising Composition for Conductivising Sheet Material. United States Patent 4,739,003. 1988.

53. A-P.S. Mandair, W.R. McWhinnie and P. Monsef-Mirzai. Charge Transfer Interactions in Smectite Clays. *Inorg. Chim. Acta.*, 1987, **134**, 99-103.

54. S.P. Bond. Interlamellar Modification of Smectite Clays. Ph.D. thesis. Aston University, Birmingham, 1991.

55. R.K. Ingam, S.D. Rosenberg and H. Gilman. Organotin Compounds. *Chem. Rev.*, 1960, **60**, 459-539.

56. R.C. Poller. The Chemistry of Organotin Compounds. Logos Press Ltd.. London, 1970.

57. N.N. Greenwood and A. Earnshaw. Chemistry of the Elements. Pergamon Press, 1984.

58. D. Petridis, T. Bakas, A. Simopoulos and N.H.J. Gangas. Pillaring of Montmorillonite by Organotin Cationic Complexes. *Inorg. Chem.*, 1989, **28**, 2439-2443.

59. W. Kemp. Qualitative Organic Analysis, Spectrochemical Techniques. McGraw-Hill. 1986.

60. G. Eng and C.R. Dillard. IR and NMR Studies of Parasubstituted Phenyl Tin Compounds. *Inorg. Chim. Acta.*, 1978, **31**, 227-231.

61. G. Barbieri and F. Taddei. ^{1}H Nuclear Magnetic Resonance Study of (d-p)π Interactions in Stannanes Containing Unsaturated Systems. *J. Chem. Soc. Perkin II*, 1972, 1323.

62. G.S. Zhdanov and I.G. Ismailzade. X-ray determination of the structures of some tetraaryl compounds of silicon, tin and lead. *Chem. Abs.*, 1949, **43**, 8764f.

63. R.N. Gedye, F.E. Smith and K.C. Westaway. The Rapid Synthesis of Organic Compounds in Microwave Ovens. *Can. J. Chem.*, 1988, **66**, 17-26.

63a. D.R. Baghurst and D.M.P. Mingos. Application of Microwave Heating Techniques for the Synthesis of Solid State Inorganic Compounds. *J. Chem. Soc. Chem. Commun.*, 1988, 829-830.

64. D.R. Baghurst and D.M.P. Mingos. Superheating Effects Associated with Microwave Dielectric Heating. *J. Chem. Soc. Chem. Commun.*, 1992, 674.

65. K. Chatakondu, M.L.H. Green, D.M.P. Mingos and S.M. Reynolds. Application of Microwave Dielectric Loss Heating Effects for the Rapid and Convenient Synthesis of Intercalation Compounds. *J. Chem. Soc. Chem. Commun.*, 1989, 1515-1517.

66. F.J. Berry and A.G. Maddock. A Tin-119 Mossbauer Investigation of the Thermal Decomposition of Tin(IV) Hydroxides. *Radiochim. Acta.*, 1977, **24**, 32-33.

67. G.E. Muilenberg. Handbook of X-ray Photoelectron Spectroscopy. Perkin Elmer Corporation. Minnesota, 1979.

68. R.C. Ashcroft, S.P. Bond, M.S. Beevers, M.A.M. Lawrence, A. Gelder and W.R. McWhinnie. ^{119}Sn Mossbauer and X-Ray Photoelectron Studies of Novel Tin Oxide Pillared Laponite formed under Ambient Conditions from Aryltin Precursors. Rapid Intercalation Reactions using Microwave Heating. *Polyhedron*, 1992, **11(9)**, 1001-

1006.

69. S.P. Bond, A. Gelder, J. Homer, W.R. McWhinnie and M.C. Perry. ^{6}Li m.a.s.n.m.r.: A Powerful Probe for the Study of Lithium Containing Materials. *J. Mater. Chem.*, 1991, **1**, 327-330.
70. K.Y. Abid, Aston University. Personal Communication.
71. K.A. Phillips. Studies of the Chemical Modification and of the Thermochemistry of some Inorganic Minerals. Final Year B.Sc. Project Report. Aston University, Birmingham, 1992.
72. L.D. Freedman and G.O. Doak. Preparation, Reactions and Physical Properties of Organobismuth Compounds. *Chem. Rev.*, 1982, **82**, 15-57.
73. G.O. Doak and L.D. Freedman. Organometallic Compounds of Arsenic, Antimony and Bismuth. Chapter IX. Wiley Interscience. 1970.
74. F. Challenger and C.F. Allpress. Organo-derivatives of Bismuth. Part IV: The Interaction of the Halogen derivatives of Tertiary Aromatic Bismuthines with Organoderivatives of Magnesium and Mercury. *J. Chem. Soc.*, 1921, **119**, 913.
75. L.A. Zhitkova, N.I. Sheverdina and A. Kocheshkov. Synthesis of Organobismuth Compounds. *Chem. Abs.*, 1939, **33**, 5819.
76. P. Pfeiffer, H. Pietsch and I. Heller. Zur Darstellung der Phenylverbindungen der Elemente der Phosphorgruppe. *Berichte der Deutschen Chemischen Gesellschaft*, 1904, **37**, 4620-4628.
77. I. Norvick. Interchange of Heavy Atoms in Organometallic Compounds. *Nature*, 1935, 1038-1039.
78. The Handbook of Chemistry and Physics. 46th Edition. Chemical Rubber Company Press Inc., Florida, U.S.A.,1966.
79. F.Kh. Solomakhina. The Reaction of Triphenylbismuth with some Metal Chlorides and Mercury. *Chem. Abs.*, 1961, **55**, 15389.
80. F. Challenger and L.R. Ridgeway. Organoderivatives of Bismuth. Part VI. The Preparation and Properties of Tertiary Aromatic Bismuthines and their Interaction with Organic and Inorganic Halogen Compounds. *J. Chem. Soc.*,1922, **121(1)**, 104-120.
81. F. Challenger and C.F. Allpress. Organoderivatives of Bismuth. Part II. The Stability of Derivatives of Quinquevalent Bismuth. *Proc. Chem. Soc. Lond.*, 1914, **30**, 292.
82. D.E. Worrall. Some Bismuth Derivatives of Diphenyl. *J. Amer. Chem. Soc.*, 1936, **58**, 1820.
83. R. Muller and C. Dathe. Organoarsenic, -Antimony, and -Bismuth Compounds. *Chem. Abs.*, 1968, **68**, 49772w.
84. F. Challenger. Organo-derivatives of Bismuth (Supplementary Note). *J. Chem. Soc.*, 1916, **109**, 250.
85. C. Glidewell. Triphenylpnictogen Chalcogenides: A Preparative and Mass-Spectrometric Study. *J. Organometal. Chem.*, 1976, **116**, 199.
86. F. Challenger. Organo-derivatives of Bismuth. Part I. The Preparation and Properties of some Tertiary Aromatic Bismuthines and their Halogen Derivatives. *J. Chem. Soc.*,

1914, **105**, 2210-2218.

87. B.J. Aylett. Organometallic Compounds. Volume One: The Main Group Elements. Part 2: Groups IV and V. Chapman and Hall. London. 1979.
88. F.A. Cotton and G. Wilkinson. Advanced Inorganic Chemistry. A Comprehensive Text. Chapter 14. Wiley Interscience, New York, 1980.
89. C.Y. Wang. Antimony. Its Geology, Metallurgy, Industrial Uses and Economics. Charles Griffin and Company Limited. London. 1952.
90. W.E. Thorneycroft. A Text-Book of Inorganic Chemistry. Volume VI, Part 5, pp38-44. Charles Griffin and Company Limited. London. 1936.
91. L.R. Mernagh. Antimony as a Constituent of Enamels. *Chemistry and Industry*, 1926, **Nov 5**, 815-816.
92. H. Bart. Uber die Synthese aromatischer Arsinsauren. *Annalen*, 1922, **429**, 55.
93. G.S. Hiers. Org. Syn., Coll. Vol. 1, p550. Wiley Interscience. New York. 1941.
94. J.I. Harris, S.T. Bowden and W.J. Jones. The Preparation and Properties of Triarylstibines. *J. Chem. Soc.*,1947, 1568-1571.
95. S.P. Olifirenko. Synthesis of Triphenyl Antimony. *Chem. Abs.*, 1965, **63**, 8401.
96. F.B. Makin and J. Waters. Decomposition Reactions of the Aromatic Diazo-compounds, Part IV. A New Synthesis of Aromatic Antimony Compounds*J. Chem. Soc.*, 1938, 843.
97. G.C. Robinson. Organometallic Compounds. *Chem. Abs.*, 1963, **58**, 6858.
98. R.R. Sauers. Cleavage of Tetraphenyl Stibonium Bromide with Lithium Aluminium Hydride. *Chemistry and Industry*, 1960, 717.
99. H. Schmidt. Uber Aromatische Antimonverbindugen. *Annalen*, 1920, **421**, 217-242.
100. R. Muller and C. Dathe. Darstellung von Organoantimon(III)- und Organobismutin(III)- verbindugen mit Hilfe von Organopentafluorosilicaten bzw. Organotrifluorsilanen in waβriger Losung. Chem. Ber., 1966, 99, 1609-1613.
101. L.H. Long and J.F. Sackman. The Heat of Formation of Antimony Trimethyl. *Trans. Faraday Soc.*, 1955, **51**, 1062-1064.
102. L.A. Harrah, M.T. Ryan and C. Tamborski. Infrared Spectra of Phenylderivatives of Group IVb, Vb and VIIb Elements. *Spectrochim. Acta.*, 1962, **18**, 21-37.
103. K.A. Jensen and P.H. Nielsen. Infra-red Spectra of some Organic Compounds of Group VB Elements. *Acta Chemica Scandinavica*, 1963, **17**, 1875-1885.
104. G.O. Doak, G.G. Long and L.D. Freedman. The Infrared Spectra of some Phenyl-substituted Pentavalent Antimony Compounds. *J. Organometal. Chem.*, 1965, **4**, 82-91.
105. M.M. Leonard. Organoantimony Compounds. *Chem. Abs.*, 1966, **64**, 9766.
106. Z.M. Manulkin, A.N.Tatarenko and F.Yu. Yusupov. Synthesis of new Antimony Organic Compounds of type Ar_2SbR where R is an Aliphatic, Alkaromatic or Alicyclic Radical. *Chem. Abs.*, 1954, **48**, 2631.
107. P.G. Sergeev and A.B. Bruker. New Method of Preparation of Aromatic Antimony

Compounds. *Chem. Abs.*, 1958, **52**, 6236.

108. A.D. Beveridge, G.S. Harris and (in part) F. Inglis. The Electrolytic Conductance of Halogen Adducts of the Triphenyl Derivatives of Group Vb Elements. *J. Chem. Soc. (A)*, 1966, 520-528.

109. A.N. Nesmeyanov, O.A. Reutov and O.A. Ptitsyna. New Possibilities of Synthesis of Organoantimony Compounds through the Double Salts of Antimony Trichloride and Diazonium Salts. *Chem. Abs.*, 1954, **48**, 11375.

110. O.A. Reutov. New Method of Synthesis of Organoantimony Compounds of Type Ar_2SbX_3 and Ar_3SbX_2. *Chem. Abs.*, 1954, **48**, 143.

111. Z.M. Manulkin, A.N. Tatarenko and F. Yusupov. Cleavage of Radicals from Organometallic Compounds IX. Cleavages of Radicals by the Action of Bismuth Trichloride on $(C_6H_5)_nMe$ where Me = Bi, Sb, Hg. *Chem. Abs.*, 1955, **49**, 5397.

112a. K.M.Mackay, D.B. Sowerby and W.C. Young. Infrared Spectra of Phenyl Derivatives of Germanium, Arsenic and Antimony. *Spectrochim. Acta*, 1968, **24A**, 611-631.

112b. K.A. Jensen. Uber die raumliche Konfiguration der verbindungen vom Typus R_3PX_2, R_3AsX_2, R_3SbX_2 und R_3BiX_2. *Z. Anorg. Allgem. Chem.*, 1943, **250**, 257-277.

113. I.G.M. Campbell, G.W.A. Fowles and L.A. Nixon. Organometallic Compounds Containing Tin-Arsenic or Tin-Antimony Bonds. *J. Chem. Soc.*, 1964, 3026-3029.

114. I.G.M. Campbell, G.W.A. Fowles and L.A. Nixon. Organometallic Compounds Containing a Tin-Phosphorus Bond. *J. Chem. Soc.*, 1964, 1389-1396.

115. W. Hewertson and H.R. Watson. The Preparation of Di- and Tri-tertiary Phosphines. *J. Chem. Soc.*, 1962, **1**, 1490-1494.

116. A.K. Sawyer. Organotin Compounds, Vol. 2, p614. Marcel Dekker. New York, 1971.

117. H. Schumann, T. Ostermann and M. Schmidt. *J. Organometal. Chem.*, 1967, **8**, 105-110.

118. H.B. Singh, W.R. McWhinnie, R.F. Ziolo and C.H.W. Jones. Donor-Acceptor Complexes of Organotellurium Compoounds. Physical Studies: Tellurium-125 Mossbauer Spectroscopy for the Measure of Charge Transfer. Crystal and Molecular Structure of the Complex Dibenzotellurophene-7,7,8,8-Tetracyano-*p*-quinodimethane. *J. Chem. Soc. Dalton Trans.*, 1984, 1267.

119. H. Van Damme, F. Obrecht and M. Letellier. Intercalation of Tetrathiafulvalene in Smectite Clays: Evidence for Charge Transfer Interactions. *Nouv. J. Chim.*, 1984, **8**, 681-683.

120. M.R. Greaves. Organotellurium Compounds for Metal Organic Vapour Phase Epitaxy. Ph.D. thesis. Aston University, Birmingham, 1991.

121a. A. McKillop, L.F.Elsom and E.C. Taylor.Thallium in Organic Synthesis.XVII. Preparation of Biaryls from ArylMagnesium Bromides and Thallium (I) Bromide. *Tetrahedron*, 1970, **26**, 4041-4050.

121b. A. McKillop, L.F.Elsom and E.C. Taylor. Thallium in Organic Synthesis.III. Coupling of Aryl and Alkyl Grignard Reagents. *J. Amer. Chem. Soc.*, 1968, **90**, 2423.

122. P.E. Fanta. The Ullmann Synthesis of Biaryls, 1945-1963. *Chem. Rev.*, 1964, **64**,

613-632.

123. J. Bergman. Tellurium in Organic Chemistry - 1. A Novel Synthesis of Biaryls. *Tetrahedron*, 1972, **28**, 3323-3331.

124. G.T. Morgan and R.E. Kellett. Interactions of Tellurium Tetrachloride and Aryl Alkyl Ethers. Part II. *J. Chem. Soc.*, 1926, 1080.

125. G.T. Morgan and F.H. Burstall. Bis-*p*-phenetyl Telluride and its Derivatives. *J. Chem. Soc.*, 1930, 2599-2601.

126. G.T.Morgan and R.E. Kellett. Interactions of Tellurium Tetrachloride and Aryl Alkyl Ethers. Part II. *Chem. Abs.*, 1926, 2669-2670.

127. G.T. Morgan and H.D.K. Drew. Interactions of Tellurium Tetrachloride and Aryl Alkyl Ethers. *J. Chem. Soc.*, 1925, **127**, 2307.

128. G.T. Morgan and H.D.K. Drew. Interactions of Tellurium Tetrachloride and Aryl Alkyl Ethers. *Chem. Abs.*, 1926, **20**, 907.

129. Carl Willetts, James River Graphics. Personal Communication.

130. P.A. Cox. Electronic Structure and Chemistry of Solids. Oxford University Press. Oxford. 1987.

131. J.M. Adams, S. Evans, P.I. Reid, J.M. Thomas and M.J. Walters. Quantiative Analysis of Aluminosilicates and Other Solids by X-ray Photoelectron Spectroscopy. *Anal. Chem.*, 1977, **49**, 2001-2008.

132. N. Davison, W.R. McWhinnie and A. Hooper. X-ray Photoelectron Spectroscopic Study of Cobalt(II) and Nickel(II) Sorbed on Hectorite and Montmorillonite. *Clays and Clay Minerals*, 1991, **39**, 22-27.

133. M.K. Bahl, R.L. Watson and K.J. Irgolic. X-ray photoemission studies of tellurium and some of its compounds. *J. Chem. Phys.*, 1977, **66**, 5526-5535.

134. Laporte Industries Ltd. Technical Document 64. Laponite. Chemistry, properties and applications.

135. H. Tateyama, S. Nishimura, K. Tsunematsu, K. Jinnai, Y. Adachi and M. Kimura. Synthesis of Expandable Fluorine Mica from Talc. *Clays and Clay Minerals*, 1992, **40(2)**, 180-185.

136. H. Tateyama, K. Tsunematsu, H. Hirosue, K. Kimura, T. Furusawa and Y. Ishida. Synthesis of the Expandable Fluorine Mica form Talc and its Colloidal Properties. *Proc. 9th Int. Clay Conf.*, Strasbourg, 1989, pp43-50. V.C. Farmer and Y. Tardy (eds.).

137. R.M. Barrer and D.L. Jones. Chemistry of Soil Minerals. Part VIII. Synthesis and Properties of Fluorhectorites. *J. Chem. Soc.(A)*, 1970, 1531-1537.

138. W.T. Granquist and S.S. Pollack. Clay Mineral Synthesis. II. A Randomly Interstratified Aluminian Montmorillonoid. *Amer. Miner.*, 1967, **52**, 212-226.

139. D.L. Hamilton and C.M.B. Henderson. The Preparation of Silicate Compositions by a Gelling Method. *Miner. Mag.*, 1968, **36**, 832-838.

140. M.E. Davis and R.F. Lobo. Zeolite and Molecular Sieve Synthesis. *Chem. Mater.*, 1992, **4**, 756-768.

141. G.P. Handreck and T.D. Smith. A Physico-chemical study of Ga-ZSM-5 Zeolite. *J. Chem. Soc., Faraday Trans.I*, 1989, **85(10)**, 3215-3220.

142. V. Luca, X. Chen and L. Kevan. Characterization of Copper(II)-Substituted Synthetic Fluorohectorite Clay and Interaction with Adsorbates by Electron Spin Resonance, Electron Spin Echo Modulation, and Infrared Spectroscopies. *Chem. Mater.*, 1991, **3**, 1073-1081.

143 D.M. Clementz, T.J. Pinnavaia and M.M. Mortland. Stereochemistry of Hydrated Copper(II) Ions on the Interlamellar Surfaces of Layer Silicates. An Electron Spin Resonance Study. *J. Phys. Chem.*, 1973,**77**, 196-199.

144 A-P.S. Mandair, P.J. Michael and W.R. McWhinnie. ^{29}Si MASNMR Investigations of the Thermochemistry of Laponite and Hectorite. *Polyhedron*, 1990, **9**, 517-525.